istituto nazionale di fisica nucleare
laboratori nazionali di frascati

2006
ANNUAL REPORT

Cover:

Bonsai naturale sull'entrata di villa Mondragon.

Natural bonsai on top of villa Mondragone entrance.

Cover artwork: *Claudio Federici*

istituto nazionale di fisica nucleare
laboratori nazionali di frascati

2006
ANNUAL REPORT

LNF-07/10 (IR)
June, 2006

Editor
Mario Antonelli

Technical Editor
Luigina Invidia

Published by
SIS-Pubblicazioni
P.O.Box 13 – I–00044 Frascati (Italia)

Available at www.lnf.infn.it/rapatt

Mario Calvetti
LNF Director

Maria Curatolo
Head, Research Division

Miro Andrea Preger, Pantaleo Raimondi
Scientific Head, Accelerator Division

Claudio Sanelli
Technical Head, Accelerator Division

LNF Scientific Coordinators

Riccardo De Sangro
Particle Physics

Marco Ricci
Astroparticle Physics

Pasquale Di Nezza
Nuclear Physics

Calogero Natoli
Theory and Phenomenology

Roberto Cimino
Techn. and Interdisciplinary Research

FOREWORD
Laboratori Nazionali di Frascati-Frascati National Laboratories (LNF)
Present and Future

1 Introduction

The Frascati National Laboratories (LNF), situated on a hill just south of Rome, is the largest laboratory of the Italian Institute of Nuclear Physics (INFN). The laboratory is organized into three substructures: the Accelerator Division, the Research Division and the Administration, for a total of about 380 staff members.

The Accelerator Division runs the DAΦNE accelerator complex, an e^+ e^- storage ring, used to produce ϕ-mesons at a high rate. Three experiments, KLOE, FINUDA and SIDDHARTA, study the ϕ decays, the charged and neutral kaon decays, the kaonic nuclei, produced when a negative kaon is absorbed in a nucleus, and the properties of any other of the particles produced in the ϕ decay chain. A linear accelerator (the Linac) accelerates electrons and positrons to fill the storage rings. The very clean electron and positron beams, with variable energy in the interval between 50 MeV and 850 MeV, variable intensity from 1 to 1010 electrons per bunch, at a rate of 50 Hz, can be deflected into an experimental area, the Beam Test Facility (BTF), where a photon tagged beam, of variable energy, is also available. The BTF facility is continuously used by internal and external users. Last year, for example, the photon calorimeter of the AGILE satellite was calibrated using the energy tagged photon beam, and the properties of several detectors, used by the LHC experiments, were also measured. Experiments with cryogenic detectors, channelling of positron with undulated crystals for x ray production, and other experiments, are planned for the coming years. The Accelerator Division participates in the construction of the CNAO (Centro Nazionale di Adroterapia Oncologica), a 1.2 GeV proton synchrotron used for cancer therapy in Pavia. A free electron laser, named SPARC, is being assembled at the LNF, in collaboration with ENEA (the Italian National Agency for New Technologies, Energy and the Environment). The scientific goal of the SPARC project consists in producing 10 ps electron bunches, with emittance smaller then 2 mm mrad, able to induce the self amplified green synchrotron laser light in the magnetic undulator placed downstream the electron gun. A very intense LASER, able to produce 200 TW of 0.8 micron wave length for 10 fs (the Frascati Laser for Acceleration and Multidisciplinary Experiments, FLAME) is being assembled nearby the SPARC linac. The possibility to accelerate a bunch of electrons in the plasma waves produced by the light in a gaseous target will be explored. The proton synchrotron in Pavia (CNAO), the SPARC free electron laser and the FLAME laser will be operational by the end of the year 2008. Physicists and engineers of the Accelerator Division also participate in the research and development in the field of accelerator technology. The construction of CTF3, the CLIC Test Facility at CERN, the TTFII, the Tesla Test Facility at DESY, the work for the future Linear Collider and the study for a possible future Super B-factory as well, are part of our research program. The DAΦNE accelerator, which is continuously being improved, produces synchrotron radiation light used by many experimental groups. The very intense infrared light from a synchrotron source is available at DAΦNE. At the moment we have three lines running, the Infra Red line, the X ray line and the UV line, a second x-ray line is under construction. More than a hundred users, in the context of the European research funding TARI program, used this facility last year.

The Research Division is composed of physicists and engineers working in many experiments at the LNF, at CERN (ATLAS, LHCb, DIRAC), at FNAL (CDFII), at SLAC (BABAR), at JLAB (AIACE), at DESY (HERMES), in Grenoble (GRAAL), at the Gran Sasso National Laboratories

LNGS (OPERA, ICARUS), at Cascina (VIRGO), in space borne experiments within the WIZARD program, and also, locally, in the search for gravitational waves with a cryogenic bar (NAUTILUS).

1.1 Short range future at LNF

In the spring of 2006 KLOE was removed from the DAΦNE ring and placed in the assembly hall, while the FINUDA detector has been placed on the machine. In the 2006-2007 run of DAΦNE, FINUDA has collected 1 ft^{-1} as expected, concluding seccesfully the data collection of the first phase of the FINUDA scientific program. DAΦNE is a beautiful opportunity to study machine physics at its cutting edge. Several possible modifications of the accelerator can be implemented to increase the luminosity. New technologies will be applied, like fast kickers, to increase the injection efficiencies, kickers that could be used for the ILC dumping rings, crab cavities, wigglers with shaped poles, to follow the particle trajectory in the alternating magnetic fields, and so on. An adequate fraction of the beam time will be dedicated to machine studies, because it is important to understand the machine limits, the new technologies and the new ideas. The LNF are also very active in the field of scientific communication. In fact, every year we have more than a thousand visitors, mainly students and teachers. Every autumn we organize a week long meeting, with lectures, discussions, visits to the labs, attended by more than 250 secondary school teachers of physics and philosophy. In the year 2005 our Scientific Information Services has organized 26 conferences.

1.2 Long range future - The LNF roadmap

The main research programs of the LNF, the CNAO, the SPARC, the FLAME projects, will either have ended or be in smooth running conditions by the end of 2008, similarly for the LNF groups that collaborate with the LHC experiments. We consider it very important to have a strong physics research program, to be pursued at Frascati beyond the year 2010. A major upgrade of the present accelerator is under evaluation, aiming at a machine able to deliver more than 50 fb^{-1} at the ϕ resonance, in 4 or 5 years of data taking, starting in 2011, and to operate with a centre of mass energy in the interval 1GeV - 2.5 GeV. Recently we have stimulated an intense effort to study the physics case of this new accelerator named DANAE. Five Letters of Intent on different research topics have recently been received and will be evaluated in the framework of this possible new future initiative. The letters of intent and the proposal for the new accelerator can be found at the following address http://www.lnf.infn.it/lnfadmin/direzione/roadmap.html. New collaborators for the experiments and the construction of a top class accelerator would be welcome at LNF.

Prof. Mario Calvetti
Director of LNF

ACKNOWLEDGMENTS

I want to thank all the authors that contributed to this report. A special acknowledgment goes to Luigina Invidia for her very pleasant and productive collaboration in the realization of this report. I would like also to thanks Claudio Federici for the excellent realization of the cover page, and Stefano Bianco for his help and suggestions.

Mario Antonelli
Editor

2006 ANNUAL REPORT
CONTENTS

5 – Technological and Interdisciplinary Research

6 – Accelerator Physics

COMMUNICATION and OUTREACH

R. Centioni, V. Ferretti (art.15), S. Miozzi (art. 2222), L. Sabatini, S. Vannucci (Resp.)
Office of Education and Public Relations
Scientific Information Service

The "Laboratori Nazionali di Frascati dell'INFN" (LNF) provide basic education in Physics for the general public, students and teachers. The LNF Educational and Public Relation programmes are made possible by the enthusiastic involvement of the laboratory graduate students, postdocs, researchers, engineers and technicians. This report describes 2006 activity including special events organized for European Researchers' Night 2006.

1 Visiting LNF

`http://www.lnf.infn.it/edu/`

- LNF Guided Tours

A well established tradition: for general public, students and teachers: about 4700 people/year, 81 volounteers have received 139 groups. A typical visit consists of:

- history of the laboratory;
- presentation of INFN-LNF activities on site and abroad;
- visit to the "en plein air museum";
- visit to experimental areas.

- LNF Scientific Week and Open day: about 600 visitors.

Scientific Coordinator G. Mazzitelli.

Since 1990.

Most of LNF employees are in action to present their research center, answer questions and care for their guests:

- guided tours;
- conferences and public lectures;
- scientific videos;
- exhibitions of students' projects;

2 Scientific Itineraries - Scienza Orienta and Frascati Scienza: about 400 visitors

The aim is to offer a more complete view of the scientific institutions operating in the area and improve the communication with the general public. In collaboration with:

- CNR Tor Vergata;

- ENEA Frascati;
- ESA-ESRIN Frascati;
- INAF Astronomical Observatory of Rome, Monte Porzio Catone;
- INAF-IASF
- COPIT, Rome;
- Frascati and Castelli Romani Municipalities;
- International non-government organizations;
- University of Rome Tor Vergata.

3 Students' programme

`http : //www.lnf.infn.it/edu/stagelnf/`

- LNF Stages for High School students.

Scientific Coordinators: D. Babusci, F. Bossi, P. Gianotti, P. Di Nezza.

Goal: enable students to acquire the knowledge and understanding of INFN research activities.

- Winter stages, 2-4 weeks: 32 students with 15 tutors;
- Masterclasses 2006, 3 days: 36 students with 6 tutors;
- Summer stages, 2 weeks: 93 students with 37 tutors;
- Lectures at school by LNF researchers, 2-3 days: 529 students with 25 tutors.

- Special Program for Primary School: QUASAR

`http : //www.lnf.infn.it/edu/quasar/`

Care of F. Murtas and B. Sciascia.
Age: 8 - 14.
First meeting with the children at their school to introduce the world of research and some concepts of modern physics. Then, visit to the Frascati National Laboratories by small groups. Total of children and teachers in visit: 310.

4 High school teachers' programme

- "Incontri di Fisica"

`http : //www.lnf.infn.it/edu/incontri/`

Organizing Committee: S. Bertolucci, D. Babusci (chair), S. Bianco, M. Calvetti, L.E. Casano, R. Centioni, C.O. Curceanu, V. Ferretti, S. Miozzi, L. Sabatini, S. Vannucci.

- Lectures for high-school science teachers and scientific journalists.

- Goal: stimulate teachers' professional training and provide an occasion for interactive and hands-on contact with the latest developments in physics.

Sixth edition (October 4-6, 2006): 205 participants and 24 LNF Tutors (researchers, engineers and technicians).

5 Online resources for teachers and students: "Lezioni di Fisica", Live lectures by scientists

`http://www.lnf.infn.it/media/`

Care of M. Calvetti, O. Ciaffoni, G. Di Giovanni.
R. Barbieri: "Matter Waves, Principle of Uncertainty".
M. Mangano: "The forces".
G. Altarelli: "Principle of Relativity, Space-Time".
N. Cabibbo: "Energy: What is it?""Electrical Energy in Italy"
C. Mencuccini: "Electrical Energy in Italy"
L. L. Cavalli Sforza: "Multidisciplinary approach to human evolution".

6 General public programme

- Seminars

`http://www.lnf.infn.it/edu/seminaridivulgativi/`

Upon request, LNF researchers presented seminars to high school students and the general public on:

- INFN Activities and Elementary Particles;
- Modern Physics and Cosmology;
- Physics and Techonology for historic and artistic patrimony.

7 Events

- European Researchers' Night 2006

`http://www.lnf.infn.it/nottedellaricerca/`

The "COME IN" (COndividiamo Mille Emozioni INsieme - Lets share thousand emotions together) project, done in the framework of the European Researchers' Night on 22 September 2006, which addressed to the general public in the Roman and the so-called Castelli Romani region has been successfully realized, by bringing about 4000 persons (so doubling the awaits) for one night in direct contact with researchers, in those places (Research Institutes) where the research is done. The key of the success was an intense and constructive collaboration between the major Italian research Institutes (INFN, ENEA, ESRIN, INAF-OAR, CNR, ROMA1, ROMA2, ROMA3), centered in Rome and in Frascati, one of the highest density

Figure 1: *European Researchers' Night 2006: Overview of the B. Touschek Auditorium during the round table. (INFN-LNF Photo).*

Figure 2: *European Researchers' Night 2006: C. Renier, Representing of the European Commission projected on the Auditorium screen, while describing the motivation of the Researchers' Night initiative. (INFN-LNF Photo).*

scientific area in Europe. This collaboration allowed to present to the general public many different and complementary activities, in an informal way.

Organizing Committee: A. Antonelli, G. Bernardi, S. Bertolucci, M. Calvetti, E. Ciarravano, C. Crisari, C.O. Curceanu, A. Gallo, D. Maselli, G. Mazzitelli, A. Paniccia, A.P. Valle, S. Vannucci, A. Viticchié.

Project Coordinator: G. Mazzitelli.

Sponsor: Regione Lazio, Filas, Provincia di Roma, Trenitalia, XI Comunitá Montana - Castelli Romani e Prenestini, Parco Regionale dei Castelli Romani, Comune di Frascati, Comune di Monte Porzio Catone, Comune di Grottaferrata, Consorzio Castelli Romani.

An important feedback of the success of the event comes from the questionnaire (available on the web site http://www.infn.it/nottedellaricerca) addressed to investigate the achievement of the main purpose of the project and of the quality of the activities.

- Christmas Concert

`http://www.lnf.infn.it/edu/eventi/index.html`

LNF 14 December, 2006

Corale Tuscolana.

Evening solidarity for Amnesty International and Associazione Sclerosi Tuberosa.

Conferences

International conferences, workshops and schools hosted and organized by the LNF:

1. ILIAS WP3, LNF 12-13 January, 2006
2. Auger Fluorescence Detector Monitoring Workshop, LNF 6 February, 2006;
3. Riunione delle Assemble Nazionali dei Rappresentanti del Personale TTA e Ricercatore, LNF 6 February, 2006;
4. CMS RPC Italia, LNF 20 - 21 February, 2006;
5. Workshop sui Monte Carlo, la Fisica e le Simulazioni a LHC, LNF 27-28 February, 2006;
6. Discoveries in Flavour Physics at e+e- Colliders, LNF 28 February / 3 March, 2006;
7. Les Rencontres de Physique de la Valle d'Aoste, La Thuile, 5-11 March, 2006;
8. Super B-Factory, LNF 16-18 March, 2005;
9. Winter School on Attractor Mechanism, LNF 20-23 March, 2006;
10. Alphagalileo, LNF 20 March, 2006;
11. Fundumental Physics in Space with small payloads (FPS-06), LNF 21-23 March, 2006;
12. Mini Workshop Kaon Interferometry, LNF 24 March, 2006;
13. Convention of Hadron Physics Project, LNF 30 March / 1 April, 2006;
14. LNF Spring School "Bruno Touschek", LNF 15-19 May, 2006;
15. I Corso Interdisciplinare di Spettro-Microscopia IR", LNF 15-17 May, 2006;
16. Spring Institute 2005, LNF 22 May / 14 July, 2006;
17. EPJA Edtorial Meeting, LNF 19-20 May, 2006;
18. Vulcano Workshop, Vulcano 22-27 May, 2006;
19. Workshop sui Monte Carlo, la Fisica e le Simulazioni a LHC, LNF 22-24 May, 2006;
20. QCD Structure of the Nucleon, Villa Mondragone (Monte Porzio Catone), 12-16 June, 2006;
21. DASIM, LNF 21-23 June, 2006;
22. Heavy Ion Reactions at Ultrarelativistic Energies, Trento 26-29, June, 2006;
23. Channelling, LNF 3-7 June, 2006;
24. Nanoscience and Nanotechonology 2006, Villa Mondragone (Monte Porzio Catone), 11-14 Septmber, 2006;
25. Convention of Hadron Physics Projects, LNF 5-7 October, 2006;
26. II Corso Interdisciplinare di Spettro-Microscopia IR, LNF 16-18 October, 2006;
27. Riunione Sighad, 12-14 October, 2006;
28. Workshop sui Monte Carlo, la Fisica e le Simulazioni a LHC, LNF 23-25 October, 2006;

29. ICFA mini-workshop on "The Frontier of Short Bunches in Storage Rings", LNF 7-8 November, 2006;

30. SuperB 2006, LNF 12-16 November, 2006;

31. La figura dell'esperto nella sorveglianza fisica dei campi elettromagnetici nei luoghi di lavoro, LNF 14 November, 2006;

32. CARE - Riunione Generale , LNF 15-17 November, 2006;

33. PANDA Software Tutorial, LNF 27 November / 1 December, 2005;

ATLAS

M. Antonelli, M. Barone, M. Beretta, H. Bilokon, E. Capitolo (Tecn.), F. Cerutti, V. Chiarella, M. Curatolo, B. Dulach, B. Esposito(Resp.), M.L. Ferrer, C. Gatti, S. Giovannella, K. Kordas, P. Laurelli, G. Maccarrone, A. Martini, W. Mei, S. Miscetti, G. Nicoletti, G. Pileggi (Tecn.), B. Ponzio(Tecn.), V. Russo(Tecn.), A. Sansoni, T. Vassilieva (Tecn.), S. Ventura (Dott.), E. Vilucchi

In collaboration with:
Servizio Progettazione Apparati Sperimentali:
C. Capoccia, S. Cerioni
Centro di Calcolo:
D. Maselli, C. Soprano

1 Introduction

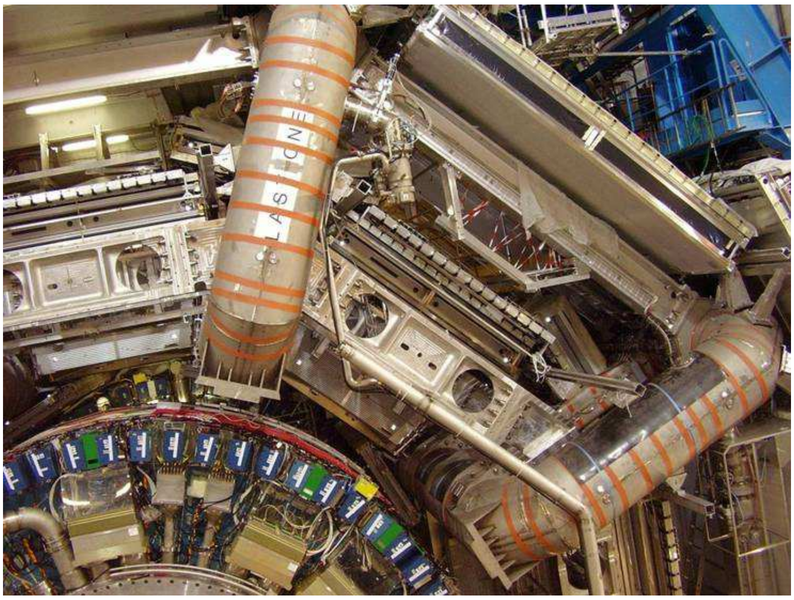

Figure 1: *An enlarged view of the top region of the Muon spectrometer*

ATLAS is a general purpose experiment at the CERN Large Hadron Collider (LHC) 7+7 TeV proton-proton machine. The experiment is aimed at the search for the Higgs boson providing a potential discovery reach over the full mass range envisageable, at the precision verification of the Standard Model and at the search for New Physics beyond the Standard Model.

The feasibility of the above physics measurements demands very challenging performances in the inner detector tracking, calorimetry, muon tracking, trigger and DAQ. The ATLAS detector, of unprecedented performances, size, complexity, has been designed, developed through many years of R&D and built by the effort of a collaboration of unprecedented size, consisting, at present, of 164 Institutes of 35 countries and 1800 members.

The LNF ATLAS group has participated to the experiment since the beginning of the study group work, at the end of the year 1989, and has been very active in the preliminary studies, the detector proposal, the R&D phase, the construction and the commissioning phase.

The area of interest of the LNF group has been the muon detection and the study of the physics channels with a muon signature in the final state. The LNF group has given a major contribution in the design, development and construction of the muon precision tracking chambers, the so-called MDT (Monitored Drift Tube) chambers. The MDT chambers, made of high pressure drift tubes, have been built with a mechanical precision in the wire position of 20 μm rms. Taking into account the large dimensions of the chambers, (up to 6 x 3 m^2) this achievement was absolutely non trivial. A great design and R&D effort was needed to find a suitable construction method and to develop suitable precision tools, in order to achieve such an unprecedented mechanical precision over such large areas. Most of this development is based on the concepts proposed by the Frascati group and on the R&D work made by the LNF group. The Frascati group has also contributed very significantly to the design and the development of the facilities for the series production and QA/QC, such as the tube wiring machine, the tube gas-leak test facility, the tube wire tension test facility, the chamber gas-leak test. Those facilities conceived for the series production are highly automated and computer controlled.

The Frascati group has taken a significant share of the MDT chamber construction, having built all the BML (Barrel Middle Large) chambers, 94 chambers of size 4 x 2 m^2, corresponding to about 28000 tubes. The availability of the highly automated construction facilities developed and realized was instrumental in order to achieve the completion of the chamber construction well in schedule, even in presence of manpower limitations.

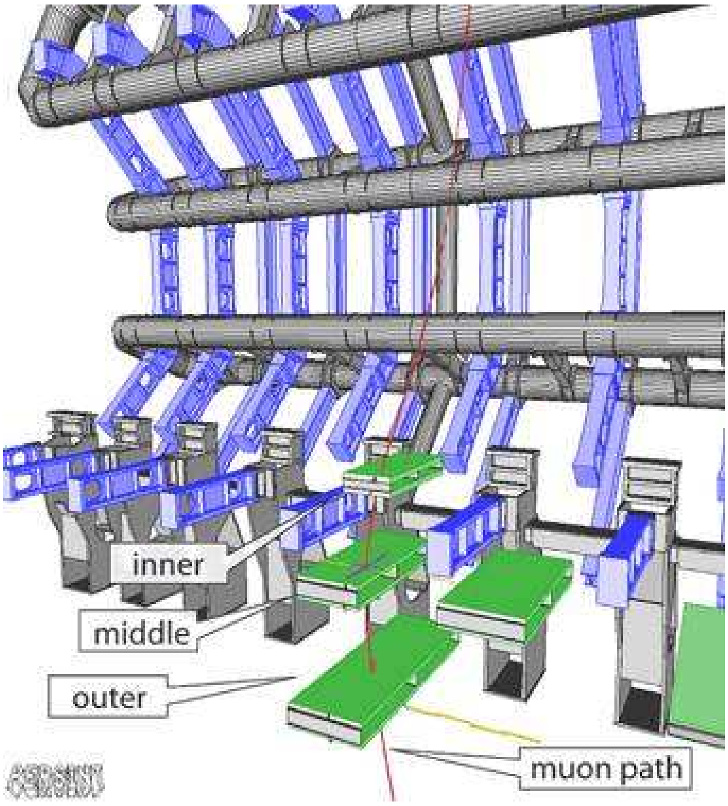

Figure 2: *Event Display of a muon passing the instrumented sectors with the Barrel Toroids at nominal field.*

2 General information about ATLAS

In 2006 the ATLAS Collaboration has been progressing towards the realization of an experimental set-up ready to record the very first proton-proton collisions at the LHC at the end of 2007. The construction of all the final components has been almost completed; the installation of the sub-detector elements of the ATLAS experiment in the underground cavern has been going on and achieved a well advanced status of completion; the commissioning of the ATLAS experiment has started.

The commissioning and field mapping of the Central Solenoid and Barrel Toroid magnet systems has been completed successfully in the second half of 2006 and the two magnet systems are ready for LHC operation.

Although detector installation can be foreseen beyond the engineering run of end 2007, the ATLAS Collaboration expects to achieve the goal of having an initial completely installed and working detector at the start of LHC operations.

The production and installation of the Level-1 trigger electronics for the calorimeter and muon triggers has been going on; one slice of the muon trigger system with cosmic rays has been successfully commissioned; the integration with the rest of ATLAS DAQ system has been progressively pursued. Concerning the High Level Trigger (HLT), progress has been achieved in exploring the HLT capabilities based on full event information.

A big effort on Data Preparation has been going on in ATLAS with the main aim to be prepared to ensure the good quality of the data from the offline processing at the Tier-0, Tier-1 and Tier-2 centers. In 2007 the commissioning of the Data Preparation is foreseen with the use of the Calibration Data Challenge reconstruction phase to test the data quality offline implementation. Finally, the recent work on physics studies has been stronghly focused to achieving the readiness to make optimal use of the early LHC data.

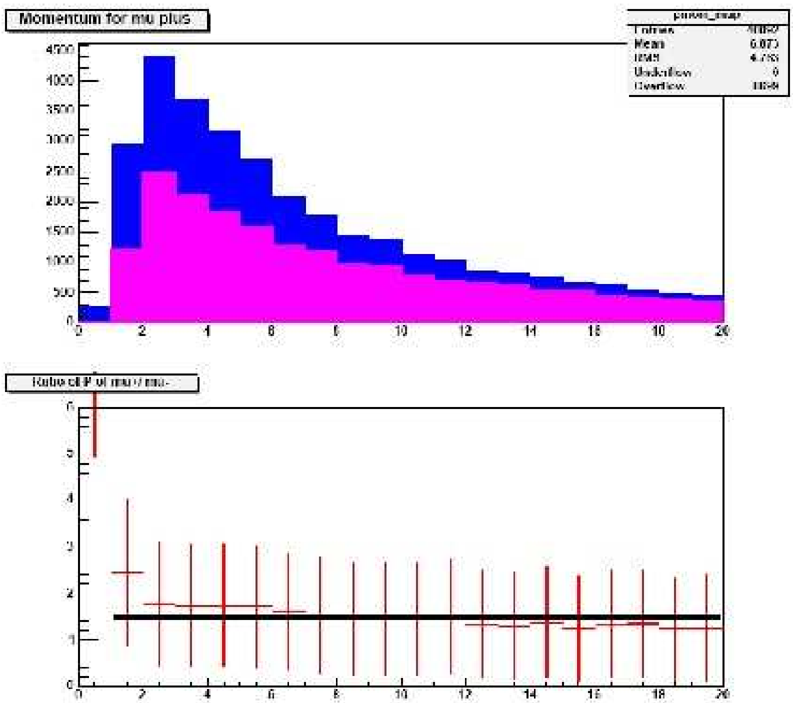

Figure 3: *Measured muon spectra*

3 Activity of the LNF group

The activity of commissioning the BML MDT chambers and installing them in the ATLAS cavern at the LHC has continued in the year 2006.

Test in situ of the muon chambers have been made, also with the toroidal magnet field on, taking data with cosmic rays.

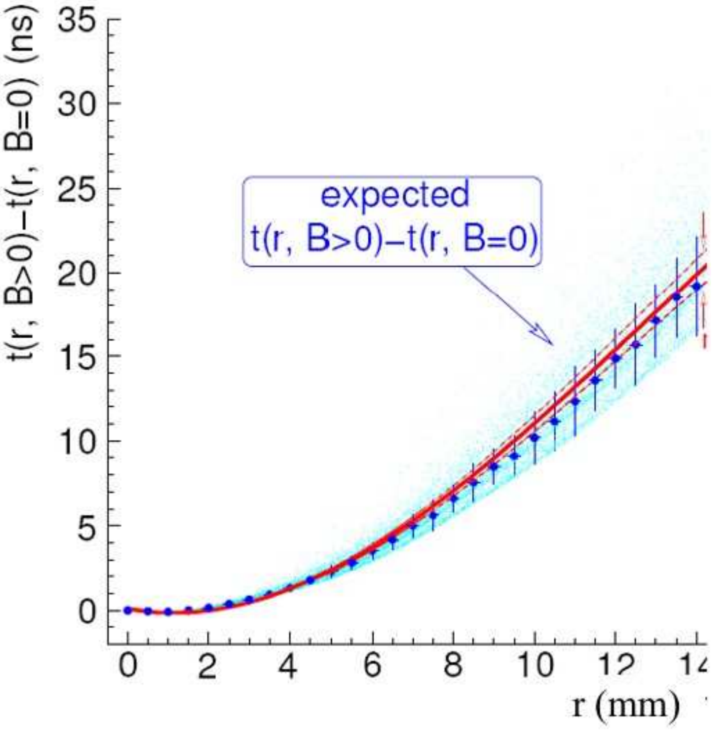

Figure 4: *Effect of the magnetic field on MDT drift*

The group has participated in the commissioning of the DAQ system.

The analysis of some interesting physics processes, characterized by the presence of muons in the final state has been pursued on MC simulated events. The potential of calibrating the muon detector by using physics events, such as $Z \rightarrow \mu^+\mu^-$ has been investigated.

The computing resources of the dedicated "proto-Tier2" farm have been installed and operated.

4 Muon Chamber commissioning

The integration of the BML chambers with the trigger detectors RPC into muon stations had to be interrupted around mid 2005 because it was found that some RPC chambers needed modifications. Many assembled stations had to be dis-assembled and then re-assembled after RPC detector repair during 2006.

Finally, in 2006 the totality (94) of the BML stations have been integrated, or re-integrated after the RPC refurbishing operations. A final cosmic ray test of the complete RPC-MDT stations at the BB5 stand has been performed to declare them ready for installation in Atlas. The number of BML stations that has undergone in 2006 this cosmic ray final test was 76.

All the muon stations arrived at ATLAS after the cosmic ray certification at the BB5 stand were re-tested at SX1 (the surface area at the ATLAS point), before being downloaded in the pit and installed in the muon spectrometer. Each single chamber was connected to the low voltages, and then readout from the CSM board via an optical fiber by a standalone PC to check the whole functionality of the FEE mounted on the chamber. Tests of the HV system, of the gas-tightness and of the optical alignment system were also performed.

5 Chamber Installation in the Atlas detector

The installation of the muon stations in the Atlas spectrometer started in summer 2005. Concerning the BML stations, 6 stations of the sector between the feet of the Atlas detector (sector 13) were successfully installed in July 2005 and correctly positioned in the Atlas spectrometer by means of auxiliary tooling designed and realized in Frascati.

In the overall ATLAS schedule, the installation of the majority of the other BML stations was scheduled in 2006 and a few of them in 2007, for reasons of detector accessibility. Indeed, 60 more BML stations were installed in ATLAS in 2006. Most of them, where possible, were also positioned in their final position, with a required precision of the order of 1 mm. In 2007, 9 more muon stations of side A and 19 more muon stations of side C remain to be installed due to the necessity of maintaining the accessibility into ATLAS up to the last moment.

A view of the top region of the ATLAS muon spectrometer is presented in Fig. 1.

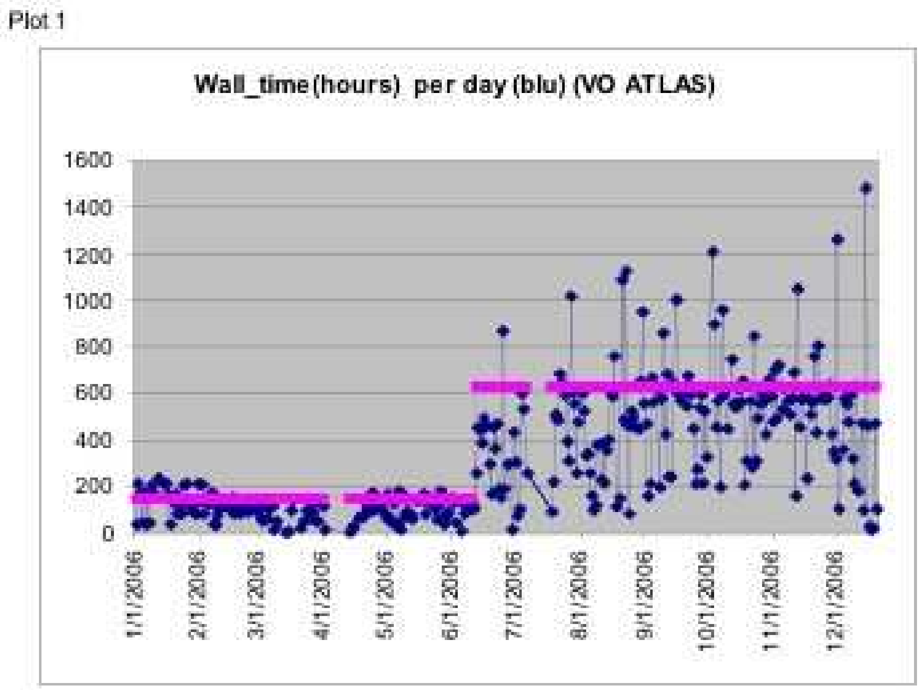

Figure 5: *Time used on the working nodes per day along all 2006: blue points measurement, purple line maximum available time*

6 Cosmics data taking in Sector 13 with magnetic field

The intense work of commissioning to test not only the functionality of the MDT chambers but the whole system (trigger, detector control system, data acquisition and online/offline monitoring), started in autumn 2005, was continued during 2006.

At the end of 2006, the ATLAS Barrel Toroid (BT) magnet was powered up, step-by-step, reaching a current of 21 kA for the first time during the night of 9 November. The BT had been first cooled down over a six-week period in July-August to reach -269 °C . The value of the current reached during this first test was 500 A above the current needed to produce the nominal magnetic field. Afterwards, the current was switched off and the stored magnetic energy of 1.1 GigaJoules, was safely dissipated, raising the cold mass of the magnet to - 218 °.

During the BT test in November, cosmic ray data were taken with the BT switched on and off and acquiring the 13 muon stations in the ATLAS feet region. The Level-1 muon trigger was provided by 3 BML-RPC/Level-1 stations and distributed to the muon system via the MUon Central Trigger Processor (MUCTP) + Central Trigger Processor (CTP). Some results coming from the data taken during the BT test are shown in the following plots: in Fig. 2 an event display of a muon crossing the apparatus with BT ON is shown. This demonstrates, not only that the muon detector is finally getting in a final working configuration, but also that all the software, DAQ and trigger infrastructure are getting together. In Fig. 3, the distribution of the muon spectra for positive and negative curvature tracks is shown. As expected, a reasonable unbalance between positive and negative tracks is observed. Finally in Fig. 4 the effect of the B-field on the drift is shown.

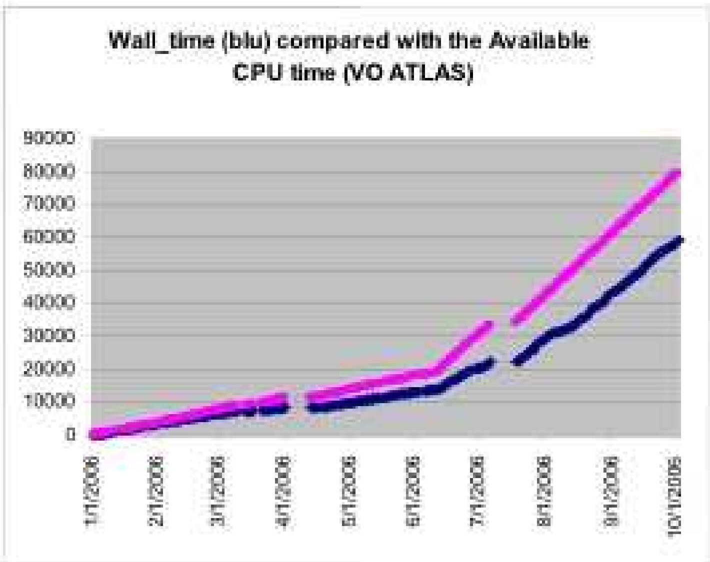

Figure 6: *Upper points maximum available running time on the working nodes. Lower points used running time.*

7 DAQ Commissioning

The activity on the Trigger and Data Acquisition (TDAQ) system has been focused, during the year 2006, on the following aspects:

1. Developments of the Event Building (EB) sub-system;
2. Validation of PC's to be used in the final installation;
3. Technical runs for TDAQ commissioning, using an increasing number of PC's and network devices approaching the final configuration;
4. Running TDAQ in the LNF cosmic ray stand.

The Event Builder sub-system has been optimized to increase the performances when running in the two different configurations of: (i) acquiring and writing events to disk, as needed to take cosmics data runs for the commissioning of the read-out system, and (ii) passing events to the Level-3 trigger sub-system.

The LNF group has been involved in the validation, installation and commissioning of the final PC's and network devices which are already installed in the ATLAS racks. This work will be continued and completed in 2007 .

The group has also been involved in the work of creating tools to easily modify the TDAQ configuration, adding/removing components, for example, so that all ATLAS users (not only the TDAQ experts) could interact in a simple way with the DAQ system.

Another field of work has been the effort in implementing more flexibility and functionalities to the Data Collection system. A full event in ATLAS is foreseen to be about 1.5 MB, recorded at a rate of 100 to 200 Hz. In some cases the complete information of an ATLAS event is not needed as, for example, for the muon detector calibration events. In 2006, the new functionality of building *partial events* has been added to the ATLAS TDAQ system. *Partial events* are based only on the data readout of a specific list of sub-detectors. For these events, a higher trigger rate than for whole events can be sustained.

In parallel, the possibility to tag events for different uses (such as physics, calibration, debugging purposes) and to stream them to the appropriate output according to a *stream tag* has been implemented. The trigger part of the TDAQ system defines the *stream tag* while the Data Collection part, responsible for the event building and the data movement between the various TDAQ components, acts accordingly. The work on the *partial event* building is part of the overall effort to add flexible streaming functionality in the Data Collection system.

8 LNF Tier-2 activity

The LNF Tier-2 computing farm is considered a proto-Tier-2 by INFN and is still in the process of getting officially approved. However, during 2006 it has worked at almost full efficiency providing computing power and data storage for official and private ATLAS simulation production campaigns.

The financial support received, both from central and local resources, made possible to expand the initial configuration. The Tier-2 is constituited by:

- 41 KSI2K of computing power;
- 6.4 TB of storage, that will be expanded to 11.5 TB after the installation of new disks which has been ordered on Dec 2006.

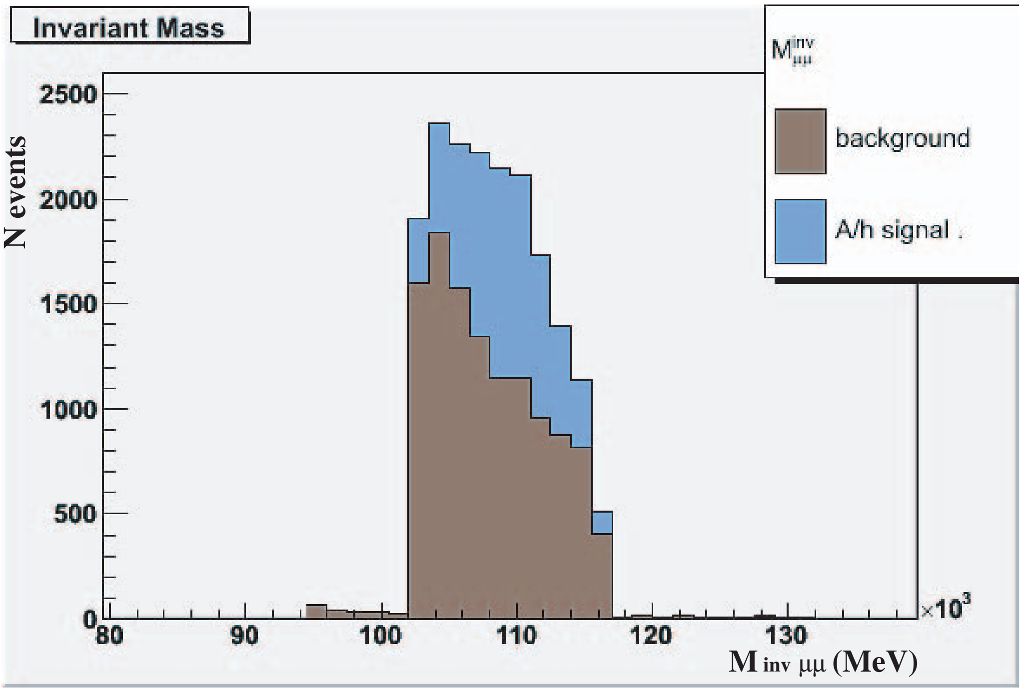

Figure 7: Distributions of the reconstructed $\mu^+\mu^-$ invariant mass for signal and background events, after all selection cuts at the reference point (tan($\beta = 45$, M$_A$ = 110.31 GeV, M$_h$ = 110.00 GeV). The two distributions are normalized at L= 300 fb^{-1}. The h/A signal (light blue) emerges over background (Z, t-tbar and ZZ) (dark brown).

At present the Tier-2 has a dedicated man-power equivalent to 4 FTE: 1 FTE from the Computing Service, responsible of maintenance and software installations, and 3 FTE from the ATLAS group, responsible of all ATLAS related interventions and users support. The computer farm provided by the LNF Computing Service is also available to local ATLAS users. To facilitate the users a parallel ATLAS software installation is maintained and a dedicated afs disk area of about 3 TB is planned.

To document the Tier-2 activity we show two reference plots. In the first plot, see Fig. 5, we compare for each day of 2006 the time accumulated by all the jobs completing execution in that day with the maximum running time available (24 hours multiplied by the number of CPU's). In the second plot, see Fig. 6, the same information is shown after integrating over the whole year. The two periods of inactivity observed are due to interventions for new installations and/or installation upgrades. The overall efficiency in the usage of the Tier-2 by the virtual organization ATLAS is about 79%.

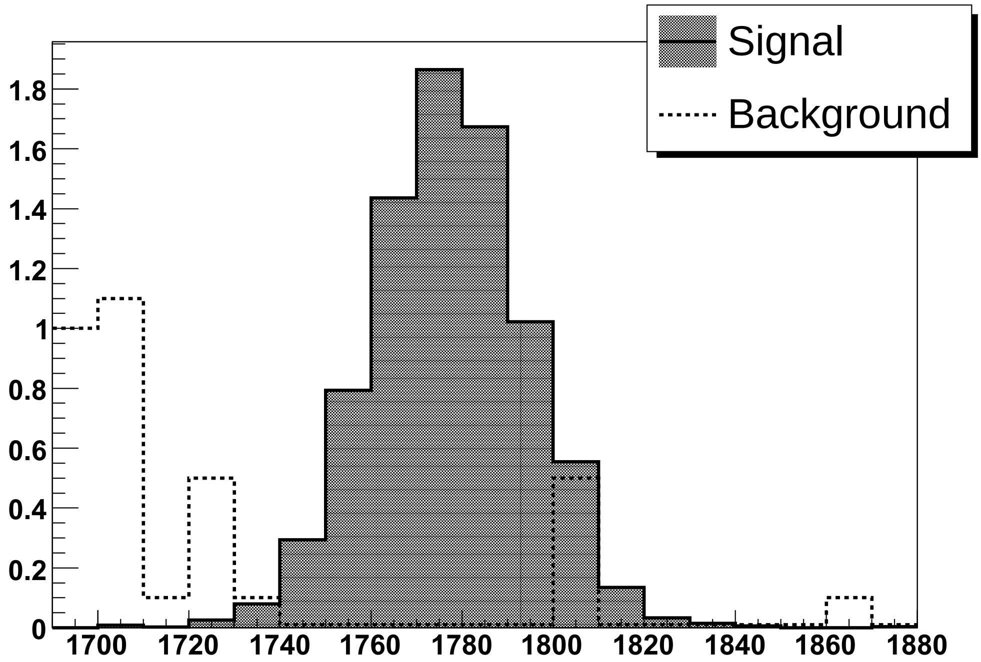

Figure 8: *Invariant mass distribution of the 3 isolated muons at the end of the search for the LFV decay $\tau \rightarrow 3\mu$: (solid) signal (dashed) background.*

9 Software and Analysis

9.1 Higgs and new physics

The LNF group is interested to analysis items related both to Standard Model Physics and to search for New Physics, the preferred signature being the presence of muons in the final states. Due to this choice, the group has contributed to the construction of the muon detector and to the test beam and commissioning work and intends to contribute actively to the verification of the calibration and reconstruction of the muons. The physics topics which at present are being studied can be summarized as follows:

1. $H \rightarrow 4\mu$ (in collaboration with Cosenza);
2. $h_0/A \rightarrow 2\mu$ (in collaboration with Roma 1);
3. $\tau \rightarrow 3\mu$;
4. $Z' \rightarrow 2\mu$.

The investigation of the ATLAS discovery potential on the SM Higgs decay to 4 muons final state has been carried out following an analysis based on multivariate techniques applied to signal and background samples [2] generated with the most up do date simulation. Variables based on the scalar and CP-even nature of the Higgs have been used to improve the rejection of the irreducible background while muon isolation criteria helped in rejecting events with muons from heavy flavour decays. A deterioration of the detector performance with respect to the physics TDR is found. Our analysis techniques and the application of the next-to-leading order correction to the Higgs production cross section allow to recover the expected discovery potential.

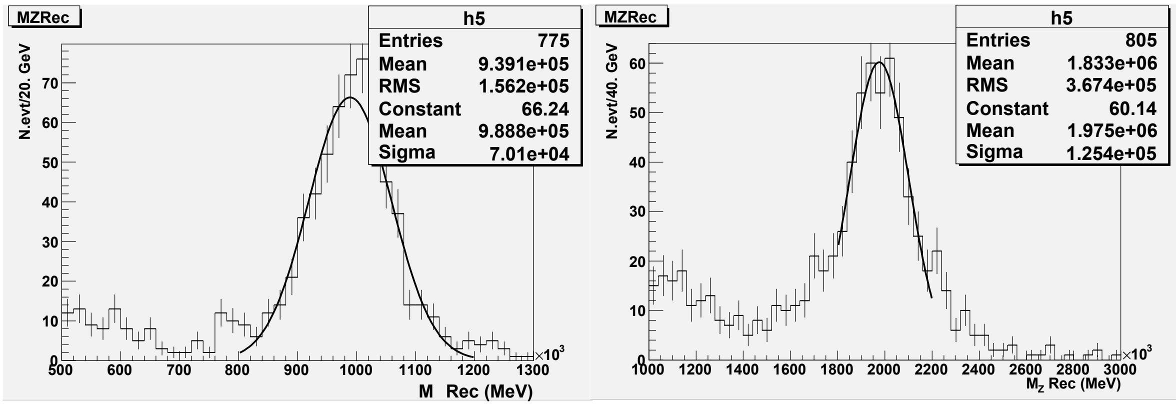

Figure 9: *Distribution of dimuon invariant mass for* $pp \to \mu^+\mu^-$ *events as expected by Drell-Yan,Z and* Z' *contributions for: (left) a* Z' *mass of 1 TeV and (right) of 2 TeV. The reconstruction is based on the Staco algorithm.*

In the analysis of the discovery potential for the MSSM neutral Higgs bosons, the unexplored region of large tanβ (15÷50) and mass between 95 and 135 GeV has been considered [3]. The h/A bosons are very close in mass in this kinematic region and are searched for in the decay channel h/A $\to \mu^+\mu^-$ with two accompaining b-jets. The most copious background is $Z \to \mu^+\mu^-$ with two b-jets which covers most of the mass region and has to be carefully estimated and subtracted. A method to control from an independent sample the quantity of this irreducible background has been developed [4].

We have also studied the feasibility of a search for the Lepton Flavour Violation (LFV) process $\tau \to 3\mu$ [7]. Many models predict the existence of such a process with BR below 10^{-7}. The only production mechanism we have simulated so far is the one of the MSSM model which expects this decay to proceed through the decay chain $\tau \to \mu\ h/A$ and the following decay of the supersimmetric higgs to $\mu^+\mu^-$. At the moment the best limit on this decay is set by the B-factories (BR$< 2 \times 10^{-7}$ at 90 % C.L.). In ATLAS, a large production cross section of clean $\tau's$ is granted from the $W \to \tau\nu$ decay. In 10 fb^{-1} we expect to produce $\sim 200 \times 10^6\tau$'s from this chain. The final state is characterized by three "isolated" muons contained in a narrow cone in the η-ϕ space and a missing transverse energy above 20 GeV. The low P_T spectra of the produced particles pushes to use the tracking in the inner detector in conjunction with segments reconstructed in the muon spectrometer. The muon spectrometer is essential for triggering purposes. The background is constituited by c-cbar and b-bbar events with a sequential decay chain in one arm such as, for istance, $D_S \to \phi\mu\nu$ and then $\phi \to \mu^+\mu^-$. The isolation and the missing E_T cut are the most important ingredients in the background rejection. A large production campaign to simulate the background has been carried out on the GRID. At the end of the analysis the invariant mass of the three selected muon, $M(3\mu)$, is reconstructed and used for the final event counting. In Fig. 8, the $M(3\mu)$ distribution is shown for signal and background. Preliminary results with the whole reconstructed events indicated that, already with the first 10 fb^{-1} produced, the limits on this decay could be lowered down to 8.7×10^{-8} at 90 % C.L.

Many theories beyond the SM predict the existence of a new heavy gauge bosons (GUT theories, Little Higgs, Technicolor, Susy ..) from the presence of a larger symmetry group. The discovery potential for a Z' in ATLAS has been investigated with the study of the channel $pp \to$

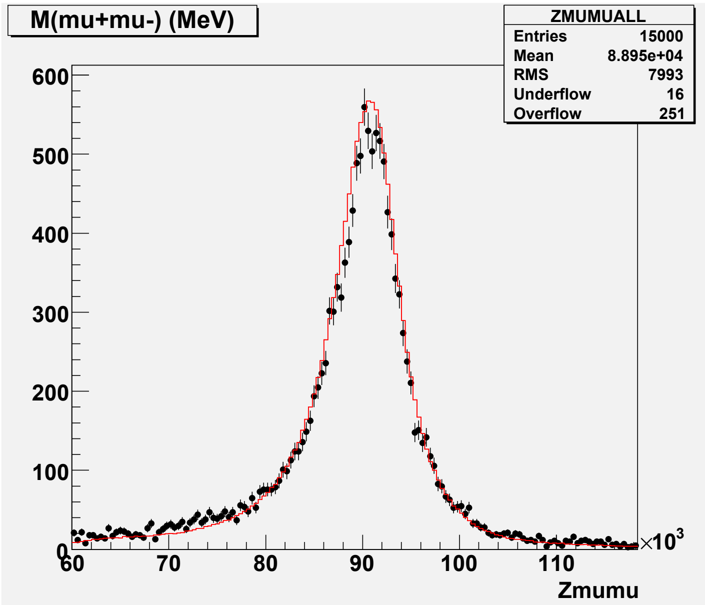

Figure 10: *Invariant dimuon mass for the calibration sample of 15000 $Z \to \mu^+\mu^-$ selected events: (black points) offline reconstructed mass, (solid line) mass reconstructed by folding the generated particle spectra with MC resolution.*

$\gamma/Z/Z' \to \mu^+\mu^-$ for a Z' mass of 1 and 2 TeV. The Z'-mediated process is simulated with Pythia according to the so-called SSM (Sequential Standard Model) in which the Z' couplings are assumed to be the same as the SM Z couplings. All interferences between the different production mechanisms have been taken into account. Data used in the analysis have been obtained from the official CSC production. Preliminary results have been based on a statistics of 1000 generated events for a Z' mass of 1 (2) TeV, corresponding to an integrated luminosity of 2 (10) fb^{-1}. In both cases, see Fig. 9, a clean mass peak emerges above a practically flat background due to the underlying Drell-Yan/Z production.

9.2 Calibration and early physics

In addition to the analysis of the above mentioned channels, we have also started the study of the $W \to \mu\nu$, $Z \to \mu\mu$ and $J/\psi \to \mu\mu$ processes with the double purpose of:

1. investigating the above physics processes since the starting LHC phase;
2. using them for calibrating the detector in general and the muon detector in particular.

In this respect, we have analized 120000 $Z \to \mu^+\mu^-$ events from the CSC initial production, to study the momentum resolution in the spectrometer and develop a method to determine from data the absolute momentum scale.

At the moment, we have used the distributions of momentum resolution from Monte Carlo in different η and ϕ bins to fold the generated momentum spectra from the Z decay to estimate the reconstructed invariant mass of the dimuons, $M_{2\mu}^{MCfold}$. In this way, it is possible to let the absolute momentum scale as a free parameter α and fit the invariant mass reconstructed with the tracking algorithm, $M_{2\mu}^{rec}$. In Fig. 10, the distribution of $M_{2\mu}^{rec}$ is shown by the black points with the best fit overimposed for the first 15000 events in the sample. This statistics should roughly be equivalent to 10 pb^{-1} of pp collisions. By using only two free momentum scale in the fit, one for the barrel and one for the endcap regions of the muon spectrometer, we determine the scale to be 1 with a few per mill error.

Moreover, the same sample has been used to determine the muon reconstruction efficiency from data with the so-called prob and tag method. By starting from a full reconstructed muon at high momenta, we add another track for the inner detector (ID), after looping over all possible tracks, to reconstruct the invariant mass and best matching the Z mass. The found ID track is called prob track and used to look for a muon in the spectrometer. This allows to estimate with data the reconstruction efficiency and compare with the MC estimates, a good agreement between these two numbers is found. We are now estending this study at the low P_T regions of the tracking by using a sample of $J/Psi \rightarrow \mu^+\mu^-$.

10 List of Conference Talks by LNF Authors in Year 2006

1. *ATLAS High Level trigger Infrastructure, RoI Collection and Event Building*, by K. Kordas, talk at CHEP2006: Computing in High Energy and Nuclear Physics, Mumbai, India, 13-17 February 2006;
2. *ATLAS Trigger and Data Acquisition system: architecture & status*, by K. Kordas, talk at HEP2006: Recent Developments in High Energy Physics and Cosmology, Ioannina, Greece, 13-16 April 2006.
3. *ATLAS Trigger and Data Acquisition system: concept & architecture*, by K. Kordas, talk at XI Frascati Spring School Bruno Touschek, LNF, Frascati, Italy, 15-19 May 2006;
4. *ATLAS Trigger and Data Acquisition system: concept, design & status*, by K. Kordas, invited talk at the 10^{th} Topical Seminar on Innovative Particle & Radiation Detectors (IPRD06), Siena, Italy, 1-5 October 2006.

References

1. **Testing on a large scale: Running the ATLAS data acquisition and high level trigger software on 700 PC nodes**, by XXX et al, ATL-DAQ-2006-002, Proceedings In International Conference on Computing in High Energy and Nuclear Physics (CHEP2006), Mumbai, India, 13-17 Feb 2006.
2. **Search for the Standard Model $H \rightarrow ZZ^* \rightarrow 4\mu$ with multivariate techniques and GEANT3 based detector simulation**, by E. Meoni, F. Cerutti, L. LaRotonda, ATL-PHYS-INT-2006-005.
3. **Search for MSSM neutral Higgs bosons decaying to a muon pair in the mass range up to 130 GeV.**, by S. Gentile, H. Bilokon, V. Chiarella and G. Nicoletti ,ATL-PHYS-COM-2006-080.
4. **Data based method for $Z \rightarrow \mu^+\mu^-$ background subtraction in ATLAS detector at LHC**, by S. Gentile, H. Bilokon, V. Chiarella and G. Nicoletti ,ATL-PHYS-PUB-2006-019.

5. **First cosmics data taking in sector 13 with the MDT precision chambers of the muon spectrometer**, by M. Antonelli et al., ATL-COM-MUON-2006-018.

6. **ATLAS Muon Barrel sagitta resolution versus momentum at the H8 test beam and comparison with GEANT4 simulation**, by G. Avolo et al., ATL-MUON-PUB-2006-011.

7. **A Monte Carlo study of the LFV decay $\tau \to 3\mu$ with the ATLAS detector**, by S. Ventura. Tesi di Dottorato per il XIX ciclo di Dottorato in Fisica della Università degli Studi di Roma Tor Vergata.

BaBar

F. Anulli, R. Baldini Ferroli, A. Calcaterra, L. Daniello (Tecn.), R. de Sangro,
G. Finocchiaro, S. Pacetti, P. Patteri, I. Peruzzi (Resp.), M. Piccolo, M. Rama, A. Zallo

1 Introduction

BaBar is the experiment running at the SLAC asymmetric B-factory PEP-II; the physics program is centered on, but not limited to, the study of the *CP* violation in the decay of neutral B mesons. The B system is the best suited to study *CP* violation because the expected effects are large, appear in many final states and, most importantly, can often be directly related to the Standard Model parameters. The large data sample being collected has already allowed significant advances in a large number of topics in B, charm and tau lepton physics; all three angles of the Unitarity Triangle have been measured, direct *CP* violation has been observed in B decays, several new B decay modes have been measured, and new charmed states have been discovered.

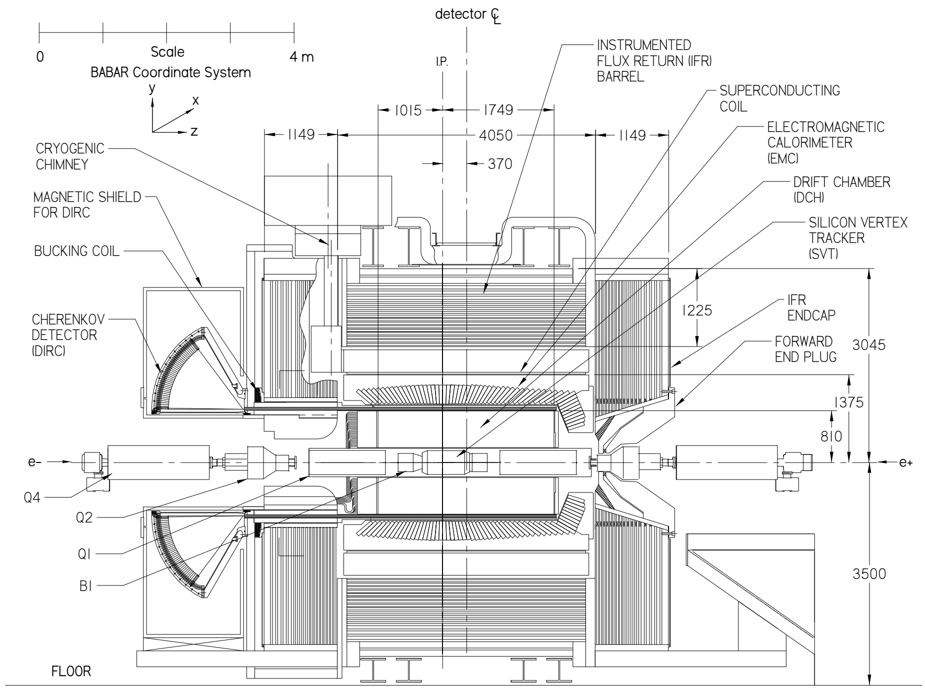

Figure 1: Elevation view of the *BaBar* Detector.

The PEP-II B factory is an asymmetric e^+e^- collider designed to operate at a center-of-mass energy of 10.58 GeV corresponding to the mass of the $\Upsilon(4S)$ resonance, which decays 50% in B^+B^- and 50% in $B^0\ \overline{B}^0$. In PEP-II the electron beam of 9.0 GeV collides head-on with the positron beam of 3.1 GeV resulting in a Lorentz boost ($\beta\gamma = 0.56$) to the $\Upsilon(4S)$ resonance, making possible the measurement of the time-dependent CP violation of the neutral B's.

The *BaBar* Collaboration includes about 540 physicists, with contributions from about 80 Institutions in 10 countries in North America, Europe, and Asia. Approximately half of the group are physicists from U.S. Universities and Laboratories, with the largest foreign contribution coming from Italy, with 12 INFN Institutions and more than 90 people.

The *BABAR* detector (fig. 1) has been designed primarily for *CP* violation studies, but it is also serving well for the other physics objectives of the experiment. The asymmetry of the beam energies is reflected in the detector design: the apparatus is centered 37 cm ahead of the collision point, along the direction of the high-energy beam, to increase forward acceptance. All services are placed on the opposite side of the detector, in order to minimize multiple scattering in the forward direction.

The momentum of the charged tracks is obtained from the curvature in a solenoidal field of 1.5 T and is measured in a low mass Drift Chamber. Different species of hadrons are identified in the DIRC, a dedicated device of a novel kind, based on the detection of Čerenkov light. Excellent photon detection and electron identification is provided by a CsI crystals electromagnetic calorimeter.

Muons and neutral hadrons are identified in the iron magnet's yoke, where a total thickness of 65 cm of Fe plates has been segmented in 18 slabs of graded thickness (from 2 to 10 cm) and instrumented with Resistive Plate Counters and Limited Streamer Tubes. This system, made of a 6-sided barrel, 2 endcaps and a double cylindrical layer inside the magnet coil, is called Instrumented Flux Return, or IFR. In 2004 two barrel sextants were upgraded with addition of copper plates in six of the gaps, to increase the amount of absorber, and instrumented with LST (Limited Streamer Tubes). In 2006, the remaining 4 barrel sextants were similarly upgradated.

The final ingredient in the *CP* asymmetry measurements, the distance between the two decay vertices, is measured by a state of the art vertex detector, with five layers of double sided silicon sensors. It also provides standalone tracking for particles with low transverse momentum that cannot be measured reliably in the Drift Chamber alone.

2 Activity

Data taking in 2006 continued with consistent high luminosity and excellent detector efficiency, until August 20, when the machine was shut down for maintenance and upgrade work. The superb machine performance allowed a delivery of approximately $80fb^{-1}$ in 2006, bringing the total data sample recorded by *BABAR* to $390fb^{-1}$. Their integrated luminosity as function of time is reported in fig. 2. *BABAR* made use of the down time for completing the barrel muon detector upgrade, following the work in Summer 2004 when two sextants had been completed. The remaining four sextants were disassembled, with all the detectors uncabled and disconnected from gas lines, power supplies, and the readout electronics. Copper slabs were added to the iron, filling some of the gaps, in order to increase the absorber thickness and improving pion rejection. The active detectors in the remaining gaps, RPC's whose efficiency had decreased in time, were replaced by Limited Streamer Tubes (LSTs). This major mechanical work was succesfully completed on time also thanks to the work of three Frascati technicians, who gave an important contribution. By November 15 the new detectors were all in place and re-cabling could start; by the end of the year the new system was commissioned and the first cosmic rays were recorded.

Data analysis activity by *BABAR* in 2006 continued regularly, covering a very wide spectrum of measurements, like the angles of the Unitarity Triangle β, α, γ, branching ratios and CP-violation of rare B decays, $|V_{ub}|$, $|V_{cb}|$, the extensive study of charm and τ decays (*BABAR* is also a charm and τ factory), and the most extensive systematic study up to now of low-energy meson spectroscopy in the energy range between 1 and 4 GeV, possible at *BABAR* using the technique of Initial State Radiation (ISR). In 2006 *BABAR* was a major contributor at all HEP Conferences. A total of 67 journal papers were published in the same year. In the next sections the items of analysis in which the Frascati group is more directly involved are shortly described.

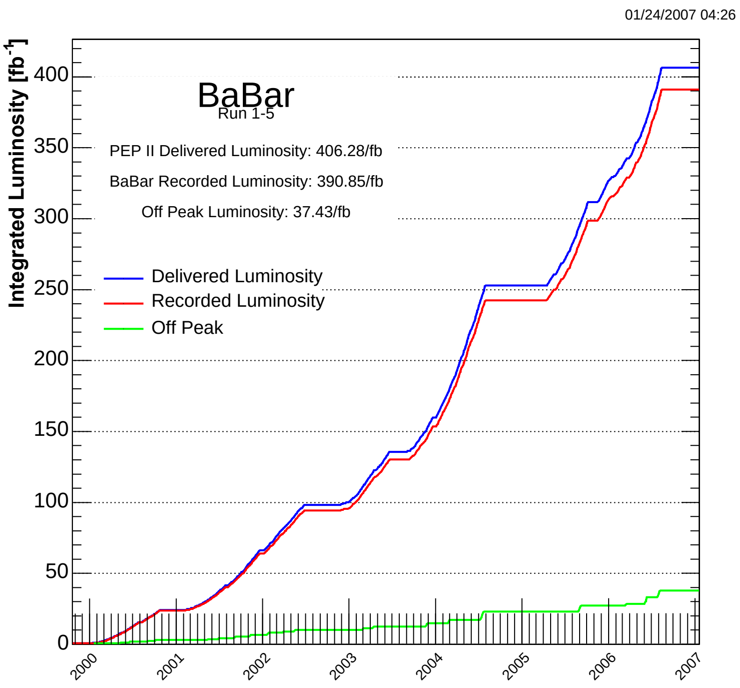

Figure 2: *BABAR* integrated luminosity from the start of the data taking in 1999 till the end of 2006.

3 Improved measurement of CP violation in neutral B decays to $(c\overline{c})K^{(*)0}$

In the Standard Model of particle physics CP violation is described as a consequence of a complex phase in the three-generation Cabibbo-Kobayashi-Maskawa (CKM) quark-mixing matrix. In this context, measurements of CP asymmetries in the proper-time distribution of neutral B decays to CP eigenstates containing a charmonium and K^0 meson provide a direct measurement of $\sin 2\beta$. The angle β is defined in terms of the CKM matrix elements V_{ij} as $\arg[-(V_{cd}V_{cb}^*)/(V_{td}V_{tb}^*)]$. At the $\Upsilon(4S)$ resonance, the CP asymmetry $\mathcal{A}_{CP} \equiv S_f \sin(\Delta m_d \Delta t) - C_f \cos(\Delta m_d \Delta t)$ is extracted from the distribution of the difference of the proper decay times Δt between the reconstructed B meson and the other B meson in the event (B_{tag}). The decay products of B_{tag} are used to identify its flavor (B^0 or $\overline{B}^0$) at its decay time. Here Δm_d is the mass difference determined from B^0-$\overline{B}^0$ oscillations.

Members of our group have contributed to the update of this flagship B-factory measurement with the new data. Since our previously published result [1] we have added about 157×10^6 decays and applied an improved event reconstruction to the complete dataset of $(384{\pm}4){\times}10^6 \Upsilon(4S) \to B\overline{B}$ decays. We have also developed a new $\eta_c K^0_S$ event selection based on the Dalitz structure of the $\eta_c \to K^0_S K^+ \pi^-$ decay and we have performed a more detailed study of the CP properties of our background events, resulting in a reduced systematic error. The preliminary measurements presented at the 2006 Summer Conferences [68] are $\sin 2\beta = 0.710 \pm 0.034\,(\mathrm{stat}) \pm 0.019\,(\mathrm{syst})$ and $|\lambda| = 0.932 \pm 0.026\,(\mathrm{stat}) \pm 0.017\,(\mathrm{syst})$.

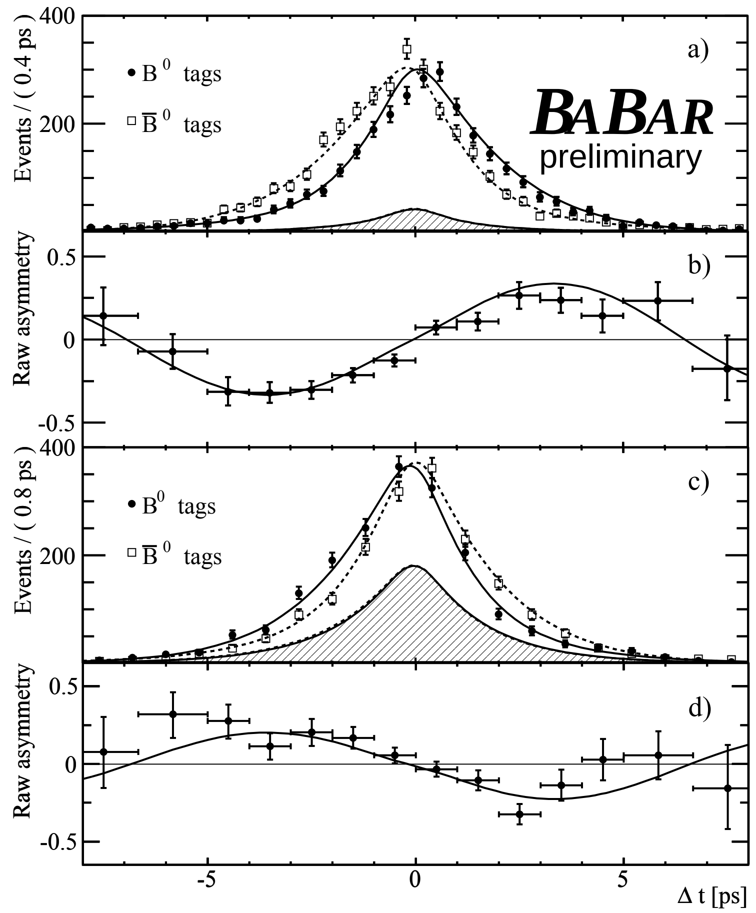

Figure 3: a) Number of $\eta_f = -1$ candidates ($J/\psi K^0_S$, $\psi(2S)K^0_S$, $\chi_{c1}K^0_S$, and $\eta_c K^0_S$) in the signal region with a B^0 tag (N_{B^0}) and with a $\overline{B}^0$ tag ($N_{\overline{B}^0}$), and b) the raw asymmetry $(N_{B^0} - N_{\overline{B}^0})/(N_{B^0} + N_{\overline{B}^0})$, as functions of Δt. Figures c) and d) are the corresponding distributions for the $\eta_f = +1$ mode $J/\psi K^0_L$. . The solid (dashed) curves represent the fit projections in Δt for B^0 ($\overline{B}^0$) tags. The shaded regions represent the estimated background contributions.

4 Measurement of *CP* violation in partially reconstructed $B^0 \to D^{*+}D^{*-}$ decays

In 2006 this analysis has been updated with inclusion of the full data set collected until August 2006, corresponding to BaBar data taking runs 1 trough 5.

The parameter sin2β is obtained measuring the time-dependent decay-rate asymmetry between B^0 and $\overline{B}^0$. This requires the reconstruction of the $B \to D^{*+}D^{*-}$ decay (*CP*-side of the event), the tagging of the B^0 or $\overline{B}^0$ flavor, looking at the other side of the event (tag-side), and the measurement of the *CP*- and tag-side decay vertices to measure the time difference Δt.

The $B \to D^{*+}D^{*-}$ decay is partially reconstructed combining a fully reconstructed $D^{*\pm}$ with a soft pion of opposite electric charge, assuming that the latter comes from the decay of the second $D^{*\mp} \to D^0\pi^{\mp}$. A candidate is selected if the kinematics is compatible with the full B decay chain, with a missing D^0.

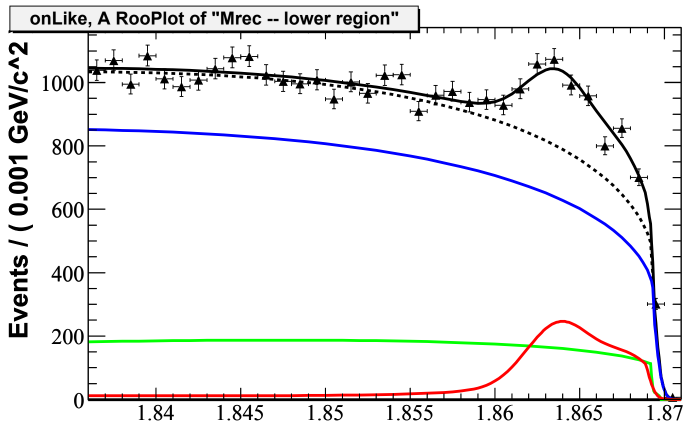

Figure 4: Missing mass for $B \to D^{*\pm}\ \pi^{\mp}\ (X)$. The curves represent the probability distribution functions (p.d.f.) for signal (red), continuum background (green), $B\overline{B}$ background (blue) and their sum (black).

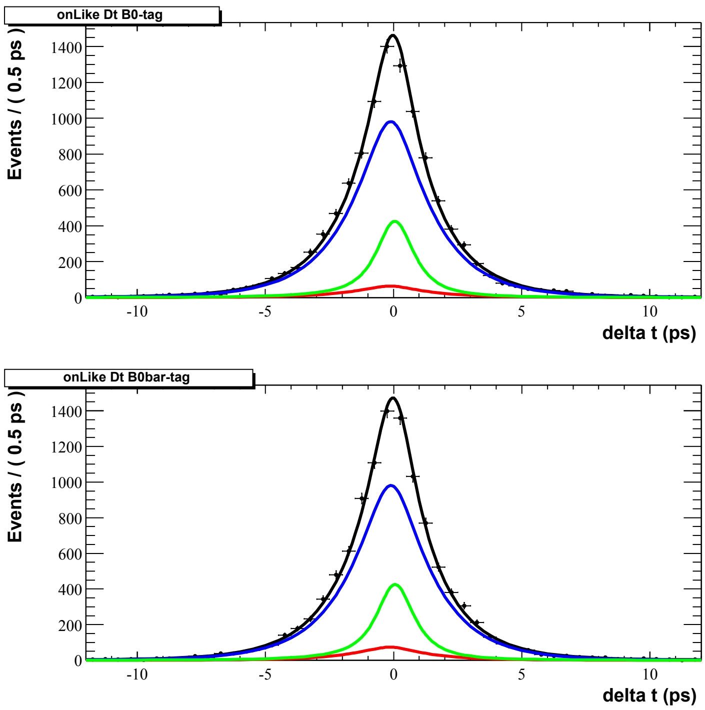

Figure 5: Δt fit to RUN 1-5 data. The curves represent the p.d.f.'s for signal (red), continuum background (green), $B\overline{B}$ background (blue) and their sum (black).

In fig. 4 we show the recoil mass distribution of collision data from RUN 1 through 5, corresponding to $\approx 350\ fb^{-1}$ of integrated luminosity. The presence of an excess of events in the signal region is evident, and a fit to the data with a PDF (black curve), made of a signal component (red) plus a continuum (green) and a $B\overline{B}$ (blue) background component, has shown that the statistical power of this measurement is comparable to that of the analysis made with the fully reconstructed sample. The two measurements of $\sin 2\beta$ can be regarded as almost independent of each other.

We also fit the time distribution in the data, and in fig. 5 we show a fit to the time difference distribution of data events including signal and background, for the full RUN 1-5 statistics.

5 Measurement of the angle γ with $B^{\pm} \to D^{(*)0}K^{(*)\pm}$ decays

The measurement of the angle γ of the Unitarity Triangle (defined as the phase of V_{ub}^{*} in the Wolfenstein parametrization of V_{CKM}) was considered hardly feasible at the B-factories till a few years ago. Instead, both *BABAR* and Belle have measured γ through the decays $B^- \to D[\to f]K^-$ (and the CP-conjugated process), where f is a state accessible from both D^0 and $\bar{D}^0$. The rate of the process is the result of the interference of the amplitudes $A(B^- \to D^0K^-)$ and $A(B^- \to \bar{D}^0K^-)$, the latter depending on V_{ub} and therefore on γ. The analysis has been performed in two steps. First, the Dalitz plot of a high-purity and high-statistics sample of flavour-tagged $D^0 \to K^0_S\pi^-\pi^+$ was fit to determine the Dalitz model. Second, we have selected $B^{\pm} \to D^{(*)}K^{\pm}$ decays with $D \to K^0_S\pi^-\pi^+$, whose Dalitz plot differs from the one found in step 1 depending on the value of γ due to the aforementioned interference. The angle γ was therefore extracted through a fit to the Dalitz plot distribution of $D \to K^0_S\pi^-\pi^+$ of the $B^{\pm} \to DK^{\pm}$ decays. On a data sample of 347×10^6 $B\bar{B}$ we have selected both $B \to DK$ and $B \to D^*K$ events [67] and we have measured $\gamma = (92 \pm 41(stat) \pm 10(syst) \pm 13(model))^o$, where the third uncertainty comes from the model assumption for the Dalitz plot of the flavour-tagged D^0's (Fig. 6). This result was presented at ICHEP 2006 and is documented in a conference paper. We're currently working on the finalization of the analysis that will be published in 2007 and will include also the $B^- \to D^0K^{*-}$ decays.

6 Light hadron spectroscopy with initial state radiation events

Initial state radiation (ISR) events can be effectively used to measure e^+e^- annihilation at a high luminosity storage ring, such as the B-factory PEP-II. A wide mass range is accessible in a single experiment, contrary to the case of fixed energy colliders, which are optimized only in a limited energy region. In addition, the broad-band coverage may result also in greater control of systematic effects because only one experimental setup is involved.

Measurements of the main hadronic final states in the energy range between 1 and 6 GeV have been carried out at *BABAR*. We have been directly involved in the measurement of the cross section of the processes $e^+e^- \to 3(\pi^+\pi^-)$, $\pi^0\pi^0 2(\pi^+\pi^-)$ and $K^+K^-2(\pi^+\pi^-)$, in collaboration with the Novosibirsk group. This analysis has been completed and published last year [52].

Our group is also involved, in collaboration with a group of the University of Cincinnati, in the study of the $KK\pi$ and $KK\eta$ final states in the energy region from threshold up to ~ 5 GeV. The cross section for the reactions $e^+e^- \to K^{*\pm}K^{\mp}$, $K^{*0}K^0_S$, $KK\pi(nonresonant)$, $\phi\eta$ and $\phi\pi^0$ are measured.

Clear peaks around 1.65 GeV in the $K^{*\pm}K^{\mp}$, $K^{*0}K^0_S$ and $\phi\eta$ channels are seen. These can be referred to decays of the resonance $\phi(1680)$, observed by the DM2 Collaboration in the K^*K channels, while the decay $\phi(1680) \to \phi\eta$ has never been observed before. The very large statistics available at *BABAR* allows to disentangle the different isospin components contributing to these final states. A Dalitz plot analysis on these data is in progress. This analysis is in the reviwing

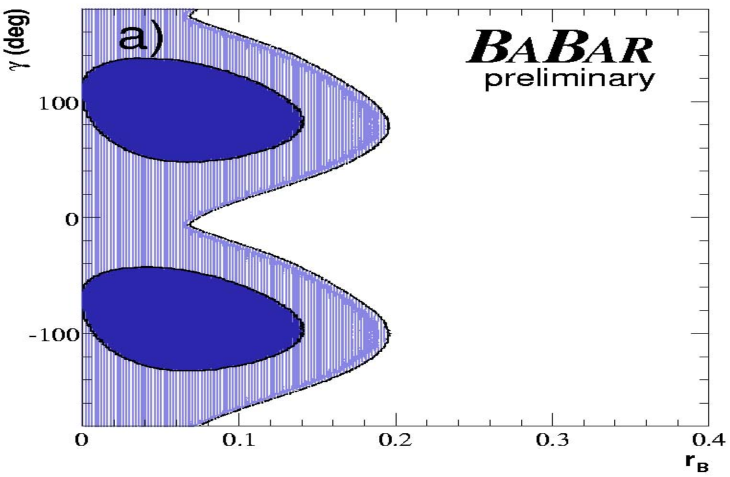

,

Figure 6: Projection in the $r_B - \gamma$ plane of the five-dimensional one- (dark) and two- (light) standard deviation regions. r_B is the ratio $|A(B^- \to \bar{D}^0 K^-)/A(B^- \to D^0 K^-)|$, unknown a priori and extracted from data together with γ. See [67] for details.

process and close to be finalized. We expect a journal paper summarizing all the results be ready by summer 2007.

7 Talks at conferences in 2006

- G. Finocchiaro, "Measurements of the angles α and β at the B-factories", presented at the *XX Rencontres de Physique de la Vallée d'Aoste*, La Thuile, Italy, 5-11 March 2006.
- P. Patteri, "Probing strong interactions at *BABAR*", presented at the *XL Rencontres de Moriond – QCD and High Energy Hadronic Interactions*, La Thuile, Italy, 18-25 March 2006.
- A. Zallo, "New *BABAR* results on electromagnetic form factors", presented at the 4^{th} *International Conference on Quarks and Nuclear Physics (QNP06)*, Madrid, Spain 5-10 June 2006.
- R. Baldini-Ferroli, "Extraction of form factors in ISR processes at the B-factories", presented at the *International Workshop on Tau-Charm Physics*, Beijing, China, 5-7 June 2006.
- F. Anulli, "Measurements of the proton form factor in the time-like region", presented at the 2^{nd} *Meeting of the APS Topical Group on Hadronic Physics*, Nashville, USA, 22-24 October 2006.

8 *BABAR* publications in 2006

References

1. *BABAR* Collab., B. Aubert *et al.*, Phys. Rev. Lett. **94**, 161803 (2005).

2. B. Aubert *et al.* [BABAR Collaboration], “Observation of the exclusive reaction e+ e- → Phi eta at s**(1/2) = 10.58-GeV,” Phys. Rev. D **74** (2006) 111103

3. B. Aubert *et al.* [BABAR Collaboration], “A structure at 2175-MeV in e+ e- → Phi f0(980) observed via initial-state radiation,” Phys. Rev. D **74** (2006) 091103

4. B. Aubert *et al.* [BABAR Collaboration], “Measurement of the absolute branching fractions B → D pi, D* pi, D** pi with a missing mass method,” Phys. Rev. D **74** (2006) 111102

5. B. Aubert *et al.* [BABAR Collaboration], “Observation of B+ → Phi Phi K+ and evidence for B0 → Phi Phi K0 below eta/c threshold,” Phys. Rev. Lett. **97** (2006) 261803

6. B. Aubert *et al.* [BABAR Collaboration], “Observation of an excited charm baryon Omega/c* decaying to Omega/c0 gamma,” Phys. Rev. Lett. **97** (2006) 232001

7. B. Aubert *et al.* [BABAR Collaboration], “Observation of B+ → anti-K0 K+ and B0 → K0 anti-K0,” Phys. Rev. Lett. **97** (2006) 171805

8. B. Aubert *et al.* [BABAR Collaboration], “Measurement of the branching fraction and time-dependent CP asymmetry in the decay B0 → D*+ D*- K0(S),” Phys. Rev. D **74** (2006) 091101

9. B. Aubert *et al.* [BABAR Collaboration], “Precise branching ratio measurements of the decays D0 → pi- pi+ pi0 and D0 → K- K+ pi0,” Phys. Rev. D **74** (2006) 091102

10. B. Aubert *et al.* [BABAR Collaboration], “Search for D0 anti-D0 mixing and branching-ratio measurement in the decay D0 → K+ pi- pi0,” Phys. Rev. Lett. **97** (2006) 221803

11. B. Aubert *et al.* [BABAR Collaboration], “Measurement of branching fractions and charge asymmetries in B decays to an eta meson and a K* meson,” Phys. Rev. Lett. **97** (2006) 201802

12. B. Aubert *et al.* [BABAR Collaboration], “Branching fraction measurements of charged B decays to K*+ K+ K-, K*+ pi+ K-, K*+ K+ pi- and K*+ pi+ pi- final states,” Phys. Rev. D **74** (2006) 051104

13. B. Aubert *et al.* [BABAR Collaboration], “Measurement of the ratio B(B+ → X e nu)/B(B0 → X e nu),” Phys. Rev. D **74** (2006) 091105

14. B. Aubert *et al.* [BABAR Collaboration], “Measurements of branching fraction, polarization, and charge asymmetry of B+- → rho+- rho0 and a search for B+- → rho+- f0(980),” Phys. Rev. Lett. **97** (2006) 261801

15. B. Aubert *et al.* [BABAR Collaboration], “Measurement of the B → pi l nu branching fraction and determination of —V(ub)— with tagged B mesons,” Phys. Rev. Lett. **97** (2006) 211801

16. B. Aubert [BABAR Collaboration], “Observation of a new D/s meson decaying to D K at a mass of 2.86-GeV/c**2,” Phys. Rev. Lett. **97** (2006) 222001

17. B. Aubert *et al.* [BaBar Collaboration], “Measurement of the branching fraction and photon energy moments of B → X/s gamma and A(CP)(B → X(s+d) gamma),” Phys. Rev. Lett. **97** (2006) 171803

18. B. Aubert *et al.* [BaBar Collaboration], “Searches for B0 decays to eta K0, eta eta, eta’ eta’, eta Phi, and eta’ Phi,” Phys. Rev. D **74** (2006) 051106

19. B. Aubert *et al.* [BABAR Collaboration], “Measurements of branching fractions, polarizations, and direct CP-violation asymmetries in B → rho K* and B → f0(980) K* decays,” Phys. Rev. Lett. **97** (2006) 201801

20. B. Aubert *et al.* [BABAR Collaboration], “Search for B+ → X(3872) K+, X(3872) → J/psi gamma,” Phys. Rev. D **74** (2006) 071101

21. B. Aubert *et al.* [BABAR Collaboration], “Measurements of the decays B0 → anti-D0 p anti-p, B0 → anti-D*0 p anti-p, B0 → D- p anti-p pi+, and B0 → D*- p anti-p pi+,” Phys. Rev. D **74** (2006) 051101

22. B. Aubert *et al.* [BABAR Collaboration], “Observation of e+ e- annihilations into the C = +1 hadronic final states rho0 rho0 and Phi rho0,” Phys. Rev. Lett. **97** (2006) 112002

23. B. Aubert *et al.* [BABAR Collaboration], “Search for the decay of a B0 or anti-B0 meson to anti-K*0 K0 or K*0 anti-K0,” Phys. Rev. D **74** (2006) 072008

24. B. Aubert *et al.* [BABAR Collaboration], “Measurement of the spin of the Omega- hyperon at BABAR,” Phys. Rev. Lett. **97** (2006) 112001

25. B. Aubert *et al.* [BABAR Collaboration], “Search for the decay B0 → K0(S) K0(S) K0(L),” Phys. Rev. D **74** (2006) 032005

26. B. Aubert *et al.* [BABAR Collaboration], “Search for doubly charmed baryons Xi/cc+ and Xi/cc++ in BABAR,” Phys. Rev. D **74** (2006) 011103

27. B. Aubert *et al.* [BABAR Collaboration], “Measurement of the D+ → pi+ pi0 and D+ → K+ pi0 branching fractions,” Phys. Rev. D **74** (2006) 011107

28. B. Aubert *et al.* [BABAR Collaboration], “Search for B+ → Phi pi+ and B0 → Phi pi0 decays,” Phys. Rev. D **74** (2006) 011102

29. B. Aubert *et al.* [BABAR Collaboration], “Study of B → D(*) D/s(J)(*) decays and measurement of D/s- and D/sJ(2460)- branching fractions,” Phys. Rev. D **74** (2006) 031103

30. B. Aubert *et al.* [BaBar Collaboration], “Search for the decay B0 → a1+- rho-+,” Phys. Rev. D **74** (2006) 031104

31. B. Aubert *et al.* [BABAR Collaboration], “Measurement of the eta and eta’ transition form factors at q**2 = 112-GeV**2,” Phys. Rev. D **74** (2006) 012002

32. B. Aubert *et al.* [BABAR Collaboration], “B meson decays to omega K*, omega rho, omega omega, omega Phi, and omega f0,” Phys. Rev. D **74** (2006) 051102

33. B. Aubert *et al.* [BaBar Collaboration], “Search for B meson decays to eta’ eta’ K,” Phys. Rev. D **74** (2006) 031105

34. B. Aubert *et al.* [BABAR Collaboration], “Dalitz plot analysis of the decay B+- → K+- K+- K-+,” Phys. Rev. D **74** (2006) 032003

35. B. Aubert *et al.* [BABAR Collaboration], “Measurement of branching fractions and CP-violating charge asymmetries for B meson decays to D(*) anti-D(*), and implications for the CKM angle gamma,” Phys. Rev. D **73** (2006) 112004

36. B. Aubert *et al.* [BABAR Collaboration], “Observation of Upsilon(4S) decays to pi+ pi- Upsilon(1S) and pi+ pi- Upsilon(2S),” Phys. Rev. Lett. **96** (2006) 232001

37. B. Aubert *et al.* [BABAR Collaboration], "A study of the D/sJ*(2317)+ and D/sJ(2460)+ mesons in inclusive c anti-c production near s**(1/2) = 10.6-GeV," Phys. Rev. D **74** (2006) 032007

38. B. Aubert *et al.* [BaBar Collaboration], "Measurement of the B- → D0 K*- branching fraction," Phys. Rev. D **73** (2006) 111104

39. B. Aubert *et al.* [BABAR Collaboration], "Measurement of anti-B0 → D(*)0 anti-K(*)0 branching fractions," Phys. Rev. D **74** (2006) 031101

40. B. Aubert *et al.* [BABAR Collaboration], "Search for the decay tau- → 3pi- 2pi+ 2pi0 nu/tau," Phys. Rev. D **73** (2006) 112003

41. B. Aubert *et al.* [BABAR Collaboration], "Study of the decay anti-B0 → D*+ omega pi-," Phys. Rev. D **74** (2006) 012001

42. B. Aubert *et al.* [BABAR Collaboration], "Measurements of branching fractions, rate asymmetries, and angular distributions in the rare decays B → K l+ l- and B → K* l+ l-," Phys. Rev. D **73** (2006) 092001

43. B. Aubert *et al.* [BABAR Collaboration], "Search for the charmed pentaquark candidate Theta/c(3100)0 in e+ e- annihilations at s**(1/2) = 10.58-GeV," Phys. Rev. D **73** (2006) 091101

44. B. Aubert *et al.* [BABAR Collaboration], "Measurement of branching fractions in radiative B decays to eta K gamma and search for B decays to eta' K gamma," Phys. Rev. D **74** (2006) 031102

45. B. Aubert *et al.* [BABAR Collaboration], "Search for T, CP and CPT violation in B0 anti-B0 mixing with inclusive dilepton events," Phys. Rev. Lett. **96** (2006) 251802

46. B. Aubert *et al.* [BABAR Collaboration], "Observation of B0 meson decay to a1(1260)+- pi-+," Phys. Rev. Lett. **97** (2006) 051802

47. B. Aubert *et al.* [BABAR Collaboration], "Measurements of CP-violating asymmetries and branching fractions in B decays to omega K and omega pi," Phys. Rev. D **74** (2006) 011106

48. B. Aubert *et al.* [BABAR Collaboration], "Branching fraction limits for B0 decays to eta' eta, eta' pi0 and eta pi0," Phys. Rev. D **73** (2006) 071102

49. B. Aubert *et al.* [BaBar Collaboration], "Measurements of the branching fraction and time-dependent CP asymmetries of B0 → J/psi pi0 decays," Phys. Rev. D **74** (2006) 011101

50. B. Aubert *et al.* [BABAR Collaboration], "Measurement of time-dependent CP asymmetries in B0 → D(*)+- pi-+ and B0 → D+- rho-+ decays," Phys. Rev. D **73** (2006) 111101

51. B. Aubert *et al.* [BABAR Collaboration], "Measurements of the B → D* form factors using the decay anti-B0 → D*+ e- anti-nu/e," Phys. Rev. D **74** (2006) 092004

52. B. Aubert *et al.* [BABAR Collaboration], "The $e^+e^- \rightarrow 3(\pi^+\pi^-), 2(\pi^+\pi^-\pi^0)$ and $K^+K^-2(\pi^+\pi^-)$ cross sections at center-of-mass energies from production threshold to 4.5-GeV measured with initial-state radiation," Phys. Rev. D **73** (2006) 052003

53. B. Aubert *et al.* [BABAR Collaboration], "Determinations of —V(ub)— from inclusive semileptonic B decays with reduced model dependence," Phys. Rev. Lett. **96** (2006) 221801

54. B. Aubert *et al.* [BABAR Collaboration], "Measurements of the branching fractions and CP-asymmetries of B- → D0(CP) K- decays," Phys. Rev. D **73** (2006) 051105

55. B. Aubert *et al.* [BABAR Collaboration], "Search for the rare decays B0 → D/s(*)+ a0(2)-," Phys. Rev. D **73** (2006) 071103

56. B. Aubert *et al.* [BABAR Collaboration], "Search for rare quark-annihilation decays, B- → D/s(*)- Phi," Phys. Rev. D **73** (2006) 011103

57. B. Aubert *et al.* [BABAR Collaboration], "A study of e+ e- → p anti-p using initial state radiation with BABAR," Phys. Rev. D **73** (2006) 012005

58. B. Aubert *et al.* [BABAR Collaboration], "A search for the rare decay $B^0 \to \tau^+\tau^-$ at BABAR," Phys. Rev. Lett. **96** (2006) 241802

59. B. Aubert *et al.* [BABAR Collaboration], "Measurements of the absolute branching fractions of B+- → K+- X/(c anti-c)," Phys. Rev. Lett. **96** (2006) 052002

60. B. Aubert *et al.* [BABAR Collaboration], "Measurement of the inclusive electron spectrum in charmless semileptonic B decays near the kinematic endpoint and determination of —V(ub)—," Phys. Rev. D **73** (2006) 012006

61. B. Aubert *et al.* [BABAR Collaboration], "Measurement of branching fractions and resonance contributions for B0 → anti-D0 K+ pi- and search for B0 → D0 K+ pi- decays," Phys. Rev. Lett. **96** (2006) 011803

62. B. Aubert *et al.* [BABAR Collaboration], "Measurements of neutral B decay branching fractions to $K^0_S\pi^+\pi^-$ final states and the charge asymmetry of $B^0 \to K^{*+}\pi^-$," Phys. Rev. D **73** (2006) 031101

63. B. Aubert *et al.* [BABAR Collaboration], "Search for lepton flavor violation in the decay $\tau^\pm \to e^\pm\gamma$," Phys. Rev. Lett. **96** (2006) 041801

64. B. Aubert *et al.* [BABAR Collaboration], "Study of $J/\psi\pi^+\pi^-$ states produced in $B^0 \to J/\psi\pi^+\pi^-K^0$ and $B^- \to J/\psi\pi^+\pi^-K^-$," Phys. Rev. D **73** (2006) 011101

65. B. Aubert *et al.* [BABAR Collaboration], "A search for the decay $B^+ \to \tau^+\nu_\tau$," Phys. Rev. D **73** (2006) 057101

66. B. Aubert *et al.* [BABAR Collaboration], "Measurement of the $\overline{B}^0$ lifetime and the $B^0\overline{B}^0$ oscillation frequency using partially reconstructed $\overline{B}^0 \to D^{*+}\ell^-\bar{\nu}_\ell$ decays," Phys. Rev. D **73** (2006) 012004

67. B. Aubert *et al.* [BABAR Collaboration], "Measurement of the CKM angle gamma in B-+ → D(*) K-+ decays with a Dalitz analysis of D0 → K0(S) pi- pi+," arXiv:hep-ex/0607104 (conference paper presented at ICHEP 2006).

68. B. Aubert *et al.* [BABAR Collaboration], arXiv:hep-ex/0607107.

CDF

A. Annovi (Art. 36), M. Cordelli (Resp.), P. Giromini,
F. Happacher (Art. 23), S. Torre (Ass.)

1 Introduction

The Tevatron, with a $p\bar{p}$ collision energy of 1.96 TeV in the center of mass system, is running with a record instantaneous luminosity, L, delivered to the experiments of 280×10^{30} $cm^{-2}s^{-1}$; the designed high luminosity phase will have 300×10^{30} $cm^{-2}s^{-1}$ ($vs.$ $\sim 10^{31}$ of Run I). At the end of year 2006, the Tevatron has delivered to the experiments $\sim$ 2500 pb^{-1}; CDF experiment has collected on tape $\sim$ 2000 pb^{-1} (see Figure 1); during the whole Run I we collected $\sim$ 109 pb^{-1}. The instantaneous luminosity is still increasing during the first months of data taking of the year 2007.

The CDF group of Frascati has built the central hadronic calorimeter (the iron-scintillator based calorimeter in the central and end-wall region, CHA and WHA) and is responsible for the hardware maintenance and for the energy scale calibration.

Since year 2005 we are also responsible of the Silicon Vertex Trigger upgrade and of its operations.

The analisys interest of the Frascati group focuses on the measurements of b quark production cross sections. Indeed, the bottom quark production at the Fermilab Tevatron has been called one of the few instances in which experimental results appear to challenge the ability of perturbative QCD to accurately predict absolute rates in hadronic collisions. We are repeating the most significant b quark cross section measurements from Run I in order to clarify the current situation.

2 Calibration of the central hadron calorimeter

The Frascati group plays a leading role in the calibration of the central hadron calorimeters, CHA/WHA.

For the WHA calorimeter the original Run I ^{137}Cs Sources system is fully working and therefore it can be used to set the absolute energy scale for all the towers; we have taken one ^{137}Cs Source run in May 2006 and we have accordingly computed a set of Linear Energy Response:

$$LER = \frac{^{137}Cs(test - beam)e^{-\Delta t/\tau}}{^{137}Cs(today)}$$

that have been downloaded in the front end electronics to correct the raw ADMEM counts. This system effectively probes the behavior of the calorimeter since the source runs in front of the inner scintillator plane of the wedges thus irradiating few of the scintillator/absorber layers of the calorimeter. In this way we monitor aging phenomena of the scintillator together with PM gain variations.

We calibrate the CHA calorimeter looking at the energy deposition of Minimum Ionizing Particles (i.e. muons from J/Ψ decays).

We briefly recall the procedure to set the absolute calorimeter energy scale using Mip's. Looking at μ's from the $\sim$ 81 pb^{-1} dimuon trigger sample collected in Run Ib, we determined the necessary statistics to determine the peaks of μ's hadronic energy, HadE, distributions with enough precision per every CHA tower. With a statistics of $\sim$ 40 pb^{-1} we find that the tower by tower peak is determined with a precision of $\sim$ 1.5%. The LER's correction factors are derived

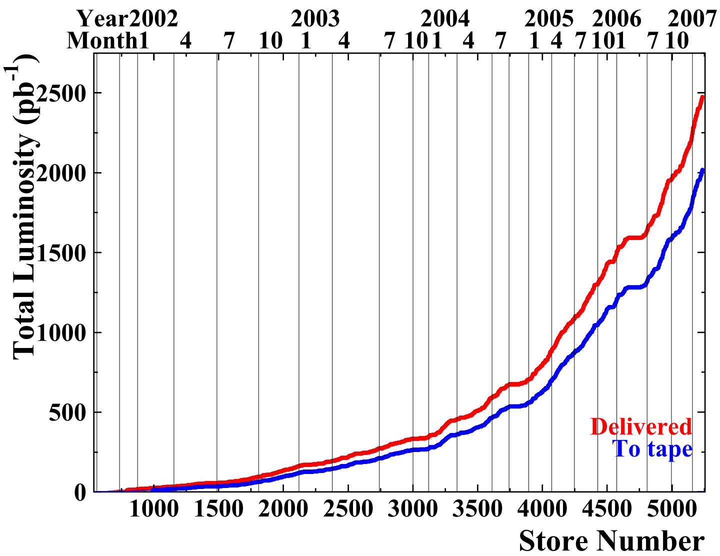

Figure 1: *Integrated Luminosity vs time*

comparing tower by tower the HadE deposition for Run I and Run II mips every 30-40 pb^{-1} of data; the LER at a given time time t are defined as the previous set of LER (t-1) multiplied by the observed ratio of the Mip's at a time t and in Run I:

$$LER(t) = LER^{t-1} \times \frac{MIP(RunI)}{MIP(t)}$$

We look at Mip's peaks response every $\sim$ 100 pb^{-1} and the typical response shows a tiny 1.5% gain variations on average and few channels that drift more than 5%.

The laser system represents a quick tool to follow the trend of the PM's gains. We have continuously acquired laser runs since year 2003 to monitor the gain variations of each photomultiplier; the CHA is stable within $\sim$ 2%.

2.1 ONLINE-OFFLINE energy scale calibration

At CDF with the current luminosity the data are being processed through the OFFLINE reconstruction every couple of months. Before producing the fully reconstructed events from the raw information of the detector we first produce small dedicated calibration samples to derive the calibrations constants for all the sub detectors. Every 6-8 weeks we run an executable called CalibExe which produces all the data ntuples for different data sets, including the dimuon trigger data sample where we reconstruct J/Ψ events; then the various calibrators use these samples to derive the calibrations. We made all this procedure automatic during the year 2006.

Usually for the Hadron calorimeters we produce two set of calibrations: ONLINE calibrations are directly downloaded in the ADMEM electronics and are intended to correct the energy response for data that have to be acquired afterwards; the OFFLINE calibrations attempts to propagate back to the data already acquired the needed corrections. The calibration constants are then filled in appropriate ORACLE data base tables called CHALINERESPONSE and CHAOFFLER. To validate the OFFLINE calibrations, the same data sets are reconstructed again picking the right calibration tables for every run range they have been produced for and the calibrators have to repeat their analysis to check that the calibrations are correct.

With this procedure the calorimeter response is kept constant at $\sim 2\%$ level over the running period.

3 SVT Upgrade

Since autumn 2005 the group has grown and we have been involved in the installation of the Silicon Vertex Trigger upgrade.

The Silicon Vertex Trigger (SVT) is part of the L2 trigger of CDF II. The SVT reconstructs tracks by associating Silicon hits to Central Tracker (COT) tracks reconstructed by the L1 trigger. By using the hits in the silicon, SVT is able to measure the impact parameter of the tracks so that this information can be used by the L2 to select data enriched of heavy flavor decays. Data collected using the SVT processor made possible the first measurement of the B_s mixing.

The SVT required an upgrade in order to perform track reconstruction within the allowed 20-40 μs/per event at the highest expected Tevatron luminosity of $300 \times 10^{30}\ cm^{-2}s^{-1}$

In order to speed up the execution of SVT we took two actions:

- improve the resolution at the pattern recognition level. With higher resolution less track candidates are found and less fits have to be performed.
- increase the clock speed of the Track-Fitter boards and of other interface boards. This allows for faster track fitting and faster I/O speed.

The pattern recognition is performed within a custom Associative Memory (AM). In order to increase the clock speed of other boards in the system we re-implemented them with Pulsar boards. Pulsar boards are flexible programmable boards developed for other CDF upgrades. They have 3 powerful FPGAs on board and all the CDF DAQ connectors. They are expansible with mezzanines that we used to increase the amount of available RAM, which was not sufficient for the demanding SVT application. Pulsars have been a key element to minimize the effort and time required for hardware development. We focused on firmware development rather than board design. This allowed us to develop and install three different kind of boards in less than 18 months.

We worked on the integration of the new boards within the existing system. This was mainly software development for the initialization of the boards, parasitic testing of the boards and development of simulation software. The other item we worked on was the study on how to actually take advantage of the higher number of patterns available. We also worked to improve the monitoring of the system and its maintainability.

The system installation has been completed in early 2006 and the system is fully operational since then. The group is currently involved in the operations of the SVT. After installation several studies and optimization of the system have been carried out, with crucial contribution from members of the group. A new system indeed requires several studies to be finely tuned and completely understood. We activate new features of the Pulsar boards that allows to have an online measurement of the processing time required by each step of the pattern recognition. We also optimize the monitoring and the simulation of the system to the point that discrepancies between data and simulation are of the order of one over ten thousand. The increase in the luminosity and the necessity to prescale (statically or dynamically) several triggers that exploit SVT information has also caused a change in the way trigger performances are evaluated. During 2006 we have studied strategies to optimize the purity of the tracking algorithm and of the cut on the impact parameter of the tracks. In particular these studies drove to the definition of new set of requirements on the beam position and slope that have been applied since the last 2006 shutdown.

In order to reduce the maintenance effort we have also improved the online and offline monitoring allowing for a better understanding of the problems and a quicker reaction when they appear during data taking.

The next challenge for SVT is a more extensive application for high-p_T triggers. The group is currently studying the performance of SVT at the highest Tevatron instantaneous luminosity and possible improvements. This work is part of the Higgs Trigger Task Force (HTTF) that is working to improve all triggers for the Higgs in view of the 6 fb^{-1} that the Tevatron is expected to deliver in the next years. The SVT plays an important role for the selection of b-quarks and taus from Higgs decays. The work of the HTTF will be crucial for a possible Higgs discovery at CDF. In fact, in addition to an increase by a factor of 8 in integrated luminosity[1], CDF expects to increase the Higgs discovery reach through several trigger and analysis improvements. The potential of these improvements is estimated to be an additional factor ≈ 10 in equivalent luminosity. By pursuing this goal and if nature is kind with us, we might see an hint of the Higgs

4 Studies of b quark cross section

4.1 Status of the Tevatron measurements

The bottom quark production at the Fermilab Tevatron has been called one of the few instances in which experimental results appear to challenge the ability of perturbative QCD to accurately predict absolute rates in hadronic collisions. In general, the data are underestimated by the exact next-to-leading-order (NLO) QCD prediction. The most recent measurement from the Tevatron is however in very good agreement with an improved QCD calculation (FONLL), and has prompted a number of studies suggesting that the apparent discrepancy has been resolved with incremental improvements of the measurements and predictions. The increase of the cross-section predicted by FONLL with respect to original NLO calculatiuons, which results into a better agreement with data, is mostly coming from new structure functions and fragmentation functions that have been computed at next-to-leading-order, in order to match the perturbative order of the FONLL calculation. The measured single b-quark cross-section is also in agreement with the prediction of LL shower MC, with an *ad hoc* tuning.

Because of the experimental difficulty inherent to each result, we reviewed all measurements of the single b cross section performed at the Tevatron, and then compared their average to the standard and to the improved QCD predictions. We have also compared the cross sections for producing both b and $\bar{b}$ quarks - centrally and above a given transverse momentum cut - to theoretical predictions. The single b-quark cross section is inferred from the measurement of the production rate as a function of the transverse momentum, p_T, of: B hadrons; or some of their decay products (leptons or ψ mesons); or jets produced by the hadronization of b quarks. Most of the Tevatron measurements correspond to b quarks produced centrally (rapidity $|y^b| \leq 1$) and with $p_T \geq 6$ GeV/c (up to $p_T \simeq 100$ GeV/c). We have performed a consistency check of all available data. For that purpose, we use the value of the single b-quark cross section extracted from the data and integrated from the p_T threshold of each experiment. We determined the ratio R of each measurement to the same theoretical prediction. We have then evaluated the average R and its dispersion. As benchmark prediction of the b-quark parton-level cross section we choose the exact NLO calculation implemented with old but consistent sets of parton distribution functions

[1]We expect to collect at least 8 fb^{-1} total, to be compared with 1 fb^{-1} used for analysis up to date.

channel	R for $p_T^{\min}$ (GeV/c) =					
	6	$8-10$	$12-15$	$19-21$	$\simeq 29$	$\simeq 40$
$J/\psi K^+$		$4.0 \pm 15\%$	(3.4)			
$J/\psi K^+$		$2.9 \pm 23\%$	(1.9)			
$\mu\ X$				$2.5 \pm 26\%$	(1.9)	
$e\ X$			$2.4 \pm 27\%$			
eD^0				$2.1 \pm 34\%$		
$J/\psi\ X$		$4.0 \pm 10\%$	(3.4)			
$J/\psi\ X$		$3.1 \pm 9\%$	(2.7)			
$\mu\ X$	$2.1 \pm 27\%$		(1.7)			
$\mu\ X$	$2.5 \pm 25\%$		(3.5)			
b jets (μ)				$2.4 \pm 20\%$		(2.0)

Table 1: Ratio R of measured single b cross sections to a prediction based on the exact NLO calculation .

(PDF), since it has been used in most published works, convoluted with the Peterson fragmentation function; B-hadron decay are modeled with the QQ Monte Carlo generator program.

There are 10 measurements of the single b cross section performed by the CDF and DØ collaborations at the Tevatron. The ratios of these measurements to the standard theory are summarized in Table 1.

Using the measurements listed in Table 1, we derive an average ratio of the data to the standard theory that is $< R >= 2.8$; the RMS deviation of the 10 measurements in Table 1 is 0.7 It has to be noticed that all the measurement involving the J/Ψ reconstruction, experimentally the cleanest, are consistently much higher than the ones based on the detection of a semileptonic decay.

The new measurement of the $B^+ \to J/\Psi(\to \mu^+\mu^-)K^+$ differential cross section (see next paragraph) carried on by the Frascati group finds a ratio R with the theory of 2.80 ± 0.24, somehow closer to the average of all measurements.

Leading-order (LO) and higher-than-LO terms are sources of b and $\bar{b}$ quarks with quite different topological structure. The production of events with both a b and $\bar{b}$ quark with $p_T \geq$ 6 GeV/c and $|y| \leq 1$ is dominated by LO diagrams and the parton-level cross sections predicted by the exact NLO calculation is comparable to that predicted by LL Monte Carlo generators.

R_{2b}, the ratio of $\sigma_{b\bar{b}}$ measured at the Tevatron to the exact NLO prediction, $\simeq 1$ would imply that the parton-level cross section predicted by LL generators (NLO) is correct and that the contribution of higher-than-LO terms has to be a factor of two larger than in the present NLO or FONLL prediction. If the ratio R_{2b} is much larger than one, then the agreement between the observed single b cross section and the prediction of LL Monte Carlo generators is fortuitous and agreement with the data may be found by using harder fragmentation functions as in the FONLL calculation.

We review five measurements, listed in Table 2, and derive a value of $< R_{2b} >= 1.8$ with a 0.8 RMS deviation. Such a large RMS deviation indicates that the experimental results are inconsistent among themselves. Additional measurements are certainly needed to clarify the experimental situation.

channel	R_{2b} for $p_T^{\rm min}$ (GeV/c) =			
	$6-7$	10	15	$\simeq 20$
$b+\bar{b}$ jets			$1.2 \pm 25\%$	
$b+\bar{b}$ jets				$1.0 \pm 32\%$
$\mu + b$ jet		$1.5 \pm 10\%$		
$\mu^+ + \mu^-$	$3.0 \pm 20\%$			
$\mu^+ + \mu^-$	$2.3 \pm 33\%$			

Table 2: Ratio R_{2b} of $\sigma_{b\bar{b}}$, the observed cross section for producing both b and $\bar{b}$ quarks, centrally and above a given $p_T^{\rm min}$ threshold, to the exact NLO prediction.

4.2 $B^+ \to J/\Psi(\to \mu^+\mu^-)K^+$

We have repeated the Run I analysis that measures the B^+ differential cross section as a function of p_T, reconstructing the decay $B^+ \to J/\Psi(\to \mu^+\mu^-)K^+$. We search for $B^\pm \to J/\psi K^\pm$ candidates in the data set selected by the $J/\psi \to \mu^+\mu^-$ trigger. We search for J/ψ candidates by using pairs of muons, reconstructed in the CMU detector, with opposite charge, and $p_T \geq 2$ GeV/c. The invariant mass of a muon pair is evaluated by constraining the two muon tracks to originate from a common point in three-dimensional space (vertex constrain) in order to improve the mass resolution. All muon pairs with invariant mass in the range $3.05 - 3.15$ GeV/c^2 are considered J/ψ candidates. If a J/ψ candidate is found, we search for $B^\pm$ mesons by considering all charged particle tracks in the event as possible kaon candidates. The invariant mass of the μ^+ μ^- $K^\pm$ system is evaluated constraining the corresponding tracks to have a common origin while the μ^+ μ^- invariant mass is constrained to the value of 3096.9 GeV/c^2. The invariant mass distribution of all $B^\pm$ candidates found in this study is shown in Fig. 2.

To measure the B^+ differential cross section as a function of p_T, we divide the sample of $B^\pm$ candidates into five p_T bins: $6-9$, $9-12$, $12-15$, $15-25$, and ≥ 25 GeV/c. In each p_T bin, we fit the invariant mass distribution of the B^+ candidates with a binned maximum likelihood method to determine the number of B^+ mesons. We use a first order polynomial function to model the combinatorial background and gaussian function to model the B^+ signal. All fits return a B^+ mass of 5279.0 ± 0.5 MeV in agreement with the PDG value.

The detector acceptance is calculated with a Monte Carlo simulation based on the NLO calculation. The $B^\pm$ decay is modeled with the EVTGEN Monte Carlo program. The detector response to the generated $B^\pm$ decay prongs is modeled with the CDF II detector simulation that in turn is based on the GEANT Monte Carlo program.

The differential cross section $d\sigma/dp_T$ is calculated as

$$\frac{d\sigma(B^+)}{dp_T} = \frac{N/2}{\Delta p_T \times \mathcal{L} \times \mathcal{A}_{\rm corr} \times BR} \tag{1}$$

where N is the number of $B^\pm$ mesons determined from the likelihood fit to the invariant mass distribution of the J/ψ $K^\pm$ candidates in each p_T bin. The factor 1/2 accounts for the fact that both B^+ and B^- mesons are used and assumes C invariance at production. Δp_T is the bin width and $\mathcal{A}_{\rm corr}$ is the geometric and kinematic acceptance that includes trigger and tracking efficiencies measured with the data. The integrated luminosity of the data set is $\mathcal{L} = 739 \pm 44$ pb$^-1$. The branching ratio $BR = (5.98 \pm 0.22) \times 10^{-5}$ is derived from the branching fractions $BR(B^\pm \to J/\psi\ K^\pm) = (1.008 \pm 0.035) \times 10^{-3}$ and $BR(J/\psi \to \mu^+\ \mu^-) = (5.93 \pm 0.06) \times 10^{-2}$.

The B^+ total cross section is $\sigma_{B^+}(p_T \geq 6.0\ \text{GeV/c}, |y| < 1) = 2.78 \pm 0.24\ \mu$b, where the 8.6% error is the sum in quadrature of the 6% error on the integrated luminosity, the 3.7% uncertainty of

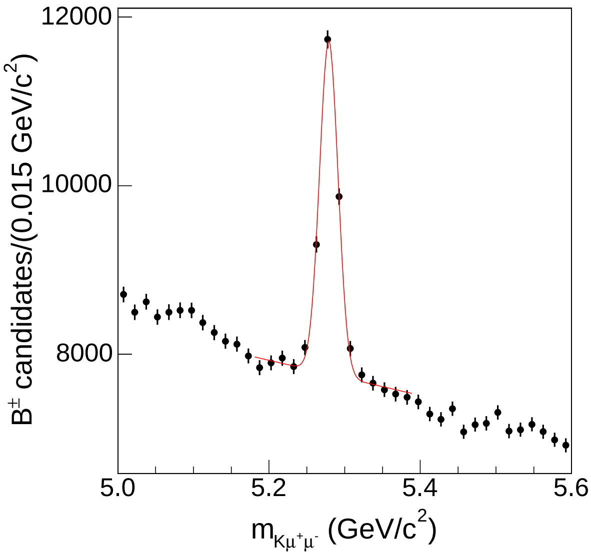

Figure 2: *Invariant mass distribution of all $B^{\pm}$ candidates. The line represents a fit to the data using a first order polynomial plus a gaussian function in order to estimate the background and the $B^{\pm}$ signal, respectively.*

the $B^+ \to J/\psi\ K^+$ and $J/\psi \to \mu^+\ \mu^-$ branching fractions, the 2.5% uncertainty of the acceptance calculation, and the 4.4% statistical error.

4.3 $b\bar{b}$ correlation

Another analisys in progress is the study of the so called $b\bar{b}$ correlation. This study is a new measurement of $\sigma_{b\bar{b}}$ that uses dimuons arising from from $b\bar{b}$ production. At the Tevatron, dimuon events result from decays of heavy quark pairs ($b\bar{b}$ and $c\bar{c}$), the Drell-Yan process, charmonium and bottomonium decays, and decays of π and K mesons. Background to dilepton events also comes from the misidentification of π or K mesons. We make use of the precision tracking provided by the CDF silicon microvertex detector to evaluate the fractions of leptons due to long-lived b- and c-hadron decays, and to the other background contributions.

The method used to determine the $b\bar{b}$ and $c\bar{c}$ content of the data is to fit the observed impact parameter distribution of the muon pairs with the expected impact parameter distributions of leptons from various sources. After data selection, the main sources of reconstructed muons are semileptonic decays of bottom and charmed hadrons, and prompt decays of onia and Drell-Yan production.

Herwig Monte Carlo simulations are used to model the impact parameter distributions for leptons from b- and c-hadron decays. The impact parameter distribution of leptons from prompt sources such as quarkonia decays and Drell-Yan production is derived using muons from $\Upsilon(1S)$ decays.

Conferences 2006

- F. Happacher, "Status of the observed and predicted $b\bar{b}$ production at the Tevatron", XIV International Workshop on Deep Inelastic Scattering - Tsukuba (Japan), April 20th-24th, 2006.
- A. Annovi, "The Silicon Vertex Trigger Upgrade at CDF", IFAE 2006, Pavia (Italy), April 19th-21st, 2006
- A. Annovi, "CDF: B physics performance & trigger - operational experience", BEAUTY 2006, Oxford (UK), September 25th-29th, 2006

Publications 2006 (partial list)

1. A. Abulencia *et al.* [CDF II Collaboration], " Measurement of the B+ Production Cross Section in p anti-p Collisions at s**(1/2) = 1960 GeV" Submitted to Phys. Rev. D December 10, 2006.
2. F. Happacher, P. Giromini and F. Ptohos, "Status of the observed and predicted b anti-b production at the Tevatron," Phys. Rev. D **73**, 014026 (2006) [arXiv:hep-ph/0509348].
3. A. Abulencia *et al.* [CDF II Collaboration], "Measurement of the helicity fractions of W bosons from top quark decays using fully reconstructed t anti-t events with CDF II," arXiv:hep-ex/0612011.
4. A. Abulencia *et al.* [CDF Collaboration], "Observation of exclusive electron positron production in hadron hadron collisions," arXiv:hep-ex/0611040.
5. A. Abulencia *et al.* [CDF Collaboration], "Search for W' boson decaying to electron-neutrino pairs in p anti-p collisions at s**(1/2) = 1.96-TeV," arXiv:hep-ex/0611022.
6. A. Abulencia *et al.* [CDF Collaboration], "Search for V + A current in top quark decay in p anti-p collisions at s**(1/2) = 1.96 TeV," Phys. Rev. Lett. **98** (2007) 072001.
7. A. Abulencia *et al.* [CDF Collaboration], "Observation of B/s0 anti-B/s0 oscillations," Phys. Rev. Lett. **97** (2006) 242003 [arXiv:hep-ex/0609040].
8. A. Abulencia *et al.* [CDF Collaboration], "Measurement of the Λ_b^0 lifetime in $\Lambda_b^0 \to J/\psi\Lambda^0$ in $p\bar{p}$ collisions at $\sqrt{s} = 1.96$-TeV," arXiv:hep-ex/0609021.
9. A. Abulencia *et al.* [CDF - Run II Collaboration], "Measurement of the t anti-t production cross section in p anti-p collisions at s**(1/2) = 1.96-TeV in the all hadronic decay mode," Phys. Rev. D **74** (2006) 072005 [arXiv:hep-ex/0607095].
10. A. Abulencia *et al.* [CDF Collaboration], "Measurement of the t anti-t production cross section in p anti-p collisions at s**(1/2) = 1.96-TeV using lepton + jets events with jet probability b-tagging," Phys. Rev. D **74** (2006) 072006 [arXiv:hep-ex/0607035].
11. A. Abulencia *et al.* [CDF Collaboration], "Observation of B/s0 –¿ K+ K- and measurements of branching fractions of charmless two-body decays of B0 and B/s0 mesons in anti-p p collisions at s**(1/2) = 1.96-TeV," Phys. Rev. Lett. **97** (2006) 211802 [arXiv:hep-ex/0607021].
12. A. Abulencia *et al.* [CDF Collaboration], "Search for excited and exotic muons in the mu gamma decay channel in p anti-p collisions at s**(1/2) = 1.96-TeV," Phys. Rev. Lett. **97** (2006) 191802 [arXiv:hep-ex/0606043].

13. A. Abulencia *et al.* [CDF - Run II Collaboration], "Measurement of the B/s0 anti-B/s0 oscillation frequency," Phys. Rev. Lett. **97** (2006) 062003 [AIP Conf. Proc. **870** (2006) 116] [arXiv:hep-ex/0606027].

14. A. Abulencia *et al.* [CDF Collaboration], "Measurement of the t anti-t production cross section in p anti-p collisions at s**(1/2) = 1.96-TeV," Phys. Rev. Lett. **97** (2006) 082004 [arXiv:hep-ex/0606017].

15. A. Abulencia *et al.* [CDF Collaboration], "Search for a neutral Higgs boson decaying to a W boson pair in p anti-p collisions at s**(1/2) = 1.96-TeV," Phys. Rev. Lett. **97** (2006) 081802 [arXiv:hep-ex/0605124].

16. A. Abulencia *et al.* [CDF Collaboration], "Top quark mass measurement from dilepton events at CDF II with the matrix-element method," Phys. Rev. D **74** (2006) 032009 [arXiv:hep-ex/0605118].

17. A. Abulencia *et al.* [CDF Collaboration], "Measurement of the b jet cross section in events with a Z boson in p anti-p collisions at s**(1/2) = 1.96-TeV," Phys. Rev. D **74** (2006) 032008 [arXiv:hep-ex/0605099].

18. A. Abulencia *et al.* [CDF Collaboration], "Search for new physics in lepton + photon + X events with 305-pb**(-1) of p anti-p collisions at s**(1/2) = 1.96-TeV," Phys. Rev. Lett. **97** (2006) 031801 [arXiv:hep-ex/0605097].

19. A. Abulencia *et al.* [CDF Collaboration], "Measurement of the ratio of branching fractions B(D0 –¿ K+ pi-)/B(D0 –¿ K- pi+) using the CDF II detector," Phys. Rev. D **74** (2006) 031109 [arXiv:hep-ex/0605027].

20. A. Abulencia *et al.* [CDF Collaboration], "Search for large extra dimensions in the production of jets and missing transverse energy in p anti-p collisions at s**(1/2) = 1.96-TeV," Phys. Rev. Lett. **97** (2006) 171802 [arXiv:hep-ex/0605101].

21. A. Abulencia *et al.* [CDF Collaboration], "Measurement of the t anti-t production cross section in p anti-p collisions at s**(1/2) = 1.96-TeV using missing E(t) + jets events with secondary vertex b-tagging," Phys. Rev. Lett. **96** (2006) 202002 [arXiv:hep-ex/0603043].

22. A. Abulencia *et al.* [CDF Collaboration], "Measurement of the B/c+ meson lifetime using B/c+ –¿ J/psi e+ nu/e," Phys. Rev. Lett. **97** (2006) 012002 [arXiv:hep-ex/0603027].

23. A. Abulencia *et al.* [CDF Collaboration], "Search for high-mass resonances decaying to e mu in $p\bar{p}$ collisions at $\sqrt{s}$ = 1.96-TeV," Phys. Rev. Lett. **96** (2006) 211802 [arXiv:hep-ex/0603006].

24. A. Abulencia *et al.* [CDF Collaboration], "Search for $Z' \to e^+e^-$ using dielectron mass and angular distribution," Phys. Rev. Lett. **96** (2006) 211801 [arXiv:hep-ex/0602045].

25. A. Abulencia *et al.* [CDF Collaboration], "Measurement of the top quark mass using template methods on dilepton events in proton antiproton collisions at $\sqrt{s}$ = 1.96-TeV," Phys. Rev. D **73** (2006) 112006 [arXiv:hep-ex/0602008].

26. A. Abulencia *et al.* [CDF Collaboration], "Observation of $B_s^0 \to \psi(2S)\phi$ and measurement of ratio of branching fractions $B(B_s^0 \to \psi(2S)\phi)/B(B_s^0 \to J/\psi\phi)$," Phys. Rev. Lett. **96** (2006) 231801 [arXiv:hep-ex/0602005].

27. A. Abulencia *et al.* [CDF Collaboration], "Measurement of $\sigma(\Lambda_b^0)/\sigma(\bar{B}^0) \times BR(\Lambda_b^0 \to \Lambda_c^+ pi-)/BR(anti-B0 \to D^+$ pi-) in $p\bar{p}$ collisions at $\sqrt{s}$ = 1.96-TeV," arXiv:hep-ex/0601003.

CMS

M. Bertani, S. Bianco (Resp.), M.A. Caponero (Ass.)
D. Colonna (Dott.), D. Donisi (Dott.), F.L. Fabbri
F. Felli (Ass.), M. Giardoni, B. Ortenzi (Tecn.), M. Pallotta, A. Paolozzi (Ass.)
L. Passamonti (Tecn.), C. Pucci (Dott.), G. Saviano (Ass.).

In collaboration with:
D. Pierluigi, B. Ponzio, A. Russo.

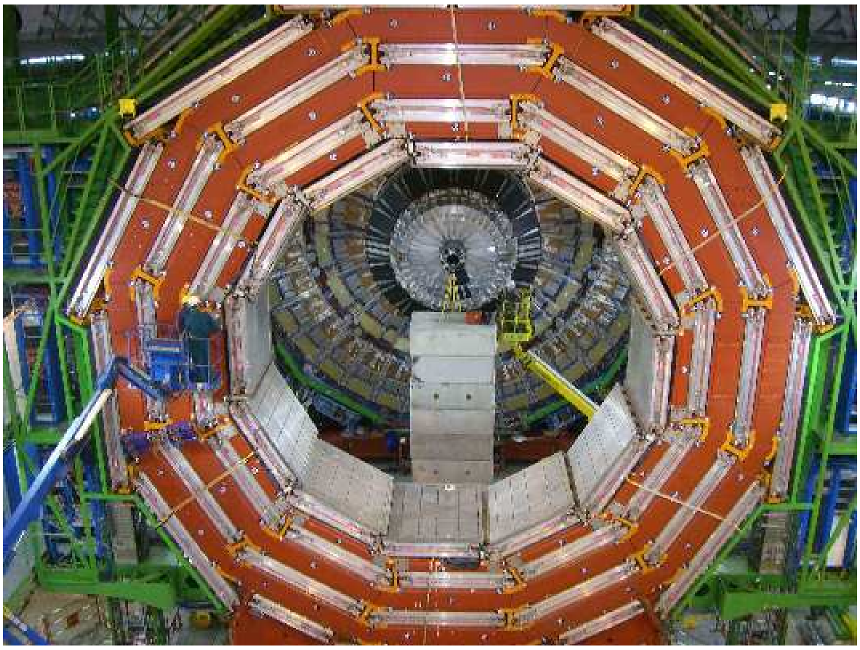

1 The CMS Experiment and the RPC Muon Detector

The Compact Muon Solenoid (CMS) experiment [1)] will search for the missing block of Nature - the Higgs boson - and for new exotic elementary particles that are predicted by theory and by cosmological observations. During 2006 CMS has rapidly progressed towards installation completion and commissioning. A major milestone was met in August 2006 when the 4 Tesla magnet was turned on exceeding specifications, and a full sector of detectors were operated with cosmic muon triggers providing the very first reconstructed tracks. Once commissioned, every wheel CMS is made of is lowered into the experimental cavern. At the end of 2006 already two out of five wheels had been lowered into the experimental cavern.

The CMS detector uses Resistive Plate Chambers (RPC) as muon detectors, coupled to Drift Tubes in the barrel region, and to Cathode Strip Chambers in the endcaps. Resistive Plate Chambers (RPC) detectors are widely used in HEP experiments for muon detection and triggering at high-energy, high-luminosity hadron colliders, in astroparticle physics experiments for the detection of extended air showers, as well as in medical and imaging applications. While gain and efficiency stability are always a must, in the case of RPC detectors in high-rate experiments which use freon-based gas mixtures, utmost care has to be paid also for the possible presence of gas contaminants. RPC counters [2] are fast, efficient and economical charged particles detectors, well-suited for operation in high magnetic field. The elementary component is a gap, a gas volume enclosed between two resistive plates. Resistive plates are made of bakelite, coated with lineseed oil for surface uniformity. Gas mix used is 96.2% $C_2H_2F_4$ / 3.5% Iso-C_4H_{10} / 0.3% SF_6, with a 45% relative humidity. Signal pulses are picked up by readout strips. In CMS, RPC counters are operated in avalanche mode to sustain high-rate operation, with the streamer suppressed by the addition of SF_6 gas in the mixture.

2 Activity of the CMS Frascati group in 2006

The Frascati group has joined CMS in the RPC muon detectors at the end of year 2005. Proposal to join was supported by the Frascati Directorate in March 2006, and funding arrived in April 2006. The initial activities of CMS Frascati have been a contribution to quality control of RPC chambers at production plant in Colli (FR), participation in detector installation and commissioning, data taking shifts for the Magnet Test Cosmic Challenge run (August 2006), responsibility of gas gain monitoring system, and material studies for gas aging of chambers. Frascati has also committed to work on physics analysis issues in B physics, with emphasis on B spectroscopy and B rare decays, such as channels decays with muon pairs (from J/ψ, $\Upsilon(4s)$) in the final state, profiting of knowledge of RPC and DT muon detectors: spectroscopy of $B_c \rightarrow J/\psi\pi$, mixing of $B_s \rightarrow J/\psi\phi$, CPV in $B_s \rightarrow J/psi\phi$, the rare decay $B \rightarrow \mu\mu$. Finally, the Frascati group has also proposed [3] the use of the FBG sensors developped in Finuda and BTeV for CMS pixel and silicon.

2.1 The CMS Closed Loop Gas System

Because of high costs and huge volumes of the freon-based gas mix used, CMS will use a recirculation (Closed Loop) gas system developed by the CERN gas group. The Closed Loop is a critical component of RPC. CMS has accumulated experience on its use and performances during the test at the Gamma Irradiation Facility at CERN in 2001 [4], and currently at the ISR where chambers are tested in CL prior to installation. At the GIF facility we observed substancial production of HF, linearly correlated with the signal current.

In the Closed Loop (CL) system, purifiers are the crucial component. Purifiers were determined after tests at the GIF in order to minimize the unknown contaminants which showed as spurious peaks besides the known gas mix components. Three filters were selected: 5A molecular sieve, Cu/Cu-Zn, Ni/Al_2O_3. A small scale CL system is currently in use at the ISR test station, where RPC chambers are tested at CERN prior to installation in the CMS detector. The system total flux is 110 l/h, with a 10% fraction of fresh mix. Our operational experience showed how the CL system works well as long as the purifiers are not saturated (about 20 days). When purifiers are saturated, contaminants are not filtered and currents in chambers start increasing (Fig.1). Currents return to standard after purifiers regeneration. We do not observe any trace in GC analysis of either impurities or pollutants.

A measurement campaign [5] on purifiers is in progress, using chemical, SEM/EDS (Scanning Electron Microscopy/Energy Dispersive Spectroscopy), XRD (x-ray Diffrattometry) analyses. We plan to characterize the CL gas system in three phases: at ISR during chamber testing, at ISR at testing finished with dedicated gaps and dedicated gas system, at the GIF in high-radiation environment. Many open questions do exist: why only some 30-40% of chambers show current increase with saturated purifiers ? Why often only one gap out of two is affected ? It is clear how full understanding of the CL system is crucial for a reliable operation of CMS RPCs.

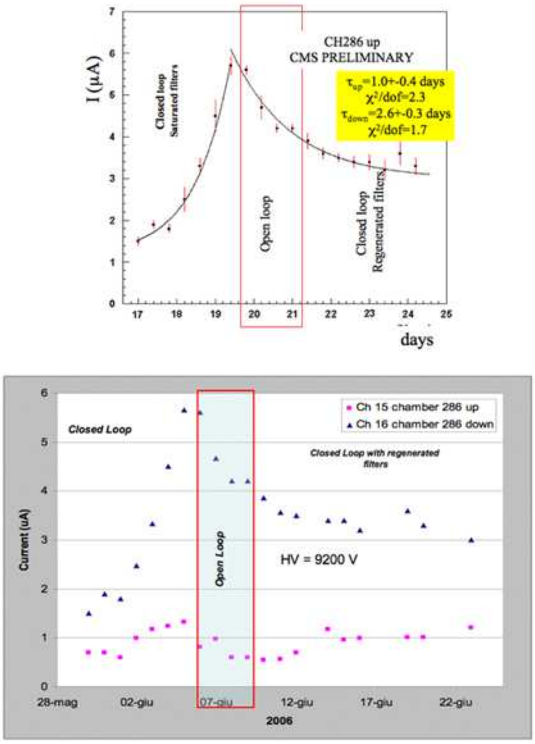

Figure 1: Increase of currents in RPC chambers under test at the ISR in CL gas system when purifiers are saturated. Currents start decreasing when chamber is set in Open Loop, and decrease further when chamber is returned to CL with regenerated purifiers. Top inset shows results of a best fit of an exponenential curve to data.

2.2 Gas Quality Monitoring System

Gas quality in CMS RPC will be monitored by a dedicated system able to accomplish a full analysis of the gas quality. The gas quality monitoring system will use specific electrodes for hydro-fluoridric acid (HF) detection, as well as SEM/EDS, XRD analyses for purifiers. The system will be flexible and open, so as to integrate other analysis devices such as GC (Gas Chromatography) and MS (Mass Spectrometry). In case of anomalies detected, we shall have the possibilities of accessing the experimental cavern where manual pickup points (one per half wheel) will be setup. Several results have been produced over the last few years with subsystems planned to be used in the gas quality monitoring system. Production of HF was found in chambers irradiated at the GIF [4)], with the concentration of HF produced in the gap found proportional to the signal charge. We recently performed new studies on irradiated RPCs. We opened small (50cm x 50cm) chambers irradiated at the GIF and observed defects on the inner surfaces (Fig.2). We performed SEM-EDS analyses on- and off-defect. The presence of Na in defects is confirmed. The origin of Na is supposedly the bakelite bulk, where NaOH is used as a catalyst in production. We performed XRD analysis of defects, preliminary results [6, 3)] show a good match of diffrattogram with the lines characteristic of NaF (Fig.3).

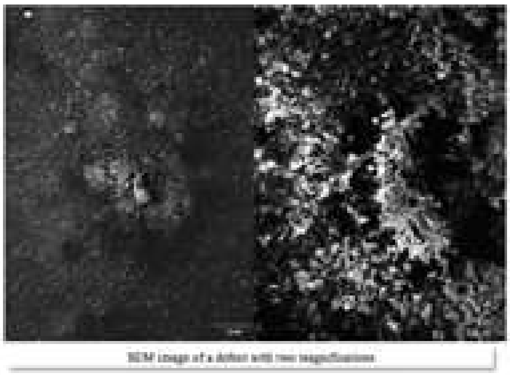

Figure 2: SEM image of a defect in a RPC chamber irradiated at the GIF under two magnifications. The defect is identified as NaF.

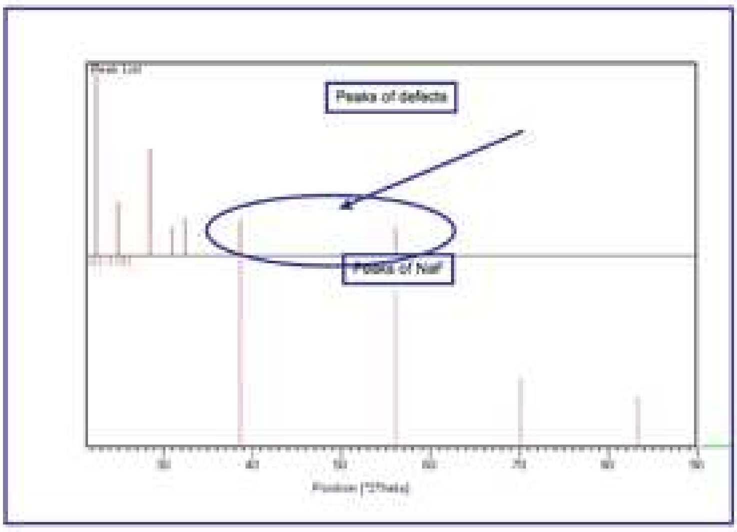

Figure 3: XRD spectrum of defects in a chamber irradiated at GIF. A very good match is observed for two characteristic peaks of NaF.

2.3 Gas Gain Monitoring System

The gas gain monitoring system will monitor the RPC working point faster and more precisely than what one could get by using the CMS RPC system, and provide a warning in case of shifts caused by the gas mixture changes. The system is designed to monitor efficiency and charge continuously in one-hour cycles with a 1% precision. The system (Fig.4) is composed of three subsystem of RPC single gaps, readout by 45cm x 45cm pads in a cosmic ray telescope located in the SGX5 gas building. Each subsystem is flushed with a different gas. The Reference subsystem is flushed with fresh open loop gas mixture. The MonitorOut subsystem is flushed with CL gas downstream of CMS RPCs. The MonitorIn subsystem is flushed with CL gas upstream of CMS RPCs. Each subsystem is composed of three gaps, whose high voltage is set to the standard working point voltage at the efficiency knee, and to 200V above and below the knee respectively. Each cosmic ray track therefore provides completely correlated pulses in the three subsystems, allowing one to study the differential response of gaps and by disentangling any effect due to changes in the gas mixture. In case a working point change is detected, an alarm condition is released and the gas quality monitoring system described in Sec.2.2 will verify what the change of work point is due to.

2.4 Prototypes

Several readout options have been considered for the RPC single gaps composing each subsystem. A double-pad readout was investigated, with each single pad read by both sides by 45cm x 45cm pads. An exploded view is shown in Fig.5.

Single gap prototypes were exposed to cosmic ray tracks triggered by a scintillator counter hodoscope. The negative and positive pads are sent to two input channels of a Tektronix TDS5600 digital sampling oscilloscope. Event-by-event pulse charges are measured and stored via LabView custom applications. The standard CMS RPC gas mixture is used, with 45% relative humidity to keep the bakelite resistivity.

Fig.2.4 shows the charge distributions of avalanches from cosmic rays for positive and negative pads, at high voltages from 9.5kV to 10kV. Fitting the charge distributions with truncated Gaussians shows the expected linear dependance of charge at the peak of distribution on the high voltage applied in case of saturated avalanche (Fig.2.4). Several amplification schemes are being explored. Even a simple passive sum of positive and negative pads, and feeding to NIM LeCroy LRS612AM amplifier improves the S/N ratio (Fig.2.4).

3 Activity planned for 2007

The CMS Frascati group is performing a detailed and complete analysis campaign since early tests at the GIF in 2001, to guarantee high-purity gas mixture for a reliable operation of the detector. A lot of work is being spent into the full understanding of the chemistry of purifiers in CL gas system. A gas analysis system has been designed, SEM-EDS analysis observes presence of Na in RPC gaps irradiated at GIF confirming previous results, while XRD analysis shows the presence of NaF. A gas gain monitoring system utilizing small RPC gaps has been designed, prototypes have been tested and preliminary results show the expected response to cosmic rays. In 2007 the gas gain system will be commissioned and installed at CERN, further tests on purifiers performed on the ISR chambers will shed new light on the issue. Physics analysis activity will start on the items in B physics of interest for the group.

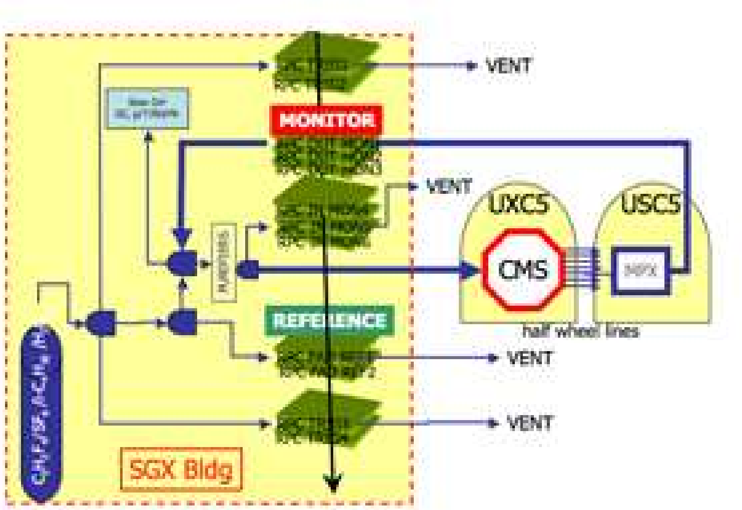

Figure 4: Gas gain monitoring system conceptual layout.

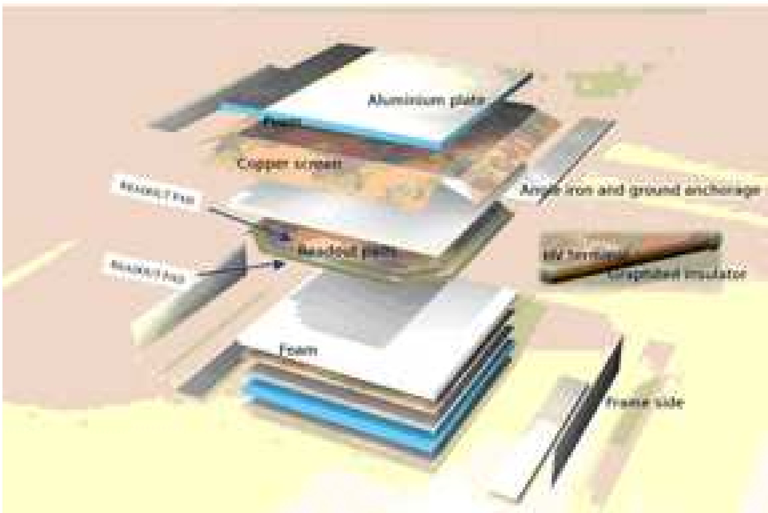

Figure 5: Exploded view of a 50cm x 50cm single gap which composes a subsystem of the gas gain monitoring system. Each single gap is read by two 45cm x 45cm pads on both sides, each one picking up negative and positive pulses from the avalanche developing in the gas gap upon the crossing of a cosmic ray track.

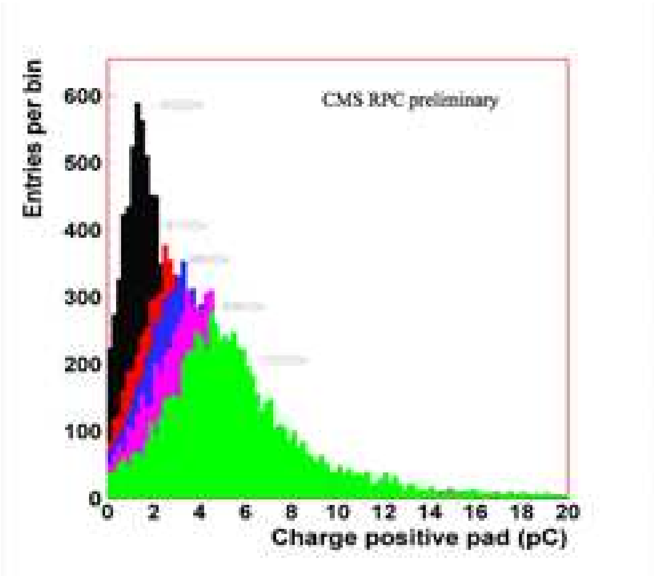

Figure 6: Charge distribution of single gap operated in avalanche regime and read by two 45cm x 45cm pads. The high voltage is increased from 9.5kV to 10kV. Pedestal is subtracted.

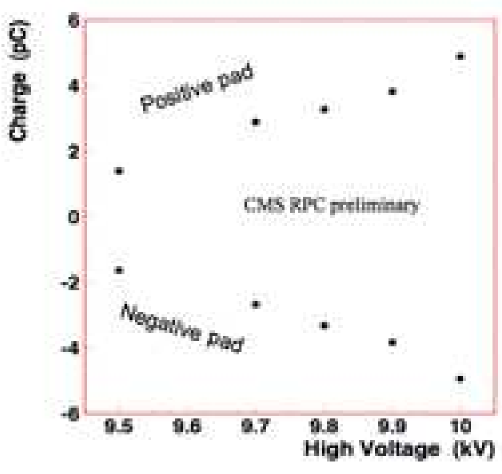

Figure 7: Dependence of peak values of charge distributions from high voltage.

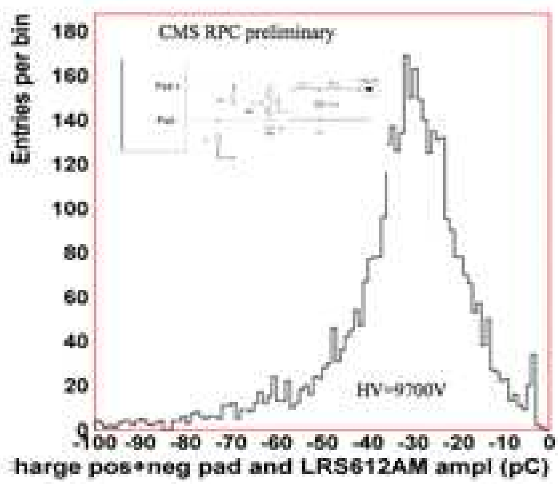

Figure 8: Charge distribution from the double pad readout scheme. A transformer (inset) sums positive and negative pads outputs. Transformer output is filtered and sent to NIM LeCroy amplifier. Pedestal is not subtracted and shown in arbitrary vertical scale at about -4pC.

4 List of Conference Talks by LNF Authors in Year 2006

1. S.Bianco on behalf of the CMS RPC Collaboration, The gas gain monitoring system for the CMS RPC detector, IEEE06, San Diego (USA), http://arxiv.org/pdf/physics/0701014
2. C.Pucci CMS RPC gas gain system, Annual Congress of Italian Physical Society, Torino 2006
3. D.Colonna Use of FBG sensors for high precision silicon detectors, Annual Congress of Italian Physical Society, Torino 2006
4. M.Caponero et al., On the use of FBG sensors in CMS, Siena conference on Adv. Detectors Nov 2006 (to appear on NIM)
5. A.Paolozzi et al., Performances of FBG sensors for application at LHC experiments, Vienna Conference Feb 2007 (to appear on NIM)

5 List of Theses in Year 2006

1. C.Pucci Analisi dei materiali nelle RPC di CMS Frascati preprint LNF-06/31(Thesis) MD Thesis
2. D.Colonna Applicazione dei sensori FBG in HEP e nelle strutture Marzo 2007, PhD Thesis

References

1. CMS Collaboration home page is /cms.cern.ch/.

2. M. Abbrescia et al., Nucl. Instr. And Meth. A533 (2994) 102-106; M.Abbrescia et al., Nucl. Instr. And Meth. A515 (2993) 342-347.

3. S.Bianco et al., Omega-Like Fiber Bragg Grating Sensors as Position Monitoring Device: A Possible Pixel Position Detector in CMS? Frascati preprint LNF- 06/13(NT).

4. M.Abbrescia et al., HF production in CMS Resistive Plate Chambers, submitted to NIM, presented by R.Guida at the RPC Conference, Seoul (Korea) 2005.

5. M.Abbrescia et al., Proposal for a systematic study of the CERN closed loop gas system used by the RPC muon detectors in CMS, Frascati preprint LNF-06/26(IR).

6. C.Pucci, Master's Degree Thesis, University of Rome La Sapienza 2006 (in Italian). Frascati preprint LNF-06/31(Thesis).

KLOE

The KLOE-LNF Collaboration

A. Antonelli, M. Antonelli, G. Bencivenni, S. Bertolucci, C. Bloise(Resp.), F. Bossi, P. Campana, G. Capon, S. Chi, P. Ciambrone, E. De Lucia(Art.23), P. De Simone, S. Dell'Agnello, M. Dreucci(Art.2222), G. Felici, G. Finocchiaro, C.Forti, C. Gatti(art.36) S. Giovannella, G. Lanfranchi, J. Lee-Franzini, M. Martini(Dott.), S. Miscetti, M. Moulson, S. Müller, F. Murtas, M. Palutan, V. Patera(Ass.)*, P. Santangelo, B. Sciascia(art.23), A. Sciubba(Ass.)*, I. Sfiligoi, T. Spadaro, G. Venanzoni, R. Versaci

**Also Dipartimento di Energetica, "La Sapienza" University, Rome*

The KLOE-LNF Technical Staff

M. Anelli, A. Balla, G. Fortugno, R. Rosellini, M. Santoni

1 Overview

On March, 2006, KLOE has completed the data taking at DAϕNE after 23 months of continuous running. During this time, about 2 fb^{-1} of integrated luminosity at the ϕ-peak, corresponding to the observation of some 6.2 billion ϕ decays, and more than 300 pb^{-1} of off-peak data, for studying resonance shape and for measuring hadronic cross section in absence of the 3π background from ϕ decays, have been collected. The efforts from KLOE and DAϕNE to maintain good data-taking conditions have resulted in collecting a large homogeneous data sample in terms of machine background, beam energy and detector performance. Smooth trigger and data-acquisition operations, and continuous running of detector calibration ensured high-quality data. At the beginning of the year, we have published several articles, mostly based on 20% of the collected sample, with new measurements that have been included in the 2006 edition of the PDG changing significantly the world averages of the kaon semileptonic branching fractions and thus the $|V_{us}|$ value, as well as the $|\epsilon|$ parameter, as a result of high precision reached in $K_L \to \pi\pi$ branching fraction (BR). During all year long we worked up about a challenge production of simulated data-sets, resulting in 3.7 billion of fully reconstructed ϕ decays. The production and the analyses on new samples have demanded the upgrade of data storage and the update of the data-handling software, successfully achieved thanks to the continuous efforts of few, fully dedicated people. Progress have been obtained in the analyses of the semileptonic form factors, on the $K_S \to \gamma\gamma$ channel and on $K_S \to e^+e^-$ decays. New upper limits on the CPT violation parameters have been published by the measurement of the time-dependent decay rates of the correlated neutral kaon pairs into $\pi^+\pi^-\pi^+\pi^-$ final state. A new measurement of the CP violating channel $K_L \to \pi^+\pi^-$ has been also published in PLB. More channels are being investigated, including among the others, $K\pi2$, $Ke2$, $K_S \to 3\pi$. In hadron physics, the f_0 study, with Dalitz plot analysis of the 2π decays, neutral and charged, has been finalized and published. A new measurement of the $\eta - \eta'$ mixing angle has been also completed. In the following, neutral and charged kaons are discussed in Sec. 2, and $f_0(980)$ and hadronic cross section are reviewed in Sec. 3.

2 Results in Kaon physics

In K_L sector, we have published the absolute measurement of the main K_L BR's, the measurement of $K_L \to \pi^+\pi^-$ and the slopes of semileptonic vector form factor from $K_L \to \pi e\nu$ decay. In K_S sector, we have published a new precise measurement of $\Gamma(K_S \to \pi^+\pi^-(\gamma))/\Gamma(K_S \to \pi^0\pi^0)$ and of semileptonic $K_S \to \pi e \nu$ decay, obtaining the first measurement of semileptonic charge asymmetry. All of these measurements have been included in the 2006 edition of Particle Data Group, greatly contributing to establish a more precise experimental picture in kaon physics.

In the same respect, KLOE is participating to a new working group created in the framework of the European network Flavia-net, on precise Standard Model (SM) tests in kaon decays. First goal of the working group is a new precise determination of V_{us}, joining the efforts from all involved, experimental and theoretical groups (see Sec. 2.1 for KLOE results).

During last year we were particularly focused on the study of the discrete symmetries. A new comprehensive analysis has been published by G. Isidori, G. D'Ambrosio and the KLOE Collaboration, in which we have used all of KLOE measurements to extract from Bell-Steinberger relation more precise CP- and CPT-violation parameters (Sec. 2.6).

Equally important is the first observation of quantum interference in the process $\phi \to K_S K_L$, giving improved limits on decoherence parameters, published on Physics Letter B (PLB) in November, 2006.

In parallel with all of these activities, a big effort has been devoted to carry on new analyses, allowing us to present to 2007 Winter conferences a new bunch of preliminary results: the scalar form factor in $K_L \to \pi \mu \nu$ decay, the BR($K_L \to \pi e \nu \gamma$), the BR($K_S \to \gamma\gamma$) and an improved upper limit on $K_S \to e^+e^-$ decay. The last two analyses, in particular, benefit of the large amount of data, ~ 2 fb^{-1}, integrated by KLOE during 2004 and 2005. These results are briefly discussed in Secs. 2.2 to 2.5.

2.1 Extraction of V_{us}

The CKM matrix element V_{us} can be extracted from the measurement of the semileptonic decay widths ($\Gamma = \mathrm{BR}/\tau$) and the most precise test of unitarity of the CKM matrix is performed from the first-row constraint: $1 - \Delta = |V_{\mathrm{ud}}|^2 + |V_{\mathrm{us}}|^2 + |V_{\mathrm{ub}}|^2$. Using V_{ud} from nuclear beta decays, a test of unitarity to one part per mil has been obtained, V_{ub} contributing only at the level of 10^{-5}. During 2006, this test has been improved by using KLOE results on K_L semileptonic decays and τ_{K_L} [1) 2)], the measurement of BR($K_S \to \pi e \nu$) [3)] and preliminary KLOE results for charged Kaon semileptonic decays; τ_{K_S} and τ_{K^+} have been taken from Ref. [4)]. V_{us} is proportional to the square root of the partial width of semileptonic Kaon decays , and can be parametrized as [5)]:

$$V_{\mathrm{us}} \times f_+^{K^0\pi^-}(0) = \left[\frac{192\pi^3\Gamma}{C_K^2 G_\mu^2 M_K^5 S_{\mathrm{ew}} I(\lambda'_+, \lambda''_+, \lambda_0, 0)}\right]^{1/2} \frac{1}{1+\delta_{\mathrm{em}}+\delta_{\mathrm{SU(2)}}}, \tag{1}$$

where $f_+^{K^0\pi^-}(0)$ is the vector form factor at zero momentum transfer and $I(\lambda'_+, \lambda''_+, \lambda_0, 0)$ is the result of the phase space integration after factorizing out $f_+^{K^0\pi^-}(0)$. In the above expression, long-distance radiative corrections for both, the form factor $f_+^{K^0\pi^-}$, and the phase space integral, have been factorized out and are included in the parameter δ_{em}, which amounts to $0.55 - 0.95 \times 10^{-2}$ for K_{e3} and $K_{\mu3}$ respectively, and $\delta_{\mathrm{SU(2)}}$, which amounts to 2.31×10^{-2} for charged Kaon decays [6)]. The short-distance electroweak corrections are included in the parameter $S_{\mathrm{ew}} = 1.0232$. [7)] λ'_+ and λ''_+ are the quadratic slopes of the vector form factor, and λ_0 is the slope of the scalar form factor. Using form factor slope averages from recent measurements by KLOE, KTeV [8)], ISTRA+ [9)], and NA48, we obtain:

$$\begin{aligned}
f_+^{K^0\pi^-}(0) \times V_{\mathrm{us}} &= 0.2155 \pm 0.0014 \;\text{ from }\; K_S \to \pi e \nu, \\
f_+^{K^0\pi^-}(0) \times V_{\mathrm{us}} &= 0.21572 \pm 0.00064 \;\text{ from }\; K_L \to \pi e \nu,
\end{aligned}$$

$$
\begin{aligned}
f_+^{K^0\pi^-}(0) \times V_{\rm us} &= 0.21633 \pm 0.00078 \text{ from } K_L \to \pi\mu\nu, \\
f_+^{K^0\pi^-}(0) \times V_{\rm us} &= 0.2171 \pm 0.0021 \text{ from } K^+ \to \pi e\nu, \\
f_+^{K^0\pi^-}(0) \times V_{\rm us} &= 0.2150 \pm 0.0028 \text{ from } K^+ \to \pi\mu\nu, \\
f_+^{K^0\pi^-}(0) \times V_{\rm us} &= 0.21595 \pm 0.00050 \text{ KLOE average.}
\end{aligned}
$$

Using $V_{\rm ud} = 0.97377 \pm 0.00027$ from Ref. [10] and $f_+^{K^0\pi^-}(0) = 0.961 \pm 0.008$ from Ref. [11] (value in agreement also with recent lattice calculations), we obtain the unitarity test:

$$
\Delta = 1 - V_{\rm us}^2 - V_{\rm ud}^2 = (-13 \pm 10) \times 10^{-4}. \tag{2}
$$

2.2 Measurement of the scalar Form-Factor slope for $K_L \to \pi\mu\nu$

Semileptonic kaon decays, $K_L \to \pi^\pm \ell^\mp \nu$, offer the cleanest way to obtain an accurate value of the Cabibbo angle, or better, V_{us}. Since $K \to \pi$ is a $0^- \to 0^-$ transition, only the vector part of the weak current gives a no-vanishing contribution. The transition is therefore protected by the Ademollo-Gatto theorem [12] against SU(3) breaking corrections to lowest order. At present, the largest uncertainty in calculating V_{us} from the decay rate, is due to the difficulties in computing the matrix element $\langle \pi | j_\mu | K \rangle$. In the following, we will use the notation in which P, p, k and k' are the kaon, pion, muon and neutrino momenta, respectively; m is the mass of the charged pion, and M that of the neutral kaon. Therefore:

$$
\langle \pi | J_\mu^V | K \rangle \quad = \quad [(P+p)_\mu f_+(t) + (P-p)_\mu f_-(t)]
$$

where $t = (P-p)^2 = (k+k')^2 = M^2 + m^2 - 2ME_\pi$ is the only L-invariant variable. It is customary to expand the vector form factor $f_+(t)$ as

$$
f_+(t) = f_+(0) \left[1 + \lambda'_+ \frac{t}{m^2} + \frac{1}{2} \lambda''_+ \left(\frac{t}{m^2} \right)^2 + \ldots \right], \tag{3}
$$

where only linear and quadratic terms are retained. In the above expression, the form factor at zero momentum transfer, $f_+(0)$, is evaluated from theory, while the form factor slopes, λ'_+ and λ''_+, are experimentally determined from semileptonic decay spectra.

A scalar form factor $f_0(t)$ is introduced in the parametrization of $f_-(t)$, defined as $f_-(t) = (f_0(t) - f_+(t))(M^2 - m^2)/t$ with $f_0(0) = f_+(0)$. As in the case of the vector form factor, the scalar form factor is expanded in powers of momentum transfer t

$$
f_0(t) = f_0(0) \left[1 + \lambda'_0 \frac{t}{m^2} + \ldots \right], \tag{4}
$$

where only the linear term is retained. Simulation studies shows that the best sensitivity to the scalar form factor slope is obtained by using the neutrino energy spectra. Using ~ 330 pb^{-1} of integrated luminosity we have obtained the preliminary result:

$$
\lambda'_0 = (15.7 \pm 1.7_{\rm stat} \pm 1.9_{\rm syst}) \times 10^{-3}, \tag{5}
$$

which is in good agreement with present world-average value [4].

2.3 Measurement of BR($K_L \to \pi e \nu \gamma$)

The study of radiative K_L decays offers the possibility to obtain information on kaon structure and to test predictions of the Chiral Perturbation Theory (χPT). Two different processes contribute to photon emission in $K_L \to \pi e \nu \gamma$ decay: the inner bremsstrahlung (IB) and the direct emission (DE). The latter describes photon radiation from intermediate hadronic states. In $K_L \to \pi e \nu \gamma$ decay, the IB component is much greater than the DE one, due to the smallness of the electron mass. Indeed, for null electron mass, the IB amplitude is infrared-divergent in the zero-limit of both, photon energy (E^*_γ), and photon emission angle (θ^*_γ) in the kaon rest frame. For testing theoretical predictions [13] and for comparison with the best experimental results achieved so far [14] [15], we have measured the ratio

$$R = \frac{\mathrm{BR}(K_L \to \pi e \nu \gamma; E^*_\gamma > 30\,\mathrm{MeV}, \theta^*_\gamma > 20^\circ)}{\mathrm{BR}(K_L \to \pi e \nu (\gamma))}. \tag{6}$$

With these cuts the theoretical predictions range between 0.95% and 0.99% . The DE contribution in any case results to be less than 1% of IB one.

To count the $K_L \to \pi e \nu \gamma$ events, we fit the observed photon energy spectrum with Monte Carlo (MC) shapes for signal and various kinds of background (see Fig. 1). A preliminary mea-

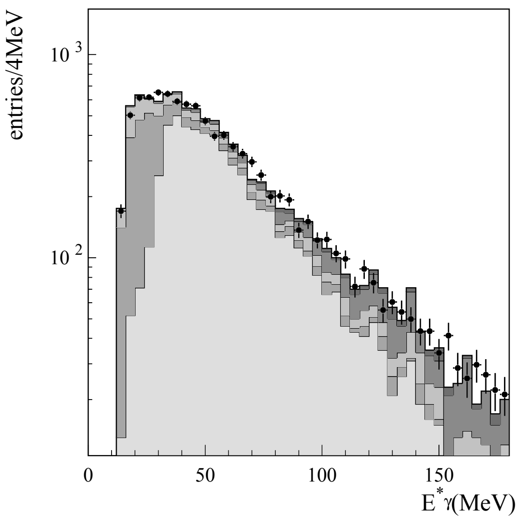

Figure 1: Photon energy spectrum observed in $K_L \to \pi e \nu \gamma$ decays; data are represented by black points, MC shapes for signal (light gray) and background contribution added to signal (dark gray) are also reported.

surement of R has been obtained by analysing 2001-2002 data sample; we get:

$$R = (0.92 \pm 0.02)\%. \tag{7}$$

A preliminary estimate of DE component gives $BR_{DE} < 2.5 \times 10^{-5}$, at 90% confidence level (C.L.).

2.4 Measurement of BR($K_S \to \gamma\gamma$)

Precise measurement of the $K_S \to \gamma\gamma$ branching ratio is of interest for χPT. The decay amplitude can be evaluated at leading $\mathcal{O}(p^4)$ order of χPT providing an estimate of the BR for this decay of $(2.1 \pm 0.1) \times 10^{-6}$ [16]. The latest experimental determination of BR($K_S \to \gamma\gamma$) is a precise measurement from NA48, $(2.78{\pm}0.07){\times}10^{-6}$ [17], which differs by about 30% from $\mathcal{O}(p^4)$ prediction of χPT, indicating the presence of important contributions from higher order corrections.

KLOE analysis on 1.6 fb^{-1} of integrated luminosity benefits from the tagging technique, which allows for the first time this decay to be identified with a pure K_S "beam", without the background from $K_L \to \gamma\gamma$ decay, and with completely different systematics with respect to fixed target experiments. Event counting is performed on the plane defined by $M_{\gamma\gamma}$, the two-photon invariant mass, and $\cos(\theta^*_{\gamma\gamma})$, $\theta^*_{\gamma\gamma}$ being the angle between photon momenta in the K_S rest frame. In this plane, the best separation between the signal and the main source of background, which is represented by $K_S \to \pi^0\pi^0$ events with two missing photons, is achieved. The observed $M_{\gamma\gamma}$ spectrum with superimposed fit using MC-predicted shapes for signal and background components, is shown in Fig. 2. We have obtained the preliminary result:

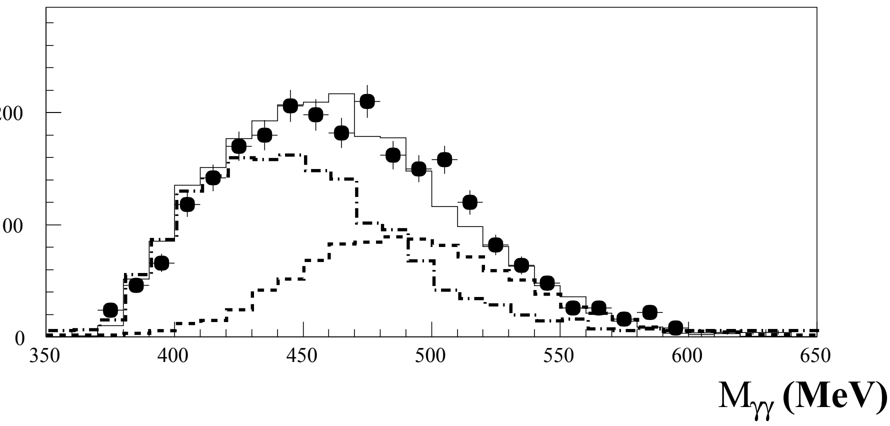

Figure 2: Two-photon invariant mass as observed at the end of $K_S \to \gamma\gamma$ selection procedure; black points are data, dashed and dot-dashed lines signal and background components, respectively, obtained using MC-predicted shapes for both contributions.

$$\mathrm{BR}(K_S \to \gamma\gamma) = (2.35 \pm 0.14) \times 10^{-6}, \tag{8}$$

which is 2.7σ less than NA48 measurement and 1.5σ greater than the value obtained from $\mathcal{O}(p^4)$ calculations in χPT.

2.5 Direct search of $K_S \to e^+e^-$

$K_S \to e^+e^-$ decay is a $\Delta S = 1$ weak neutral current process. The Standard Model expectation is BR($K_S \to e^+e^-$) $= 1.6 \times 10^{-15}$, which has been evaluated [18] by χPT with $\sim$ 10% error. The best experimental limit on this decay, from CPLEAR, is BR($K_S \to e^+e^-$) $< 1.4 \times 10^{-7}$, at 90% C.L. [19].

We have performed a direct search for $K_S \to e^+e^-$ decays by analysing 1.3 fb^{-1} of data belonging to the whole KLOE data taking period. The analysis exploits the KLOE drift chamber (DC) momentum resolution to identify the signal by e^+e^- invariant mass (M_{inv}) reconstruction. Further background rejection comes from calorimeter (EMC) particle identification, which is based on time of flight, shower depth and E/p measurements; all of this information is used to build a χ^2 function, peaking at low values for e^+e^- final states. In Fig. 3 the scatter plot of χ^2 versus

M_{inv} is shown for MC signal and background events. Optimized selection cuts in this plane give as preliminary result the upper limit on $K_S \to e^+e^-$ decay:

$$\mathrm{BR}(K_S \to e^+e^-) < 2.1 \times 10^{-8}, \quad \text{at } 90\% \text{ C.L.}. \tag{9}$$

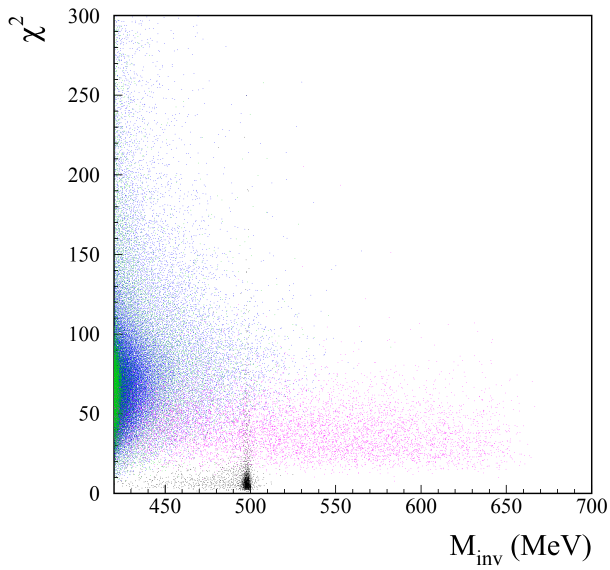

Figure 3: MC events as observed in $M_{inv} - \chi^2$ plane: points clustering at low χ^2 values and $M_{inv} = 500\ MeV$ are $K_S \to e^+e^-$ events, while those at low M_{inv} values belong to $K_S \to \pi^+\pi^-(\gamma)$ background, and those spread out over the entire M_{inv} window are $\phi \to \pi^+\pi^-\pi^0$ decays.

2.6 CP, CPT violation parameters using Bell-Steinberger relation

The three discrete symmetries of quantum mechanics, charge conjugation (C), parity (P) and time reversal (T), are known to be violated in nature, both, separately, and in bilinear combination. Only CPT appears to be an exact symmetry of nature. Exact CPT invariance holds in quantum field theory, under assumption of Lorentz invariance, locality and unitarity [20]. Testing the validity of CPT invariance therefore probes the most fundamental assumptions of our present understanding of particles and their interactions.

The neutral kaon system offers unique possibilities for the study of CPT invariance. From the requirement of unitarity, Bell and Steinberger have derived a relation (BSR) [21], which connects possible violation of CPT invariance ($m_{K^0} \neq m_{\bar{K}^0}$ and/or $\Gamma_{K^0} \neq \Gamma_{\bar{K}^0}$) in the time-evolution of the K^0-$\bar{K}^0$ system to the observable CP-violating interference of K_L and K_S decaying into same final state f. Strictly speaking, the BSR links the $CP-$ and $CPT-$violating parameters $\mathrm{Re}(\epsilon)$, $\mathrm{Im}(\delta)$ with the physical K_S and K_L decay amplitudes, $\mathcal{A}_S(f)$ and $\mathcal{A}_L(f)$:

$$\left(\frac{\Gamma_S + \Gamma_L}{\Gamma_S - \Gamma_L} + i \tan\phi_{\mathrm{SW}}\right)\left(\frac{\mathrm{Re}(\epsilon)}{1+|\epsilon|^2} - i\mathrm{Im}(\delta)\right) = \frac{1}{\Gamma_S - \Gamma_L}\sum_f \mathcal{A}_L(f)\mathcal{A}_S^*(f), \tag{10}$$

where $\phi_{\rm SW} = \arctan\big(2(m_L - m_S)/(\Gamma_S - \Gamma_L)\big)$. The advantage of the neutral kaon system is that only the $\pi\pi(\gamma)$, $\pi\pi\pi$ and $\pi\ell\nu$ decay modes give significant contributions to the right hand side of Eq. 10.

A phenomenological analysis has been published by KLOE during 2006, in which recent results from the KLOE experiment [1) 2) 3) 22) 23) 24)] have been used to improve the determination of the Re(ϵ) and Im(δ). Our analysis benefits in particular from three new measurements: i) the branching ratio BR($K_L \to \pi^+\pi^-$), which is relevant for the determination of Re(ϵ); ii) the new upper limit on BR($K_S \to \pi^0\pi^0\pi^0$), which is necessary to improve the accuracy on Im(δ); and iii) the measurement of the K_S semileptonic charge aymmetry A_S, which allows, for the first time, the complete determination of the contribution from semileptonic decay channels. We find

$$\mathrm{Re}(\epsilon) = (159.6 \pm 1.3) \times 10^{-5}, \qquad \mathrm{Im}(\delta) = (0.4 \pm 2.1) \times 10^{-5}\,. \tag{11}$$

The allowed region in the Re(ϵ), Im(δ) plane at 68% C.L. and 95% C.L. is shown in the left panel of Fig. 4. Our results, Eq. 11, improve by a factor of two previous experimental sensitivity [25)]. The limits on Im(δ) and Re(ϵ) can be used to constrain the mass and width difference between

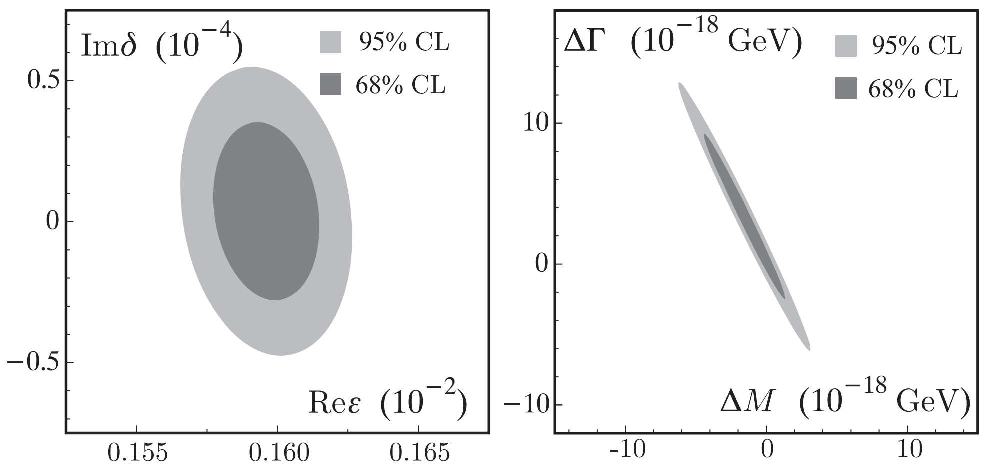

Figure 4: Left: allowed region at 68% and 95% C.L. in the Re(ϵ), Im(δ) plane. Right: allowed region at 68% and 95% C.L. in the ΔM, $\Delta\Gamma$ plane.

K^0 and $\bar{K}^0$. The allowed region in the $\Delta M = (m_{K^0} - m_{\bar{K}^0})$, $\Delta\Gamma = (\Gamma_{K^0} - \Gamma_{\bar{K}^0})$ plane is shown in the right panel of Fig. 4. Since total decay width is dominated by long-distance dynamics, in models where CPT invariance is a pure short-distance phenomenon, it is natural to consider the limit $\Gamma_{K^0} = \Gamma_{\bar{K}^0}$. In this limit (i.e. neglecting $CPT-$violating effects in the decay amplitudes), we obtain for neutral kaon mass difference:

$$-5.3 \times 10^{-19}\ \mathrm{GeV} < m_{K^0} - m_{\bar{K}^0} < 6.3 \times 10^{-19}\ \mathrm{GeV}, \quad \text{at 95 \% C.L.}\,.$$

2.7 First observation of QM interference in $\phi \to K_S K_L \to \pi^+\pi^-\pi^+\pi^-$

A ϕ-factory provides unique opportunities for testing quantum mechanics (QM) and CPT symmetry. In the decay $\phi \to K^0\bar{K}^0$, the neutral kaon pair is produced in a $J^{PC} = 1^{--}$ state:

$$|\,i\rangle \;\; = \;\; \frac{1}{\sqrt{2}}\,\big(|K^0,\,\mathbf{p}\rangle|\bar{K}^0,-\mathbf{p}\rangle - |\bar{K}^0,\,\mathbf{p}\rangle|K^0,\,-\mathbf{p}\rangle\big)$$

$$= \frac{N}{\sqrt{2}} \left(|K_S,\ \mathbf{p}\rangle |K_L, -\mathbf{p}\rangle - |K_L,\ \mathbf{p}\rangle |K_S,\ -\mathbf{p}\rangle \right) \tag{12}$$

where $\mathbf{p}$ is the kaon momentum in the ϕ meson rest frame, and $N = (1 + |\epsilon|^2)/(1 - \epsilon^2)$.

The decay intensity for the process $\phi \to$(2 neutral kaons)$\to \pi^+\pi^-$, $\pi^+\pi^-$ is then given by [26]:

$$\begin{aligned} I(t_1,\ t_2) &= \frac{1}{2} \left| \langle \pi^+\pi^- | K_S \rangle \right|^4 |\eta_{+-}|^2 \Big(e^{-\Gamma_L t_1 - \Gamma_S t_2} + e^{-\Gamma_S t_1 - \Gamma_L t_2} \\ &\qquad - 2 e^{-(\Gamma_S + \Gamma_L)(t_1+t_2)/2} \cos\left(\Delta m\, (t_1 - t_2) \right) \Big) \end{aligned} \tag{13}$$

where t_i are proper times of the two kaon decays, Γ_S and Γ_L are the decay widths of K_S and K_L, $\Delta m = m_L - m_S$ is their mass difference and $\eta_{+-} = \langle \pi^+\pi^- | K_L \rangle / \langle \pi^+\pi^- | K_S \rangle = |\eta_{+-}| e^{i\phi_{+-}}$. The two kaons cannot decay into the same final state at the same time, even though the two decays are space-like separated events. Correlations of this type in QM were first pointed out by Einstein, Podolsky, and Rosen (EPR) [27].

While it is not obvious what a deviation from QM might be, the assumption that coherence is lost during time evolution of QM states, does violate QM. One can therefore introduce a decoherence parameter ζ [28], simply multiplying the interference term in Eq.(13) by a factor of $(1-\zeta)$. The meaning and value of ζ depend on the basis in which the initial state (12) is written. Eq. (13) is modified as follows:

$$\begin{aligned} I(t_1, t_2; \zeta_{SL}) &= \frac{1}{2} \left| \langle \pi^+\pi^- | K_S \rangle \right|^4 |\eta_{+-}|^2 \Big(e^{-\Gamma_L t_1 - \Gamma_S t_2} + e^{-\Gamma_S t_1 - \Gamma_L t_2} \\ &\qquad - 2\,(1 - \zeta_{SL})\, e^{-(\Gamma_S + \Gamma_L)(t_1+t_2)/2} \cos\left(\Delta m\, (t_1 - t_2) \right) \Big) \end{aligned} \tag{14}$$

in the K_S-K_L basis, and:

$$\begin{aligned} I(t_1, t_2; \zeta_{0\bar{0}}) &= \frac{1}{2} \left| \langle \pi^+\pi^- | K_S \rangle \right|^4 |\eta_{+-}|^2 \Big(e^{-\Gamma_L t_1 - \Gamma_S t_2} + e^{-\Gamma_S t_1 - \Gamma_L t_2} \\ &- 2 e^{-(\Gamma_S + \Gamma_L)(t_1+t_2)/2} \cos\left(\Delta m\, (t_1 - t_2) \right) \\ &+ \frac{\zeta_{0\bar{0}}}{2} \Big(- e^{-\Gamma_L t_1 - \Gamma_S t_2} - e^{-\Gamma_S t_1 - \Gamma_L t_2} \\ &+ 2 e^{-(\Gamma_S + \Gamma_L)(t_1+t_2)/2} \left(\cos\left(\Delta m (t_1 - t_2) \right) - \cos\left(\Delta m (t_1 + t_2) \right) \right) \Big) \\ &+ \frac{1}{2} \frac{\zeta_{0\bar{0}}}{|\eta_{+-}|^2} e^{-\Gamma_S (t_1+t_2)} \Big) \quad \text{to the lowest order in } |\eta_{+-}|, \end{aligned} \tag{15}$$

in the K^0-$\bar{K}^0$ basis.

KLOE has recently published the analysis on quantum interference based on data acquired during 2001-2002. From about 5×10^4 neutral kaon pairs both decaying to $\pi^+\pi^-$ pairs we obtain the distribution of Δt, the difference between the two kaon decay times, which is shown in Fig. 5. We fit the observed $\Delta t = |t_1 - t_2|$ distribution between 0 and 35 τ_S with decay intensity derived from Eqs. 14 and 15, after having integrated over the sum, $t_1 + t_2$, for fixed Δt and including the contribution from regeneration. From the fit we have obtained the decoherence parameter values:

$$\begin{aligned} \zeta_{SL} &= 0.018 \pm 0.040_{\text{stat}} \pm 0.007_{\text{syst}} & \chi^2/\text{dof} = 29.7/32; \\ \zeta_{0\bar{0}} &= \left(0.10 \pm 0.21_{\text{stat}} \pm 0.04_{\text{syst}} \right) \times 10^{-5} & \chi^2/\text{dof} = 29.6/32. \end{aligned}$$

which are consistent with $\zeta = 0$ and no QM modification. The above results represent a considerable improvement on those obtained from CPLEAR [29].

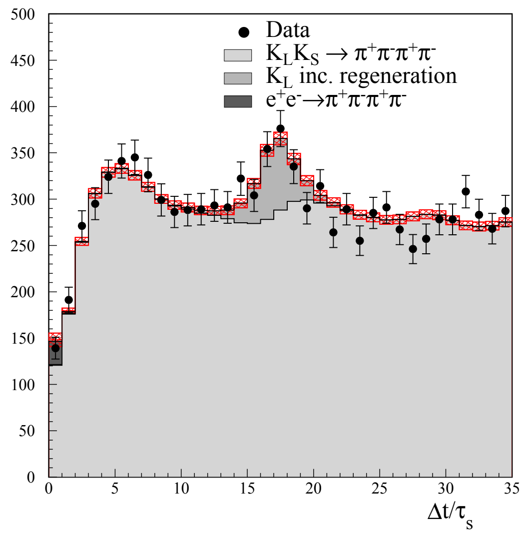

Figure 5: Δt distribution from the fit used to determine ζ_{SL}; the black points with errors are data and the solid histogram is the fit result; the uncertainty arising from the efficiency correction is shown as the hatched area.

2.8 The absolute branching ratio $K^\pm \to \pi^\pm\pi^0$

A new precise measurement of the absolute $K^\pm \to \pi^\pm\pi^0(\gamma)$ BR, fully inclusive of radiative decays, has an impact also on the world average of the semileptonic BR's because NA48, ISTRA+ and E865 experiments use $\pi^+\pi^0$ decay in the normalization sample. A pure K^+ beam is tagged at KLOE by reconstruction of $K^- \to \mu\nu$ decays. Signal counting is given by a fit to the distribution, shown in Fig.6, of the charged-particle momentum in the kaon rest frame, under the pion-mass hypothesis, taking into account all the contributing processes to the spectrum, i.e. $\pi^+\pi^0$, $\mu\nu$ and three-body decays. The shape of the background contribution from $K_{\mu 2}$ decays has been obtained in our previous work, published in PLB [30]. For three-body decays we have used MC-predicted shapes.

The selection efficiency has been evaluated directly on data, using as control sample $K^+ \to X^+\pi^0$ events selected by π^0 reconstruction, requiring that the neutral vertex is on the K^+ flight path as given by tag reconstruction.

At present, a precise evaluation on data of the signal shape is underway, including also the comparison among different control samples.

2.9 The measurement of the $K^\pm$ lifetime

$K^\pm$ lifetime is an experimental input to the determination of V_{us}, and affects, through the evaluation of the geometrical acceptance, also the BR measurements. The present fractional uncertainty is about 0.2%; however available data show large discrepancies between "in-flight" [31] and "at-rest" [32] measurements.

Two different methods for the measurement of the $K^\pm$ lifetime, $\tau_{K^\pm}$, have been exploited at KLOE. The first is based on the measurement of the decay lengths, from the reconstruction of the charged vertices in the drift chamber, DC. The other method uses the decay times of the kaons, obtained by the calorimeter time reconstruction of the photons from $K^\pm \to X^\pm\pi^0$ decays.

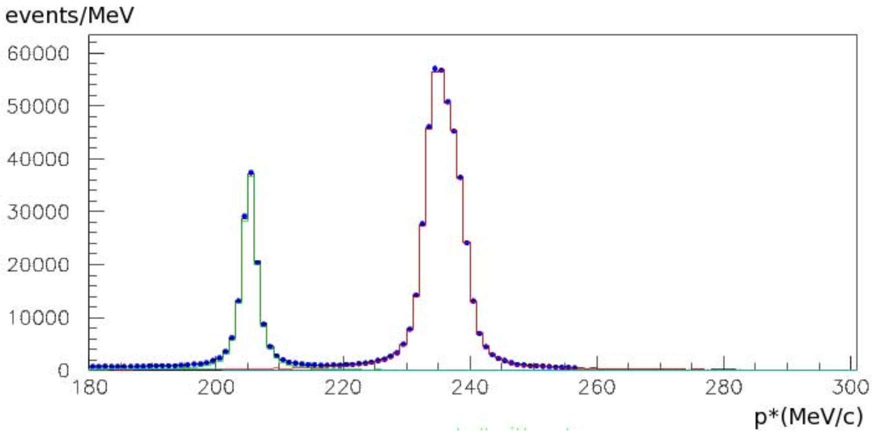

Figure 6: Distribution of charged particle momentum from K^+ decays, in the kaon rest frame, under the pion-mass hypothesis.

With both methods we have reached accuracies of a few per mil. They are independent and their comparison is really useful to assess part of systematics. The signal events are tagged by $K_{\mu 2}$ decays. With the first method, the fit to the proper-time distribution and the evaluation on data of the vertex-reconstruction efficiency and resolution effects, has given the preliminary result,

$$\tau_{K^+} = (12.367 \pm 0.044_{\text{stat}} \pm 0.065_{\text{syst}}) \text{ ns},$$

with $\chi^2/\text{dof} = 17.7/15$. With the second method we have obtained a proper-time distribution that is in agreement with the result from charged vertex measurement. We are finalizing the evaluation of tiny corrections and systematics coming from selection efficiency, resolution effects and background contaminations.

3 Results in hadronic physics

3.1 Dalitz plot analysis of $e^+e^- \to \pi^0\pi^0\gamma$ events

The Dalitz plot of the $e^+e^- \to \pi^0\pi^0\gamma$ events at center of mass energy ($\sqrt{s}$) around M_ϕ has been studied with ~ 410 pb^{-1} of e^+e^- collisions collected during the 2001-2002 data taking [33]. Events are divided in $\sqrt{s}$ bin of 100 keV. The sample with higher statistics ($\sqrt{s} = 1019.75$ MeV), corresponding to $\sim 65,000$ events, has been used to fit data with two different theory models. The two kinematic variables used to describe the Dalitz plot are the invariant mass of the two reconstructed π^0, $M_{\pi\pi}$, and the invariant mass of each π^0 and the radiative photon, $M_{\pi\gamma}$. There are therefore two entries per event. In Fig. 7 the reconstructed Dalitz plot is shown for the data sample after background subtraction. The two bands at $M_{\pi\pi}$ masses below 700 MeV are due to the non-resonant process $e^+e^- \to \omega\pi^0$ with $\omega \to \pi^0\gamma$ whereas, for higher $M_{\pi\pi}$ values, the radiative ϕ decay to a scalar meson is the dominant mechanism.

The sample is selected with high efficiency by requiring five prompt photons in the events with loose energy and angular cuts to maximize the acceptance and the efficiency for low energy photons. A two steps procedure of kinematic fitting is used. It first imposes the 4-momentum conservation of the ϕ meson and the time of flight of the photons; it then pairs photons to π^0's

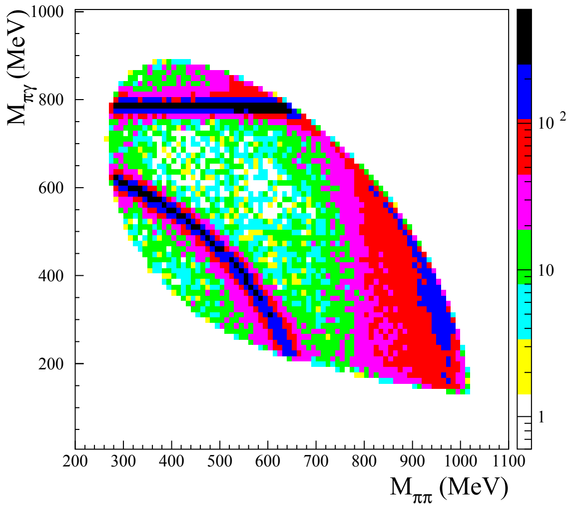

Figure 7: Dalitz plot in logarithmic scale after background subraction.

and constrains also the π^0 masses, thus largely improving the photon energy resolution. At the end of the fitting procedure the invariant $\pi^0\pi^0$ mass is reconstructed with a resolution of 5-6 MeV. Different from the previous published analysis [34], the pairing of photons to π^0's has been done without considering the intermediate state of the process. This allows to consider in the fit to the Dalitz plot all possible interferences between the considered intermediate processes.

In the fit to the Dalitz plot, the not resonant contribution is described by standard VMD [35]. For the resonant term we used two different models. In the Kaon Loop (KL) model [36] the scalar propagator, due both to the $f_0(980)$ and a wide $\sigma(600)$, is coupled to the ϕ through a kaon loop which provides a dumping of the cross section at low $M_{\pi\pi}$. There are ten fit variants due to the different $\sigma(600)$ parameters used. In the No Structure model [37] the scalar has a pointlike coupling to the ϕ with a simpler propagator. A single particle, the $f_0(980)$, is used. In this formulation the low mass $M_{\pi\pi}$ behaviour is described by three free parameters, representing the continuum background.

For each model, the $f_0(980)$ mass and its coupling to $\pi\pi$, $K\overline{K}$ and to the ϕ, are extracted. For the Kaon Loop only six variants of the fit originate acceptable $P(\chi^2)$ and are therefore considered, producing an extra error associated with the theoretical model. This last error is evaluated as the maximum variation between the central value obtained by the best fit and the other five accepted fits. The systematics on the extracted parameters are estimated by repeating the fit when varying the normalization scale, the photon efficiency curve, the smearing matrix and the background contribution. In Tab. 1 the main parameters extracted for both models are reported. For both models, the resulting fit curve reproduces also the mass spectrum of all other $\sqrt{s}$ bins around M_ϕ.

The extracted couplings show that the Kaon Loop model provides a stable description of the data with large coupling of $f_0(980)$ to kaons, as also indicated by the study of the $\pi^+\pi^-\gamma$ final state [38]. Therefore, these results add evidences to a 4-quark structure of the $f_0(980)$ meson. On the other hand, in the fit with the No Structure model the $f_0(980)$ coupling to kaons get substantially reduced with respect to what found in the $\pi^+\pi^-\gamma$ channel. However, the physical interpretation is

Parameter	Kaon Loop	No Structure
M_{f_0} (MeV)	$976.8 \pm 0.3_{\rm fit}\,{}^{+0.9}_{-0.6}{}_{\rm syst} + 10.1_{\rm mod}$	$984.7 \pm 0.4_{\rm fit}\,{}^{+2.4}_{-3.7}{}_{\rm syst}$
$g_{f_0 K^+K^-}$ (GeV)	$3.76 \pm 0.04_{\rm fit}\,{}^{+0.15}_{-0.08}{}_{\rm syst}\,{}^{+1.16}_{-0.48}{}_{\rm mod}$	$0.40 \pm 0.04_{\rm fit}\,{}^{+0.62}_{-0.29}{}_{\rm syst}$
$g_{f_0 \pi^+\pi^-}$ (GeV)	$-1.43 \pm 0.01_{\rm fit}\,{}^{+0.01}_{-0.06}{}_{\rm syst}\,{}^{+0.03}_{-0.60}{}_{\rm mod}$	$1.31 \pm 0.01_{\rm fit}\,{}^{+0.09}_{-0.03}{}_{\rm syst}$
$g_{\phi f_0 \gamma}$ (GeV^{-1})	$2.78\,{}^{+0.02}_{-0.05}{}_{\rm fit}\,{}^{+0.13}_{-0.05}{}_{\rm syst} + 1.31_{\rm mod}$	$2.61 \pm 0.02_{\rm fit}\,{}^{+0.31}_{-0.08}{}_{\rm syst}$

Table 1: Fit parameters for both KL and NS models.

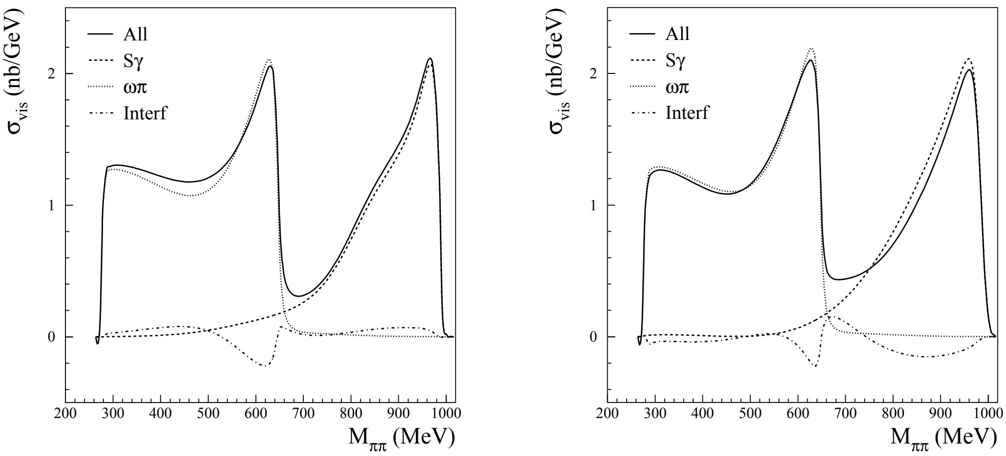

Figure 8: Resulting $\pi^0\pi^0\gamma$ contributions for Kaon Loop (left) and No Structure (right) models.

more difficult due to the presence of the continuum background which differs substantially in the $\pi^0\pi^0$ and $\pi^+\pi^-$ cases.

To understand the relative importance of the different fitting terms, their contributions are shown in Fig. 8. As expected, the VMD (scalar) term is dominating in the region below (above) 700 MeV. The interference term is concentrated around 600 MeV.

By integrating the KL, NS distributions and normalizing to the ϕ production cross section, an effective BR for the $\phi \to S\gamma \to \pi^0\pi^0\gamma$ process is extracted:

$$\mathrm{BR}(\phi \to S\gamma \to \pi^0\pi^0\gamma) = (1.07\,{}^{+0.01}_{-0.03}{}_{\rm fit}\,{}^{+0.04}_{-0.02}{}_{\rm syst}\,{}^{+0.05}_{-0.06}{}_{\rm mod}) \times 10^{-4} \tag{16}$$

The central value is given by the KL model with the best $P(\chi^2)$; the fit error has been evaluated as the maximum variation on the branching ratio obtained when varying the results of the fit of the Dalitz plot by $\pm 1\sigma$, and the model error corresponds to the maximum variation of the central value with respect to the other five accepted fit results of the KL model and to the NS description.

3.2 The measurement of the hadronic cross section

In 2006, the analysis of $\pi^+\pi^-\gamma$ final state for the measurement of the hadronic cross section, relevant for calculating the muon anomaly, has been focused on two aspects:

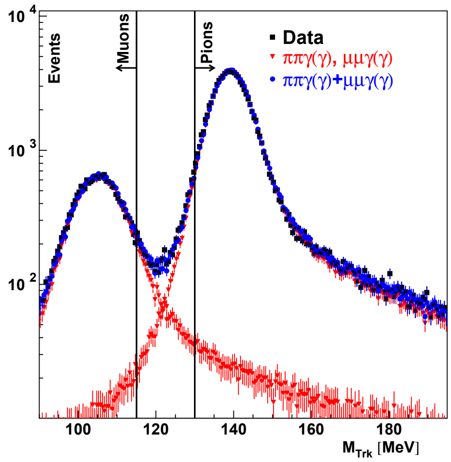

Figure 9: Trackmass distribution of data with MC-predicted shapes of $\mu\mu\gamma(\gamma)$ and $\pi\pi\gamma(\gamma)$ events in the region $0.72 < M^2_{\pi\pi} < 0.74$ GeV^2. The cuts used to separate pions from muons are also shown.

- the improvement of our published analysis [39], using 240 pb^{-1} and working on the optimization of systematics, normalising to the Bhabha sample;
- a new analysis, selecting muons from the process $e^+e^- \to \mu^+\mu^-\gamma(\gamma)$ to extract the hadronic cross section from the ratio $\frac{d\sigma(e^+e^-\to\pi^+\pi^-\gamma(\gamma))}{ds'} / \frac{d\sigma(e^+e^-\to\mu^+\mu^-\gamma(\gamma))}{ds'}$

On the first point, improvements have been already obtained thanks to the cleaner and more stable running conditions, better trigger performance and the revision of reconstruction algorithms applied to the new data sample. Moreover, the methods used to evaluate background contamination and selection efficiencies have been studied and refined mostly for improving the control of systematics. The *trackmass*[1], m_{trk}, distribution from data is shown in Fig. 9. The superimposed fit results have been obtained using MC-predicted shapes for $\mu\mu\gamma$ and $\pi\pi\gamma$ events.

Main issue of the second point is muon identification and separation from pion events. It has been addressed using as discriminating variable m_{trk} and putting a cut so that the events with $m_{trk} < 115\ MeV$ are considered as muons, and events with $m_{trk} > 130\ MeV$ as pions (see Fig. 9). Fig. 10 shows the number of signal events obtained both, for pion, and muon samples, together with the background contributions estimated from MC simulations. To obtain an independent control sample for the muons, we have used a pion-muon identifier based on a neural net mostly based on calorimeter information. The procedure is extremely useful to evaluate selection efficiencies for the muon analysis.

For both analyses we are studying procedures to understand and keep under control systematic effects. Special care has been put, in close collaboration with the theorists, on the treatment of radiative corrections.

Additional work, in collaboration with the LNF theory group, has been undertaken in order to create a Monte Carlo generator including a detailed description of the $\pi^+\pi^-\gamma$ final state [40].

[1]Defined under the hypothesis that the final state consists of two charged particles with equal mass m_{trk} and one photon.

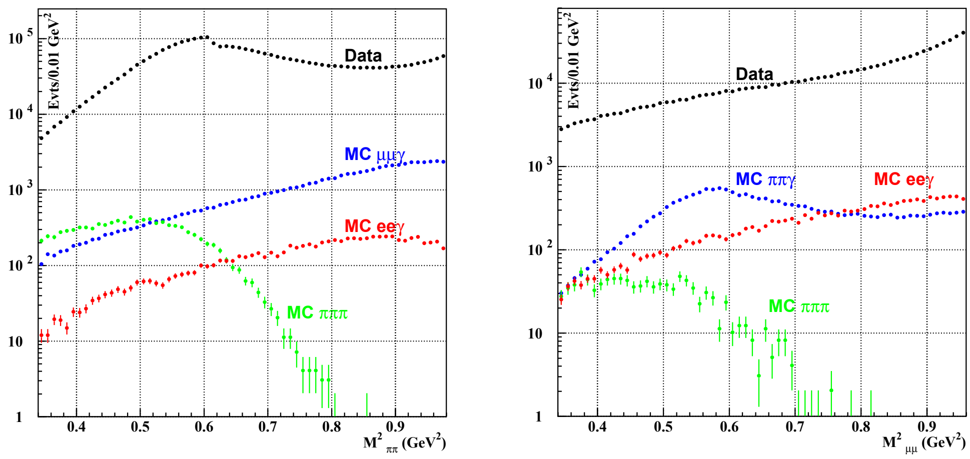

Figure 10: Number of $\pi\pi\gamma(\gamma)$ (left) and $\mu\mu\gamma(\gamma)$ events (right) obtained from 242 pb^{-1} of data, with MC expectation for background contributions.

4 KLOE papers in year 2006

1. *F. Ambrosino et al.*, "Measurement of the absolute branching ratios for the dominant K_L decays, the K_L lifetime, and V_{us} with the KLOE detector", Phys. Lett **B632** (2006) 43.

2. *F. Ambrosino et al.*, "Measurement of the $K^+ \to \mu^+\nu$ decay with the KLOE detector", Phys. Lett **B632** (2006) 76.

3. *F. Ambrosino et al.*, "Study of the decay $\phi \to f_0(980)\gamma \to \pi^+\pi^-\gamma$ with the KLOE detector", Phys. Lett **B634** (2006) 148.

4. *F. Ambrosino et al.*, "Measurement of the form-factor slopes for the decay $K_L \to \pi^\pm e^\mp \nu$ with the KLOE detector", Phys.Lett.B636:166-172,2006.

5. *F. Ambrosino et al.*, "Measurement of the branching ratio of the $K_L \to \pi^+\pi^-$ decay with the KLOE detector", Phys.Lett.B638:140-145,2006.

6. *F. Ambrosino et al.*, "Measurement of the DAFNE luminosity with the KLOE detector using large angle Bhabha scattering", Eur.Phys.J.C47:589-596,2006.

7. *F. Ambrosino et al.*, "Study of the branching ratio and charge asymmetry for the decay $K_S \to \pi e\nu$ with the KLOE detector", Phys.Lett.B636:173-182,2006.

8. *F. Ambrosino et al.*, "Precise measurement of $\Gamma(K_S \to \pi^+\pi^-(\gamma))/\Gamma(K_S \to \pi^0\pi^0)$ with the KLOE detector at DAFNE", Eur.Phys.J.C48:767-780,2006.

9. *F. Ambrosino et al.*, "First observation of quantum interference in the process $\phi \to K_S K_L \to \pi^+\pi^-\pi^+\pi^-$: A Test of quantum mechanics and CPT symmetry", Phys.Lett.B642:315-321,2006.

10. *F. Ambrosino et al.*, "Determination of CP and CPT violation parameters in the neutral kaon system using the Bell-Steinberger relation and data from the KLOE experiment", JHEP 0612:011,2006.

11. *F. Ambrosino et al.*, "Dalitz plot analysis of $e^+e^- \to \pi^0\pi^0\gamma$ events at $\sqrt{s}$ approximately $M(\phi)$ with the KLOE detector", Eur.Phys.J.C49:473-488,2007.

5 Public notes in year 2006

1. C. Gatti, T. Spadaro, " Measurement of the branching fraction and the charge asymmetry for the decay $K_S \to \pi e \nu$" KLOE Note 208, January 2006.
2. C. Gatti, M. Palutan, T. Spadaro, "Measurement of $\Gamma(K_S \to \pi^+\pi^-(\gamma))/\Gamma(K_S \to \pi^0\pi^0)$ with 2001-2002 data", KLOE Note 209, January 2006.
3. M. Antonelli, M. Dreucci, C. Gatti, "Measurement of K_{e3} Semileptonic Form Factor Slope and Curvature and Pole in the Decay $K_L \to \pi^\pm e^\mp \nu$ at KLOE", KLOE Note 210, January 2006.
4. M. Antonelli, M. Testa, "Measurements of the Branching Ratio of the $K_L \to \pi^+\pi^-$ decay with the KLOE Detector, KLOE Note 211, March 2006.
5. S. Giovannella, S. Miscetti, "Study of the $e^+e^- \to \pi^0\pi^0\gamma$ process using 2001/2002 data", KLOE Note 212, August 2006.
6. S. Giovannella, S. Miscetti, "Fit to the $\pi^0\pi^0\gamma$ Dalitz plot", KLOE Note 213, August 2006.

6 Contributions to Conferences

1. *R. Versaci* , "Charged Kaons at KLOE", e+e- Collisions from phi to psi, Novosibirsk, February 27-March 2, 2006.
2. *B. Sciascia* , "Experimental Status and Future Perspectives on Vus", Discoveries in Flavour Physics at e+e- Colliders, Frascati, February 28-March 3, 2006.
3. *E. De Lucia* , "Kaon Physics at KLOE", Les Rencontres de Physique de la Vallee d'Aoste, La Thuile, March 5-11, 2006.
4. *M. Palutan* , "Kaon Physics at KLOE", Rencontres de Moriond, Electroweak Interactions and Unified Theories, La Thuile, March 11-18, 2006.
5. *M. Dreucci*, "Risultati di KLOE sui decadimenti dei K neutri", IFAE, Pavia, April 19-21, 2006.
6. *S. Giovannella*, "Highlights on Hadron Physics at KLOE", CIPANP06, Puerto Rico, May 30-June 3, 2006.
7. *P. De Simone*, "Status of Vus", CIPANP06, Puerto Rico, May 30-June 3, 2006.
8. *C. Gatti* , "Highlights on neutral Kaon Decays", BEACH2006, Lancaster, July 2-7, 2006.
9. *A. Antonelli* , "Semileptonic K decays: recent measurements on Vus", BEACH2006, Lancaster, July 2-7, 2006.
10. *B. Sciascia* , "Kaon Physics", Physics in Collisions, Buzios, July 6-9, 2006.
11. *M. Antonelli* , "Vus Measurement and CKM Unitarity", ICHEP06, Moscow, July 26-August 2, 2006.
12. *T. Spadaro* , "Recent KLOE Results", ICHEP06, Moscow, July 26-August 2, 2006.
13. *C. Bloise* , "Physics Highlights from KLOE", Final Euridice Workshop, Kazimierz, August 24-27, 2006.

14. *S. Mueller* , "The determination of sigma-hadronic with KLOE", Final Euridice Workshop, Kazimierz, August 24-27, 2006.

15. *C. Bloise* , "Recenti risultati dell'esperimento KLOE a DAFNE", Congresso nazionale della Societa' Italiana di Fisica, Torino, September 18-23, 2006.

16. *M. Moulson* , "Kaon Decays: Recent experimental Results", Chiral Dynamics, Chapel Hill, September 18-22, 2006.

17. *M. Martini* , "Results on light meson decays and dynamics at KLOE", Chiral Dynamics, Chapel Hill, September 18-22, 2006.

18. *G. Venanzoni*, "Status Report on the KLOE measurement of the hadronic cross section with ISR", Tau 2006, Pisa, September 19-22, 2006.

19. *R. Versaci* , "New results from KLOE", Heavy Quarks and Leptons, Munich, October 16-20, 2006.

20. *T. Spadaro* , "KLOE results on Kaon decays and summary status on Vus", Workshop on the CKM Unitarity Triangle, Nagoya, December 12-16,2006.

References

1. F. Ambrosino *et al.*, KLOE Collab., Phys. Lett. B632 (2006) 43.
2. F. Ambrosino *et al.*, KLOE Collab., Phys. Lett. B626 (2005) 15.
3. F. Ambrosino *et al.*, KLOE Collab., Phys. Lett. B636 (2006) 173.
4. W.-M. Yao *et al.*, Particle Data Group, Journal of Physics G33, 1 (2006).
5. M. Battaglia *et al.*, Workshop on the CKM Unitarity Triangle, Geneva, Switzerland, February 13-16 2002, CERN report 2003-002, hep-ph/0304132 (2003).
6. V. Cirigliano, H. Neufeld, H. Pichl, Eur. Phys. J. C35 (2004) 53.
7. A. Sirlin, Nucl. Phys. B196 (1982) 83.
8. T. Alexopoulos *et al.*, KTeV Collab., *Phys. Rev. Lett.* **93**, 181802 (2004).
9. O. P. Yushchenko *et al.*, ISTRA+ Collab., *Phys. Lett.* **B589**, 111 (2004).
10. A. Czarnecki, W. J. Marciano, A. Sirlin, Phys. Rev. D70 (2004) 093006.
11. H. Leutwyler, M. Roos, Z. Phys. C25 (1984) 91.
12. M. Ademollo, R. Gatto, Phys. Rev. Lett. 13 (1964) 264.
13. J. Gasser *et al.*, Eur. Phys. J. C40 (2005) 205.
14. T. Alexopoulos *et al.*, KTeV collab., Phys. Rev. D71 (2005) 012001.
15. A. Lai *et al.*, NA48 Collab., Phys. Lett. B605 (2005) 247.
16. G. D'Ambrosio and D. Espriu, Phys. Lett. B175 (1986) 237.
17. J.R. Batley *et al.*, NA48 Collab., Phys. Lett. B551 (2003).

18. G. Ecker and A. Pich, Nucl. Phys. B366 (1991) 189.

19. A. Angelopoulos *et al.*, CPLEAR Collab., Phys. Lett. B413 (1997) 232.

20. G. Lueders, Ann. Phys. (NY) 2 (1957) 1, reprinted in Ann. Phys. (NY) 281 (2000) 1004.

21. J.S. Bell and J. Steinberger, Proceedings Oxford Int. Conf. on Elementary Particles (1965).

22. F. Ambrosino *et al.*, KLOE Collab., Phys. Lett. B619 (2005) 61.

23. F. Ambrosino *et al.*, KLOE Collab., Eur. Phys. J C48 (2006) 767.

24. F. Ambrosino *et al.*, KLOE Collab., Phys. Lett. B638 (2006) 140.

25. A. Apostolakis *et al.*, CPLEAR Collab., Phys. Lett. B456 (1999) 297.

26. I. Dunietz, UJ. Hauser, J.L. Rosner, Phys. Rev. D35 (1987) 2166.

27. A. Einstein, B. Podolsky, N. Rosen, Phys. Rev. 47 (1934) 777.

28. P.H. Eberhard, The Second DAΦNE Handbook, vol.I, INFN-LNF, Frascati, 1995.

29. A. Apostolakis *et al.*, CPLEAR Collab., Phys. Lett. B422 (1998) 339.

30. F. Ambrosino *et al.*, KLOE Collab., Phys. Lett. B632 (2006) 76.

31. V.P. Koptev *et al.*, JETPL 61 (1995) 877; R.J. Ott and T.W. Pritchard, Phys. Rev. D3 (1971) 52.

32. F. Lobkowicz *et al.*, Phys. Rev. 185 (1969) 1676; V.L. Fitch *et al.*, Phys. Rev. 140B (1965) 1088.

33. F. Ambrosino *et al.*, KLOE Collab., Eur.Phys.J. C 49 (2007) 473.

34. A. Aloisio *et al.*, KLOE Collab., Phys. Lett. B 537 (2002) 21.

35. N. N. Achasov and A. V. Kiselev, private communication following [?] and [?].

36. N. N. Achasov and V. N. Ivanchenko, Nucl. Phys. B 315 (1989) 465.
N. N. Achasov and V. V. Gubin, Phys. Rev. D 56 (1997) 4084.
N. N. Achasov and A. V. Kiselev, Phys. Rev. D 73 (2006) 054029.

37. G. Isidori, L. Maiani, M. Nicolaci and S. Pacetti, J. High Energy Phys. 05 (2006) 049.

38. F. Ambrosino *et al.*, KLOE Collab., Phys. Lett. B 634 (2006) 148.

39. A. Aloisio *et al.*, KLOE Collab., Phys. Lett. B 606 (2005), 12

40. G. Pancheri, O. Shekhovtsova and G. Venanzoni, Phys. Lett. B **642** (2006) 342 [arXiv:hep-ph/0605244].

LHCb

M. Alfonsi (Dott.), M. Anelli (Tecn.), G. Bencivenni, P. Campana, G. Capon,
M. Carletti(Tecn.), P. Ciambrone, E. Dané, P. de Simone, D. Domenici,
A. Di Virgilio(Tecn.), C. Forti, G. Lanfranchi, F. Murtas, M. Pistilli(Tecn.), M. Poli Lener,
R. Rosellini (Tecn.), M. Santoni (Tecn.), A. Saputi (Tecn.), A. Sarti, A. Sciubba (Resp.Ass.),
S. Valeri (Tecn.), A. Zossi (Tecn.)

In collaboration with:
A. Battisti, E. Capitolo, A. Cassará, G. Pileggi, B. Ponzio, V. Russo, T. Vassilieva
In collaboration with the "SSCR":
M. Arpaia, G. Bisogni, E. Iacuessa, U. Martini, M. Meli
In collaboration with the "Servizio di Elettronica":
A. Balla, G. Corradi, C. De Padova,
G. Felici, M. Gatta, G. Paoluzzi, G. Papalino, R. Vaccaro.

1 Introduction

The LNF group of LHCb operates on the **muon subdetector** [1, 2] with responsibilities on detectors (MWPC and GEM), electronics and mechanics. The detector production started in autumn 2003: the MWPC production ended in November 2006, while the GEM production is expected to be completed by may 2007. The electronics production started in 2006: since September detailed tests of the electronics performance have started. The detector installation started in 2006: the gas lines, signal and service cables (LV, HV) are being installed, as well as the MWPC chambers. The electronics and services are being put into place (HV, LV modules, patch panels, etc etc). The installation of the first 200 MWPC chambers took place before the December CERN shutdown. The MWPC and GEM installation will end in August 2007.

2 Multiwire Proportional Chambers

The LNF group of LHCb has the responsibility for the construction of $\sim 1/4$ of the MWPCs of the muon detector. Depending on the position inside the detector, there are different chamber dimensions with different readout: anode pads, cathode pads, anode & cathode pads.

We designed, collaborating with the Ferrara group, all the details of 10 different chambers types (with active dimensions ranging from $29{\times}35$ cm^2 to $31{\times}151$ cm^2). With these characteristics 292 chambers will be assembled and tested in LNF. The same design is applied to the remaining 1170 chambers that will be built in Ferrara, Firenze, CERN and S.Petersbourg.

2.1 Brief description of the LHCb MWPC

The MWPC chambers of the LHCb muon detector must fulfill stringent requirements on time response: for triggering purpose $\sim$ 99% minimum efficiency must be exploited in 20 ns. Each chamber is constituted by four layers assembled as two independent bigaps with hardwired-OR of the readout. In each 5 mm gap there are 30 microns gold-plated tungsten wires stretched at about 65 grams with a pitch of 2 mm.

2.2 Main goals reached in 2006

2.2.1 STATUS OF PRODUCTION

By the end of 2005 we completed the production of M3R3, M5R3 and M5R4 chambers. In January 2006 we started the production of the chambers of region M1R4 of the Muon System. We completed the production (48 chambers + 12 spare) in April 2006. Then, we started the production of the M1R3 chambers. We built 59 chambers (48 chambers + 11 spare). The production of MWPC chambers has ended in November 2006 in perfect agreement with the MWPC production schedule.

2.2.2 CHAMBER QUALITY CONTROL

All the chambers built are expected to pass successfully three main tests:

- Test of gas tightness: the chamber is inflated at an overpressure of 5 mbar and the pressure drop ΔP is measured as a function of time. The requirement is $\Delta P < 2$ mbar/hour.
- HV training: the chamber is slowly conditioned and is required to reach at least 2.85 kV of high voltage, drawing a negligible dark current.
- Test of gap gain uniformity: the gain fluctuation of each double-gap detector must be compatible with the plateau width measured at test beams (see below).

For what concern the gas tightness test on chambers produced in 2006: 1 M1R3 and 4 M1R4 chambers have a big gas leak that is under repair, while 4 M1R3 chambers need still to undergo the gas leakage measurement.

Concerning the HV training and dark current measurements: all the M1R3 and M1R4 chambers tested up to now, except for C010,C033,C035 M1R3 (that have loose or broken wires) and C008 M1R4, satisfy the requirements on dark current ($<$ 10 nA/gap at 2.85 kV). These four chambers showing problems have not been measured with the radioactive source (see below).

The uniformity of each gap gain is tested with a 40 mCi ^{137}Cs source. The current drawn by each gap is monitored while the source is moved over the chamber surface. These measurements allow to check the gain uniformity within each gap and to compare different chambers among them. The nominal gas mixture was used for the test: $Ar/CO_2/CF_4$ 40/55/5. Results are presented below (for the classification criteria, as well as for the detailed explanation of the plots, you can refer to [3] and [4]).

Results for M3R3, M5R3 and M5R4 chambers

In 2006 the quality tests of all the M3R3, M5R3 and M5R4 chambers produced have been finalized. The gas tightness of the chambers was tested: only 6 chambers over the 185 built had a gas leakage larger than the experiment requirements and in five of them this problem will be probably fixed. The gain uniformity measurements performed on each chamber are presented in fig.1. Results show that all the M3R3 chambers tested but one (number 58) can be classified *good* as well as 55 (out of the 59) produced M5R3 chambers and all the 68 M5R4 ones.

Results for M1R4 and M1R3 chambers

In Fig. 2 the mean values of $< I >$ for each double-gap of the 59 M1R4 and 56 M1R3 chambers tested are reported, with the maximum spread found superimposed, once corrected for T and P by means of the single-gap data.

From Fig.2 it is possible to see that all tested chambers are “good”.

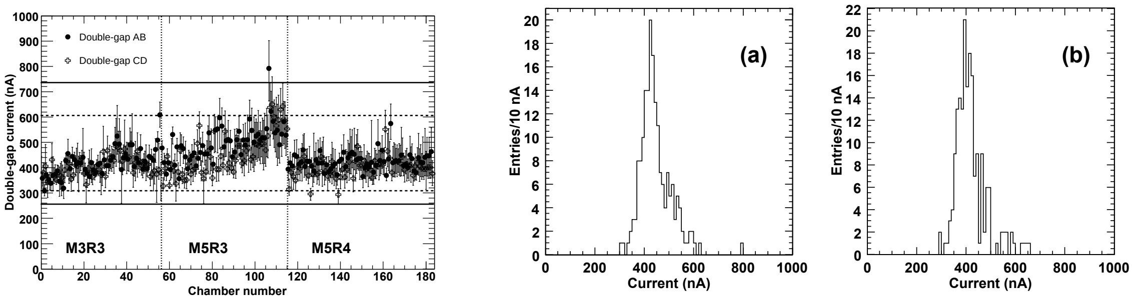

Figure 1: Average values of $< I >$ for the two double-gaps of the chambers produced in 2005, with the maximum spread found superimposed, after the correction for the T and P effects. (for the detailed explanation of the plots, you can refer to [3] and [4])

2.3 Electronics tests

Since August 2006 the Front End Boards (FEBs) dressed with final cardiacs and the Spark Protection Boards (SPBs) were avaiable. LNF has the responsibility of mounting the Front End electronics on all the chambers, after having dressed them with the Faraday Cages (FCs), and of testing the equipped chamber. For each chamber we test:

- that the I2C chain is properly working
- that the internal and external counters are giving the same results
- if there are noisy/dead channels
- if the electronics readout is uniform performing a counting scan on all the channels at 2.7kV with the nominal gas mixture

Chambers are tested in several places in order to ensure that the chamber remains good after shipping or handling (in the Capannone Gran Sasso at the LNF, in building 156 at CERN) and in the pit after the installation on the wall. So far all the installed chambers fulfill the requirements:

- no dead channel, no short circuits
- I2C line properly working
- ACQ and interal counters consistency
- low noise: all channels <1kHz with 8(14)fC threshold for the positive(negative) cardiacs.

Plots of the noise measured with a threshold of 8fC in LNF, at CERN and with the chamber on the PIT wall are shown in fig 3, separately for chambers M5R2, M5R3 and M5R4.

3 Triple GEM detectors

For the innermost part (regions R1, ~ 0.6 m^2 area) of the first muon station (M1) of the LHCb experiment the LNF group, in collaboration with INFN-Cagliari, proposes a detector based on Gas Electron Multiplier (GEM) technology. The requirements [1] for detectors in M1R1 are: a rate

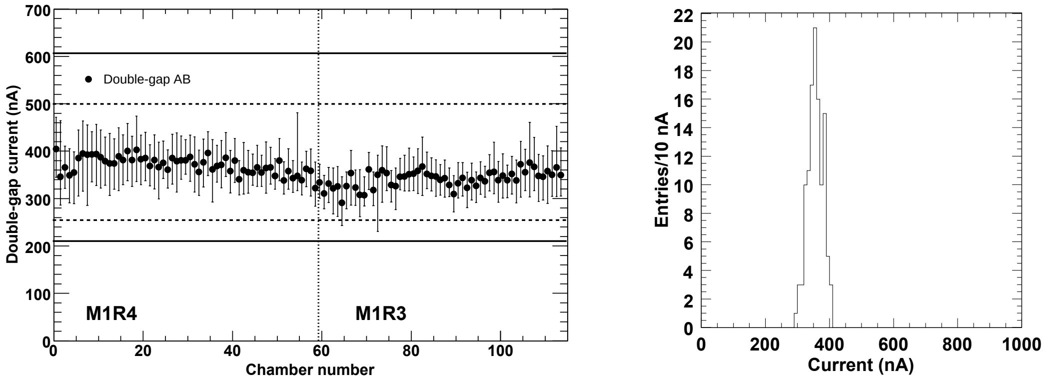

Figure 2: Average values of $< I >$ for the two double-gaps of the M1R4 chambers, with the maximum spread found superimposed, after the correction for the T and P effects. (for the detailed explanation of the plots, you can refer to [3] and [4])

capability of $\sim$ 500 kHz/cm^2; each station must have an efficiency of $\sim$ 96% in a 20 ns time window (two independent detector layers per station, logically OR-ed, are foreseen); a cluster size, i.e. the number of adjacent detector pads fired when a track crosses the detector, should not be larger than 1.2, for a 10$\times$25 mm^2 pad size. In addition the detector must tolerate, without damages or large performance losses, an integrated charge of $\sim$ 0.88 C/cm^2 in 10 years of operation at a gain of $\sim$6$\times$10^3 and an average particle flux of 184 kHz/cm^2, for an average machine luminosity of 2$\times$10^{32} $cm^{-2}s^{-1}$.
The GEM [6] consists of a thin (50 μm) kapton foil, copper clad on each side, chemically perforated in order to obtain a high density of holes having bi-conical structure, with external (internal) diameter of 70 μm (50 μm) and a pitch of 140 μm. In safe condition, gains up to 10^4 are reachable using multiple structures, realized assembling more than one GEM at close distance one to each other.
After a long period of R&D, spent to qualify the GEMs as detectors suitable for the intense and radioactive environment around the beam pipe of LHCb, we chose to operate the detector with the $Ar/CO_2/CF_4$(45/15/40) gas mixture with an overall gain of $\sim$8000 (see the activity report of the 2004 for details).
In the 2005 the triple-GEM detectors were officially approved by LHC Committee to equip the M1R1 region of the Muon apparatus [7].

In the 2006 the group was manly involved in the construction and the tests of the detectors, the finalization of all off-detector components and the integration studies on the LHCb apparatus. The construction and the quality tests of the 12 triple-GEM chambers of LNF responsibility started in April 2006. Each M1R1 station is composed by two of such detectors, with corresponding channels logically OR-ed through the front-end electronics. With respect to the 2005 prototypes a minor fix on gas connectors was applied, removing any part that could introduce metallic dust on the gas mixture. In December 2006 the production and the tests were completed with the construction of 6 additional spare chambers. The results of gas leak test and the measurement of gain uniformity of the whole production are shown in Fig. 4(a). The gas leak is measured by introducing a low overpressure (10mbar) in a chamber and monitoring its drop rate. The effects of environmental

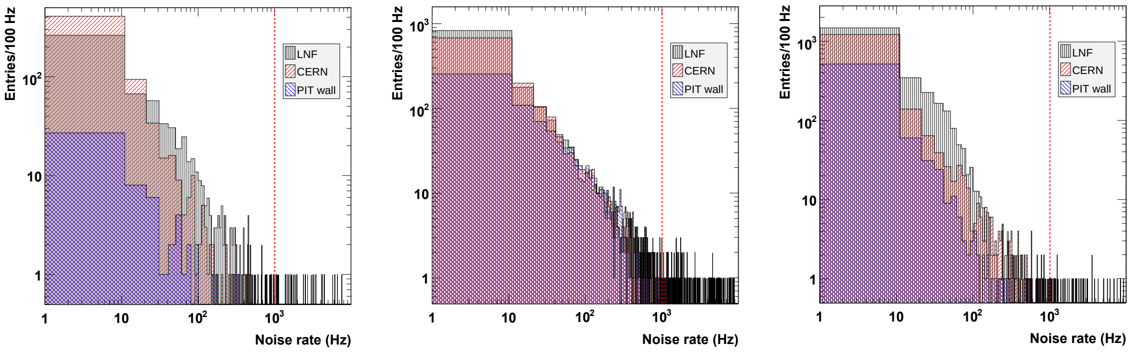

Figure 3: Noise values measured in LNF, CERN and PIT wall for M5R2 (left), M5R3 (center) and M5R4 (right) chambers.

parameters such as temperature and atmospheric pressure are taken into account with a reference fake chamber built with the same materials. The gas leak of the reference chamber was measured to be about 2 mbar/day, that corresponds to a water contamination less than 100ppmV with the foreseen gas flux of 80 cc/min. Most of the produced chambers has a gas leak lower than the one of the reference chamber. Gain uniformity is measured with a X-ray beam obtaining a tomography of the chamber pad by pad.
The first couples of chambers of the two production sites were instrumented with FEE and the performances were measured in September 2006 at the LNF-BTF beam, and at the CERN-SPS beam. In the second case, the beam exhibited a bunch structure of 25 ns, similar to LHC environment, and also the official LHCb DAQ electronics was used. The results of previous works have been confirmed. In Fig. 4(b) the efficiency in the bunch crossing time window (25ns) is shown as a function of detector gain for a FEE threshold of about 3fC, as measured in the CERN-SPS test beam.

A new custom HV system has been proposed as replacement of a passive HV divider. It consists of seven independent floating HV channels, each of them refereed to the voltage of the previous one. This instrument allows the same flexibility of the independent channels solutions, with the addition of safety of not exceeding the maximum allowed voltage between two of the detector electrodes in case of fault of one of the HV channel. The prototype, under test since the previous year, showed high long-term voltage stability. The final crate for the experiment, containing 24 of such HV device together with 24 current-meters with nano-amp sensitivity, has been designed and production has started. HV filter boards have been designed to be placed inside the Faraday Cage, and HV lines exit from the Faraday Cage with a multi-polar radiation-hard connector. A proper multi-polar HV cable has been ordered. The Fadaray Cage design has been completed to include the new HV connector, and all the components have been delivered at the end of December 2006. The integration problem of the detectors in the tight space around the beam pipe has been studied, taking into account all the cabling and the gas piping required for the operation. In particular, a distribution card for signal and power supply FEE lines has been introduced. HV filter boards and distribution cards will arrive in January 2007. Dressing of the chambers will start in February and installation will begin in April 2007.

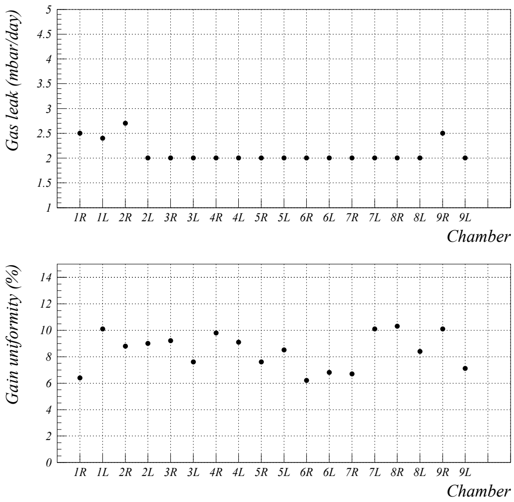

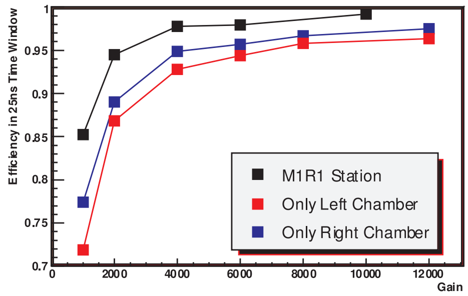

Figure 4: (a) Quality tests performed on the whole production: (top) Gas leak measured as loss of overpressure (mbar/day); (bottom) Gain uniformity. (b) Efficiency in the bunch crossing time window (25ns) as a function of detector gain, for the station (black) and with only one chamber switched on (red and blue). The FEE threshold was about 3fC

4 Electronics

The LHCb muon trigger architecture relays on 1248 Trigger Sectors (TS) built by the first stage of the front-end electronic chain. About 122,112 physical channels are merged to generate about 26,000 logical channels both in the chamber front-end and in the Intermediate Boards (IB) system.

The off detector front-end chain is mainly made of two components : the IB system and the ODE system. The IB system is used to merge part of the physical channels and is made of 176 boards. Each IB board can manage up to 192 LVDS input signals and 60 LVDS output signals. To minimize the number of boards (because the chamber/TS geometries we have 5 different IB I/O configurations) the logic functions have been implemented using programmable devices. That choice allowed us to design a single PCB to match the whole detector geometry. The use of anti-fuse technology for programmable devices (ACTEL devices) gives also an intrinsic robustness in moderate radiation environment (like the levels foreseen near the LHCb detector).

In the Off Detector Electronics (ODE) boards, the logical channels are synchronized to the bunch crossing, arranged to implement the required TS, and, finally sent to the Level-0 (L0) trigger logic through 1248 optical links at 1.6 Gbit/s. The ODE board also provides a measure of signal arrival times (1.5 ns time resolution) and implements L0-pipelines and DAQ interface via a 1,6 Gbit/s optical link and ECS interface. Because the huge number of input channels per boards (192 LVDS) and the very strict requirements on timing performances for optical link connections (less than 100 ps peak to peak on clock jitter) the design of this board has been very challenging. To fully instrument the muon detector 152 ODE boards will be used.

Due to the huge number of I/O managed by each board both IB and ODE system use a passive Transition Board (TB) to arrange the different topologies of input logical channels. All boards are hosted in a mechanical standard 7U VME crate with custom backplane. The backplane

allows to interconnect IB and TB boards and to distribute low voltage (+2.5V and + 3.3V) to the IB boards. Each crate can host up to 21 boards.
To minimize the cables length both IB and ODE systems are localized close to the detector. Then all boards have been implemented using radiation tolerant components, while critical components (anti-fuse and flash based FPGA) have been qualified (vs radiation) at the Louvain La Neuve irradiation facility with 70 MeV proton beam at a maximum fluence of $6{\times}10^{11}$ p/cm^2.
Two main tests have been successfully performed: a full chain and the optical high speed data transmission test.
The full chain test was carried out by means of a fully instrumented chamber (192 channels), an IB board and an ODE board, while in the data transmission test both the ODE board and the L0 trigger electronics was used.
Concerning the front-end electronics LNF was responsible for the production of 328 Transition Boards (TBs), 176 Intermediate Boards (IBs), 152 Off Detector Electronics boards (ODEs), Low Voltage boards and the HV filter boards.

At the moment the production of all boards has been completed and only the test of the ODE boards is still in progress while all other cards has already been fully qualified.
Besides the electronics shown before the LNF electronic workshop has also developed:

- A 64 channels VME SCALER used in the chamber test setup for rate measurements
- A 192 channels MONITOR BOARD to check chamber readout connections.
- A 8 channels 3.2 Gbits/sec VME board equipped with optical transmitter/receiver for the ODE boards production qualification.

Finally the LNF Electronic Workshop supplies services to the detector setup (chamber/readout installation).

5 Muon system infrastructure

During 2006, much work has been done in the development of the infrastructure. At begin of the year, only the iron filters and the part of the gantry structure (including the rack towers and the beams to hang the detector walls) were in position. The installation of the support beams was completed in February. In the period February-May 2006, the installation of the eight Aluminum walls was performed, starting from the Cryogenics side. Each station (M2-M5) requires two separate walls (one on Access side, the second on the Cryogenics side). Each wall is made of several (5 to 6) panels in Aluminum honeycomb. The panels were glued and riveted together and lifted up one by one, until the whole wall was completed. The walls were dressed with balconies (to handle the chambers) and cable clamps. The design of the walls and of the lifting system was realized in LNF. Tests of resistance to load were performed in LNF using a prototype wall.

The walls were dressed with guides, allowing to close the structure inside the iron filters in a safe way.

The alignment of each wall was measured after assembly. First, we checked the wall planarity. Then, the relative alignment of the walls between them. We plan to verify as soon as possible the alignment of the walls with respect to the beam.

5.1 Services installation

Once the walls were mounted, we could start to install services (cables and gas pipes) on them. One team of three people worked full time on the installation of copper braids for grounding and cables (signal, control, HV and LV cables). A second team worked on the gas piping (after cables were in position). At the end of 2006, the stations M3,M4 and M5 of the C side were completed (both cables and pipes) and the stations M4 and M5 of the side A were cabled.

5.2 Cables

Nearly 1500 HV cables, needed to connect the MWPC chambers to the CAEN HV power supplies, have been produced in LNF from June to December 2006. Those cables have been already mounted on the PIT wall in station M5, M4 and M3. The cabling of the remaining stations will be accomplished before July 2007.

5.3 Gas piping

LNF has the responsibility to design and build the Distribution Muon Gas System (from gas-racks to MWPCs). The layout that has been finalized during 2006 foresees six gas racks (RK1,...,RK6) that are placed on both sides of the Muon System to supply the 1368 MWPCs. Each rack supplies 2 half-stations (for a total of 276 MWPCs), except the two racks (RK1 and RK2) that are connected only to M1 (and thus supply 132 chambers each).
Each gas rack has 72 gas connectors: 36 used as inlets (to the chambers) and the other 36 as outlets (from the chambers), with the exception of RK1 and RK2 that have 18 inlets and 18 outlets.

The details of the gas connections are the same for all the sides of each half-station: 69 chambers are connected to 9 gas lines (L1,L2,...,L9). Each line connects 8 chambers, except for line L9 (5 chambers): chambers are flushed in parallel, in order to minimize the amount of dust and impurities going from chamber to one other, using two distributors (IN and OUT) as shown in figure 5. The gas piping is placed between the wall and the chambers in columns A and C in the Cryogenic side (B and D in the Access side), corresponding to the chambers 93mm away from the wall.

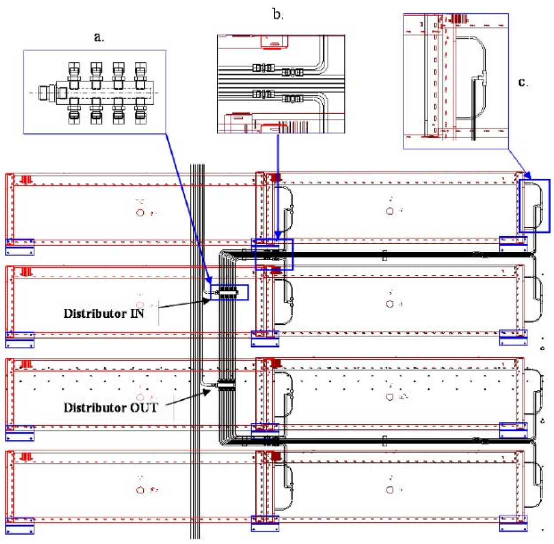

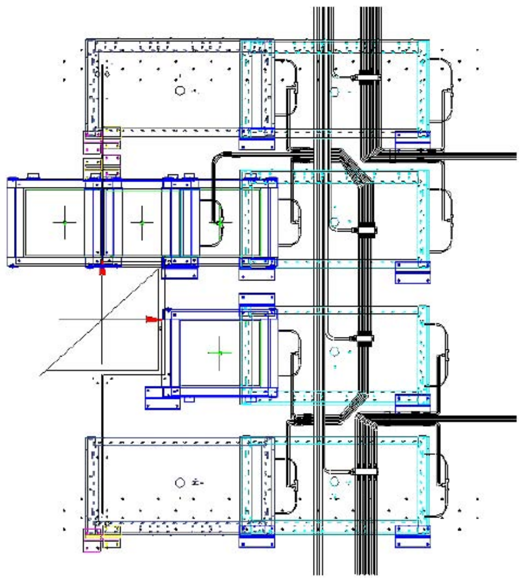

Figure 5: (a) Left: Design of Gas Line 1; a. Distributor IN; b. Connectors between copper and plastic tube; c. T connector with plastic tube. (b) Right: Design of Gas Line 9. This Gas Line supplies 5 chambers: 2 R2 and 3 R1.

A block scheme of a single gas line is shown in (Fig.6). To reduce joints, and hence costs and possible sources of gas leakage, each couple of gas chamber connectors are joined through 2 pieces of 15cm long plastic tube (Rilsan) and a T connector. From the T-connector another piece of plastic tube is linked through an I connector to the copper tube and so on to the gas distributor. It's important to note the presence of a capillary in the inlet branch that works as a gas impedance that is needed to equilibrate the system.

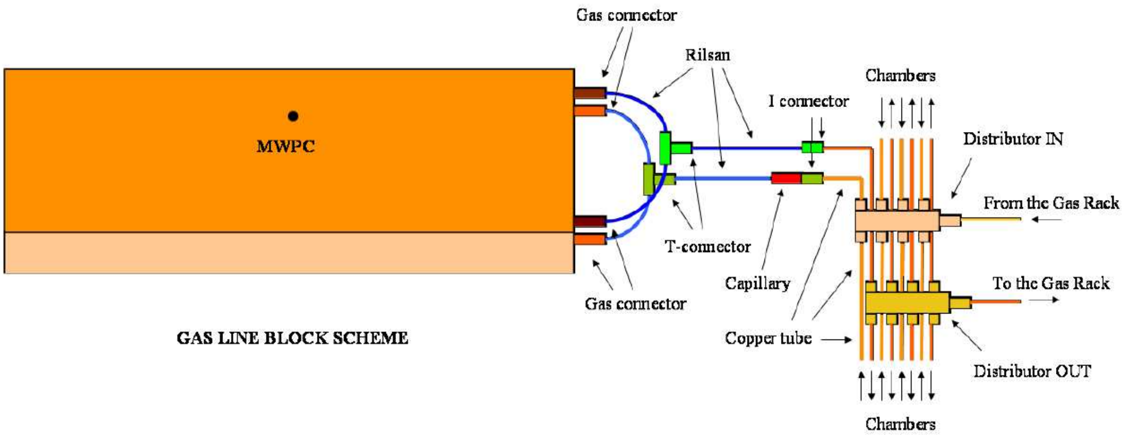

Figure 6: Scheme of a single gas line.

In the beginning of 2006 the layout has been designed and the gas piping components (copper tubes and connectors) have been ordered and cleaned.

In July, the work at CERN Laboratories did start. In six months the following items, necessary for gas the distribution of about 690 MWPC, have been prepared:

- 2000m 6x4 copper tubes;
- 1000m 10x8 copper tubes;
- 1000m 12x10 copper tubes
- 180 distributors (also tested).

In the same period the installation of about the 40% of the gas piping in the LHC PA 8 has been completed.

During the installation some tests were made to check the gas line tightness. All the gas lines have been given an overpressure of 1bar (with respect to the atmospheric pressure). Results of the test performed on gas lines of station five (cryogenic side), front and back, are shown in table 1: the average loss is reported in column 4 and 8 while the expected loss, for an overpressure of 5mbar, is quoted in columns 5 and 9. Those value have been obtained performing an exponential fit to the overpressure decrease. It can be clearly seen that the pressure loss is well below the limit of 2mbar/h and that the quality of the gas system is really good.

The end of the gas system installation is foreseen in June 2007.

Table 1: Tests performed on on gas lines of station five (cryogenic side) front and back side. DT is the elapsed time of the test and DP is the related pressure loss. To be noted that the tests are made starting from 1 bar over the atmospheric pressure. In the last two columns the data are reported considering 5 mbar of overpressure as requested by the requirements.

Lines	DT [h]	DP [mbar]	mbar/h average	mbar/h exp fit	DT [h]	DP [mbar]	mbar/h average	mbar/h exp fit
		M5C	back.			M5C	front.	
1	12	0	0.00	0.00	12	20	1.67	0.01
2	15	40	2.67	0.01	7	0	0.00	0.00
3	7.5	0	0.00	0.00	6	0	0.00	0.00
4	4	5	1.25	0.01	7.5	50	6.67	0.03
5	17	60	3.53	0.02	12	0	0.00	0.00
6	6	0	0.00	0.00	4	30	7.50	0.04
7	7.5	0	0.00	0.00	7.5	0	0.00	0.00
8	4	0	0.00	0.00	4	30	7.50	0.04
9	16	0	0.00	0.00	6	10	1.67	0.01

5.4 Rack Preparation

In October 2006, we could start the rack preparation. First we installed heat exchangers and cooling, then we started to put cables in the LV patch panels. These panels has been completed in 2006. At the end of the year, we started to put signal cables in the Transition Boards.

6 The Mock-up tests

From August to October 2006, we set up a test station in the laboratory in Meyrin. Several types of chambers (with cathode pad, wire pad and mixed readouts) were tested. The MWPCs were installed on a Aluminum panel identical (but smaller) to the one used in the experimental setup. The wall was dressed with the same ground copper braids which are actually used in the experiment. We measured the counting rate of cosmic rays (by putting the two double gaps of each detector in AND logic readout) and measured the electronics noise as function of the high voltage, trying several layouts of ground connections. The tests were successful and allowed to verify the grounding scheme, define a standardized test procedure to be used for all chambers before installation in the experiment and trigger the completion of the software tools needed for the test setup.

7 Chambers installation

At the end of 2006, the installation of all the MWPCs of the C side of the stations M4 and M5 were completed. About half of these chambers were also re-tested in the pit. Our goal is to complete the installation of stations M3 and M2 (on C side), within the end of March 2007. In the meantime, from begin of March, we will start installation of chambers on the side A (station 5).

7.1 Chambers tests after installation

All INFN chambers arriving at CERN undergo several tests to verify that they have not been damaged during the transport. We check the gas tightness (with mbar/hour precision), perform again a HV conditioning and test the chamber for the electronics noise (measured by internal and external counters) and measure the cosmic ray counting rate as a function of the working voltage. After transport to the pit and installation on the support walls, the chambers are tested again. We check again the gas tightness (by means of simple bubbler) and verify the noise rate together with the connectivity of all cables (control, signal, HV and LV) as explained in sec. 2.3.

8 Test Beam activities

In 2006 we participated in a testbeam with 25 ns interbunch. The beam was composed of pions and muons of 180 GeV/c with a Spot size nearly 4x4 cm2 and 1k-10k particles/spill. This test was an important step in the Commissioning of the Muon detector: the test of both type of detectors (MWPC and GEM). All the components of the system were present:

- chambers, FEE, TB, ODE, TELL1
- control systems of FEE, ODE and TELL1
- TFC systems (ODIN, TFC control)
- DAQ control

This testbeam allowed to check the time alignment procedure and the SW tools to control all devices (FEE, ODE, TELL1). The test was a success: we were able to align the system with respect to the beam and the 2 detectors (GEM and MWPC) between them. The Coarse (x25 ns) and the Fine (x1.6 ns) time alignment procedures were tested. The SW tools (simple C programs) used in the testbeam were OK for the very simplified system under test, but would be inadequate for more complex systems.

This experience gave a boost to the work on:

- the appropriate PVSS+FSM tools to control the whole Muon System: more and more people involved in the SW of the Experiment Control System;
- the SW dedicated to the Time Alignment Events (or multi-bunch events), to be used for the time alignment in the Pilot Run (A.Lai et al).

9 Software and analysis work

During 2006 several software and analysis work started:

- Bound to the deep involvment in the Muon detector construction, a work on the Muon Detector geometry implementation (needed for MC event simulation and reconstruction) did start in 2006, in collaboration with other INFN sections.
- The study of muon idenditification, its calibration on data, the development of HLT muon trigger algorithm was started in 2006 as well.
- The study of $B_d \to J/\psi K_s$, $B_s \to \mu\mu$ and $D^0 \to \mu\mu$ (all channels involving muons in the final state) started as well.
- The study of $B_{d,s} \to h^+h'^-$ decays, started in 2005, is reaching a mature status. Some first evaluations on the sensitivity of this channels on the angle γ (as well as on the underlying SU(3) assumptions) have been presented in a Flavour Workshop at cern in November 2006.

10 List of Conference Talks by LNF Authors in Year 2006

- M. Alfonsi *et al.*, “The triple-GEM detector for the M1R1 muon station at LHCb Experiment”, presented at International Symposium on the development of detectors for particle, astro-particle and synchrotron radiation experiments, SLAC, California, April 3 - 6 2006.
- M. Alfonsi *et al.*, “Production and Performances of LHCb Triple-GEM Detectors Equipped with the dedicated CARDIAC-GEM front-end electronic”, presented at the X Pisa Meeting on Advanced Detectors, La Biodola, Isola d’Elba (Italy), May 21 - 27, 2006.
- A. Sarti, “LHCb Level-0 Trigger detectors”, presented at the X Pisa 2006 Meeting frontier Detectors for Frontier Physics La Biodola, Isola d’Elba, Italy; 21-27 May, 2006.
- A.Sarti, “Bs,d $\rightarrow$h+h’- @ LHCb”, presented at the Flavour in the Era of the LHC CERN, October 9-11, 2006.

References

1. LHCb Collaboration, “LHCb: muon system technical design report”, CERN LHCC MUON 2001-010, LHCb TDR 4, 28 May 2001.
2. LHCb Collaboration, “LHCb: Addendum to muon system technical design report”, CERN LHCC MUON 2003-002, LHCb TDR 4 Addendum 1, 15 January 2003.
3. M. Anelli *et al.* “Quality tests of the LHCb muon chambers at the LNF production site ”, Poster presented at the IEEE 2004 (Rome, Italy, October 16-22, 2004), and submitted to Transaction on Nuclear Science.
4. D.Pinci and A.Sarti, “Production and test of the LHCb Muon Chambers”, presented at Hadron Collider Physics Symposium (HCP05), Les Diablerets, Switzerland July 4-9, 2005.
5. M. Anelli *et al.*, “Test of a MWPC for the LHCb Muon System at the Gamma Irradiation Facility at CERN”, Public Note LHCb MUON-2005-003. `http://cdsweb.cern.ch/search.py?recid=815058&ln=en`
6. F. Sauli, Nucl. Instrum. Meth. **A386** (1997) 531.
7. LHCb Collaboration, “LHCb: Second addendum to muon system technical design report”, CERN LHCC MUON 2005-012, LHCb TDR 4 Addendum 2, 9 April 2005.
8. M. Alfonsi *et al.*, presented at Puerto Rico 2005 IEEE conference (Oct. 23-29) and submitted to Transaction on Nuclear Science.
9. A. Balla *et al.*, Muon Off-Detector electronics: The IB system, LHCb note, LHCb 2003-023.

BENE_DTZ

F. Terranova

BENE-INFN is a study group closely related to the European initiative BENE (Beams for European Neutrino Experiments). The latter is aimed at developing novel sources for high intensity neutrino beams and is focused on the conceptual design of Superbeams, Beta Beams and Neutrino factories. In 2006 the activity in Frascati has been mainly devoted to Beta Beams [1, 2], particularly in its medium and high gamma configuration. Interesting studies have also been carried out in connection with the exploitation of laser-driven proton sources [3, 4]. Moreover, future applications of OPERA-like detectors [5], i.e. hybrid emulsion cloud chambers with and without magnetic field, have also been considered in connection with the Neutrino Factories.

References

1. A. Donini et al., Eur. Phys. J. **C48**, 787 (2006).
2. A. Donini et al., **PoS** HEP2005, 178 (2006).
3. F. Terranova et al., Nucl. Instr. Meth **A558**, 430 (2006).
4. F. Pegoraro et al., AIP Conf. Proc. **827**, 130 (2006).
5. G. De Lellis et al., "On a possible magnetized emulsion cloud chamber for a neutrino factory", contribution to the International Scoping Study (Detector working group).

LARES

G. Bellettini, (Ass.), A. Boni (Bors.), C. Cantone (Bors.), A. Colantoni (Laur.)
S. Dell'Agnello (Resp.),G.O. Delle Monache, M. A. Franceschi, M. Garattini (Bors.),
N. Intaglietta (Tecn.), M. Martini (Bors.), T. Napolitano (Art. 23),
A. Paolozzi (Ass.), G. Sindoni (Dott.), R. Tauraso (Ass.)

1 Introduction

Gravity can be studied in detail in Near Earth Orbits (NEO) using laser-ranged test masses tracked with few mm accuracy by ILRS. The two LAGEOS satellites have been used to measure frame dragging (a truly rotational effect predicted by GR) with a 10% error. A new mission and an optimized, second generation satellite, LARES (I. Ciufolini PI), is in preparation to reach an accuracy of 1% or less on frame dragging, to measure some PPN parameters, to test the $1/r^2$ law in very weak field and, possibly, to test select models of unified theories (using the perigee). This requires a full thermal analysis of the test mass and an accurate knowledge of the asymmetric thermal thursts due to the radiation emitted by Sun and Earth. A Space Climatic Facility (SCF) has been built at INFN-LNF (Frascati, Italy) to perform this experimental program on LAGEOS and LARES prototypes. It consists of a 2 m $\times$ 1 m cryostat, simulators of the Sun and Earth radiations and a versatile thermometry system made of probes and an infrared digital camera.

The SCF has been commissioned in summer 2006, using a LAGEOS 3×3 retro-reflector array built at LNF (the "matrix"). This prototype has been thermally modeled in detail with a commercial simulation software. The first space-climatic measurements of the matrix were performed in December 2006. Following a special agreement, an original engineering prototype of LAGEOS I built in the 1990's has been sent by NASA-GSFC to LNF to be tested in the SCF in 2007.

LARES received the scientific approval by INFN in December 2006 and is now awaiting from ASI the availability of a launch on one of the first flights of VEGA, the new small ESA launcher.

2 Probing Gravity in Near Earth Orbits (NEO) with LAGEOS and LARES

The LAGEOS (LAser GEOdynamics Satellite) I and II satellites have been launched, respectively, in 1976 (by NASA) and 1992 (NASA-ASI) into orbits with high inclinations (i = 109.9^o and 52.65^o), low eccentricities (e = 0.004 and 0.014) and large semi-major axes (a = 12,270 and 12,163 km). They are high-accuracy, passive, spherical test masses, whose orbit is tracked with <1 cm precision by the 40+ stations of ILRS (International Laser Ranging Service) scattered all over the Earth. They have a weight of about 400 Kg, a 60 cm diameter and 426 fused silica cube corner retro-reflectors (CCRs) for the satellite laser-ranging measurement (SLR).

The LAGEOS data were used in 1998 for the first-ever measurement of the phenomenon of dragging of inertial frames by a central rotating mass (the Earth in this case) acting on its orbiting satellite. This effect was predicted by Einstein (who named it "frame dragging"), Lense and Thirring in 1916-1918. For its formal similarity with electromagnetism, it is also referred to as the Earth "gravitomagnetism". Frame dragging can be observed also with point-like spinning bodies (ie, gyroscopes): this is the goal of the Gravity Probe B mission, launched in 2004, which ended data taking in 2006. GP-B is an active, high-technology satellite (one of the most sophisticated ever), aimed at a one-time only measurement of frame dragging with an accuracy $\leq$ 1%.

Recently, a larger set of LAGEOS data (about 11 years), in conjunction with a very improved determination of the Earth geopotential field (mainly due to the two GRACE satellites), were used to re-measure the frame dragging effect in NEO with 10% accuracy. 3) The measured value of the frame dragging precession of the two combined orbital nodes, $\dot{\Omega}_{FD} = 47.9$ mas/yr (milliarc-sec/yr), is in good agreement with the GR prediction, $\dot{\Omega}_{FD} = 48.2$ mas/yr. For the LAGEOS altitude $h \sim 6000$ km, this amounts to a nodal precession of about 2 m/yr.

In the next years, the knowledge of the geopotential is expected to improve thanks to the GRACE, CHAMP and GOCE missions. Since the LAGEOS have a virtually limitless orbit lifetime ($\sim$1 million years), the non-gravitational perturbations (NGPs) will become an important experimental error on $\dot{\Omega}_{FD}$. Among NGPs, the main sources of error are non-conservative thermal forces due to the varying and asymmetric space climatic conditions. These contribute to $\sigma(\dot{\Omega}_{FD})$ with *few* %. A very detailed error analysis and error budget can be found in Ref. [4].

A LAGEOS follow-up mission, LARES (LAser RElativity Satellite), is being considered since the late '90s. Because SLR is a consolidated technique, the LAGEOS data analysis is mature, and thanks to the SCF, the time is right to launch a modern, second generation test mass.

Laboratory measurements of the thermo-optical properties of the LAGEOS retro-reflectors have been advocated for many years by the leading experts in this field (Rubincan, Farinella, Slabinski, etc.). Tests like these in a NEO SCF were not conducted on either LAGEOS I or LAGEOS II. Due to their larger temperature asymmetry and emissivity, the CCRs give rise to a thermal drag perturbation by far much larger than that of the aluminum structure of the satellite. The orbital perturbations depend significantly on the Yarkovsky effects; specifically the diurnal Yarkovsky effect, the seasonal Yarkovsky effect (also known as *thermal drag* and first understood, in the case of LAGEOS, by Rubincam), and the Yarkovsky-Schach effect. The seasonal Yarkovsky effect is due to the Earth infrared radiation, while the Yarkovsky-Schach effect is due to the modulation of the solar radiation by the Earth shadow. The magnitude of these effects depends upon the spin axis orientation, spin rate and the thermal properties of the satellites. Among the thermal properties, of particular importance and concern for the orbital dynamics of LAGEOS and LARES, is the *thermal relaxation time* of the CCRs (τ_{CCR}). This constant has never been measured before and the spread of its calculated values in the literature is ~ 250 %, which gives $\sigma_{LT}(TT) \sim 2 - 3\%$.

For LARES, it will be critical to have an accurate measurement of τ_{CCR} to use in the NASA GEODYNE orbit determination program used for data analysis. The SCF has been designed to achieve $\sigma(\tau_{CCR})/\tau_{CCR} \leq 10\%$ for the LARES retro-reflectors [5], which are the same as the LAGEOS ones. This will make the effect of TTs on $\sigma_{LT}(TT)$ negligible [6].

3 The LNF Space Climatic Facility

A schematic view of the SCF is shown in Fig. 1. The size of the steel cryostat is approximately 2 m length by 1 m dimeter. The inner copper shield is painted with the Aeroglaze Z306 black paint (0.95 emissivity and low outgassing properties) and is kept at T = 77 K with liquid nitrogen. When the SCF is cold, the vacuum is typically in the 10^{-6} mbar range.

A support fixture on the ceiling holds the prototype spacecraft in front of the Earth infrared simulator (inside the SCF). The solar simulator is outside, behind a quartz window (40 cm diameter, 4 cm thickness), which is transparent to the solar radiation up to 3000 nm. A side flange with a Germanium window allows to take thermograms of the prototypes with a FLIR infrared camera. The Earth simulator is a 30 cm diameter disk painted with Aeroglaze Z306, kept at the appropriate temperature (250 K) and distance from the satellite prototype in order to provide the CCRs with the same viewing angle in orbit ($\sim 60^o$ for LAGEOS). The sun simulator (from `www.ts-space.co.uk`) provides a 40 cm diameter beam with close spectral match to the AM0 standard of 1 Sun in space (1366.1 W/m^2), with a uniformity of $\pm 5\%$ over an area of 35 cm diameter. The spectrum is formed from the output of two sources, namely an HMI arc lamp (UV-V), together with a tungsten filament lamp (Red-IR). The quartz halogen lamp (with the tungsten

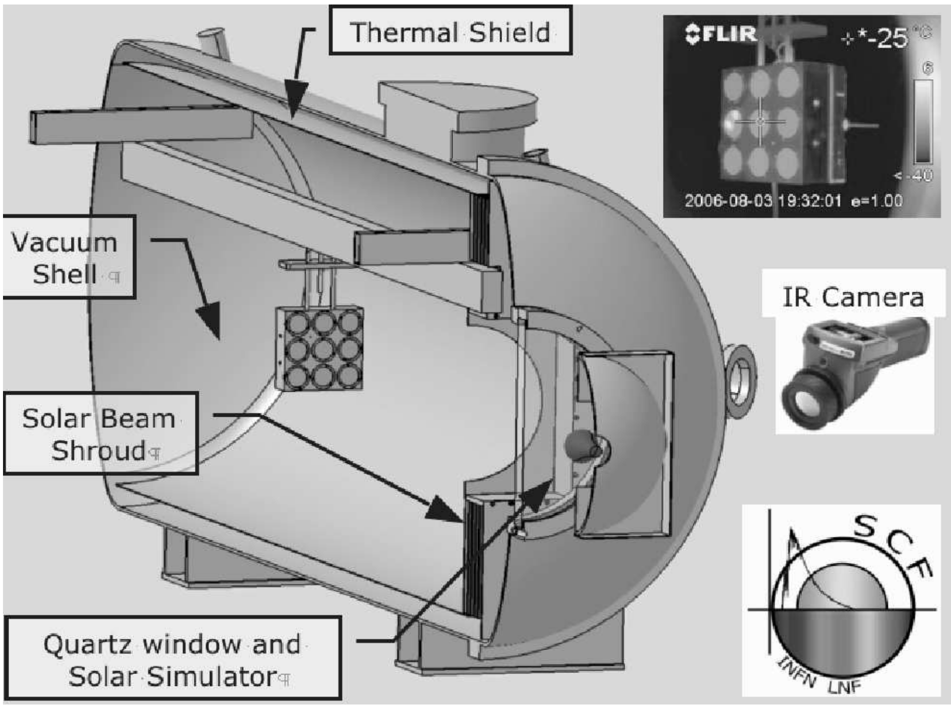

Figure 1: Sketch of the LNF Space Climatic Facility

filament) has a power of 12 KW, while the metal halide lamp has 6 KW power. These two sources are filtered such that when the two beams are combined with a beam splitter/filter mirror, the resulting spectrum is a good match to AM0 in the range 400-1800 nm. The spectrum has also been measured up to $\lambda = 3000$ nm (important for $\dot{\Omega}_{TD}$) and found to be in reasonable agreement with the AM0.

The absolute scale of the solar simulator intensity is established by exposing the beam to a reference device, the *solarimeter*, which is a standard `www.epply.com` thermopile. The solarimeter is a calibrated blackbody, accurate and stable over 5+ years to $\pm 2\%$. It is used over long times to adjust the power of the lamps and compensate for their ageing. During continuous operation, the beam intensity is monitored and controlled by means of a feedback PID photodiode which reads a portion of the beam with a small optical prism. The SCF is described in greater detail in [7].

4 Thermal Simulations and Experimental Measurements

The simulations have been performed with a commercial specialized satellite software by $C\&R-Tech$ (`www.crtech.com`), Thermal Desktop (geometric thermal modeler) + RadCad (radiation analysis module) + Sinda-Fluint (solver) + orbital simulator (TRS). SCF measurements and TRS simulations will be iterated.

The overall strategy of the program is described in the following.

1) Hold T(Aluminum) to the expected 300 K [8] and measure in the SCF:
   - A) emissivity (ϵ) and reflectivity (ρ) of CCRs and Al retainer rings;
   - B) τ_{CCR} and τ_{AL} for the Al retainers,;
   - C) surface temperature distribution (ie, thermal forces).

2) Repeat the above for T(AL) different from 300K.

3) Tune TRS models to SCF data for "static" conditions (Sun ON and OFF).

4) Use validated TRS models to predict TTs along full satellite orbits.

5) The sequence of the prototype simulations and measurements will be:

   A) Test the LNF matrix in detail and then the NASA prototype.

   B) Use the matrix results to optimize the design of LARES.

   C) Build a LARES prototype and test it in the SCF.

6) Test the effect of satellite spin, first in the simulation and then in the SCF.

Several simulations results have been obtained and are reported in ref. [6].

4.1 Parametric model of the thermal forces

A parametric model of the thermal forces on LAGEOS has been performed, which shows the strong capabilities of the TRS software and some of the basic features of the thermal NGPs.

The simulated SCF configuration is: (1) satellite pole facing the Sun and Earth simulators, (2) steady state with both simulators turned on at t=0, (3) Sun turned off between t = 0 and 4500 sec, (4) zero thermal conductance between the Al retainer screws and the Al satellite body. This configuration can be easily implemented in the SCF and it mimics, approximately, the satellite passage through the Earth shadow and a satellite spin directed along the ecliptic plane. TTs are estimated in a parametrized way, using a single CCR in a cavity of an aluminum block held fixed at 300 K. For each row, the single CCR is iluminated by the solar lamp at the appropriate angle and the thermal thrust is computed from the software. The contribution of all CCRs in a row, of all rows and of the two hemispheres is then summed. The results are shown in Fig. 2.

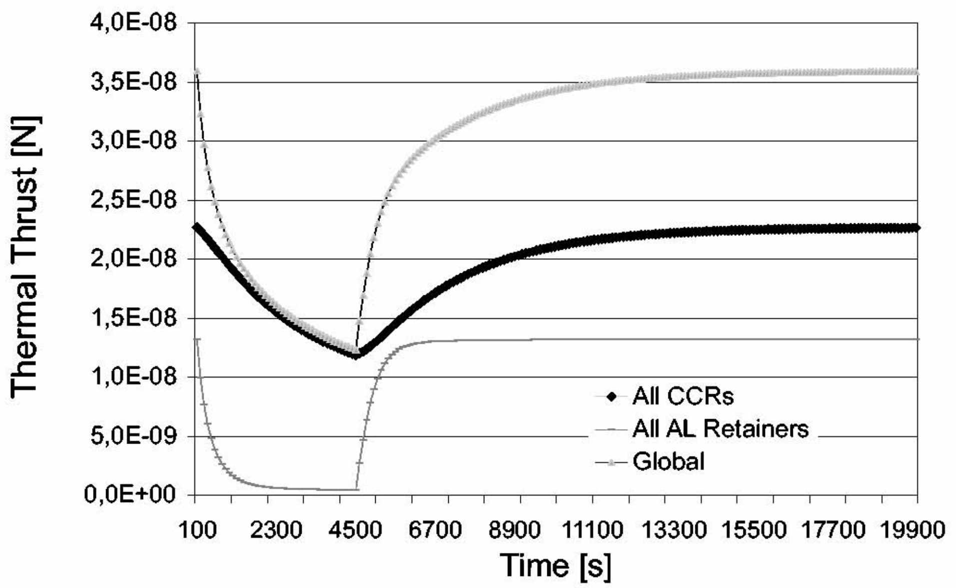

Figure 2: Parametric simulation of the thermal thrusts on LAGEOS due to the SCF Sun and Earth simulators for CCR solar absorptivity = 1.5%.

4.2 SCF measurements

A preliminary thermal measurement with the Earth IR simulator as the only thermal input has been performed at the SCF in December 2006. The measured steady-state temperature of the CCR shows a fair agreement with the simulated thermal model of the matrix (see fig. 3). This preliminary test has been carried out with a non-optimized configuration of the screws and retainer rings (materials used and the torque on the screws) and that the temperature scale of IR camera was not fully calibrated.

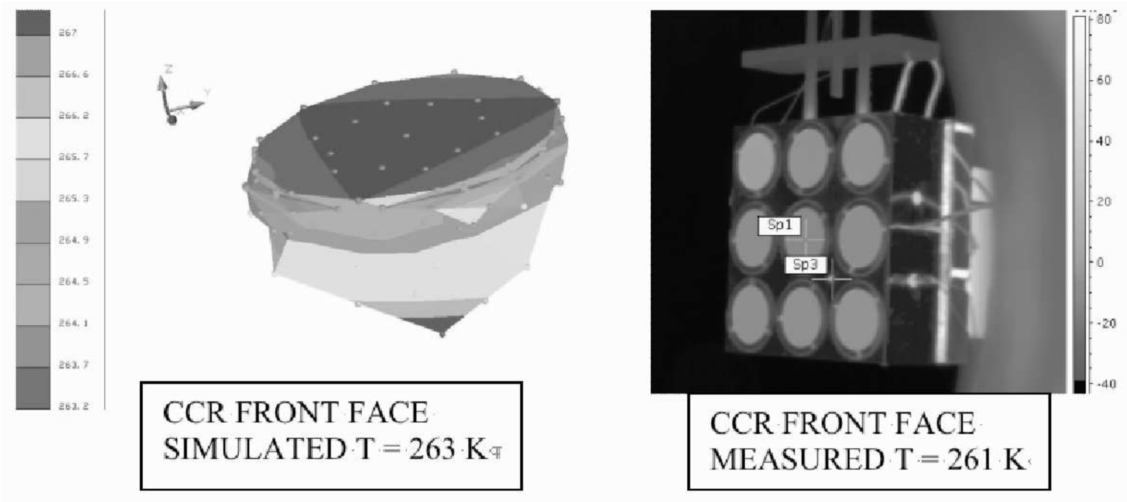

Figure 3: Simulated and measured temperature of the CCR in the SCF (Earth IR only).

Another preliminary space-climatic measurement has been performed with the Solar Simulator (and not Earth IR simulator) in December 2006. During this test the vacuum was around 10^{-6} mbar, the inner shield was cold at T ¡ 100 K. The matrix Al temperature was varied by several degrees by means of thermo-electric coolers (TECs) and the temperatures of the CCR and its plastic (KEL-F) and metal (Al retainer) mounting rings were measured with PT100 probes (see fig. 4). This was done mainly to cross-check the temperature scale of the infrared camera, but it introduced some bias in the thermal balance of the CCR and rings. The test proved that the overall system works well, and indicated what modifications are necessary to complement the measurements of the IR camera with the PT100 probes. The calibration of the temperature scale is in progress. Once it is performed, the plot of fig. 4 will allow the measurement of τ_{CCR} with the required statistical accuracy. Systematics effect are under study.

5 Talk by LARES-LNF Collaborators

M. Garattini, "LAGEOS and LARES" InnovactionFair, Udine, Italy, February 2006.
S. Dell'Agnello, "Quantum to Cosmos" NASA Workshop, Warrenton (VA), USA, May 2006.
S. Dell'Agnello, "1rst J. A. Wheeler School" E. Maiorana Institute, Erice, Italy, June 2006.
G. O. Delle Monache, "European Geoscience Union" Conference, Vienna, Austria, April 2006.
G. O. Delle Monache, "Fundamental Physics in Space" INFN Work., Frascati, Italy, March 2006.
G. O. Delle Monache, "Int. Laser Ranging Service" Conference, Canberra, Australia, Oct. 2006.
M. A. Franceschi, "SpacePart06" Conference, Beijing, China, August 2006.
C. Cantone, "Experimental Gravity in Space" GGI Workshop, Florence, Italy, Sep. 2006.

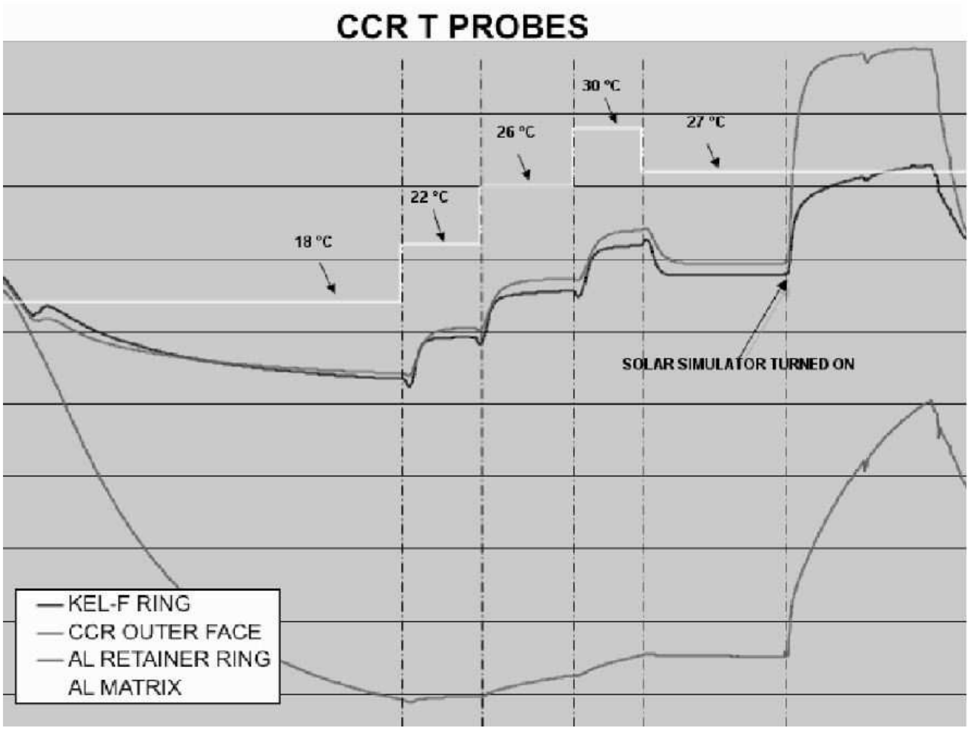

Figure 4: Space-climatic test of the LAGEOS 3x3 CCR matri prototype at the SCF with the Sun Simulator only. Temperature (AU) of CCR and its mounting rings vs. time (AU).

References

1. I. Ciufolini, E. C. Pavlis, Nature, Vol. **431**, 21 October 2004.
2. G. Dvali, A. Gruzinov, and M. Zaldarriaga, Phys. Rev. D **68**, 024012 (2003).
3. I. Ciufolini, E. C. Pavlis, *Nature* **431**, 21 October 2004.
4. I. Ciufolini, E. C. Pavlis, R. Peron *New Astronomy* **11**, 527-550 (2006).
5. A. Bosco, Thesis, University of Rome Tor Vergata, 2006, LNF Report LNF-06/32(T).
6. A. Bosco et al, LNF Report LNF-06-24(P), May 2006; to be pub. on Int. Jour. Mod. Phys. D.
7. A. Bosco et al, LNF Report LNF-06-26(IR), Feb. 2006.
8. V. J. Slabinski *Cel. Mech. Dyn. Astr.* **66**, 131-179 (1997)

NEMO

M. Cordelli, A. Martini, H. Roberto (Ass.), L. Trasatti (Loc.Coor.)

In collaboration with:
Bari Section, Bologna Section, Catania Section, Genova Section,
LNS, Messina Section, Roma1 Section

1 Activity

The NEMO project aims at the construction of a kilometer cube detector for neutrino astronomy. During the year 2006 the NEMO group has deployed with success the first tower, called NEMO Phase 1. The tower, made up of 4 floors, has been deployed at the Catania Test Site, at a deptth of 2000m, in Decembe 2006. During 2007 a 100 km electrooptical cable will be installed between Porto Palo (Capo Passero) and the chosen site. During 2008 the second tower, made up of 12 floors, will be deployed .in the final site.

Meanwhile work is in progress on the properties of deep Mediterranean sea, and the group has produced several instruments to study the marine depths. The LNF group has designed and built NERONE, an instrument to measure with great accuracy the water transparency using measurements performed at several distances from the source. During a cruise in June 2006 the first good results were obtained from a series of measurements at the Catania Test Site. The group has also developed the console software for the NEMO Phase 1 project.

2 Publications

LNF-01 / 029 (NT) (30 novembre 2001).
M. Cordelli, R. Habel, A. Martini, L. Trasatti: NERONE: First Tests in Sea Water

OPERA

F. Bersani Greggio (Ass.), A. Cazes (Ass.Ric.), V. Chiarella, C. Di Troia (Ass.Ric.),
B. Dulach, G. Felici, A. Franceschi, F. Grianti (Ass.), A. Gambarara (Tecn.),
A. Mengucci (Tecn.), T. Napolitano, A. Paoloni (Art.36),
M. Spinetti (Resp.), F. Terranova, M. Ventura (Tecn.), L. Votano

in collaboration with

LNF-SEA: A. Balla, G. Corradi, U. Denni, A. Frani, M. Gatta, G. Paoluzzi, G. Papalino
LNF-SPAS: A. Cecchetti, D. Orecchini
LNF-SSCR: G. Catitti, A. Ceccarelli, A. Tiburzi
LNF Divisione acceleratori: M. Incurvati, F. Iungo, L. Pellegrino, C. Sanelli

1 The experiment

OPERA [1] has been designed to provide a very straightforward evidence for $\nu_\mu \to \nu_\tau$ oscillations in the parameter region indicated by Super-Kamiokande as the explanation of the zenith dependence of the atmospheric neutrino deficit. It is a long baseline experiment located at the Gran Sasso Laboratory (LNGS) and exploiting the CNGS neutrino beam from the CERN SPS. The detector is based on a massive lead/nuclear emulsion target. The target is made up of emulsion sheets interleaved with 1 mm lead plates and packed into removable "bricks" (56 plates per brick). The bricks are located in a vertical support structure making up a "wall". Nuclear emulsions are used as high resolution tracking devices for the direct observation of the decay of the τ leptons produced in ν_τ charged current interactions. Electronic detectors positioned after each wall locate the events in the emulsions. They are made up of extruded plastic scintillator strips read out by wavelength-shifting fibers coupled with photodetectors at both ends. Magnetised iron spectrometers measure charge and momentum of muons. Each spectrometer consists of a dipolar magnet made of two iron walls interleaved with pairs of precision trackers. The particle trajectories are measured by these trackers, consisting of vertical drift tube planes. Resistive Plate Chambers (RPC) with inclined strips, called XPC, are combined with the precision trackers to provide unambiguous track reconstruction in space. Moreover, planes of RPCs (Inner Tracker) are inserted between the magnet iron plates. They allow a coarse tracking inside the magnet to identify muons and ease track matching between the precision trackers. They also provide a measurement of the tail of the hadronic energy leaking from the target and of the range of muons which stop in the iron. A block of 31 walls+scintillator planes, followed by one magnetic spectrometer constitutes a "super-module". OPERA is made up of two supermodules located in the Hall C of LNGS (see Fig. 1). The total number of bricks amounts to 206,336 resulting in a target mass of 1766 tons. Bricks are automatically produced in situ by a "brick assembly machine" (BAM) and inserted into the wall support structure through a dedicated robot (BMS).

OPERA is able to observe the ν_τ signal with an impressively low background level. The direct and unambiguous observation of $\nu_\mu \to \nu_\tau$ appearance will constitute a milestone in the study of neutrino oscillations. Moreover, OPERA has some sensitivity to the sub-dominant $\nu_\mu \leftrightarrow \nu_e$ oscillations in the region indicated by the atmospheric neutrino experiments. It has been shown [2]

Figure 1: OPERA as in spring 2006.

that the CNGS beam optimized for ν_τ appearance, will improve significantly (about a factor of three) the current limit of CHOOZ.
Opera is an international collaboration (Belgium, China, Croatia, France, Germany, Israel, Italy, Japan, Russia, Switzerland, and Turkey) and the INFN groups involved are Bari, Bologna, LNF, LNGS (Gran Sasso), Naples, Padova, Rome and Salerno. The Technical Coordinator of the experiment (M. Spinetti), the Chairperson of the Collaboration Board (L. Votano) and two of the OPERA project leaders (A. Franceschi for the wall construction and F. Terranova for the magnets) are LNF researchers.

2 Overview of the OPERA activities in 2006

2006 has been a crucial year for the CNGS/OPERA project: both the beamline and the electronic detectors at the far location were commissioned and the first physics run took place in August. In particular, the construction of CNGS has been completed in winter 2006. The beamline was commissioned between April and July. In August the CNGS has been fully operational and it performed a physics run between 8/18 and 8/31. At that time 70% of the nominal intensity has been achieved with an integrated number of protons on target (pot) of 7.6 10^{17}. This intensity was sufficient to commission the electronic detectors of Opera and provided the first events at the far location. Opera observed 319 events: muons coming from the rock surrounding the experiment and internal events (i.e. charged current neutrino interactions mainly in the iron of the magnets) [3]. The artificial origin of these events are testified by the time correlation with the CERN accelerator complex. Moreover, rates and angular distributions are in agreement with expectations. In summer, a preproduction of about 1000 bricks has been done with the BAM, however, the planned October run of CNGS has been canceled due to a problem in the cooling system of the reflector.

Repairing of this horn and a full overview of the system are in progress and will be completed by summer 2007. In the meanwhile, the Brick assembling Machine is being commissioned and brick production is in progress.

3 Activities in Frascati

The Frascati group is responsible for the design and construction of the dipolar magnets and the general support structure for the subdetectors. It shares responsibility with INFN Padova and LNGS for the construction and installation of the bakelite RPC planes (Inner Tracker). Frascati and Naples also designed and prototyped the wall support structures housing the lead/emulsion bricks and LNF is responsible for their production and installation. Moreover, the group contributes to software development and to the analyses aimed at assessing the performance of the experiment after the completion of the CNGS programme. Since 2002 LNF is involved in the construction of the Brick Assembly Machine (BAM) and will contribute to the emulsion scanning with two dedicated microscopes located in Frascati.

3.1 OPERA General layout

The OPERA general support structure is a project by LNF-SPAS and external firms and it has been mounted in parallel with the electronic subdetectors and the brick walls between 2003 and 2006. Before the August run, nearly all the structure has been installed. LNF-SPAS also designed the tools for the positioning and alignment of the drift tubes and for positioning of the drums containing the bricks in the loading station near the BMS. In autumn 2006, the balcony in front of the second supermodule was positioned and a new access stair in front of the experiment has been mounted. The project is therefore completed. In 2007, only auxiliary installations are planned: a support floor to ease rock-side access to Opera, a protecting fence near the area of operation of the BMS and an access line to the elctronics of the drift tubes in the second supermodules.

3.2 Magnets

The Opera magnets have been commissioned in spring 2006 and were fully operative during the first CNGS run. In February, the power supplies of the magnets were delivered at Gran Sasso after completion of tests at firm. They were subsequently installed in the top platform of the experiment and connected to the driving coils by means of flexible cables. The magnets have been switched on for the first time in March using a temporary cooling system. Commissioning was completed in collaboration with LNF Acc. Div. (M. Incurvati, F. Iungo, C. Sanelli) and INFN Padova (A. Bergnoli): in particular, a systematic assessment of the properties of the magnets has been done in June-July 2006; it was demonstrated that the magnetic fields in the bulk of the iron fulfill the physics requirements for OPERA and are consistent with specifications. In general, fields agree with expectations within 5%, the deficit being related with non-ideal mechanical contacts within the slabs [4]. The difference of fields between the two magnets is below 3% while fringe field in air at the location of the photomultipliers reading the plastic scintillators never exceeds 30 Gauss.

The water cooling system for Opera has been designed by LNF-Acc.Div. (L. Pellegrino) and LNGS-Tech.Div. (R. Adinolfi-Falcone) and it was completed in March 2006; executive drawings and installation have been carried out by external firms. The commissioning was divided into two phases: short term thermal response has been tested immediately after the completion of the works while long term studies were done during the first CNGS run. It has been demonstrated that the magnet coils reach thermal equilibrium after ~ 30 hours and the temperature ranges between 35 and 80 degrees depending on the location of the copper bars and the presence of heat exchangers. No significant increase of temperature has been observed in the proximity of the RPC after the physics run of August.

During the physics run, the magnet closer to Borexino ("Magnet 1") was operated very smoothly (100% livetime) while several power interruptions were observed in Magnet 2. The problem was traced to the power supply regulator and has been solved by the supplier (EEI srl, Vicenza) in September 2006.

Current activities on the magnets are focused mainly on the slow control system and on remoting of the sensors. Similarly, remoting of the chiller for the water cooling system is in progress. We expect the slow control to be fully operative by spring 2007.

3.3 Inner Trackers

In 2006 [5, 6], the electronics of both the spectrometers have been completed and commissioned. All RPC have been fully operational during the CNGS run and took data with nearly 100% livetime.

For what concerns the electronics, the 22 RPC planes per magnet are equipped with horizontal and vertical readout strips, for a total amount of about twenty-five thousand digital channels. The front end electronics is self-triggered and has single plane readout capability. It is made of four different subsystems: the Front End Boards (FEBs) system (486 boards hosted in 28 crates) provides the discrimination of the strip incoming signals and produces a FAST OR prompt output for the Trigger Plane signal generation; the Controller Boards (CBs - 56 boards hosted in 4 crates) acquire FEB discriminated signals and manages the communications to the experiment DAQ and Slow Control. A Trigger Board allows to operate in both self-trigger (the FEB FAST OR signal starts the plane acquisition) and external-trigger (different conditions can be set using the OR signals generated from the planes) modes. Finally, the Timing Boards (TBs) system is made of 252 Timing Boards on the detector and 22 OPE boards hosted in 4 crates on the top platform. It exploits the RPCs good timing features to generate a plane prompt timing signal for Precision Tracker front-end electronics. Timing Boards are used to discriminate at low threshold signals at the end of the horizontal read-out strips. OPE boards manage the communication between the TBs and both the slow control (for channel masking, threshold setting and rate monitoring) and the drift tubes trigger board (to which they provide the RPC plane fast OR). Figure 2 shows the main elements of the TB system. The readout electronics is also equipped with a Monitor System made of 30 boards hosted in the FEB crates. It uses one of the two FAST-OR of the FEB boards to produce an on-line monitor of the RPCs counting rates.

The tasks concerning the design and construction of the RPC electronics are shared among LNF-SEA (strip boards [7], current monitoring [7], timing boards), Padova (front-end boards)

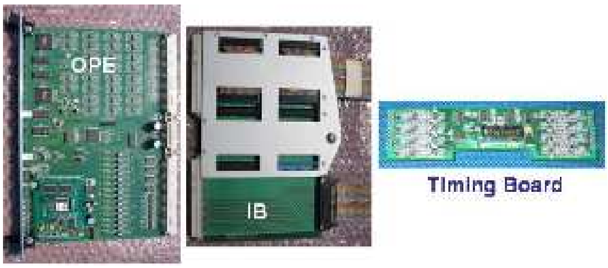

Figure 2: The picture shows the main elements of the timing system: the Timing Board, the Interconnection Board (IB), receiving the cables from 14 TBs, and the OPE Board, connected to the IB.

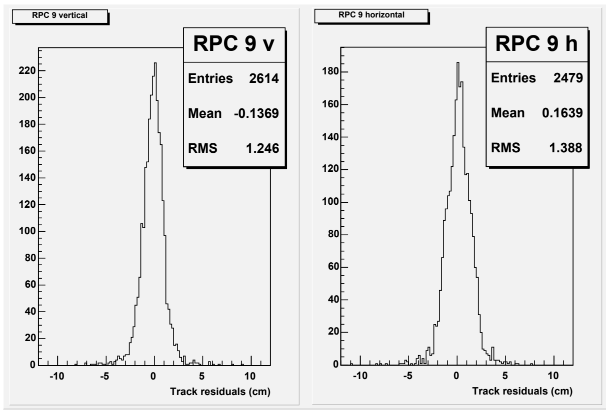

Figure 3: Examples of tracking residuals of one RPC layer, for the bending projection (plot at left) and for the non-bending projection (plot at right).

and Napoli (controller and monitor boards) and coordinated by LNF-SEA. LNF-SEA, together with LNGS Tech.Div. (A. Candela), also designed the overall power distribution system for the experiment; this system has been installed and commissioned in winter 2006 [8].

In 2006, both magnets have been fully instrumented with DAQ and Timing Systems, while only one spectrometer has been instrumented with the Monitor System. At time of writing, the full integration of the Monitor System with the experiment Slow Control is in progress. During the first half of 2006 the Front-end electronics of the RPCs has been fully commissioned in both spectrometers, as well as the gas system. OPERA RPCs are operated at 5.8 kV with the gas mixture $Ar/C_2H_2F_4/i-C_4H_{10}/SF_6$ = 75.4/20.0/4.0/0.6. Signals coming both from horizontal and vertical strips are discriminated at 40 mV. As mentioned before, the full system ran smoothly during the whole CNGS beam physics runs, with almost no dead-time. The performances of the RPCs have been tested on a sample of about 12000 tracks (mostly cosmics) acquired during the run. Beam events are easily distinguished around (θ, ϕ)=(0,0), where ϕ (θ) is the angle with respect to the beam axis in the bending (not-bending) projection.

Typical tracking resolution values for the Inner Trackers are around 1.3 cm, as shown in figure 3.

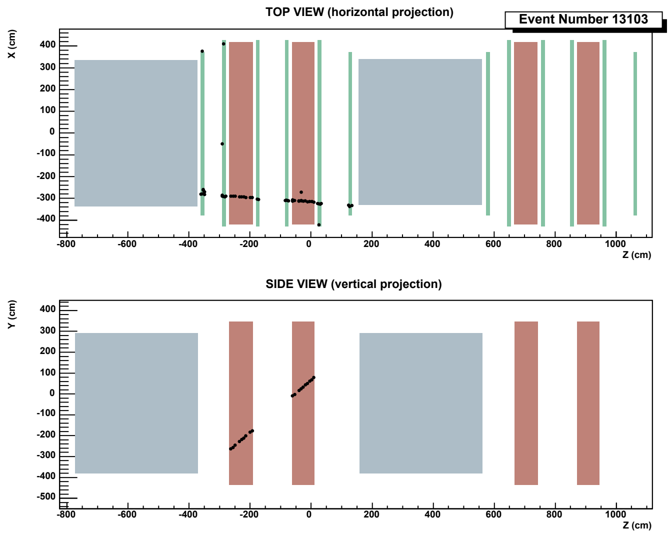

Figure 4: Event reconstructed in the drift tubes of the first spectrometer. Drif tubes are represented in green, while the iron magnet with the installed RPCs are plotted in brown. The other electronic detectors where off.

Average cluster sizes are about 2.4 strips in the bending projection and 1.4 strips in the other projection. The average efficiency of each RPC layer has been measured to be 95%, due to geometric inefficiency. Typical counting rates between 1 and 2 kHz/layer have been observed, with operating currents around 500 nA for each RPC row (3 chambers, corresponding to a sensitive area of 9 m^2). During october and november 2006, dedicated runs have been performed for the integration of the precision trackers in the trigger and acquisition systems. In figure 4 one of the first events reconstructed in the drift tubes is shown.

3.4 Wall support structure

The wall support structure ("walls") is made of thin stainless steel vertical bands welded to light horizontal trays where the bricks are positioned with a precision of one millimeter. The structure is suspended through rods and joints from the general support structure and tensioned from the bottom through a spring system. The walls are installed in parallel with the plastic scintillators (Target Trackers, TT). In particular, all the wall+TT planes of the second supermodule have been positioned in spring 2006. The installation speed of the second supermodule exceeded expectations (1.2 planes/week) and the wall project has been successfully completed by May 2006.

3.5 Brick Assembly Machine

In 2006, the activity of LNF has been mainly focused to the follow-up of the BAM construction at firm and its commissioning at LNGS. Moreover, LNF-SSRC finalized the materials and tools for brick packing ("Al spiders"). LNF also contributed to the installation, configuration and maintenance of the BAM database server. In spring 2006 the system was completed at firm but only partially commissioned: in particular only one over five piling stations was fully operative.

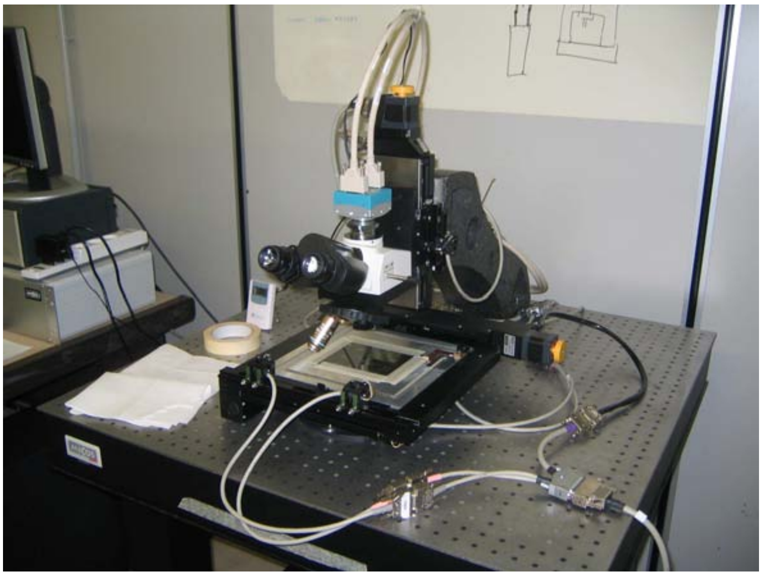

Figure 5: One of the microscopes installed at LNF.

The BAM was installed at LNGS in summer 2006. LNF contributed to the commissioning of the piling stations and wrapping system; they also take care of the monitoring of the quality of the lead and of several lead handling issues.

3.6 The LNF scanning station

Emulsion layers are made of gel with interspersed AgBr crystals; in the case of OPERA, two such layers, each 40 μm thick are poured on a 200 μm plastic base. A particle crossing an emulsion layer ionises the meduim, leaving a sequence of "sensitized" sites. After development, these sites are turned into silver grains, with a linear dimension of about 0.6 μm. About 30 grains every 100 μm are left by a minumum ionising particle.

Nuclear emulsions are analized by means of optical microscopes: adjusting the focal plane of the objective lens through the whole emulsion thickness allows to obtain an optical tomography of each field of view, in order to reconstruct 3D tracks. A detailed description of the automatic microscopes developed for OPERA can be found in Ref. [9)].

During 2006, two microscopes have been installed in Frascati (see figure 5) and at present are under commissioning with a set of emulsions exposed to a pion beam at CERN PS. The design scanning speed of about 20 cm^2/h per side has been reached. The alignment of the microscope optics at the mrad level has also been verified.

Finally, it's worth mentioning that emulsion tests have been done at LNF using the BTF electron beams, particularly for the quality tests of the Opera "changable sheets" (see the BTF report in this document).

3.7 Software and analysis

LNF contributes to the simulation of the magnetic spectrometers, the embedding of the magnetic field maps and the development of reconstruction algorithms for charged particles in the new offline framework for OPERA. Moreover, LNF in collaboration with Lyon and INFN Padova, has provided crucial tools for the first CNGS run: the online event display, the definition and implementation of the data format for the electronic detectors, the muon predictions extrapolated at the locations of the emulsion bricks [3], the full simulation of neutrino interactions in the material surrounding the experiment, especially in rock. More recently, a new optimization of the reconstruction codes has been carried out to ease data analysis with cosmics and improve 3D track reconstruction. Finally, LNF contributes to the development of the spectrometer slow control (SC) and in particular handles the interface with the overall OPERA DAQ/SC through a dedicated CORBA server.

4 List of Conference Talks by LNF Authors in Year 2006

1. A. Paoloni, "The start-up of the OPERA experiment", CalTech Informal High Energy Physics Seminar, Pasadena, CA.
2. A. Cazes, "Construction and commissioning of the magnets for the Opera experiment", 2006 Nuclear Science Symposium and Medical Imaging Conference, NSS-MIC IEEE, San Diego, CA.
3. F. Terranova, "The instrumented magnets for the OPERA experiment: construction and commissioning", 10th Topical Seminar on Innovative Particle and Radiation Detectors, Siena, Italy.
4. C. Di Troia, "Monitoraggio del fascio CNGS con gli spettrometri di Opera", XCII Congresso Nazionale della Societá italiana di fisica, Torino, Italy.

References

1. M. Guler *et al.*, OPERA proposal, CERN/SPSC 2000-028, SPSC/P318, LNGS P25/2000.
2. M. Komatsu, P. Migliozzi, F. Terranova, J. Phys. **G29**, 443 (2003);
   P. Migliozzi, F. Terranova, Phys. Lett. **B563**, 73 (2003).
3. R. Acquafredda *et al.* [OPERA Collaboration], New J. Phys. **8**, 303 (2006).
4. A. Cazes et al., "Electromagnetic characterization of the 990 ton gapless magnets for the Opera experiment", Opera Internal Note.
5. A. Bergnoli *et al.*, Nucl. Phys. B (Proc. Suppl.) **158**, 93 (2006).
6. A. Bergnoli *et al.*, Nucl. Phys. B (Proc. Suppl.) **158**, 35 (2006).
7. See "LNF 2005 Annual report", E. Nardi ed., LNF-06/10 (IR), p.78, "LNF 2004 Annual Report", E. Nardi ed., LNF-05/5 (IR), p.70; "LNF 2003 Annual Report", S.Dell'Agnello ed., LNF-04/08 (IR), p.64.
8. A. Candela, G. Felici, F. Terranova, "The Opera power distribution system", LNF-07/7 (NT).
9. N. Armenise *et al.*, Nucl. Inst. Meth. **A551**, 261 (2005).

STUDY OF MAGNETO-OPTICAL PROPERTIES OF GASES AND VACUUM AT PVLAS

E. Zavattini[1]†, G. Zavattini[2], G. Ruoso[3], G. Reiteri[1], E. Polacco[4], E. Milotti[1], M. Karuza[1], U. Gastaldi[3], G. Di Domenico[2], F. Della Valle[1], R. Cimino (Resp.loc)[5], S. Carusotto[4], G. Cantatore[1], M. Bregant[1]

1) Dipartimento di Fisica and INFN, Trieste; 2)Dipartimento di Fisica and INFN, Ferrara;
3) INFN, Laboratori Nazionali di Legnaro; 4) Dipartimento di Fisica and INFN, Pisa;
5) INFN, Laboratori Nazionali di Frascati;
† Deceased on 9-01-2007 PVLAS activities during 2006 have been focussed on apparatus upgrades

and additions, on data analysis and publication of previously obtained results, and on the continued search for a possible instrumental source of the observed signals.

Figure 1: *View of the PVLAS optics tower showing the new aluminum access structure.*

Upgrades included the construction and installation of a new structure to access the optics tower and the cryostat and the layout of new signal cables. The old iron tubing scaffolding, was replaced with a new structure entirely made of aluminum. This structure, besides being amagnetic, allows easy operator access to the upper optical bench and to the top and sides of the rotating cryostat. The structure, which is visible in the photograph shown in figure 1, rests entirely on the concrete beam spanning the PVLAS dugout and supporting the turntable-magnet-cryostat assembly.

A new gasline for the insertion of ultrapure gases in the interaction region was also added, along with sets of Helmholtz coils around the Fabry-Pèrot (FP) cavity mirrors to compensate both the static magnetic field due to the earth and the variable fringe fields due to the rotating magnet. Furthermore, a setup for the performance of a photon regeneration test was designed as an addition to the main apparatus and its construction was started. This test is based on the fact that should hypothetical particles be produced from a two-photon vertex in the interaction region two beams of such particles will propagate vertically along the cavity in both directions. Being the particles weakly interacting with normal matter, these beams will pass through the mirrors and the granite optical tables. The downward propagating beam can be intercepted by placing a permanent dipole magnet below the lower optical bench. Within this field, particles can decay back into regenerated photons which can then be detected downstream. The observation of such regenerated photons would be a direct confirmation of the particle interpretation of the observed signals, and indeed, a major physics result.

In 2006, data analysis efforts were concentrated both on gas measurements, from which we obtained apparatus calibrations and performance tests and novel determinations of the Cotton-Mouton effect in gases, and on disentagling the wealth of information on the vacuum magnetic birefringence and rotation effects. The latter effort was distinctly aimed at identifying possible spurious sources in order to validate the already published results on vacuum ?).

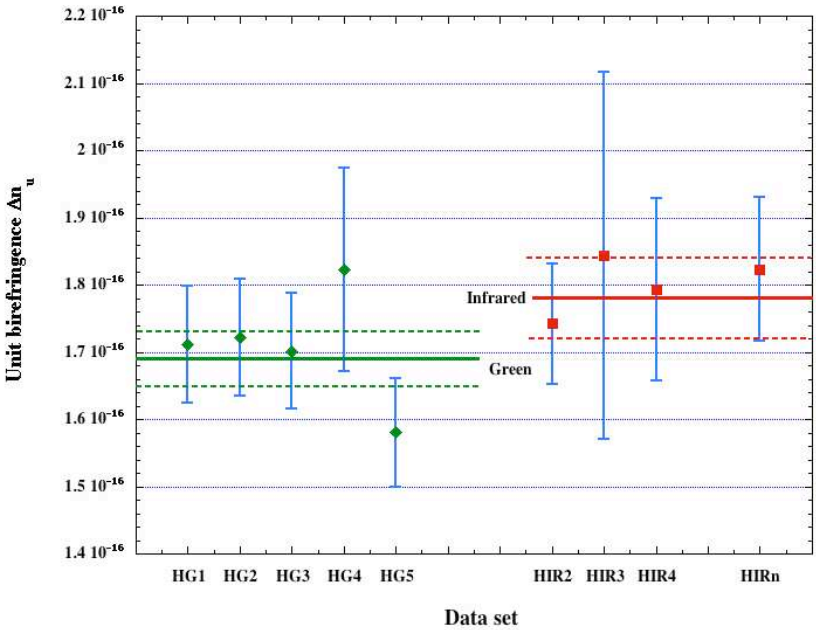

Figure 2: *Unit birefringence of He as a function of data set. Green refers to a laser wavelength of 532 nm while Infrared refers to 1064 nm. Different data sets where acquired at different times spanning about two years from HG1 to HIRn. The dotted lines represent 1σ error bands. Notice the stability of the apparatus over time.*

The remaining suspect as a source of instrumental artifacts is the residual stray field (of the order of 1-5 G when the magnet is runnign at 5 T). We have measured and excluded the direct action of the stray field on the FP cavity mirrors as a source of systematics. This is also the case for the SOM modulator and the other optical elements. It remains, therefore, the possibility of some indirect stray field-polarization coupling which could affect our signal. The actual mechanism causing such a coupling is however unknown. A possible solution has been searched by studying, without conclusive results, the effect on the FP cavity due to the residual mirror birefringence [?]. We are also trying to implement the existing set-up as follows: compensate the local stray fields on the mirrors using Helmholtz coils, move the laser and the feedback electronics away from the magnet using optical fibers to bring the light into the interaction region, energize the magnets at 2.3 T to keep al field lines contained within the soft iron yoke. This strategy needs, among other things, rather extended data taking periods with the magnet cold and energized. Due to the poor duty cycle of the experiment, the currently available statistics is too limited to draw immediate conclusions. In these runs we also performed routine gas magnetic birefringence measurements (Cotton-Mouton effect) on Helium, Neon and Nitrogen. A series of measurements of the Cotton-Mouton effect in He at 1064 nm is shown in figure 2 where the unit birefringence of He is plotted as a function of the data set and of the laser wavelength. The stability of the apparatus over time is apparent from the plot. It must also be noted that the reported values for the He reduced bifrefingence differ by about 20 % well out of the 3σ confidence interval, from current theoretical values.

References

1. "Experimental observation of optical rotation generated in vacuum by a magnetic field", E. Zavattini et al. [PVLAS Collaboration], Phys. Rev. Lett. **96**, 110406 (2006) [hep-ex/0507107].
2. "On measuring birefringences and dichroisms using Fabry-Pèrot cavities" G. Zavattini, G. Cantatore, R. Cimino, G. Di Domenico, F. Della Valle, M. Karuza, E. Milotti, G . Ruoso: Appl. Phys. B 83, 571577 (2006)

RAP

B. Buonomo (Bors.), G.O. Delle Monache, G. Cavallari (Osp.), G. Ceccarelli (Tecn.), R. Ceccarelli (Tecn.), M. De Giorgi (Tecn.), D. Di Gioacchino, V. Fafone, C. Ligi (Art.23), R. Lenci (Tecn.), A. Marini (Resp. Naz.), G. Mazzitelli, G. Modestino, G. Pizzella (Ass.), L. Quintieri (Art.23), F. Ronga (Resp.), S.M. Vinko (Laur.)

1 Aim and description of the experiment

The primary scope of the experiment RAP is to measure the longitudinal vibrations of cylindrical test masses, that are impinged by the electrons provided by the DAΦNE Beam Test Facility (BTF), in order to investigate if the mechanism of the particle energy loss conversion into mechanical energy depends on the conduction state of the bar.
The motivation of the experiment is related to the fact that the gravitational wave antenna Nautilus has detected high energy cosmic rays at a rate higher than expected when the bar was operated at $T = 0.14$ K, that is in the superconductive (s) state. On the contrary, the observed rate of high energy cosmic rays was in agreement with expectations when the bar was operated at $T = 1.5$ K, that is in the normal (n) state.
The expectations rely on models [1, 2, 3] that account for the excitations of the longitudinal modes of vibration of a cylinder due to pressure sources related to the energy lost by particles in the interaction. For a thin cylinder in the n state, if a particle normally impinges on the middle point of the generatrix then the maximum amplitude of the first longitudinal mode of oscillation (FLMO) is given by [1]:

$$B_0^n = \frac{2\alpha^n LW}{\pi c_V^n M} \ , \tag{1}$$

where L and M are the cylinder length and mass, W is the total energy lost by the particle in the cylinder, α^n and c_V^n are respectively the linear thermal expansion coefficient and the specific heat at constant volume of the material in the n state. B_0 is related to the pressure source due to thermal effects. The expected FLMO maximum amplitude is given by $X_{exp} = B_0^n(1+\epsilon)$, where ϵ is estimated by a montecarlo simulation, which takes into account the solutions at the 2nd order for the modes of oscillation of a cylinder, the transverse dimension of the beam at the impact point and the angles with the cylinder axis of the secondary particles generated in the bar. To evaluate B_0 at different temperatures and for each beam pulse, α and c_V are computed by interpolating data available on the literature, while W is given by $N_e \times \Delta E$. The number of electrons per pulse, N_e, is measured by the BTF beam monitor facility, while the average energy lost by each electron in the interaction, ΔE, is estimated by the montecarlo simulation. In order to assess the models, X is compared with the values of the measured FLMO maximum amplitude, which is given by $X_{meas} = V_{meas}/(G\lambda)$, where λ is the electro-mechanical conversion factor of the piezoelectric transducers (Pz), G is the amplifier gain and V_{meas} is the maximum amplitude of the signal component at the FLMO frequency, which is obtained by Fast Fourier Transform algorithms applied to the digitized Pz signals. Two ways of comparing data and expectations are possible when the bar is in the s state. In the first mode data are compared against $X_{exp} = B_0^s(1+\epsilon)$, where B_0^s is given by (1) using α^s and c_V^s. The second way [2, 3] takes into account two pressure sources: one due to $s-n$ transitions in small regions centered around the particle tracks and the other due to thermal effects in these regions. Therefore X_{exp} is given by:

$$X_{exp} = X_{tr} + X_n = \left[\frac{2\rho W L}{3\pi M}\frac{\Delta V/V}{\Delta\mathcal{H}/V} + B_0^n\right](1+\epsilon) \ , \tag{2}$$

where ρ is the density and $\Delta V/V$, $\Delta\mathcal{H}/V$ are the specific variations of volume and enthalpy in the $s-n$ transition, respectively.
The experimental setup (*viz.* the beam, the test masses, the suspension system, the cryogenic and vacuum system, the mechanical structure hosting the cryostat, the readout and the data acquisition system) is described in [4]. In particular two test masses have been used: one made of AL5056, the same material of NAUTILUS, which has a critical temperature $T_c \sim 0.9\ K$, and one made of Nb ($T_c \sim 9\ K$).
INFN and Physics Department Università di Roma Tor Vergata and Kamerlingh Onnes Laboratory, Leiden University (The Netherlands) are participating Institutions to the experiment.

2 Activities in the year 2006

Two lines of activity were performed in the year: *a*) the commissioning of the dilution refrigerator, needed to cool the AL5056 bar at temperatures below 1 K where the material is in the *s* state and *b*) the completion of the analysis of the data taken with the Nb bar.

a) The manufacturer completed the shipment of the dilution refrigerator components on January, 2006. The assembly of the refrigerator inside the cryostat required the $ex-novo$ realization of parts and the first cooling at LHe temperature occurred on September, revealing leaks in the cryogenic system. The completion of the commissioning is planned for Spring 2007.

b) The data collected in the year 2005 with the Nb bar have been fully analyzed and the results have been published [5]. A good agreement is found among observed and expected values for Nb in *n* state, as shown in Table 1. For Nb in *s* state a linear dependence of X_{meas} on the measured energy deposited by the beam pulses in the bar is found (Fig. 1).

$T[K]$	m	Δm
275	0.96	0.01
81	1.03	0.01
12.5	0.95	0.02

Table 1: *Nb - Values of m fitting* $X_{meas} = m\ X_{exp}$ *and error* Δm.

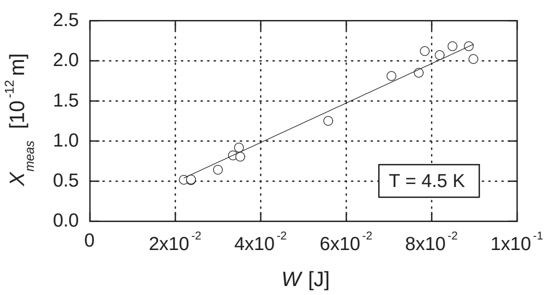

Figure 1: *Nb,T = 4.5K. Correlation between measured FLMO maximum amplitudes (X_{meas}) and energy (W), deposited by beam pulses in the bar, as derived by N_e measurements.*

Fig. 2-left shows the measured FLMO maximum amplitudes normalized to W above and below T_c, together with the expectations computed using the first mode of comparison (B_0^n for $T > T_c$ and B_0^s for $T < T_c$). The quantity $X_{meas} - B_0^n(1+\epsilon)$ is checked against X_{tr}, as given by (2), for assessing the second mode of comparison (Fig. 2-right), which seems to explain better the data in the region $4K < T < 8K$.

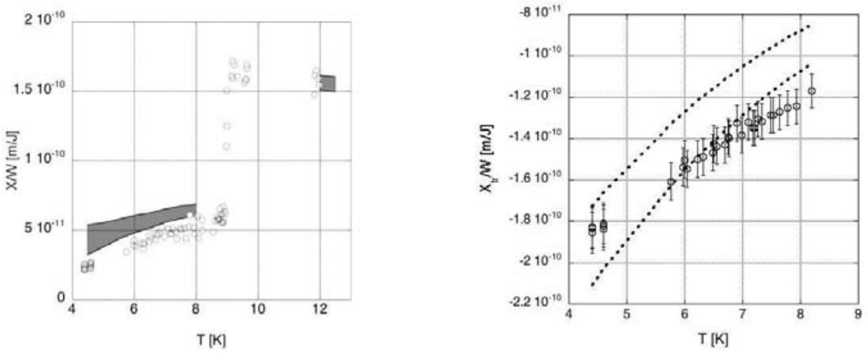

Figure 2: *Nb - Left: FLMO maximum amplitudes (X) normalized to the total energy lost per beam pulse (W) vs. temperature (T). Circles: measured values. Bands: expected values. Right: The component of the FLMO maximum amplitude due to local transitions normalized to the energy lost (X_{tr}/W) vs. temperature (T). Circles : observed values. The region enclosed by the broken lines shows the expected values.*

The expected rate of cosmic ray coincidences in NAUTILUS was evaluated by using (1) in n state. The results obtained by RAP with the Nb bar suggest that the amplitude of oscillations due to the energy released by particles impinging on the bar depends on the state of conduction. While for niobium in the s state the FLMO maximum amplitude is observed and expected smaller than in the n state, the contrary is expected for aluminum. However, a final confirmation will be obtained by performing the measurements with the AL5056 bar cooled at temperatures below 1 K.

3 List of Conference Talks by LNF Authors in the Year 2006

- L. Quintieri, "The RAP experiment: acoustic detection of particles", IPRD06: 10th Topical Seminar on Innovative Particle and Radiation Detectors. Siena - 1-5 October 2006.

References

1. A.M. Grassi Strini *et al.*, J. Appl. Phys. **51**, 948 (1980).
2. A.M. Allega and N. Cabibbo, Lett. Nuovo Cim. **38**, 263 (1983).
3. C. Bernard *et al.*, Nucl. Phys. B **242**, 93 (1984).
4. B. Buonomo *et al.*, Astropart. Phys., **24**, 65 (2005).
5. M. Bassan *et al.*, Europhys. Lett. **76**(6), 987 (2006).
6. M. Bassan *et al.*, J. Phys.: Conf. Ser. **39**, 46 (2006).
7. M. Bassan *et al.*, J. Phys.: Conf. Ser. **32**, 393 (2006).

ROG

D. Babusci, V. Fafone (Resp.), G. Giordano, M. Iannarelli (Tecn.),
R. Lenci (Tecn.), A. Marini, G. Modestino, G.P. Murtas (Ass.),
G. Pizzella (Ass.), L. Quintieri (Art. 23), F. Ronga (Resp.), E. Turri(Tecn.)

Collaboration with: LNGS, INFN Genova,
University of Rome La Sapienza and INFN Roma 1,
University of Rome Tor Vergata and INFN Roma 2,
Geneva University, Leiden University

1 Introduction

The ROG group is currently operating two cryogenic gravitational wave (GW) bar detectors: EXPLORER (at CERN) and NAUTILUS (in Frascati). The main goal of this search is the direct detection of the GW's that could be emitted by astrophysical sources (such as Supernovae or Coalescent Binaries). Such detection would be of enormous interest for general relativity and astrophysics.

Both detectors consist of an aluminum cylindrical bar having a mass of $\simeq 2.3$ tons, with a capacitive resonant transducer mounted on one of the bar faces. They are contained in a vacuum cryostat, cooled at cryogenic temperatures ($\simeq 3$ K) to reduce thermal noise, and are isolated from seismic and acoustic disturbances.

The capacitive transducer is coupled to a very low noise superconducting amplifier (d.c. SQUID) whose output is acquired by a VME ADC board, sampled at 5 kHz.

A GW signal would excite the mechanical resonant modes of the bar-transducer system. When searching for impulsive signals, the data are filtered with an adaptive filter matched to a delta-like signal. This search for bursts is suitable for any transient GW which shows a nearly flat Fourier spectrum at the two resonance frequencies of each detector.

Both EXPLORER and NAUTILUS have been kept in continuous observational mode since 2003, with a duty cycle between 80 and 90%, mainly limited by the necessary periodic cryogenic operations.

The LNF group has major responsibilities in the maintenance and running of NAUTILUS (including the production of liquid Helium), in the maintenance, upgrading and running of the cosmic ray detectors, in the development of a new nearly quantum limited signal read-out, in the data acquisition and in many items of data analysis.

During 2006, ROG continued the collaboration with the Leiden University group for the development of MiniGRAIL, a resonant spherical detector located in Leiden (Holland). This collaboration, ongoing since several years, has regarded mainly the read-out chains and the data acquisition system. This last period effort was mainly devoted in the preparation of a first scientific run of MiniGRAIL, preparing its full configuration of 6 transducers in the so called TIGA configuration, able of determining all the parameters of a GW wave (direction, tensorial characteristics and polarization state).

2 NAUTILUS and EXPLORER

The ultra-cryogenic detector NAUTILUS is operating at the INFN Frascati National Laboratory since December 1995. It is equipped with a cosmic ray detector based on a streamer tube assembly.

The present data taking started in 2003, with a new bar tuned at 935 Hz, where a pulsar, remnant of the SN1987A, is supposed to emit GW's, with a more sensitive readout chain (the same as for EXPLORER), and a new suspension cable, to provide a more stable position setting. At present, the temperature of the bar is 3.5 K and the resulting strain noise (the minimum detectable spectral density) is $\tilde{h} \simeq 1 \div 2 \cdot 10^{-21}$ $/\sqrt{Hz}$ around 935 Hz, and $\tilde{h} \leq 10^{-20}$ $/\sqrt{Hz}$ over about 30 Hz. The noise temperature is less than 2 mK, corresponding to an adimensional amplitude of GW bursts $h = 3.4 \cdot 10^{-19}$.

NAUTILUS is the only resonant detector capable of reaching a temperature as low as 0.1 K, being equipped with a ^{3}He-^{4}He dilution refrigerator. This ultra-cryogenic operational mode would result in a better sensitivity but also in a decrease of the duty cycle. Up to now, we decided to give the priority to the observational time and so we keep the standard operation at 3 K.

The EXPLORER antenna is located at CERN and is very similar to NAUTILUS, but can operate only down to 2.6 Kelvin. Also the duty cycle of EXPLORER is very high (of the order of 90%) and the noise temperature of the order of 2 mK, with a strain sensitivity $\tilde{h} \simeq 2 \div 3 \cdot 10^{-21}$ $/\sqrt{Hz}$ around the two resonances at 904 Hz and 927 Hz, and $\tilde{h} \leq 10^{-20}$ $/\sqrt{Hz}$ over about 30 Hz. Also EXPLORER is equipped with a cosmic ray detector, based on a set of long plastic scintillators.

The read-out systems installed in 2001 on EXPLORER and in 2003 on NAUTILUS, obtained a larger bandwidth and consequently improved the time resolution (now less than 10 ms), as it is also been checked with the events due to cosmic ray showers.

3 Read-out developments

The read-out of all the resonant-mass GW detectors is based on an electromechanical transducer (capacitive or inductive) and a d.c. SQUID amplifier.

In most practical applications the sensitivity of a SQUID with a standard electronics is usually good enough. However GW detectors require the highest possible sensitivity of a d.c. SQUID. In this case the standard read-out may not be the best solution, because the overall sensitivity can be limited by the room-temperature preamplifier noise. With this standard setup the typical energy resolution measured by the detector is about $20000\hbar$.

The sensitivity of a resonant-mass detector is limited by three sources of noise which, referred to the output are: the narrowband thermal noise, due to the input wideband brownian motion of the resonant masses, which appears at the output after passing through the mechanical transfer function of the system; the wideband amplifier noise, which appears directly at the output and the narrowband back-action noise, originated from the back-energy flow from the amplifier, which excites the resonant masses.

The useful bandwidth of such detectors is by no means limited to the very narrow width of the high Q mechanical resonance. Rather, it is the amplifier noise that limits the bandwidth. The lowest spectral noise is found in the frequency region where the narrowband (thermal plus back action) noises dominate the amplifier noise, and there the noise level is the sum of the two. As a consequence, any reduction in the amplifier noise and/or increase in transducer coupling, increases the antenna bandwidth.

In the last years, it has been shown that a double-SQUID system can reach quantum limit energy resolution and that a double-SQUID system can be arranged in a stable configuration when connected to a high-Q resonant circuit. The double-SQUID amplifier of the ROG Collaboration is made of a sensor d.c. SQUID, developed by the Institute of Photonic and Nanotechnologies of CNR, while the preamplifier SQUID is a commercial Quantum Design d.c. SQUID. The performances of the device are very good: with open input and open loop it exhibited energy resolutions equal to $28\hbar$ at 4.2 K and $5.5\hbar$ at 0.9 K. The system has been successfully tested with a high-Q resonant input load in the temperature range 2 K-4.2 K. The device showed very good stability and an energy resolution of about $(70 \pm 8)\hbar$ at 2 K has been measured.

With this new device, the expected NAUTILUS sensitivity at 0.1 K is around $3 \cdot 10^{-22}\text{Hz}^{-1/2}$ and the bandwidth, at the level of $10^{-21}\text{Hz}^{-1/2}$, is about 35 Hz. The noise temperature of the detector should be around 7μK corresponding to a sensitivity to 1 ms bursts $h = 2.1 \cdot 10^{-20}$.

An even better type of d.c. SQUID has recently been produced by CNR and is currently under test.

4 Data analysis

In the last years a continuos effort has been payed in improving the data analysis system already present and in testing independent algorithms and new methods. As a result of these, still going, efforts we were able to improve the accuracy in the reconstruction of both the amplitude and time characteristic of the signals. At the same time, we performed detailed studies of the detectors response to other class of signals than the simple delta-like burst previously considered. All this was done also with a particular eye on the perspective of performing joint analyses with the interferometric type of GW detectors.

4.1 EXPLORER-NAUTILUS coincidences

The data collected in 2004 were analyzed with some delay, because we were developping the improvements described above. Moreover, we had to understand the features in the results of the new software. In particular, the number of candidate events in each detector increased by about a factor of 2, due to the increase, by a factor 16, in the sampling rate of the filtered data. This produces a number of accidental coincidences about 4-5 times larger than before. We have then started a study to try and identify possible wide-band noises that can result in a candidate event and also, through simulations and software injections of signals, to find the event characteristics (e.g. length vs. amplitude) that an event due to a real excitation must have. All this aims to reduce the number of candidate events, but, being this study not yet finalized, we decided to maintain the same analysis conditions used in 2003, namely a threshold at 19.5 in energy signal to noise ratio and a coincidence window fixed at 30 ms.

In 2004 we had a total overlap of 218.5 days of good data periods for both Explorer and Nautilus. The average number of accidentals, estimated as usual with realtive shifs in time between the Explorer and Nautilus events, was 84.88, the true coincidences were 89. Fig.1 shows the distribution of coincidences and accidentals as a function of the sidereal time.

Exactly the same analysis was performed for the 2005 data. There we had an overlap time of 182.1 days, an average number of accidentals equal to 113.51 and the true coincidences were 136. The distributions in sidereal time are shown in Fig.2.

About these results, we can comment that, while for 2004 the numbers of coincidence and accidentals are really very close, and nothing noticeable can be seen in the sidereal time distribution, this is not the case for the 2005 results. The sidereal time distributions show some differences, but the main feature is the significant difference between the numbers of true coincidences and accidentals, 136 against an expected value of 113.51, meaning a fluctuation of probability about 0.022.

4.2 IGEC-2 collaboration

The bar detectors distributed worldwide operated for a few years (1997-2000) as a network, giving for the first time significant upper limits to the yearly rate of GW burst events in the Galaxy. In 2003 and 2004 EXPLORER and NAUTILUS have been the only two detectors in data taking over long time periods. Since 2005 both Auriga at LNL and Allegro at the Lousiana State University

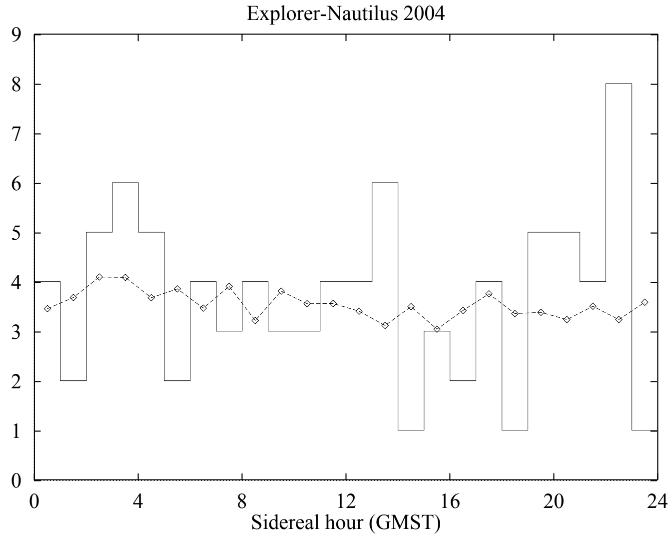

Figure 1: Explorer-Nautilus coincidences in 2004. Number of coincidence and average accidentals as a function of sidereal hour.

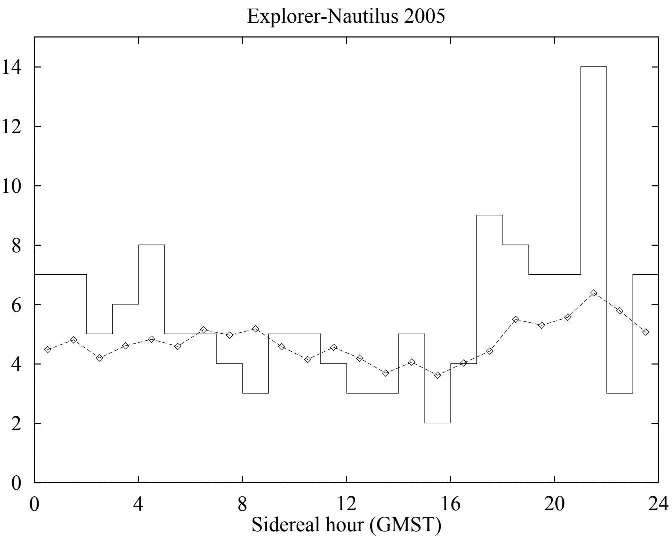

Figure 2: Explorer-Nautilus coincidences in 2005. Number of coincidence and average accidentals as a function of sidereal hour.

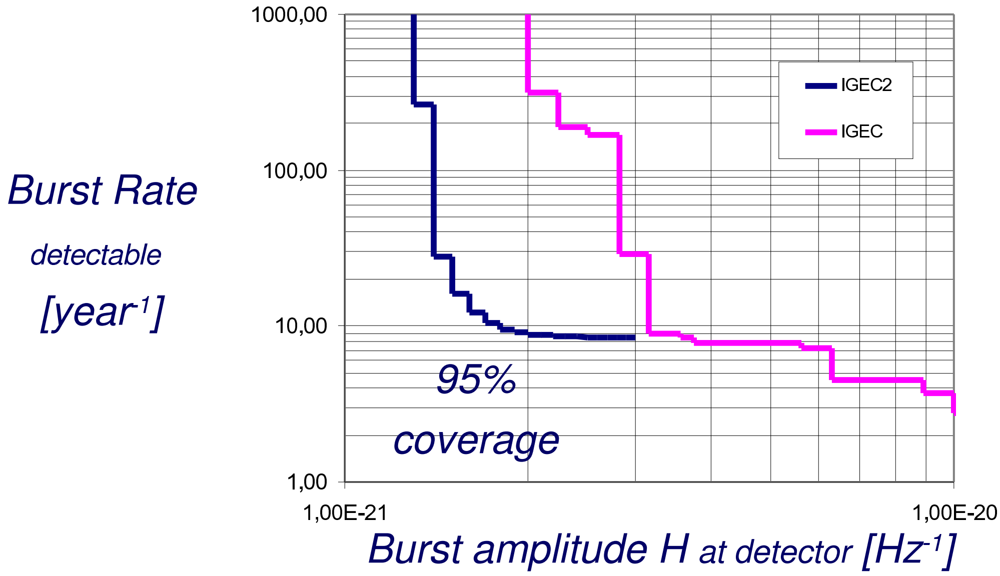

Figure 3: Upper limit at 95% on the rate of detectable GW events as a function of the threshold in amplitude used in the search.

restarted regular operation, so the former IGEC collaboration was restarted, under a new agreement (IGEC-2) between the 4 bar detectors.

This new agreement produced in 2006 the joint analysis of six months of 2005 data from AURIGA, EXPLORER and NAUTILUS (ALLEGRO was not able to produce in due time its event list). The period, from May to November 2005, was covered for $\simeq$ 73%, for a total overlapping time between the three detectors of 130 days. The search was based on three-fold coincidences at a very low level of accidental rate, namely 1 per century, and no triple coincidences were found. A subset of the data was used to compute upper limits in the rate of GW burst (see fig.3), showing a clear improvement in sensitivity with respect to the previous IGEC-1 search.

At the moment, we are establishing a new agreement for the joint analysis of the data collected up to the end of 2006, than of more than 1 year.

4.3 Collaborations between resonant bars and interferometers

A first joint data analysis between all the INFN GW detectors (AURIGA, EXPLORER, NAUTILUS and VIRGO) has been performed for the period of the VIRGO C7 run (September 2005). Since the period was really short (VIRGO could provide only less than 1 day of good data), the analysis has addressed more methodological than scientific issues. The efficiency of each detector separately, and then of the network, was extensively studied through a large number of software injections of damped sinusoid signals with 11 different carrier frequencies or damping times. The detailed knowledge of the efficiency as a function of time has been employed in the study of possible optimized ways for the selection of vetoes and thresholds. A publication concerning the results obtained is currently in preparation.

An agreement between LIGO and all the groups forming the IGEC collaboration (Allegro, Auriga and ROG) is being established. Likely, this agreement will conceive the common analysis of about 1$\div$2 months of data, that is the period of the LIGO S5 run, started in November 2004 and still going, when only one of the LIGO interforemeters was in operation. In such periods, LIGO cannot hope to perform any detection by itself and so the addition of the IGEC bar detectors will retrieve these periods.

4.4 Other type of analyses

- Cosmic Rays - The study of the response of our detectors to cosmic ray showers continues to demonstrate experimentally the actual capability to detect very small mechanical excitations of the bars. While the study of the timig characteristics of the larger events produced by the rare very high density showers allows us a real measure of the accuracy in the time reconstruction, the study of the much more numerous cases of low density showers, performed with a cumulative-type analysis, constitutes an independent cross-check of the amplitude response calibration.

- Search for monochromatic signals - Also this kind of analysis continued in 2006, both with the already tested coherent algorithms and a new non-coherent one, developed by the Geneva group and currently under test. In principle, a non-coherent method should exhibit a loss of sensitivity with respect to a coherent one, but, being extremely faster, allows to analize in a reasonable time and on standard computers an amount of data larger by 2-3 orders of magnitude, thus obtaining at the end a better overall sensitivity.

- Search triggered by astrophysical events - The analysis of our detectors data at the time of a large number of Gamma-ray bursts allowed us to set upper limits on the amplitude of possible GW signals associated to them. This kind of study is continuing and actually has been extended to detailed analysis of the data collected in coincidence with some rare astrophysical events, like the giant flares happened 1998 and 2004.

5 ROG publications in 2006

1. P. Astone *et al*, "Status report on the EXPLORER and NAUTILUS detectors and the present science run", Classical and Quantum Gravity, **23**, S57 (2006).
2. A. de Waard *et al*,"Preparing for science run 1 of MiniGRAIL", Classical and Quantum Gravity, **23**, S79 (2006).
3. P. Astone *et al*, "The 2003 run of the EXPLORER-NAUTILUS gravitational wave experiment", Classical and Quantum Gravity, **23**, S169 (2006).
4. V. Fafone, "Developments in resonant-mass detectors", Classical and Quantum Gravity, **23**, S223 (2006).
5. P. Astone *et al*, "All-sky search of EXPLORER data: search for coincidences", Classical and Quantum Gravity, **23**, S687 (2006).
6. M. Bassan *et al*, "A new capacitive read-out for EXPLORER and NAUTILUS", Journal of Physics Conf.Ser. **32** 89 (2006).
7. P. Astone *et al*, "Validating delta-filters for resonant bar detectors of improved bandwidth foreseeing the future coincidence with interferometers", Journal of Physics Conf.Ser. **32** 192 (2006).
8. F. Ronga, "Detection of gravitational waves with resonant antennas", Journal of Physics Conf.Ser. **39** 18 (2006).
9. I. Modena and G. Pizzella, "Coincidences between the gravitational wave detectors EXPLORER and NAUTILUS in 1998, during the activities of the black hole candidate XTE J1550-564 and the magnetar SGR1900+14", Int. Journal of Modern Physics **D15** 485 (2006).

WIZARD

G.Basini, F.Bongiorno (Ass.), L.Bongiorno (Bors.),
G.Mazzenga (Tecn.), M.Ricci (Resp.)

Participant Institutions:

ITALY: INFN Bari, LNF, Firenze, Napoli, Roma Tor Vergata, Trieste;
CNR Ist. Fisica Applicata "Nello Carrara" Firenze;
ASI (Italian Space agency);
Electronic Engineering Department, University of Roma 2 "Tor Vergata";
RUSSIA: MePhi Moscow;
FIAN Lebedev Moscow;
IOFFE St Petersburg;
TsSKB-Progress Samara;
SWEDEN: KTH Stockholm;
GERMANY: Siegen University;
USA: NASA Goddard Space Flight Center;
New Mexico State University.

1 Experimental Program and Scientific Objectives

The WIZARD experimental program is devoted to the extensive study of cosmic ray spectra (particles, antiparticles, isotopes, abundances and search for antimatter) in several energy ranges achievable through different instruments on board stratosferic balloons and long duration satellite missions. WIZARD is an International Collaboration between several Universities and Research Institutions from Russia, Sweden, Germany, USA togheter with the Space Agencies NASA, RSA (Russia), SNSB (Sweden), DLR (Germany) and ASI. The experimental activities have been and are carried out through three main programs:

- Stratospheric Balloon flights;
- Satellite missions NINA-1 and NINA-2;
- Satellite mission PAMELA.

We refer to previous editions of this report for the descrition of the activities related to the balloon flights and to the two NINA missions.

1.1 The satellite mission PAMELA

PAMELA is a cosmic ray space experiment installed on board a Russian satellite (Resurs-DK1) which has been successfully launched on June 15th, 2006 from the cosmodrome of Baikonur, Kazakhstan, by a Soyuz TM2 rocket. Fig. 1 shows the lift-off of the rocket.

The satellite will fly for at least 3 years in a low altitude, elliptic orbit (300-600 km) with an inclination of 70.4 degrees. The PAMELA telescope consists of a magnetic spectrometer composed of a permanent magnet coupled to a silicon tracker, an electromagnetic silicon-tungsten calorimeter, a time-of-flight system, an anticoincidence system, a shower tail catcher scintillator and a neutron detector [1, 2]. A sketch of the PAMELA instrument is shown in fig.2 and a photo of the completed Flight Model is shown in fig. 3.

Figure 1: Lift-off of the Soyuz rocket from the Baikonur cosmodrome.

The total height of PAMELA is $\sim$ 130 cm, the mass is 470 kg and the power consumption is 355 W.

The observational objectives of the PAMELA experiment are to measure the spectra of antiprotons, positrons and nuclei over an extended range of energies, to search for antimatter and for indirect signatures of dark matter and to study cosmic ray fluxes over a portion of the Solar cycle.

The main scientific goals can be schematically listed as the following:

a) measurement of the antiproton spectrum in the energy range 80 MeV-190 GeV;
b) measurement of the positron spectrum in the energy range 50 MeV-270 GeV;
c) measurement of the electron spectrum in the energy range 50 MeV-400 GeV;
d) measurement of the proton spectrum in the energy range 80 MeV-700 GeV;
e) measurement of the electron+positron spectrum up to 2 TeV;
f) measurement of light nuclei spectra (up to Z=6) at energies 100 MeV/n - 250 GeV/n;
g) search for antinuclei with a sensitivity of the order of 10^{-7} in the $\overline{He}/He$ ratio (95% C.L.).

In addition, the PAMELA experiment will be able to measure the light nuclear component of cosmic rays and investigate phenomena connected with Solar and Earth physics.

So far, the satellite and the PAMELA instrument are functioning nominally and the overall performance of the detectors is fairly good. Every day, an average of 14 GBytes of data are transmitted to the main Receiving Station NTsOMZ located in Moscow. Then, alla data are transferred through high-speed networks to CNAF, Bologna and to the participating institutions of the PAMELA International Collaboration where preliminary analysis of data has started. A sample of events gathered in flight is displayed in figs. 4, 5 and 6 where a 4.2 GeV electron, a 1.56 GeV positron and a 35 GeV interacting proton are shown, respectively.

Activity in the year 2006 has covered the following items:

- Pre-launch readiness tests and launch in orbit (15 June 2006) from Baikonur Cosmodrome (Kazakhstan).

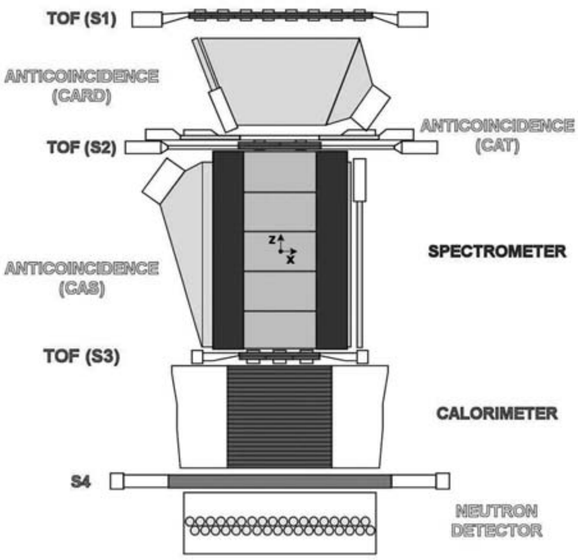

Figure 2: Sketch of the flight detectors the PAMELA telescope.

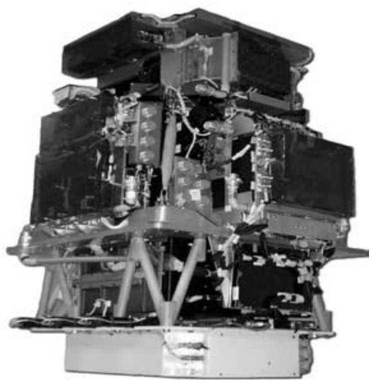

Figure 3: The PAMELA Flight Model.

- Commissioning of Resurs satellite and PAMELA instrument in orbit.
- Data taking in flight: first phase and establishment of downlink procedures.
- Additional Beam tests of detectors of the Technological/Engineering Model at GSI/Darmstadt (nuclei) and CERN/SPS (protons).
- Final set-up and operation of the main (Moscow, Russsia) and peripheric (Roma Tor Vergata) ground control and data receiver centers.

2 Activity of the LNF group during year 2006

The LNF WIZARD group has been fully involved in all the previous balloon and present satellite programs. During the year 2006 the activity for the PAMELA experiment has been carried on as follows:

- Responsibility of the Mechanical Ground Support Equipment (MGSE) for the assembly and integration of the whole apparatus.
- Preparation, assembly and tests of the Flight Model.

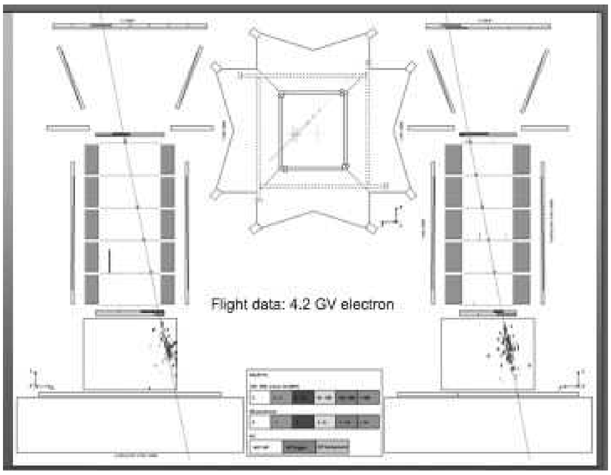

Figure 4: Display of an in-flight 4.2 GeV electron

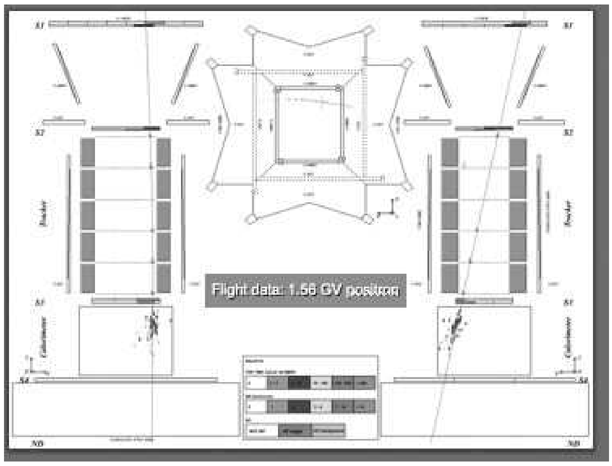

Figure 5: Display of an in-flight 1.56 GeV positron

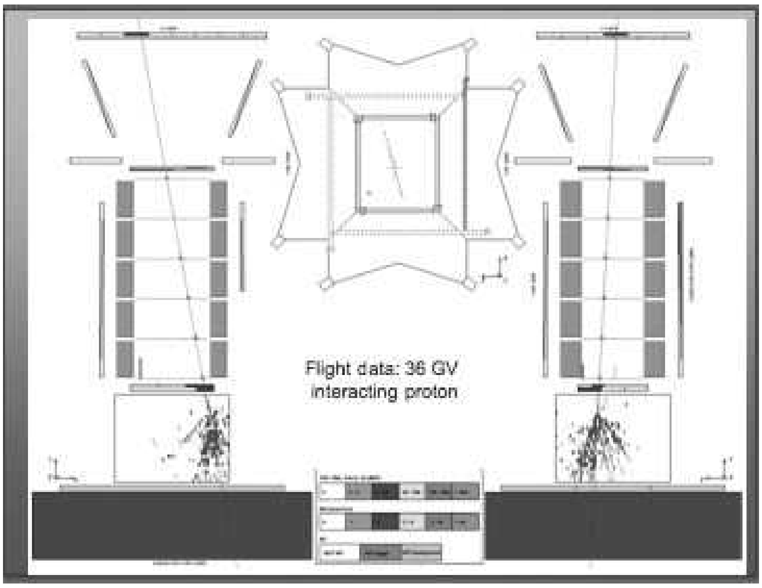

Figure 6: Display of an in-flight 35 GeV interacting proton

- Definition and organization of the data base of the command-control procedures from ground.
- Responsibility of the beam test at CERN SPS.

3 Planned activity in 2007

- Shifts at NTsOMZ ground control center for the monitoring of the mission and data transmission to ground.
- First analysis of data, presentation to Conferences and publication of first results.
- Continuation of Beam tests of detectors of the Technological/Engineering Model at GSI/Darmstadt (nuclei) and CERN/SPS (protons).

4 A selection of Publications in 2006

1. S. Orsi *et al.*,"Second Level Trigger for the PAMELA Satellite Experiment ", Astrop. Phys.**25**, 33 (2006)
2. S. Straulino *et al.*,"Spatial Resolution of Double-Sided Silicon Microstrip Detectors for the PAMELA Apparatus ", Nucl. Instr. and Meth. **A556**, 100 (2006)
3. M. Boezio *et al.*,"The electron-hadron separation performance of the PAMELA electromagnetic calorimeter", Astrop. Phys.**26**, 11 (2006)
4. P. Picozza *et al.*,"PAMELA - A Payload for Antimatter Matter Exploration and Light-nuclei Astrophysics", astro-ph/0608697 (paper accepted in Astrop. Phys.)

References

1. P. Picozza *et al.*, "PAMELA - A Payload for Antimatter Matter Exploration and Light-nuclei Astrophysics ", astro-ph/0608697
2. R.Sparvoli *et al.*,"Launch in orbit of the Space Telescope PAMELA and Ground Data Results", Proc. 9th ICATPP Conf. on Astroparticle, Particle, Space Physics and Medical Physics Applications (Como, Italy, 2005)

AIACE

M. Aghasyan (Bors. PD), E. De Sanctis, M. Mirazita (Art. 36),
J. de Oliveira Echeimberg (Dott.), A. Orlandi (Tech.), S. A. Pereira (Ass.),
W. Pesci (Tech.), E. Polli, F. Ronchetti (Art. 23), P. Rossi (Resp. Naz.), A. Viticchié (Tech.)

1 Introduction

AIACE stands for Attività Italiana A CEbaf. It is the collaboration of the INFN groups of Frascati and Genova which participate into the physics program carried in the Hall B at the 6 GeV Continuous Electron Beam Accelerator Facility (CEBAF) at the Jefferson Laboratory (JLab). The Hall B collaboration counts about 140 physicists from 35 Institutions from seven Countries.

The scientific program of Hall B, which is equipped with the CLAS detector, is the precision study of the structure of the nucleon and the nature of the strong interaction.

The scientific activity of the Frascati AIACE group, in the period covered by this report, can be summarized in the following main topics:

- **search for exotic baryons**
  - the publication on Physical Review Letters of the paper "*Search for the Θ^+ pentaquark in the $\gamma d \to \Lambda n K^+$*".
  - The data analysis of the reactions $\gamma d \to \Lambda p K^0$ for the pentaquark search.
- **study of exclusive reactions**
  - The data analysis of the reaction $\gamma n(p) \to p\pi^-(p)$.
  - The start-up of the analysis of a "*Comprehensive study of exclusive Δ photoproduction on the deuteron.*"
- **study of strangeness photoproduction**
  - The data analysis of the reactions $\gamma n(p) \to K^+\Sigma^-(p)$ and $\gamma p(n) \to K^+\Lambda(n)$.

The Frascati AIACE group is also involved in the proposal for the complete measurement of the nucleon form factors in the time-like region with the new upgraded DAΦNE electron-positron ring. In the past year the study of feasibility of a proton polarimeter for the measurement of the time-like nucleon form factor from threshold up to 1.2 GeV has been carried on.

2 Search of the pentaquark baryon state Θ^+

Exotics, i.e. particles with more complex quark configurations than $q\bar{q}$ pairs (mesons) or 3-quarks states (baryons), have been proposed since the early 70's. The lack of experimental evidence did not stop the theoretical work on this subject, and in 1997 Diakonov, Petrov and Polyakov, in the framework of the Chiral Quark Soliton Model predicted an antidecuplet of 5-quarks baryons with $J^\pi = 1/2^+$ [1). The lowest mass member is an isosinglet state, the Θ^+, with quark configuration ($uudd\bar{s}$) giving S=+1, mass $\sim$ 1.54 GeV and width $\sim$ 15 MeV.

Experimental evidence for a S=+1 baryon resonance, dubbed the Θ^+, has been reported for the first time by the LEPS Collaboration [2)]. Evidence for an additional narrow exotic S=-2 state, called the Ξ^{--} with mass close to 1862 MeV was reported by the NA49 Collaboration [3)]. Immediately after the LEPS announcement, several other groups analyzed low statistics old data taken for other purposes, and found the exotic baryon Θ^+ in both pK^0 and nK^+ decay channels [4]. At the same time, a similar number of high statistics and high energy experiments [5] reported null results.

During the year 2004-2005, high statistics, new dedicated experiments (**G10, G11, EG3, SUPER G**) have been started in Hall B with the aim to clarify the existing experimental situation.

The CLAS pentaquark search experimental program is summarized in Table 1.

Table 1: The CLAS pentaquark program.

Exp	Target	Reaction		Egamma	Status
G10	**d**	$\gamma d \rightarrow pK^-\Theta^+$	Θ^+	0.8-3.6	Published
		$\gamma d \rightarrow \Lambda(1116)\Theta^+$	"	"	Published
		$\gamma' n' \rightarrow K^-\Theta^+$	"	"	In progress
G11	**p**	$\gamma p \rightarrow K^0\Theta^+$	Θ^+	1.6-3.8	Published
		$\gamma p \rightarrow K^-\Theta^{++}$	Θ^{++}	"	Published
EG3	**d**	$\gamma d \rightarrow K^+K^+\Xi^{--}(p)$	Ξ_5	4.0-5.4	In progress
SUPER G	**p**	$\gamma p \rightarrow K^-\pi^+\Theta^+$	Θ^+	3.8-5.7	Data to be taken

The Frascati group performed the analysis for the Θ^+ search in the reaction channel $\gamma d \rightarrow \Theta^+\Lambda(1115)$.

Searching for Θ^+ through photoproduction on the deuteron together with a Λ hyperon has various positive aspects. The main advantage of this reaction channel is that it allows identification of the final state without the need of removing competing channels, while at the same time it excludes kinematical reflections of heavy mesons in the NK invariant mass spectrum, possible in other channels, like $pK^+K^-(n)$ or $pK^+K^0(p)$. Moreover, the presence of the Λ allows a "strangeness tag" ($S_\Lambda = -1$) in both the nK^+ and the pK^0 decay modes.

After selecting the $\Lambda K^+(n)$ events, the Θ^+ has been searched for calculating the invariant mass of the nK^+ system. Since the nK^+ mass spectrum did not show any evident structure, kinematical cuts on non-spectator-neutron and on photon-energy, according to the model [6] have been applied. Several cuts on the neutron momentum (p_n) and on the photon energy (E_γ) have been tested. However, also under these stringent kinematic conditions, no narrow peaks having statistical relevance was observed in the mass region around 1.54 GeV/c^2.

Since no structures with relevant statistical significance appeared in the nK^+ invariant mass for any of the kinematic cuts that have been studied, the upper limit on the cross section was calculated using the Feldman-Cousins method. The acceptance was computed with the aid of a Monte-Carlo simulation that reproduces the response of the CLAS detector and was found to be on the order of 1-2%. The $\Lambda \rightarrow p\pi^-$ decay branching ratio (64%) was included in the calculation of the luminosity, as well as the Θ^+ decay branching ratio for the nK^+ mode, which was assumed to be 50%. The resulting upper limit on the $\gamma d \rightarrow \Lambda\Theta^+$ total cross section is shown in Fig. 1 (top), as a function of $M(nK^+)$ for photon energies below 1.6 GeV. In the mass range between 1.52 and 1.56 GeV/c^2 it is 2-5 nb.

The upper limit on the $\gamma d \rightarrow \Lambda\Theta^+$ differential cross section as a function of the momentum transfer t, with $t = (p^\mu_\gamma - p^\mu_\Lambda)^2$, was also calculated. The data were divided into five t bins, as shown in the lower plot of Fig. 1. For each t bin, the upper limit on the cross section was extracted according to the procedure described above for the total cross section. The maximum value of the upper limit in the $M(nK^+) = 1.52 - 1.56$ GeV/c^2 range for each t bin was then used to get the upper limit on the differential cross section, as shown in the bottom plot of Fig. 1. It varies between less than 0.5 nb/(GeV/c)^2, at the highest values of $-t$, to 11 nb/(GeV/c)^2, as t approaches

0. The kinematic region around $t \simeq 0$, however, corresponds to the forward-most part of the CLAS detector, where its acceptance drops down to zero, and the dependence on the model used in the event generator becomes stronger. This explains the higher upper limit for the last bin in Fig. 1.

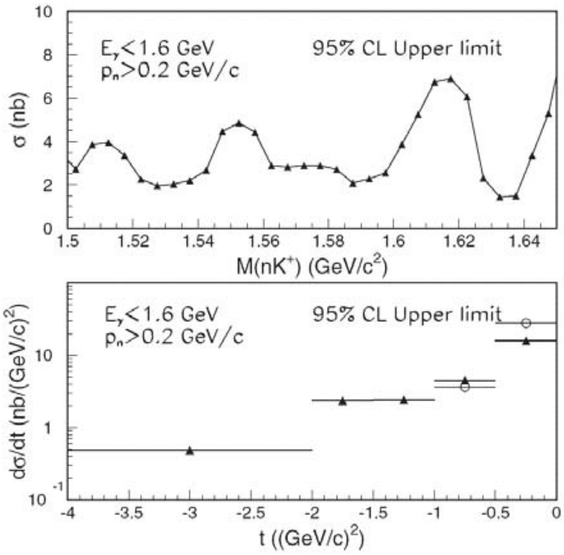

Figure 1: Top: 95% confidence level upper limit of the $\gamma d \rightarrow \Lambda\Theta^+$ reaction total cross section as a function of the nK^+ invariant mass. Bottom: 95% confidence level upper limit of the differential cross section $d\sigma/dt$ as a function of t, for $1.52 < M(nK^+) < 1.56\ GeV/c^2$. The triangles and the circles represent the results obtained using two different model for the acceptance calculation.

3 Study of exclusive reactions

The interplay between the nucleonic and partonic pictures of the strong interaction represents one of the major issues in contemporary nuclear physics. Although standard nuclear models are successful in describing the interactions between hadrons at large distances, and Quantum Chromodynamics accounts well for the quark interactions at short distances, the physics connecting the two regimes remains unclear. In fact, the classical nucleonic description must break down once the probing distances become comparable to those separating the quarks. The challenge is to study this transition region by looking for the onset of some experimentally accessible phenomena naturally predicted by perturbative QCD. Exclusive processes are essential probes to accomplish this aim.

The simplest signature of the partonic picture is the validity of the constituent counting rule (CCR) for high-energy exclusive reactions [7]. CCR predicts the energy dependence of the differential cross section at fixed center-of-mass angle for an exclusive two-body reaction at high energy and large momentum transfer as:

$$d\sigma/dt = h(\theta_{cm})/s^{n-2} \tag{1}$$

where s and t are the Mandelstam variables, respectively, for the square of the total energy in the center-of-mass frame and the momentum transfer squared. The quantity n is the total number of elementary fields in the initial and final states, while $h(\theta_{cm})$ depends on details of the dynamics of the process.

Single pion photoproduction reactions are essential probes to study this transition from meson-nucleon degrees of freedom to quark-gluon degrees of freedom in exclusive processes. The cross sections of these processes are also advantageous, for investigation of the oscillatory behavior around the quark counting prediction, since they decrease relatively slower with energy (s^{-7}) compared with other photon-induced processes. Recent data from JLab Hall A show dramatic change in the scaled differential cross section from the $\gamma n \to \pi^- p$ and $\gamma p \to \pi^+ n$ processes in the c.m. energy between 1.8 GeV to about 2.4 GeV and for $\theta_{CM} = 90°$. The Frascati group has continued the analysis of the G10 data on the $\gamma n \to \pi^- p$ to investigate this behavior in much finer photon energy bins and for a wide angular range and to study the angular dependence of the scaling behavior. The analysis is almost finished and the results will be released soon.

On the same track is the study of the **exclusive Δ photoproduction on the deuteron**. The Frascati group, using the G10 data, has started the analysis of he reactions $\gamma n(p) \to \Delta^- \pi^+(p)$, $\gamma n(p) \to \Delta^+ \pi^-(p)$, $\gamma p(n) \to \Delta^{++} \pi^-(n)$ and $\gamma p(n) \to \Delta^0 \pi^+(n)$ for which an s^{-7} scaling of the cross sections is expected. Also the double-Δ photoproduction reaction, $\gamma d \to \Delta^{++} \Delta^-$ will be studied to look for a signature of the hidden-color states of the deuteron.

4 Strangeness photoproduction

The long-standing question of "missing resonances", i.e. experimentally not established baryon states which are predicted by SU(6) x O(3) symmetric quark models but not expected by the di-quark model, can only be settled if experiments unambiguously identify some of these resonances. Symmetric quark models predict several "missing" baryon states to couple strongly to γp as well as $K\Lambda$ or $K\Sigma$ but not significantly to πN. Thus, resonances with these properties would not have been observed in pion experiments on which most of the data analyses are based.

The electromagnetic strangeness production is an important part of the JLab's experimental program and several experiments have been approved to run in all the three halls.

The Frascati group, taking advantage of the high quality of the G10 data collected for the pentaquark search, has continued the analysis of the $\gamma n(p) \to K^+ \Sigma^-(p)$ and $\gamma p(n) \to K^+ \Lambda(n)$ reactions in the invariant mass range from 1.54 to 2.76 GeV where data are not available, in order to study the baryon resonance spectrum to emphasize resonances not otherwise revealed.
In particular, in the period covered by this report, for the $\gamma n(p) \to K^+ \Sigma^-(p)$ reaction, a detailed study of the neutron detection in the CLAS electomagnetic calorimeter, never done before, has been undertaken. An analysis note has been written and it is almost ready for release.

5 Nucleon form factor in the time-like region

The study of the electromagnetic form factors of the nucleon plays a key role for the understanding of the internal structure and dynamics of this basic building block of the matter. They are also necessary for the interpretation of many other measurements in reactions involving nucleons. In spite of being under investigation by more than fifty years, form factors are far from being fully exploited and more experimental effort is needed for their determination.

The possibility to fully measure nucleon form factors in the time-like region at Frascati in the proposed high energy upgrade of DAΦNE storage ring is under investigation by the AIACE group. Differential $e^+e^- \to p\bar{p}$ and $e^+e^- \to n\bar{n}$ cross section should be measured, in order to extract the moduli of proton and neutron form factors. The relative phase between electric and magnetic form factors (never measured yet) can be obtained by measuring the polarization of the outgoing nucleon in the normal direction to the scattering plane.

In 2006, an addendum to the Letter of Intent, submitted in 2005 and signed by 80 physicists from 24 institutions in 7 countries , for the measurement of the time-like nucleon form factor from threshold up to 1.2 GeV has been written. The paper addresses the suggestion of the LNF Scientific Committee, to consider that all future experiments should be developed around the KLOE detector, which is well suited for the mesurements of the moduli while for the measurement of the form factor phases a polarimeter should be added.

During the reporting period, the study of feasibility of a proton polarimeter has be undertaken. The polarization of the produced nucleons is measured through secondary scattering in a strong-interaction process. The strong spin-orbit coupling causes an azimuthal asymmetry from which the polarization perpendicular to the nucleon momentum can be extracted. Then a polarimeter consists of a thin scatter layer (usually carbon) placed between two tracking systems. Referring to the KLOE geometry, the second tracking system is made by the drift chamber, while the scatterer and the first tracking system should be built and installed in the ~ 25 cm between the beam pipe and the drift chamber wall. The installation of the polarimeter must be carefully studied, in order not to spoil the tracking resolution of the detector. A simulation of the polarimeter, in order to give an estimate of its parameters (carbon analyzer thickness, magnetic field value, angular cuts and so on) and to study the sensitivity in the measurement of the relative phase between the two proton form factors has been made. The results of these studies have been reported in an internal note.

6 List of Publications

1. Search for $\Theta^+(1540)$ pentaquark in high statistics measurement of $\gamma p \to \bar{K^0} K^+ n$ at CLAS.
   M. Battaglieri *et al.* and CLAS collaboration, Phys. Rev. Lett. 96 (2006), 042001.

2. Electron scattering from high-momentum neutrons in deuterium.
   A. Klimenko *et al.* and CLAS collaboration, Phys. Rev. C73 (2006), 035212.

3. Measurement of 2 and 3 nucleon short range correlation probabilities in nuclei.
   K. Egiyan *et al.* and CLAS collaboration, Phys. Rev. Lett. 96 (2006), 082501.

4. η' photoproduction on the proton for photon energies from 1.527 to 2.227 GeV.
   M. Dugger *et al.* and CLAS collaboration, Phys. Rev. Lett. 96 (2006), 062001.

5. Differential cross section for $\gamma p \to K^+ + Y$ for Λ and Σ^0 hyperons.
   R. Bradford *et al.* and CLAS collaboration, Phys. Rev. C73 (2006), 035202.

6. Measurement of the deuteron structure function F2 in the resonance region and evaluation of its moments.
   M. Osipenko *et al.* and CLAS collaboration, Phys. Rev. C73 (2006), 045205.

7. Single π^+ electroproduction on the proton in the first and second resonance regions at 0.25 $GeV^2 < Q^2 < 0.65\ GeV^2$ using CLAS.
   H. Egiyan *et al.* and CLAS collaboration, Phys. Rev. C73 (2006), 025204.

8. Search for Θ^+ pentaquark in the reaction $\gamma d \to p K^- K^+ n$.
   B. McKinnon *et al.* and CLAS collaboration, Phys. Rev. Lett. 96 (2006), 212001.

9. Search for Θ^+ pentaquark in the $\gamma d \to \Lambda n K^+$ reaction measured with CLAS.
   S. Niccolai, M. Mirazita, P. Rossi *et al.* and CLAS collaboration, Phys. Rev. Lett. 97 (2006), 032001.

10. Search for Θ^{++} pentaquarks in the exclusive reaction $\gamma p \to K^+ K^- p$.
    V. Kubarovsky *et al.* and CLAS collaboration, Phys. Rev. Lett. 97 (2006), 102001.

11. Measurement of Deeply Virtual Compton Scattering with a polarized proton target.
S. Chen *et al.* and CLAS collaboration, Phys. Rev. Lett. 97 (2006), 072002.

12. Measurement of the x- and Q^2- dependence of the spin asymmetry A_1 of the nucleon.
K. V. Dharmawardane *et al.* and CLAS collaboration, Phys. Lett. B 641 (2006), 11.

13. Measurement of the N- and $\Delta(1232)$ transition at high momentum transfer by π^0 electroproduction.
M. Ungaro *et al.* and CLAS collaboration, Phys. Rev. Lett. 97 (2006), 112003.

14. Search for Θ^+ pentaquark in the reactions $\gamma p \to \bar{K}^0 K^+ n$ and $\gamma p \to \bar{K}^0 K^0 p$.
R. De Vita *et al.* and CLAS collaboration, Phys. Rev. D 74 (2006), 032001.

15. Quark-Hadron Duality in spin structure functions g_1^p and g_1^d.
P.E. Bosted *et al.* and CLAS collaboration, accepted by Phys. Rev. C, hep-ph/0607283.

16. Separated structure functions for the exclusive electroproduction of $K^+\Lambda$ and $K^+\Sigma^0$ final states.
P. Ambrozewicz *et al.* and CLAS collaboration, accepted by Phys. Rev. C, hep-ph/0611036.

17. First measurement of beam-recoil observables C_X and C_Z in hyperon photoproduction.
R. Bradford *et al.* and CLAS collaboration, accepted by Phys. Rev. C, hep-ph/0611034.

18. Measurement of the nucleon Time-Like Form Factors at DAFNE2.
P. Rossi, hep-ex/0604004.

19. Nucleon form factors stride into the future.
A. Fantoni and E. Tomasi-Gustafsson, CERN Courier, Volume 46, number 3, may 28-June 2, 2006.

20. Study of a polarimeter for protons with 0.2 GeV kinetic energy.
M. Mirazita, http://www.lnf.infn.it/conference/nucleon05/FF/related papers

7 Presentation at Conferences

1. *Measurement of the nucleon Time-Like Form Factors at DAFNE2*
Patrizia Rossi - Invited talk at the "XLIV International winter meeting on nuclear physics" - Bormio (Italy), January 29 - February 5, 2006.

2. *Measurement of the $\gamma n(p) \to K^+\Sigma^-(p)$ at Jefferson Lab*
Sergio Anefalos Pereira - "XLIV International winter meeting on nuclear physics" - Bormio (Italy), January 29 - February 5, 2006.

3. *The search for pentaquarks: where do we are now?*
Marco Mirazita - Invited talk at the "Hadron Structure and Nonperturbative QCD" - Schladming, Styria (Austria) March 11-18, 2006.

4. *Project of upgrade of the DAFNE accelerator and the associated programme*
Patrizia Rossi - Invited talk at the "JINR Programme Advisory Committee for Particle Physics 25th meeting" - Dubna (Russia), April 20, 2006.

5. *DANTE: DAnae Nucleon Time-like form factor Experiment*
Patrizia Rossi - Invited talk at the "RNP2006" - Modra-Harmonia (Slovenia) May 22-27, 2006.

6. *DANTE: DAnae Nucleon Time-like form factor Experiment*
Patrizia Rossi - "32nd LNF Scientific Committee" - Frascati (Italy) May 31, 2006.

7. *Measurement of time-like nucleon form factors at Frascati*
Marco Mirazita - Invited talk at the "QCD 06" - Montpellier (France) July 3-7, 2006.

8. *Measurement of the* $\gamma n(p) \rightarrow K^+\Sigma^-(p)$ *at Jefferson Lab*
Sergio Anefalos Pereira - "18th International IUPAP Conference on Few-Body Problems in Physics (FB18)" - Santos (Brazil) August 21-26, 2006.

9. *Measurement of the* $\gamma n(p) \rightarrow K^+\Sigma^-(p)$ *at Jefferson Lab*
Sergio Anefalos Pereira - "NN2006" - Rio de Janeiro (Brazil) August 28- September 1, 2006.

10. *Search for pentaquarks in high statistics experiments at CLAS*
Patrizia Rossi - Invited talk at the "EMIN-2006 XI International Seminar on Electromagnetic interactions of Nuclei" - Moscow (Russia), September 21-24, 2006.

11. *Search for pentaquarks at CLAS*
Patrizia Rossi - Invited talk at the "XVIII International Baldin Seminar on High Energy Physics Problems" - Dubna (Russia) September 25-30, 2006.

12. *Misura dei fattori di forma del nucleone a DAFNE2*
Marco Mirazita - "SIF 2006" - Torino (Italy), September 18-23, 2006.

13. *Measurement of the g n (p) -¿ K+ Sig- (p) at Jefferson Lab*
Sergio Anefalos Pereira - "SIF 2006" - Torino (Italy), September 18-23, 2006.

14. *DANTE: Status and Plans*
Marco Mirazita - "33rd LNF Scientific Committee" - Frascati (Italy) November 27, 2006.

References

1. D. Diakonv, V. Petrov, M.V. Polyakov, Z. Phys. **A359**, 305 (1997).

2. T. Nakano et al., Phys. Rev. Lett. **91**, 012002 (2003).

3. C. Alt et al., Phys. Rev. Lett. **92**, 042003 (2004).

4. V. Barmin et al., Phys. Atom. Nucl. **66**, 1715 (2003); S. Stepanyan et al., Phys. Rev. Lett. **91**, 252001 (2003); V. Koubarovsky et al., Phys. Rev. Lett. **92**, 032001 (2004); J. Barth et al., Phys. Lett. **B572**, 127 (2003); A. Airapetian et al., Phys. Lett. **B585**, 213 (2004); A.E. Asratyan, A.G. Dolgolenko, M.A. Kubantsev, Phys. Atom. Nucl. **67**, 682 (2004); A. Aleev et al., Phys.Atom.Nucl. **68**, 974 (2005); Yad.Fiz. **68**, 1012 (2005); M. Abdel-Bary et al., Phys. Lett. **B595**, 127 (2004); S. Chekanov et al., Phys. Lett. **B591**, 7 (2004) .

5. J.Z. Bai et al., Phys.Rev. **D70**, 012004 (2004). K.T. Knoepfle et al., J.Phys. **G30**, S1363 (2004); M.I. Adamovich et al., Phys.Rev. **C70**, 022201 (2004); C. Pinkeburg et al., Eur.Phys.J. **C37**, 91; BABAR, hep-ex/0408064; Yu.M. Antipov et al., Eur.Phys.J. **A21**, 455 (2004); S. Schaet et al., Phys. Lett. **B5**, 99 (2004); CDF, E690, LEP, Focus, HyperCP (QNP2004 conference presentation).

6. V. Guzey, Phys. Rev. **C69**, 173 (2004).

7. S.J. Brodsky and G.R. Farrar, Phys. Rev. Lett. **31**, 1153 (1973); Phys. Rev. D **11**, 1309 (1975); V. Matveev *et al.*, Nuovo Cimento Lett. **7**, 719 (1973).

FIsica NUcleare a DAΦNE - FINUDA

L. Benussi (Art. 23), M. Bertani, S. Bianco, M. A. Caponero (Ass.), F. L. Fabbri
P. Gianotti (Resp.), M. Giardoni, V. Lucherini, E. Pace, M. Pallotta (Ass.), S. Tomassini,
L. Passamonti (Tecn.), D. Pierluigi (Art. 15), F. Pompili (Art. 23), A. Russo (Art. 15)

1 Introduction

FINUDA (FIsica NUcleare a DAΦNE) is an experiment devoted to hypernuclear physics studies. Hypernuclei are nuclear systems in which one or more nucleons are replaced by a hyperon. This feature adds explicit strangeness to the nuclear system allowing to study, in a more general environment, the baryon-baryon interaction.

FINUDA produces hypernuclei via the reaction:

$$K^- +^A Z \rightarrow^A_\Lambda Z + \pi^- \tag{1}$$

stopping K^- from $\phi(1020)$ decay almost at rest into a thin (~ 0.2 g cm^{-2}) target. The spectroscopy of the hypernuclear levels produced is performed by measuring the momentum of the outgoing π^-. Moreover, the products of the sub-sequent decay of the Λ bound to the nucleus can be detected by FINUDA, allowing to investigate simultaneously the decay mechanisms of hypernuclei.

The FINUDA detector is a large acceptance magnetic spectrometer housed inside a superconducting solenoid (2.7 m length and 2.4 m diameter) providing a field of 1 T. The apparatus can be sub-divided in two distinct areas: the interaction-target region and the outer tracking zone. The former, surrounding the DAΦNE beam pipe, consists of a barrel of plastic scintillators, a layer of double-sided silicon microstrips, and the target station, which can house up to 8 different materials. The latter consists of several layers of tracking detectors: a double-sided silicon microstrips array, two layers of planar drift chambers, and six layers of straw tubes. The outermost detector of the whole complex is a second barrel of plastic scintillators, for trigger purposes and neutron detection. The whole FINUDA tracking volume (~ 8 m^3) is filled with helium to reduce multiple-Coulomb scattering that is the main factor limiting the momentum resolution.

The FINUDA Collaboration consists of 60 physicists coming from LNF, several INFN sections and Italian universities (Torino, Bari, Trieste, Pavia, Brescia) plus foreign researchers from the TRIUMF laboratory of Vancouver, Canada, the KEK laboratory of Tsukuba, Japan, the Seoul National University, South Korea, and the Joint Institute for Nuclear Research of Dubna, Russia.

2 FINUDA activity in 2006

The activity of the LNF FINUDA group during 2006 has been devoted mainly to two aspects: the detector re-installation inside the DAΦNE hall and the preparation of all the tools necessary for the fortcoming running period, and to the analysis of the data collected in the first data taking to produce scientific results.

The FINUDA apparatus was completely re-assembled and rolled-in at the end of July 2006 with a new set of nuclear targets and a inner tof system (TOFINO). The target installed for the new data taking are: 2 ^{6}Li, 2 ^{7}Li, 2 ^{9}Be, D_2O, and ^{13}C. TOFINO has been completely re-built with new thinner scintillators. The previously used Hybrid Photo Diode devices (HPD) have been replaced with Hamamatsu R5505 photomultipliers, which can work with good gain and low noise inside magnetic fields. Nevertheless, the photomultipliers gain is lower than that of HPD and to compensate this, low noise preamplifiers, designed at LNF, have been mounted on each channel. To discriminate the analog signals, new, lower walk constant fraction discriminators have been

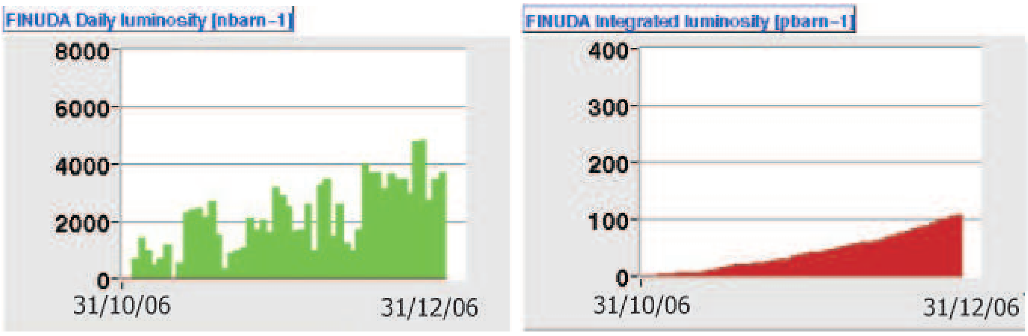

Figure 1: Daily and total integrated luminosity by FINUDA during 2006 data taking.

adopted. All these changes have improved the time resolution of TOFINO that now is about 250 ps FWHM.

Starting from August 2006 a cosmic ray data taking with magnetic field off started. These data are necessary to calibrate and align the different sub-detectors composing the FINUDA spectrometer. At the middle of November 2006, the new data taking of FINUDA started with the goal of collecting an integrated luminosity of 1 fb^{-1}. The FINUDA DAQ system has been completely changed in order to have a more stable system able to stand the higher DAΦNE luminosity. The new DAQ layout is based on CAEN V2718-A2818 optical system [1)] which allows a data transfer rate up to 70MByte/s. During the data taking, either the new DAQ or the all set of FINUDA sub-detectors showed a high level of reliability allowing to collect, by the end of December, about 100 pb^{-1} (see fig. 1). Furthermore, during Christmass DAΦNE shutdown, FINUDA collaboration continued the cosmic ray data taking with magnetic field off, to improve the statistics of the data alvailable for the calibnration procedure.

The LNF FINUDA group is overseeing all the activities on the floor, and has the responsibility for the data taking quality insurance.

3 Analysis results

FINUDA research program is extremely wide and spans over the search for deeply bound kaon-nuclear states, the study of Λ-hypernuclei production, spectroscopy and decay, the investigation of neutron rich hypernuclei existence, and the search for Σ-hypernuclei. In all these fields FINUDA has been able to produce high quality results.

3.1 Hypernuclear physics

The spectroscopy of Λ-hypernuclei has been a powerful tool to study ΛN interaction instead of difficult and low statistic ΛN scattering experiments. This field received a boost with the production of high precision data coming from Ge-detectors experiments measuring γ-ray transitions of hypernuclear levels. Thanks to that, ΛN spin-dependent contributions to the interaction are finally being measured.

FINUDA cannot compete with these measurements, but can produce complementary information by combining the spectroscopic studies to the investigation of the decay modes of hypernuclear states. With the first set of acquired data, FINUDA produced good results in this field for ${}^{12}_{\Lambda}$C, and ${}^{7}_{\Lambda}$Li, hypernuclear systems. Figures 2 and illustrates ${}^{12}_{\Lambda}$C and ${}^{7}_{\Lambda}$Li hypernuclear spectra. The

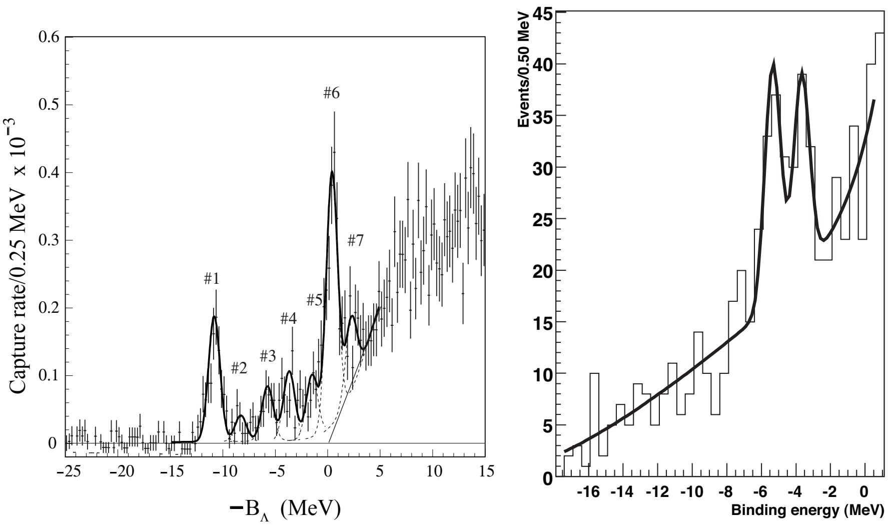

Figure 2: ${}^{12}_{\Lambda}$C (right) and ${}^{7}_{\Lambda}$Li (left) hypernuclear spectra measured by FINUDA

spectrum of ${}^{12}_{\Lambda}$C [2] closely resembles that measured by E369 experiment [3]. This is expected, as the production of hypernuclear states is, in first approximation, determined by the momentum transferred to the Λ, which, for both experiments, is grossly comparable ($\sim$ 250 MeV/c for FINUDA, $\sim$ 350 MeV/c for E369). The use of Carbon targets during the first data taking was essentially meant for testing the detector capabilities on a well known hypernuclear system. The energy resolution of the spectrometer finally turns out to be 1.1 MeV. ${}^{7}_{\Lambda}$Li hypernucleus is one of the most studied. Recently, the experiments E419 at KEK and E930 at BNL by using a large acceptance Germanium array (Hyperball) performed high resolution spectroscopy of ${}^{7}_{\Lambda}$Li, defining precisely the level scheme and the energies of the bound states [4].

Regarding the two levels identified by FINUDA analysis, we have tried to place them in the level scheme determined with the Hyperball. The first (left) peak could be a mixture of the ground state with the first excited state ($3/2^+$) since the value of the energy is laying in between the two. In the same way, the second (right) peak can be the $5/2^+$ state, or the $7/2^+$ state or a mixture of the two.

Concerning the decay of Λ hypernuclei, the scarce statistics collected so far allows only to attack the investigation of ${}^{12}_{\Lambda}$C since three carbon targets were mounted inside the spectrometer during the first data taking. The FINUDA spectrum of protons from non-mesonic weak-decay ($\Lambda n \rightarrow np$) is reported in fig. 3. The proton energy distribution is centered around 80 MeV with a width of $\sim$ 60 MeV, corresponding to the Q-value of the weak reaction widened by the Fermi momentum of the interacting nucleon. The low energy rise, is probably due to Final State Interactions of the outgoing particles and/or to the contribution of the two nucleon induced reaction $\Lambda(np) \rightarrow nnp$. The shape of the distribution is also consistent with early theoretical works [5]. However, the comparison with an high statistic similar spectrum measured at KEK by E462/E508 experiments [6] shows some differences. The scenario will be better understood with new high statistics measurements [7].

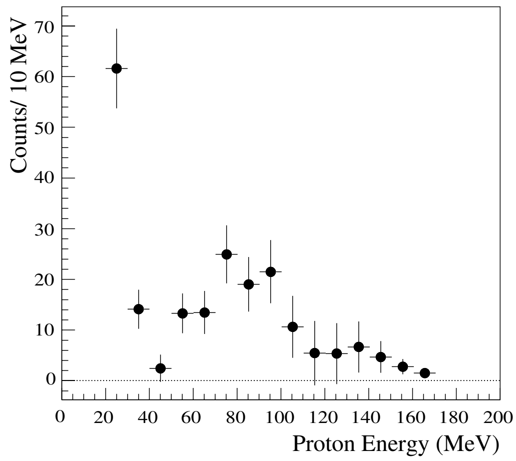

Figure 3: Energy spectrum of the protons from non-mesonic weak-decay of ${}^{12}_{\Lambda}$C hypernucleus

3.2 Nuclear bound kaonic systems

The search for nuclear bound kaonic systems was not included in the original scientific program of FINUDA. Nevertheless, the detector characteristics have turned out to be excellent to give clear results on a topic that has became of extreme interest in the last years. In fact, the existence of kaon-nucleon bound systems is not accepted world-wide. The main features of $\bar{K}N$ and $\bar{K}A$ interactions don't foresee clearly detectable levels since the expected binding energies are around 10-30 MeV, and the widths of 80-100 MeV exclude the possibility of an experimental observation. Nevertheless, a different approach of recent theoretical works by Akaishi and Yamazaki [8] shows the possibility that $\bar{K}N$ interaction, under certain conditions, could became strongly attractive allowing the formation of kaon-multinucleon systems with a binding energy varying from 86 MeV to 113 MeV, depending on the target nucleus, and with widths of 20-40 MeV. These Authors also suggest that the presence of a K^- inside the nucleus should enhance the binding energy of the system increasing the density several times that of the ordinary nuclei. Furthermore, these aggregates should be formed with higher probabilities when the kaon interacts with light nuclei.

The capability of the FINUDA apparatus to detect almost all the particles emitted after K^- absorption by the nucleus is extremely useful to clarify the experimental situation. This is the reason why FINUDA is carrying out a complete set of analyzes studying the invariant-mass spectra of exclusive final states where kaon-nucleon aggregates could be formed. With the present data, some results have been already presented [9], but with the new set of targets mounted on the apparatus, the collaboration hopes to draw some firm conclusions on this topic.

3.3 Neutron-rich Λ-hypernuclei

Neutron-rich hypernuclei are systems with a large N/Z ratio. By studying such systems it would be possible to get more information on baryon-baryon interaction, and on the importance of the ΛNN force related to the "coherent $\Lambda - \Sigma$ coupling" in connection with nuclear astrophysics implications [10]. In particular there is great interest on the existence of ${}^{6}_{\Lambda}$H since theoretical calculations including $\Lambda - \Sigma$ coupling predict a stable state with a binding energy of 5.8 MeV below the ^{5}H + Λ threshold [11]. On the other hand, without considering the $\Lambda - \Sigma$ coupling the

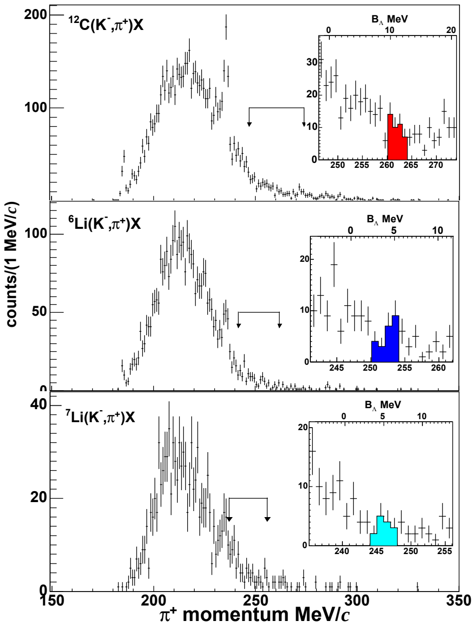

Figure 4: Inclusive π^+ momentum spectra of ^{6}Li, ^{7}Li and ^{12}C targets. The insets show an enlarged view of of the region where neutron rich Λ hypernuclei signals are expected.

state would be very close to the ${}^{4}_{\Lambda}$H + $2n$ threshold [12].

In FINUDA the search for neutron rich Λ hypernuclei has been carried out studying the reaction:

$$K^-_{stop} +^A Z \rightarrow^A_\Lambda (Z-2) + \pi^+ \quad (2)$$

By measuring the momentum of the outgoing π^+, it is possible to determine the energy level of the hypernucleus that could be formed. For ${}^{6}_{\Lambda}$H and ${}^{7}_{\Lambda}$H the momentum of the outgoing π^+ is expected to be $\sim$ 252 and 246 MeV/c respectively.

FINUDA looked to the inclusive π^+ spectrum from ^{6}Li, ^{7}Li and ^{12}C targets (see fig. 4) which shows no evidences for the formation of Λ bound states. The upper limits for the production rates have been evaluated; the values are $(2.5 \pm 0.4_{stat}\ {}^{+0.4}_{-0.1}{}_{syst}) \times 10^{-5}$ per $K^-_{stopped}$ for ${}^{6}_{\Lambda}$H, $(4.5 \pm 0.9_{stat}\ {}^{+0.4}_{-0.1}{}_{syst}) \times 10^{-5}$ per $K^-_{stopped}$ for ${}^{7}_{\Lambda}$H, and $(2.0 \pm 0.4_{stat}\ {}^{+0.4}_{-0.1}{}_{syst}) \times 10^{-5}$ per $K^-_{stopped}$ for ${}^{12}_{\Lambda}$Be [13].

With the new set of targets the statistics on ${}^{6}_{\Lambda}$H and ${}^{7}_{\Lambda}$H will be increased, while new neutron-rich hypernuclear system will be studied: ${}^{9}_{\Lambda}$He, ${}^{13}_{\Lambda}$Be, and ${}^{16}_{\Lambda}$C.

4 List of publications

1. M. Agnello *et al.*,“ Search for ${}^{\Lambda}_{6}$H and ${}^{\Lambda}_{7}$H with the (K$^-_{(stop)}$, π^+) reaction”, Phys. Lett. B640, 145, 2006.

2. M. Agnello *et al.*, “ A study of the proton spectra following the capture of K$^-$ in ^{6}Li and ^{12}C with FINUDA”, Nucl. Phys A775, 35, 2006.

5 Conference presentations by LNF collaborators

1. L. Benussi, "Study of the proton weak decay of $^{12}\Lambda C$ g.s. with FINUDA", presented at IX Int. Conference on Hypernuclear and Strange Particle Physics HYP 2006, 10-14 Oct 2006 Mainz, Germany.

2. P. Gianotti, "FINUDA: a hypernuclear factory ", presented at IX Int. Conference on Hypernuclear and Strange Particle Physics HYP 2006, 10-14 Oct 2006 Mainz, Germany.

3. M. Bertani "Recent results and future perspectives from FINUDA experiment", presented at CIPANP 2006 - Conference on the Intersection of Particle and Nuclear Physics, May 30-June 3 2006, Puerto Rico.

References

1. CAEN S.p.A. Costruzioni Apparecchiature Elettroniche Nucleari, Via Vetraia, 11 55049 - Viareggio (LU) - ITALY, http://www.caen.it

2. M. Agnello *et al.*, Phys. Lett. B **622** (2005), 35.

3. H. Hotchi *et al.*, Phys. Rev. C **64** (2001), 044302.

4. H. Tamura *et al.*, Nucl. Phys. A **754** (2005), 58c.
   H. Tamura *et al.*, Nucl. Phys. A **691** (2001), 86c.

5. A. Ramos *et al.*, Phys. Rev. C **55** (1997), 735.

6. S. Okada *et al.*, Phys. Lett. B **597** (2004), 249.

7. L. Benussi *et al.* , *Proceedings of the IX Int. Conference on Hypernuclear and Strange Particle Physics HYP 2006, 10-14 Oct 2006 Mainz, Germany, to be published.*

8. Y. Akaishi, T. Yamazaki, Phys. Rev. C **65** (2002), 044005.
   T. Yamazaki, Y. Akaishi, Nucl. Phys. B535 (2002), 70.
   Y. Akaishi *et al.*, nucl-th/0501040.

9. M. Agnello *et al.*, Nucl. Phys A775, 35, 2006.
   A. Filippi *Proceedings of the IX Int. Conference on Hypernuclear and Strange Particle Physics HYP 2006, 10-14 Oct 2006 Mainz, Germany, to be published.*
   S. Piano *et al.*,*Proceedings of the IX Int. Conference on Hypernuclear and Strange Particle Physics HYP 2006, 10-14 Oct 2006 Mainz, Germany, to be published.*

10. Y. Yamamoto *et al.*, Nucl. Phys. A **691** (2001), 432c.

11. A. A. Korsheninnikov *et al.*, Phys. Rev. Lett. **87** (2001), 092501.

12. K. S. Myint *et al.*, Few-Body Sys. Suppl. A **12** (2000), 383.

13. M. Agnello *et al.*, Phys. Lett. B **640** (2006), 145.

GRAAL

P. Levi Sandri (Resp.), D. Pietreanu

1 Introduction

The Graal experiment aims at a more detailed knowledge of the baryon spectrum via the precise measurement of cross sections and polarisation observables in photo-induced reactions on the nucleon.

The use of the electromagnetic probe and of it's polarisation, coupled to large acceptance detectors with cylindrical symmetry and high efficiency in the detection of all final state particles, is the technique chosen in many laboratories to perform the ambitious program of a full determination of the scattering amplitude of a given photonuclear reaction. Such determination requires, for each reaction channel, the measurement of the cross section, of the three single polarisation observables and of four appropriately chosen double polarisation observables.

The Graal esperiment is performed in collaboration between 6 INFN Sections (Roma2, LNF, Catania-LNS, Roma1, Genova and Torino), LPSC-Grenoble and INR-Moscow. The Frascati group is responsible of running and maintaining the ΔE/Δx scintillator barrel detector, the Montecarlo simulation program LAGGEN, the off-line reconstruction of events in the BGO calorimeter, the data analysis for coherent η photoproduction off the deuteron and contributes to the data analysis of π^0 and η photoproduction from the neutron bound in a deuteron in the quasi-free kinematics regime.

2 The Graal Beam and the Lagranγe apparatus

The Graal facility provides a polarised and tagged photon beam by the backward Compton scattering of laser light on the high energy electrons circulating in the ESRF storage ring [1]. Using the UV line (350 nm) of an Ar-Ion laser we have produced a gamma-ray beam with an energy from 550 to 1550 MeV. Its polarisation is 0.98 at the maximum photon energy and the energy resolution has been measured to be 16 MeV (FWHM).

The Lagranγe detector is formed by a central part surrounding the target and a forward part. Particles leaving the target at angles from 25^o to 155^o are detected by two cylindrical wire chambers with cathode readout, a barrel made of 32 strips of plastic scintillator parallel to the beam axis, used to determine the ΔE/Δx of charged particles, and the BGO rugby-ball made of 480 crystals of BGO scintillator.

The BGO ball is made of crystals of pyramidal shape with trapezoidal basis which are 21 radiation lengths long (24 cm). This calorimeter has an excellent energy resolution for photons [2], a good response to protons [3], a high detection efficiency for neutrons [4] and is very stable in time due to a continuous monitoring and to the calibration slow control system [5].

Particles moving at angles smaller than 25^o encounter two plane wire chambers, (xy and uv) two walls of plastic scintillator bars, 3 cm thick, located at 3 m from the target point, that provide a measurement of the time-of-flight for charged particles (700 ps FWHM resolution) followed by a shower wall made by a sandwich of four layers of lead and plastic scintillators, 4 cm thick, that provides a full coverage of the solid angle for photon detection (with 95 percent efficiency) and a 20 percent efficiency for neutron detection [6].

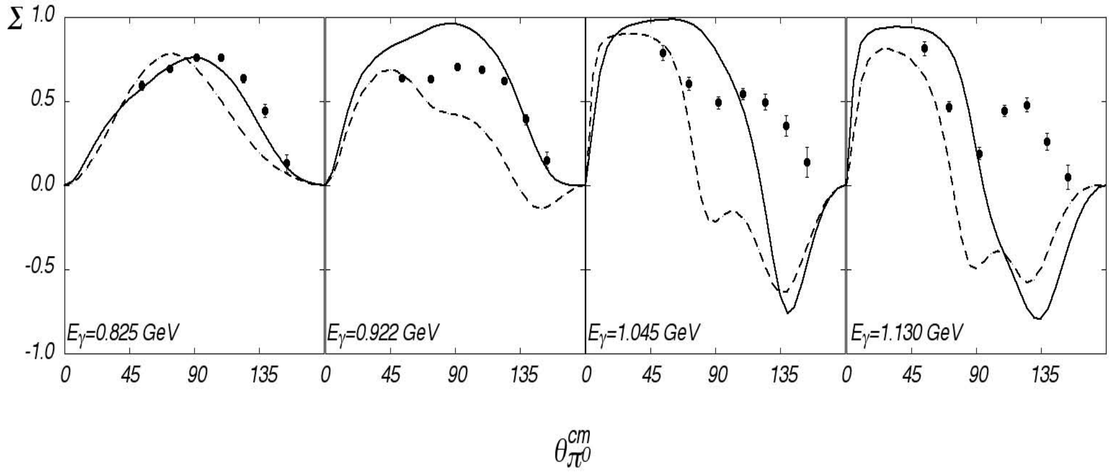

Figure 1: *Preliminary result for beam asymmetry for π^0 photoproduction from the neutron compared with MAID2003 (full line) and SAID standard solution (dashed line)*

The beam intensity is continuously monitored by a flux monitor, composed by three thin plastic scintillators and by a lead/scintillating fibre detector that measures energy and flux [7].

3 2006 Activity

During the year 2006 the Graal experiment has collected data with deuterium target. The data have been analysed in the quasi free kinematical regime for both proton and neutron. Data analysis was continued for Hydrogen and Deuterium target.

3.0.1 Hydrogen Target

The data analysis activity was mainly focused upon the study of strangeness photoproduction. The reactions $\gamma + p \rightarrow K^+ + \Lambda$ and $\gamma + p \rightarrow K^+ + \Sigma^0$ where analysed and the beam asymmetry and recoil polarisation were extracted for both reactions.

The result is the more extended data base for strangness photoproduction that includes, for the Λ channel, 66 data points in the beam asymmetry and 66 data points in the recoil polarisation while for the Σ^0 channels the points produced were 42 (beam asymmetry) and 8 (recoil polarisation). In the case of the Σ^0 channel, these are the very first data available in literature.

The data were compared to the most recent theoretic approaches allowing for a better determination of some resonance parameters and strengthening the need for a new D_{13} state around 1900 MeV.

Also the total photoabsorbtion cross-section for Hydrogen was measured and compared to the existing data. In the second and third resonance region this is the first measurement for long time

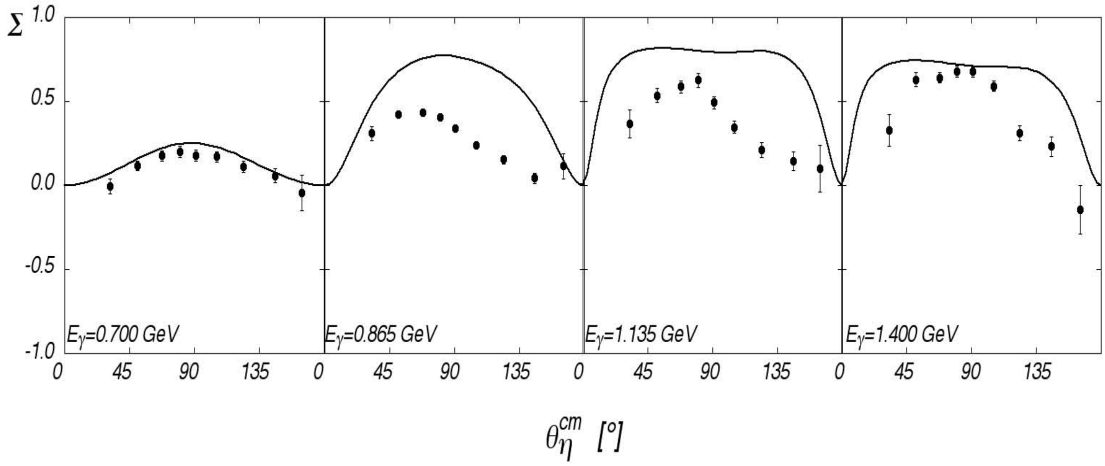

Figure 2: *Preliminary result for beam asymmetry for η photoproduction from the neutron compared with MAID2001 prediction.*

and confirms the existing data though introducing some small differences that can have impirtant consequences for the study of resonance propagation inside nuclei.

3.0.2 Deuterium Target

The deuteron was used at Graal as a target of quasi-free neutrons in order to bring in complementary information and towards a full multipole analysis including the isospin structure.

The data analysis was focused on the π^0 and η photoproduction for which reactions a large data base was produced in recent years by Graal. As a first step, data for free and quasi free protons were compared and found quite consistent allowing, as far as the beam asymmetry is concerned, to extract the neutron asymmetry from the deuteron target. Some of the preliminary data points are shown in fig. 1 for π^0 and in fig. 2 for η photoproduction.

Following the announced results coming from SPRING-8 [8], a search for pentaquark states (θ^+ and non-strange antidecuplets members) was performed and some preliminary results were presented in international conferences. The possible signal of non strange member of the antidecuplet was searched for in the process of η photoproduction on the neutron. The preliminary results for η photoproduction on the quasi-free neutron are shown in figure 3. A clear peak is evident in the total center-of-mass final state enrgy on the quasi-free neutron which is absent in the same spectrum for the quasi-free proton as predicted by Diakonov et al. [9]: this peak could be ascribed to a narrow baryon resonance at W=1.675 GeV and could be an indication of a non strange antidecuplet pentaquark member (crypto-pentaquark) [10]. Further investigations (i.e. beam asymmetry) have been performed and indicate a different behaviour of the Σ beam asymmetry as measured from the proton and from the neutron at the same c.m. energy where the peak shows up.

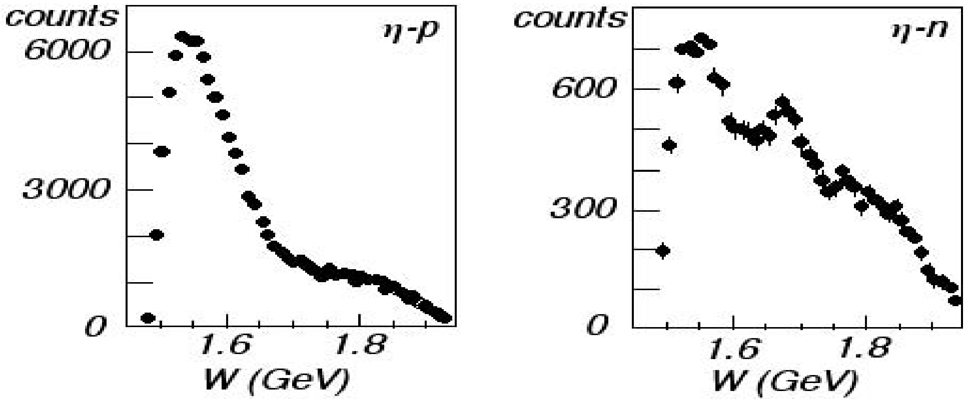

Figure 3: *Preliminary ηn (right) and ηp (left) total c.m. energies when the η meson is detected at backward angles. The difference between proton and neutron indicates clearly that a different resonant state contributes to the neutron-η asymmetry around 1650-1700 MeV.*

4 Activity in 2007 and Conclusions

The Graal experiment started data taking in 1997. It was run both with the green laser line giving rise to a photon beam of maximum energy of 1100 MeV and with UV multi-line with the corresponding gamma-ray beam of 1550 Mev maximum energy. The typical intensity was $2 \cdot 10^6 \, s^{-1}$ for the UV line and $5 \cdot 10^6 \, s^{-1}$ for the green line, reaching the design intensity. The detector was found very stable during the eight years of operation, with only minor maintenance problems.

Proton and deuteron targets of different lenghts were used and asymmetry data and cross sections have been produced for η, π^0, π^+, $2\pi^0$ and and ω photoproduction channels providing, for these reactions, the most extended and coherent data base available until now. Also the strangness photoproduction from the proton with $K^+\Lambda$ and $K^+\Sigma^0$ final states has been analysed and the final results are being published. The total photoabsorption cross section has been measured and will be published soon. The analysis of the Compton process on the proton, and of all the mentioned photoreactions on the quasi-free neutron of the deuteron target are underway.

During the year 2007 Graal will continue the data taking with deuteron (and eventually other medium nuclei) in order to increase the available statistics and to study the behavior of η and π^0 photoproduction cross sections and asymmetries as a function of the atomic number A.

5 Recent Publications

- ”Neutron detection efficiency of BGO calorimeter at GRAAL” NIMA562, 85, 2006..
- ”Meson photoproduction on the neutron at Graal” Int. J. Mod. Phys. A22 .341, 2007.
- ”Polarization observable measurement for $\gamma p \to K^+\Lambda$ and $\gamma p \to K^+\Sigma^0$ for energies up to 1.5 GeV” Eur. Phys. J. A31,79, 2007.
- ”Measurement of Total Photoabsorption Cross Section on Proton in 600 - 1500 MeV Energy Region at the GRAAL” Rus. J. Nucl. Phys. 2007.

References

1. Graal Collaboration, Nucl. Phys. A622, (1997) 110c.
2. P. Levi Sandri *et al.* Nucl. Inst. and Meth. in Phys. Research A370, (1996), 396.
3. A. Zucchiatti *et al.*, Nucl. Inst. and Meth. in Phys. Research A321, (1992), 219.
4. O. Bartalini *et al.*, Nucl. Inst. and Meth. in Phys. Research A562, (2006), 85.
5. F. Ghio *et al.*, Nucl. Inst. and Meth. in Phys. Research A404, (1998), 71.
6. V. Kouznetsov *et al.*, Nucl. Instr. and Meth. in Phys. Research A487 (2002), 396.
7. V. Bellini *et al.*, Nucl. Inst. and Meth. in Phys. Research A386, (1997), 254.
8. T. Nakano *et al.* Nucl. Phys. A721, (2003), 112c.
9. D.Diakonov, V. Petrov and M. Polyakov, Z. Phys. A359 (1997) 305.
10. arXiv:hep-ph/0512136v1 (12/12/2005).

HERMES

E. Avetisyan (Ass.), N. Bianchi (Resp. Naz.), G.P. Capitani, E. De Sanctis,
P. Di Nezza, A. Fantoni (Resp.), A. Funel (Dott.), C. Hadjidakis (Ass. Ric.),
D. Hasch (Art.23), V. Muccifora, A. Orlandi (Tecn.), W. Pesci (Tecn.),
E. Polli, C. Reidl (Bors. PD), A.R. Reolon, A. Viticchié (Tecn.)

1 Introduction

HERMES (HERa MEasurement of Spin) is an experiment at DESY mainly dedicated to study the spin structure of the nucleon. Nucleons (protons and neutrons) are the basic ingredients of the matter of the known universe and their most important quantum number is the spin 1/2. The nucleon is a composite object which can be described in terms of moving quarks of different flavors (up, down and strange) in different configurations (valence and sea) and gluons. Up to year 2000, HERMES collected data with a longitudinally polarized positron beam of 27.5 GeV on longitudinally polarized H, D and ^{3}He internal gas targets. From these runs HERMES provided the most accurate and complete data set for the polarized structure function g_1 and allowed for the first time a direct flavor decomposition of the nucleon spin. The use of a tensor polarised deuteron gas target with only a negligible residual vector polarization enabled the first measurement of the tensor asymmetry A^d_{zz} and of the tensor structure function b^d_1. Runs on several unpolarized nuclear gas targets have been also collected.

In the years 2002-2005 data HERMES has taken data with a transversely polarized hydrogen target. The azimuthal asymmetries are evaluated in two dimensions (ϕ and ϕ_S) and the amplitudes for the Collins and Sivers mechanism were extracted simultaneously. Preliminary results for charged pions and kaons, base on the first three years which correspond to about 30% of the total statistic, have been published. The average Collins amplitude is positive for π^+ and negative for π^-, with a magnitude for π^- comparable or larger than the one for π^+: one explanation could be a substantial magnitude for the disfavoured Collins fragmentation function with an opposite sign than the favoured one. These non-zero asymmetries provide clear evidence for the existence of both the transversity distribution and the Collins fragmentation function. The significant positive Sivers amplitudes for π^+ and K^+ provide the first evidence for a T-odd parton distribution function appearing in leptoproduction and imply a non-vanishing orbital angular momentum of the quarks inside the nucleon. The 2005 data set is under study, the final results are expected for the end of the present year. The transversity distribution $h_1(x)$ is the missing function in the leading twist description of the nucleon, together with the better known momentum $f_1(x)$ and helicity $g_1(x)$ distributions.

HERMES has measured longitudinal double spin asymmetries as a function of transverse momentum p_T using charged inclusive hadrons from electroproduction off a deuterium target. At $p_T >$ 1 GeV, the asymmetries are sensitive to the spin dependent gluon distribution Δg. To extract the gluon polarization $\Delta g/g$, information on the background asymmetry and the subprocess kinematics has been obtained from a Leading Order Monte Carlo model. Values for $\Delta g/g$ have been calculated both as a function of the measured p_T and x, using two different methods, in the region $p_T >$1.05 GeV, assuming $\Delta g/g$ constant in the measured x range or a functional form. The data favour a very small Δg, or $\Delta g(x)$ has a node at x around 0.1. Results are shown in Fig.1.

During the shutdown at the end of 2005, the Recoil Detector have been installed and since the beginning of 2006 HERMES has taken data with it, with the aim of providing new results in the exciting field of hard exclusive production of mesons and real photons with positron and electron beams. Moreover, as previously done, unpolarized hydrogen and deuterium runs at high density have been also collected for studying nuclear effects.

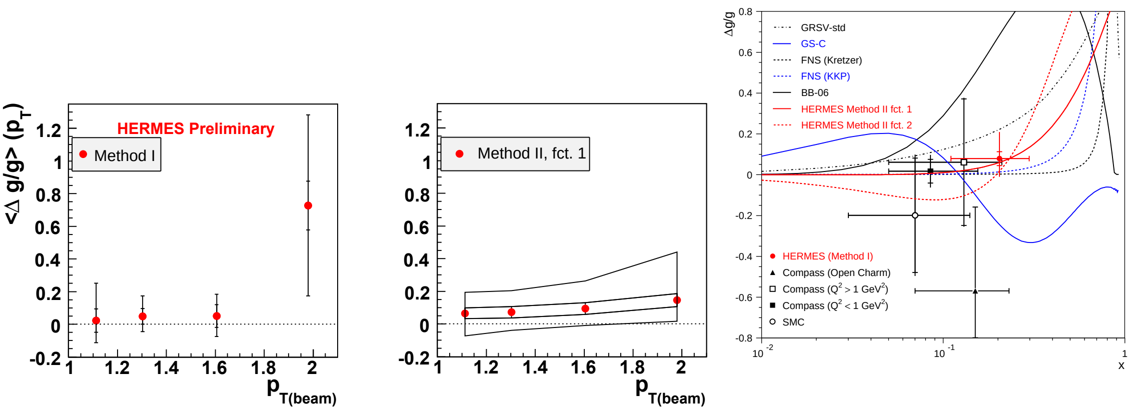

Figure 1: *HERMES results for $\Delta g/g$ vs p_T (left and center panels) and compilation of world data on $\Delta g/g$. The curves represent two fit functions from Method II and results from several NLO-QCD fits.*

2 The LNF HERMES group

HERMES is a Collaboration of about 180 physicists from 31 Institutions from 12 Countries. Italy participates with 4 groups and more than 30 physicists from Bari, Ferrara, Frascati and Rome. A Frascati physicist (P. Di Nezza) is the deputy spokesman, and an other one (D. Hasch) is the analysis coordinator of the experiment. The Frascati group is responsible for the electromagnetic calorimeter and has participated in the project and in the construction of two dual RICH detectors. It has been involved in the project and in the construction of Photon Detector, a part of the new Recoil Detector, installed at the end of 2005. A Frascati physicist (C. Hadjidakis) has the responsibility of the analysis working groups of azimuthal asymmetries in semi-inclusive processes and of the pseudoscalar meson exclusive production. A Frascati physicist (P. Di Nezza) has the responsibility of the nuclear physics analysis working group. Frascati physicists are involved in the analysis of many other physics processes. In addition they are playing a major role in the physics paper draftings and in the editorial process being the leading authors of about one third of the HERMES Collaboration physics publications.

3 Experimental activity of the LNF group in 2006

3.1 Calorimeter and TOF

In the period of data taking 2006-2007 with Recoil detector, one of the most important physics goals of HERMES is the investigation of the properties of the Deeply Virtual Compton scattering, a process where a virtual photon is transforming to a real one. For the detection of real photons the HERMES electromagnetic calorimeter, consisting of 840 lead-glass blocks, is used. It's basic purposes are the first level trigger on leptons and offline separation of charged hadrons from leptons by comparing their momentum from the energy of the electromagnetic showers deposited in the clusters of the calorimeter. In addition it allows to measure the energy and the angle of single photons from DVCS as well as double photons from π^0 and η meson decays. The responsibility for the calorimeter required the online monitoring of the status of the detector for the whole period of data taking. During 2006 all the data collected in the past has been reprocessed with recalibration of many detectors, including the calorimeter. During the long shutdown at the end of 2005 and beggining of 2006 the key components of the calorimeter (the high voltage power supplies and the readout electronics) were tested and maintained to assure their reliable service for the high intensity running of next years.

A precise energy and position reconstruction of electromagnetic showers allowed to separate leptons and hadrons with high efficiency by comparing their energy with momentum measured in the tracking system. An improved method of the energy reconstruction accounting for the losses in the preshower lead layer allowed to improve the resolution of the measured energy by ∼25%.

HERMES has two sets of scintillator hodoscope paddles which were mainly designed for charge particle triggering and lepton/hadron separation. The second one is also working as a preshower detector. Nevertheless, it turned out that they can be used also as a time-of-flight system to distinguish different hadron types from each other by their mass extracted from speed and momentum. A method was therefore developed to allow a nice separation of pions from protons in the momentum range of 0.6-3 GeV/c with total efficiency of 98% and pion contamination in proton sample of less then 5%. This momentum range is complementary to the one provided by the HERMES dual RICH detector.

3.2 Recoil detector

The recent proof of factorization for exclusive processes and their interpretation in terms of Generalized Parton Distributions to describe the nucleon structure, suggested the detailed investigation of these processes in which a fast meson or a photon is emitted in the forward direction while the slow nucleon is recoiling intact at large angle. Several exclusive processes have been already investigated by HERMES with the missing mass technique. To better identify these processes, a compact Recoil Detector has been constructed and installed around the target in autumn 2005. It consists of three part: an inner Silicon Detector inside the beam vacuum, a SciFi (Scintillating Fibre) Detector that is situated concentrically outside the beam pipe and an outer Photon Detector that is made of scintillator blocks, with the purpose to reconstruct the paths of protons involved in DVCS reactions from a hydrogen target cell located at the center of the detector. The Frascati group has built the Photon Detector, used to detect photons from the π^0 decay. It consists of three layers of scintillating strips with a WLS fiber system readout. Multi-anode photomultipliers are used with specially designed fan-in/preamplifiers to ensure capable transmittance of the signal. The Photon detector has been assembled in Frascati, transported to DESY and tested with cosmic rays with different trigger configurations. The cosmic rays have been used to test the full readout of the detector, using the Photon Detector as a trigger and a stand-alone tracking system, since the magnet was not included in the test. The reconstruction algorithm, the event display and the wire maps were developed, ensuring effective data acquisition, data processing and interpretation for standard HERMES software analysis tools. The Photon Detector is nicely working, some plots are shown in Fig.2. The Recoil Detector has been installed at the end of 2005 and it is entering in the data taking of 2006 and 2007.

3.3 Technical software

LNF members were main responsible for Particle Identification (PID). In particular they worked on the maintenance and code development of the PID library function, on the PID calibration, on the new data productions of 2004, 2005 and part of the 2006, on the flux corrections to PID for different physics analyzes, mainly dedicated to the transversity group. LNF has also the responsibility of the online data quality. In 2006 the code for taking into account the Recoil detector in the upcoming

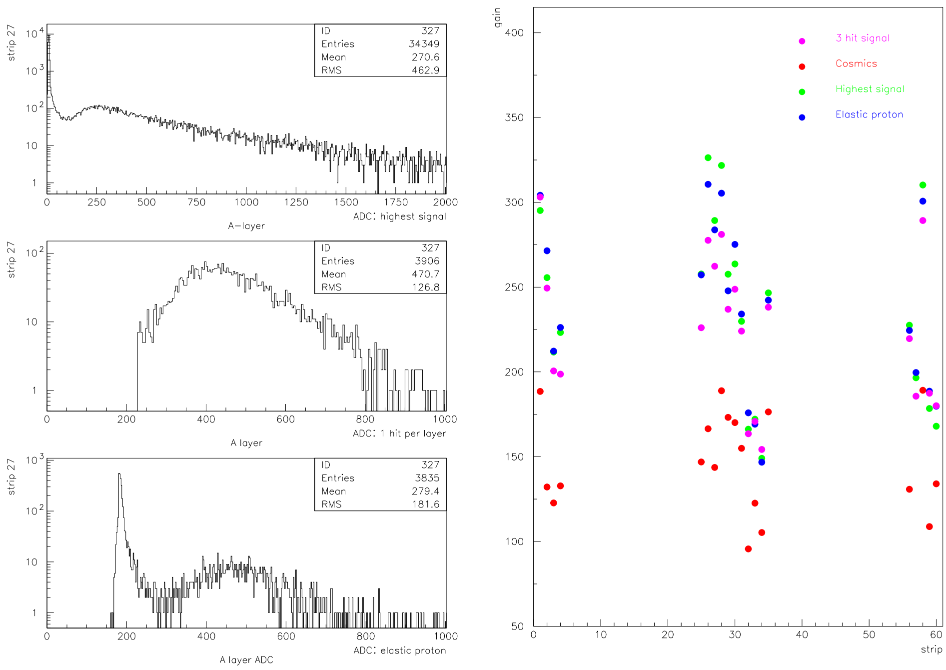

Figure 2: *Left: Tree types of event selection for the Photon Detector, requiring everytime a lepton track in the forward spectrometer. On top the ADC spectrum in the case that strip A27 gave the highest signal in the Photon Detector A layer for this event; on the middle the ADC spectrum, of strip A27 in case of 1 hit in each of the three Photon Detector layers and on the bottom the signal of the elastic proton peak. Right: Comparison of the previous plot with cosmic test: the three cases are always higher than cosmics because of protons.*

data has been completed and tested and the display of the online data quality chain has been implemented.

The LNF group acted also as HERMES Linux administrator and represented HERMES on DESY Linux user meeting, where user requirements and future strategy for Linux support were discussed. HERMES has a powerful Linux-based PC-farm with 2 workgroups servers, 4 fileservers and 40 batch nodes for various types of analysis. Several new powerful nodes were purchased to replace the master application server and the interactive workgroups servers, based on Intel Dual Core Xeon CPUs. The computer farm was upgraded to a newer operating system - Scientific Linux v.3.0.8 to allow better consistency with world standards and future participation in GRID computing. A suitable Linux distribution for this cluster has been set up to meet the growing demands of the users on data analysis and Monte-Carlo productions. The maintenance of the computers is provided through SNMP protocol plugged through an SMS gateway, which allows immediate knowledge in case of failures. In addition, there are about 40 desktop PCs acting as terminals for users and about 20 notebook computers for working use. server and the interactive workgroups servers, based on Intel Dual Core Xeon CPUs.

4 Data analysis and physics results of the LNF group in 2006

4.1 Inclusive spin structure functions

The cross-check of the moments of the polarised structure function g_1 have been performed, as well as the checks for the compatibility of the HERMES and SLAC measurements of g_1 for the deuteron, performing also studies on the parameterisation of the unpolarised structure function F_2. All these studies have been reported in the long paper on the precise determination of the spin-dependent structure function g_1 of the proton, deuteron and neutron. The final HERMES result for the polarised structure function g_1 from all data taken with longitudinally polarised hydrogen and deuterium targets is presented in Fig. 3 (left panel). The statistical precision of the proton data is comparable to that of the hitherto most precise data from SLAC and CERN in the same x range, while the deuteron data provide the most precise determination of $g_1^d(x, Q^2)$, compared to previous measurements. The right panel of Fig. 3 shows the integrals of $g_1^{p,d,n,NS}$ over the range $0.021 < x < 0.9$, corresponding to the event selection $Q^2 > 1$ GeV^2, as function of the low-x limit of integration evaluated at $Q_0^2 = 5$ GeV^2. For $x < 0.04$, g_1^d becomes compatible with zero and its measured integral shows saturation. Based on the *assumed* saturation of the integral of g_1^d, the flavour-singlet axial charge has been determined in the $\bar{M}S$ scheme at $Q_0^2 = 5$ GeV^2 using only the g_1^d integral and the axial charge a_8 as inputs: $a_0 = 0.330 \pm 0.011(\text{theo.}) \pm 0.025(\text{exp.}) \pm 0.028(\text{evol.})$. In this factorisation scheme, the result can be interpreted as the contribution $\Delta\Sigma$ of quark spins to the spin of the nucleon. The data therefore suggest that the quark helicities contribute a substantial fraction to the nucleon helicity, but there is still need for a major contribution from gluons and/or orbital angular momenta of more than half of the total decomposition of nucleon spin.

4.2 Beam-spin asymmetries in semi-inclusive deep inelastic scattering

Single-spin asymmetries in semi-inclusive deep-inelastic-scattering (SIDIS) are known as a powerful tool for probing the structure of the nucleon. If the orbital motion of the quarks is neglected, the structure of nucleon can be described in the leading twist by three parton distribution funtiosn (PDF) defining the momentum f_1, helicity g_1 and transversity h_1 distributions. The observation of different azimuthal asymmetries and in particular single spin asymmetries (SSAs) were an indication of a more complex inner structure if the nucleon. They give access to transverse momentum dependent parton distributions and time-reversal-odd fragmentation functions with prominent examples like the transversity h_1 and Sivers $f_{1T}^{\perp}$ distributions and Collins $H_1^{\perp}$ fragmentation functions. These quantities have been studied so far with unpolarized beam and both transverse and longitudinally polarized targets. Semi-inclusive pion production ($ep \rightarrow e'\pi X$) wiht an underlying mechanism of quark fragmentation is diluted by exclusive vector meson production which can contribute significantly in certain kinematic regions at HERMES. To access the effect of the exclusive processes, the amplitude $A_{LU}^{sin\phi}$ has been extracted for pions identified as decay products of exclusive ρ^0 mesons in the data, and compared with a Monte-Carlo simulation based on a vector meson dominance model and spin-density matrix elements extracted from HERMES data. The information obtained from a Monte Carlo simulation was used to subtract the contribution from exclusive vector meson production to the measured asymmetry amplitudes $A_{LU}^{sin\phi}$. The corrected asymmetry is shown in Fig.4 for charged pions. The asymmetry is roughly constant at about 0.01 for π^+ and compatible with zero for π^- in the low and middle range of z and exhibits a steep rise in the highest z bin for both π^+ and π^-. For the first time the pure semi-inclusive asymmetries are extracted from data through explicit subtraction of the exclusive vector meson contribution.

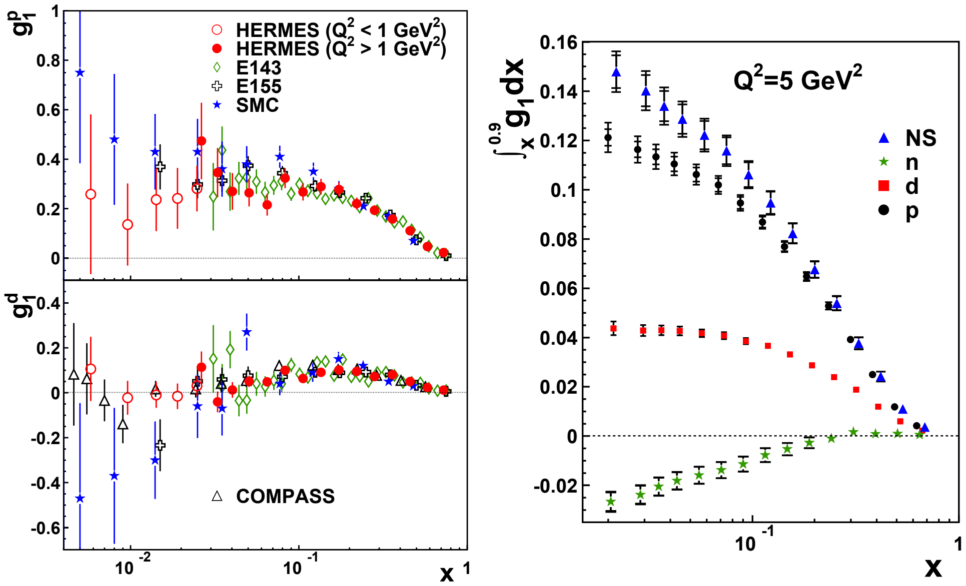

Figure 3: *Left: HERMES results on xg_1^p and xg_1^d vs x, shown on separate panels, compared to data from SMC, E143, E155 and COMPASS. The error bars represent the sum in quadrature of statistical and systematic uncertainties. The HERMES data points shown are statistically correlated by unforlding QED radiative and detector smearing effects. The E143 and E155 data points are correlated due to the method for correcting for QED radiation. For the HERMES data, the closed (opne) symbols represent values derived by selecting events with Q^2 >1 GeV^2 (Q^2 <1 GeV^2). Right: Integrals of $g_1^{p,d,n,NS}$ over the range* $0.021 < x < 0.9$ *as function of the low-x limit of integration.*

4.3 Semi-inclusive deep inelastic scattering measurements on deuterium, helium, neon, krypton and xenon in order to study the hadronization process

The process that leads from the partons produced in the elementary interactions to the hadrons observed experimentally is commonly referred to as hadronization or fragmentation. As at the length scales involved in the process (fentometer to few tens of fentometers) the magnitude of the strong coupling constant is such that perturbative techniques cannot be applied, experimental results are fundamental to develop theoretical models for hadronization. Leptoproduction of hadrons offers the advantage that the energy and the momentum of the struck parton are well determined, as they are tagged by the scattered lepton. In addition, by using nuclei of increasing size one can investigate the time development of hadronization. Hadron multiplicities on a nucleus A relative to those of deuterium have been studied at HERMES for various identified hadrons (π^+, π^-, π^0, K^+, K^-, p, $\bar{p}$) and as a function of the virtual photon energy ν, the fraction of this energy transferred to the hadron z, the photon virtuality Q^2 and the hadron transverse momentum $p-t^2$. The multiplicity ratio R_A^h decreases with increasing value of the mass number A and the ratio becomes larger (smaller) with increasing value of ν (z). The behaviour of the R_A as a function of $/nu$ and z is shown in Fig.4-right for charged pions and He, Ne and Kr nuclei. Furthermore, R_A^h increases slightly with increasing Q^2 , and it's almost independent of p_t^2, except at large values of p_t^2 where R_A^h increases strongly showing evidence of the Cronin effect.

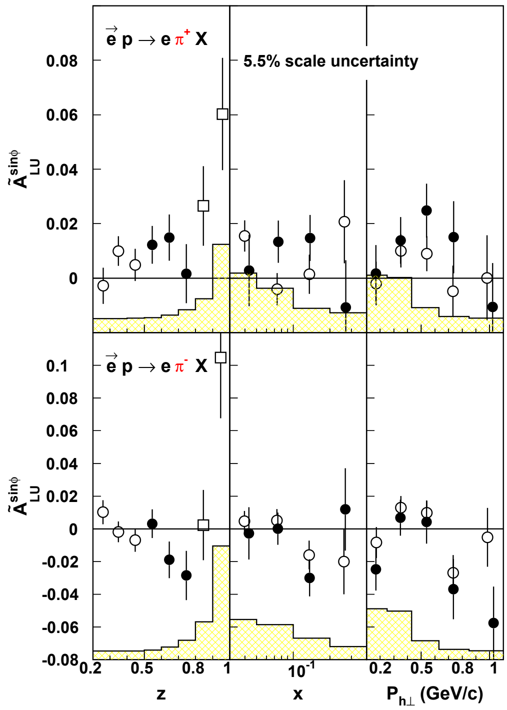

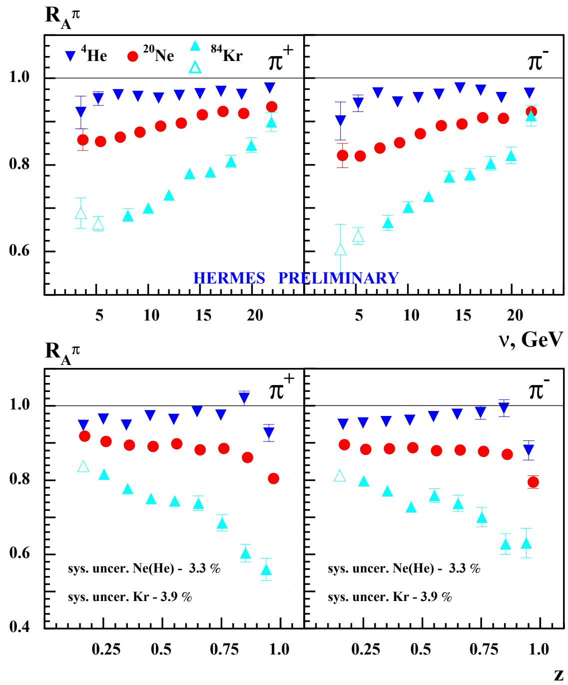

Figure 4: *Left: Dependence of the corrected asymmetry on z, x and P_{hL} for charged pions. The contribution from vector meson decays has been determined from a Monte Carlo simulation and subsequently subtracted from the asymmetries. The measurement of the x and P_{hL} dependences is made separately for low (0.2< z <0.5) and middle (0.5< z <0.8) $z-$ranges (indicated by open and full circles, respectively). The error band indicates the uncertainties from PYTHIA and rhoMC. Right: Multiplicity ratio as a function of ν and z for π^+ and π^- produced from He, Ne and Kr targets.*

4.4 p_t broadening and parton energy loss

Measurements performed up to now of semi-inclusive production of hadrons in deep-inelastic scattering off nuclei have provided precious information about the space-time development of the hadronization process Lately, by these measurements, HERMES is studying p_t-broadening, defined as $\Delta < p_t^2 >^h = < p_t^2 >^h_A - < p_t^2 >^h_D$ that is also strongly related to the interpretation of high-p$_t$ hadron production in heavy ion collisions. Recent results are shown in Fig.5. Moreover, an additional goal is to access the initial momentum distribution of quarks in a free nucleon. HERMES is well equipped to study these effects as in deep inelastic scattering no Initial State Interaction are possible which means a suppression of competitive processes. These new data will be available soon and show that the hadronization process is a powerfull tool for probing the medium properties also as an inputfor the, so-called, "jet quenching" mechanism representing the driving idea of the probe for the creation of dense matter in relativistic heavy ion collisions.

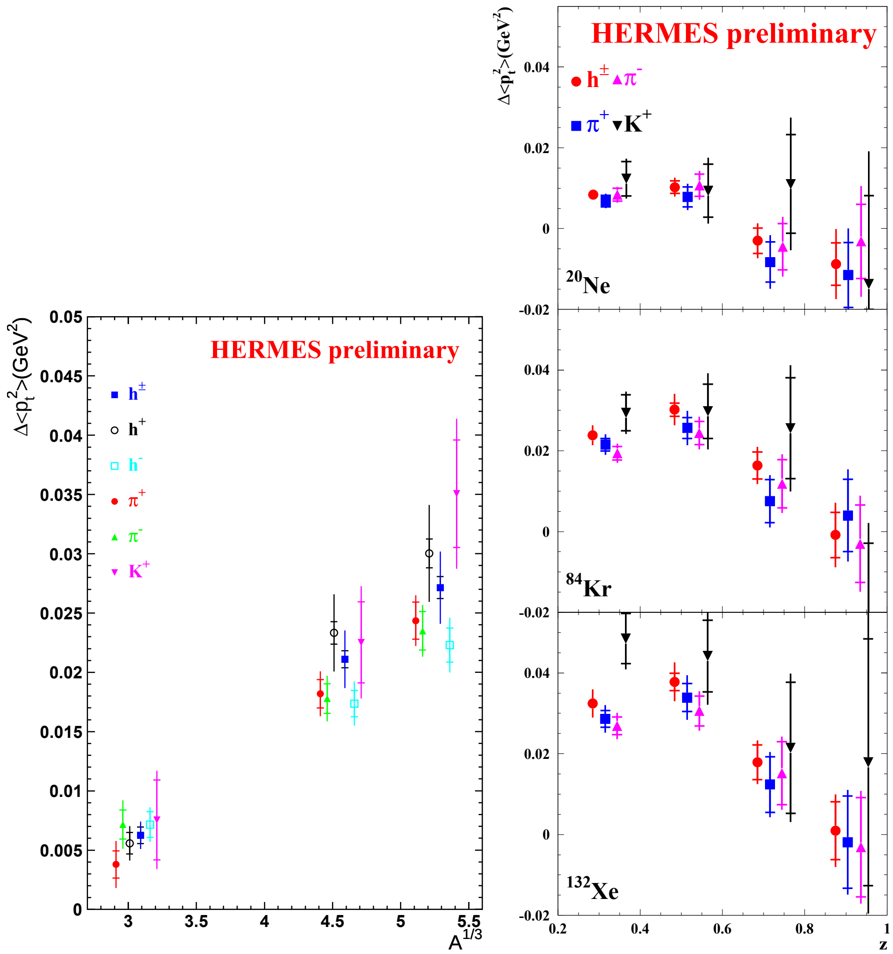

Figure 5: *Left: Dependence of p_t broadening on the atomic number of several hadron types. Right: $z-$dependence of p_t broadening for different hadron types produced on several targets.*

4.5 Exclusive production of single pion

The interest in the hard exclusive electroproduction of mesons has grown since a QCD factorization theorem was proved in the case of longitudinal photon at large Q^2. The amplitude for such reactions can be factorized into a hard lepton scattering part and two soft parts which parametrize the produced meson by a distribution amplitude and the target nucleon by four Generalized Parton Distributions (GPDs). In case of exclusive electroproduction of pion, the reaction provides essential information of the largely unknown space-like form factor and of the polarized GPDs ($\tilde{H}$ and $\tilde{E}$). First preliminary results for the unpolarized $ep \rightarrow en\pi^+$ has been extracted as a function of Q^2 for different x ranges and recently as a function of $t' = -t + t_0$ for different Q^2 range as shown in Fig. 6. The measurements have been compared to calculations based on GPD and Regge models. The full lines show the leading order calculations for the longitudinal part computed by the GPD-model. This model parametrizes $\tilde{E}$, which is dominated by the $t-$channel pion pole contribution, as a function of the pion electromagnetic form factor F_π. The GPD $\tilde{H}$ is neglected here as a first approximation as $\tilde{E}$ is expected to dominate the cross section at low t.

A Regge-inspired t-dependence is used for $\tilde{E}$. The dashed lines include power corrections mainly due to the soft overlap type contributions. The t-dependence is sharper in the model and does not reproduce the dependence of the data. While the leading-order calculations underestimate the data, the evaluation of the power corrections reproduce the Q^2 dependence of the data for $t' = 0.07$ GeV^2. The dotted lines show the cross section computed by a Regge-model. Pion production is described by the exchange of the meson trajectories π and ρ. In this formalism, the meson-nucleon coupling constants are fixed by pion photoproduction data and, at the electromagnetic vertices, the parameters F_π and the $\pi\rho\gamma$ transition form factor are fixed by existing electroproduction data. In particular, the form factors are both Q^2 and t dependent. The model calculations describe well the t' dependence but overestimate the data at low t' for $Q^2 < 3$ GeV^2.

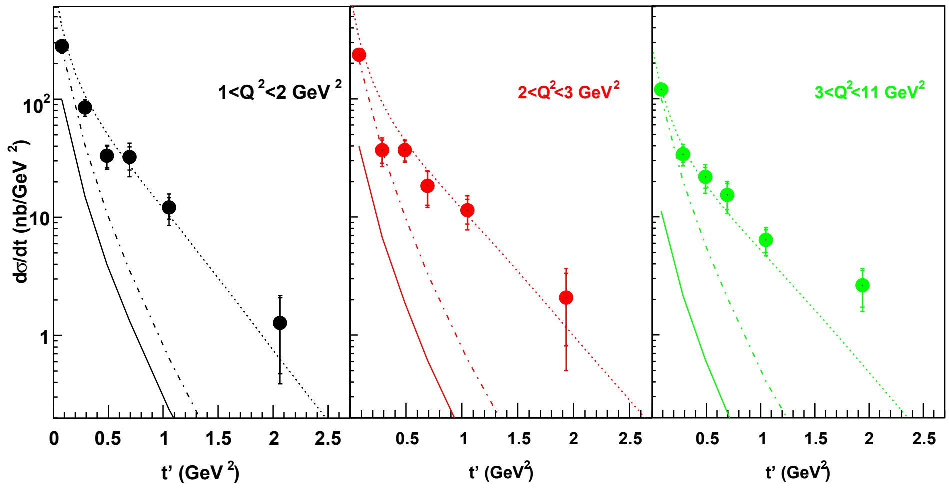

Figure 6: *Cross section for exclusive π^+ production as function of t' for three different Q^2 ranges. The inner error bars represent the statistical uncertainty and the outer error bars the quadratic sum of statistical and systematic uncertainty. The curves represent calculations based on GPD and on Regge models.*

5 Phenomenology on HERMES physics of the LNF group in 2006

5.1 Quark-hadron duality

Parton-hadron duality is generally defined as the similarity between hadronic cross sections in the Deep Inelastic Scattering region and in the resonance region. It encompasses therefore a range of phenomena where one expects to observe a transmogrification from partonic to hadronic degrees of freedom, a question, the latter, at the very heart of Quantum ChromoDynamics. A perturbative QCD NLO analysis including target mass corrections and large x re-summation effects has been extended to the integrals of both unpolarized and polarized structure functions in the resonance region. Both effects have been quantified and disentangled for the first time. A different behavior for unpolarized and polarized structure functions has been found. The discrepancy of the ratio from unity has been interpreted in terms of higher twists (HTs). The extraction of the dynamical HT terms from the resonance region for the unpolarised structure function F_2 is shown in Fig.7-left, where a clear discrepancy is seen for F_2, marking perhaps a breakdown of the twist expansion at low values of W^2. The analysis has been done also taking into account the recent data from Hall B in the resonance region and also using the Bodek-Stein parameterisation. A discrepancy between the two set of data from Jlab is seen in the region of high x: a more detailed study is going on. A comparison with other results obtained in the DIS region is also shown. Compared to previous analysis, new data form JLab have been added for the polarized structure function g_1 and the experimental values of the ratio $R = \sigma_L/\sigma_T$ from recent JLab measurements in the resonance region have been used (Fig.7-right). The latter introduce an oscillation around the original result of about 2%, well within the error bars. The new data introduced confirme a large violation of duality at $Q^2 \approx 1$ GeV^2 in the polarised case. A complete analysis of these results in comparison with other HT extractions is under study.

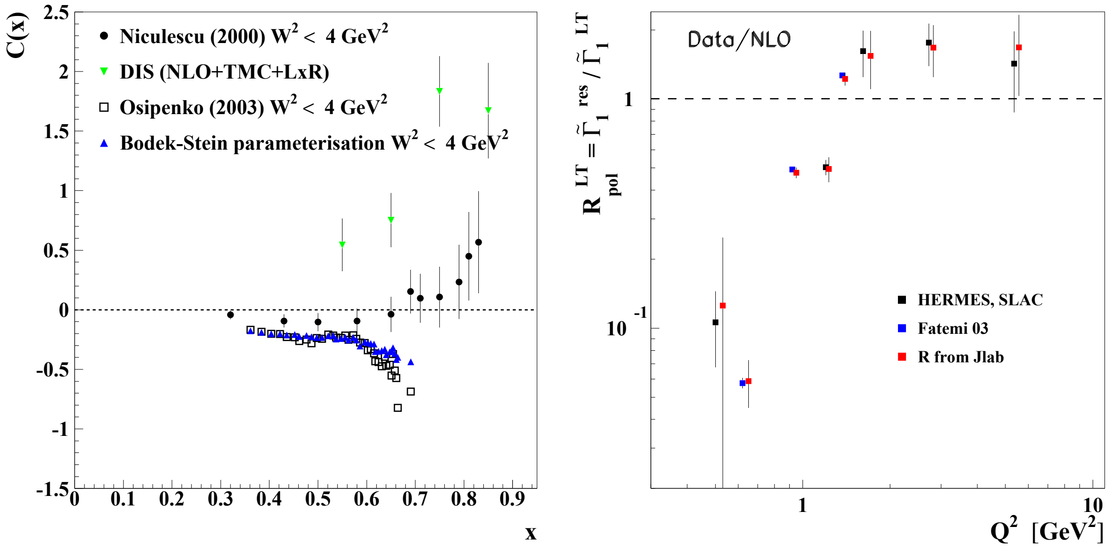

Figure 7: *Left: Comparison of HT contributions for the structure function F_2 in the DIS and resonance regions, respectively. Symbols are described in the legend of the picture. Right: Ratio of the experimental data on g_1 and the PQCD extrapolation to the resonance region. The Fatemi results agree with the trend of the Hermes data.*

6 Outlook

The data taking with Recoil Detector installed started at the beginning of 2006 and it will continue until the end of HERA, scheduled in June 2007. New precision data on hard exclusive reactions will be collected and analyzed, providing results on the exciting and new field of hard exclusive production of mesons and real photons with positron and electron beams. More precise results from HERMES are also expected soon for the full analysis of data with a transversely polarized hydrogen target. The results to date provide a demonstration of a new tool for studying the transverse structure of the nucleon. The ongoing physics analysis and the phenomenological investigations will be completed.

7 Conferences by LNF Authors in Year 2006

7.1 List of Conference Talks

1. N. Bianchi, "Hadron Leproproduction on Nuclei" (invited talk), XLIV International Winter Meeting on Nuclear Physiscs Bormio (Italy), Jan. 29-Feb. 5 2006 Bormio (Italy)
2. N. Bianchi, "Review on DIS Electro-production on Nuclei" (invited talk), 5th International Conference on Perspectives in Hadronic Physics Trieste (Italy), May 22-26 2006 Trieste (Italy)
3. N. Bianchi, "Nuclear Modification of two-hadron Correlations from HERMES" (invited talk), 2nd International Conference on Hard and Electromagnetic Probes of Hig-Energy Nuclear Collisions, Asilomar (USA), June 9-16 2006
4. P. Di Nezza, "The spin of the nucleon" (invited talk), International School on High Energy Physics (LISHEP 2006), Itacuruca (Brazil), April 1-7 2006
5. P. Di Nezza, "Parton propagation in cold nuclear matter" (invited talk), Jet Physics in Heavy Ion Collision at the LHC, ECT* Trento (Italy), September 2006
6. E. De Sanctis, "Status Report of the N7 project", Annual I3HP Meeting, Laboratori Nazionali di Frascati, Oct.6-7 2006
7. A. Fantoni, "Recent Results from the HERMES experiments at DESY" (invited talk), 9th International Workshop on Meson Production, Properties and Interaction, Kracow (Poland), June 9-13 2006; proceeding to be published in Journal of Modern Physics A
8. A. Fantoni, "Measurement of polarised distribution functions at HERMES" (invited talk), 13th International QCD Conference (QCD 06), Montpellier (France) July 3-7 2006; proceeding to be published by World Scientific.
9. C. Hadjidakis, "HERMES Results on Exclusive Reactions" (invited talk), 2nd Workshop on the QCD Structure of the Nucleon (QCD-N06), Monte Porzio Catone (Roma), June 12-16 2006
10. D. Hasch, "New Results from HERMES", open session of the PRC62, Desy Zeuthen, May 2006
11. D. Hasch, "Spin Physics at HERMES", 17th International Spin Physics Symposium (SPIN 06), Kyoto (Japan), Oct. 2-7 2006

7.2 Conference organization and advisory, Projects, Seminars, Lectures, Editors

1. N. Bianchi, (International Advisory Committee), 5th International Conference on Perspectives in Hadronic Physics, Trieste (Italy), May 22-26 2006
2. N. Bianchi, (International Advisory Committee), 2nd Workshop on the QCD Structure of the Nucleon (QCD-N06), Monte Porzio Catone (Roma), June 12-16 2006
3. N. Bianchi, (Editor) The European Physical Journal A
4. E. De Sanctis, (chair of the International Organizing Committee), 2nd Workshop on the QCD Structure of the Nucleon (QCD-N06), Monte Porzio Catone (Roma), June 12-16 2006
5. E. De Sanctis, (Convener) HERMES-LNF TARI at DESY
6. E. De Sanctis, (Convener) Studio di effetti di spin trasverso nel nucleone, PRIN 2006 project of the MIUR
7. E. De Sanctis, (Convener) N7-Transversity: Exploring the unknown transverse spin structure of the nucleon, Project of the I3-HP program of the European Commission
8. E. De Sanctis, member of HERMES Nominating Committee
9. P. Di Nezza, member of HERMES Editorial Board

10. P. Di Nezza, (Local Organizing Committee) 2nd Workshop on the QCD Structure of the Nucleon (QCD-N06), Monte Porzio Catone (Roma), June 12-16 2006
11. A. Fantoni, (chair of the Local Organizing Committee) 2nd Workshop on the QCD Structure of the Nucleon (QCD-N06), Monte Porzio Catone (Roma), June 12-16 2006
12. C. Hadjidakis, (Seminar) "Derniers resultats de l'experience HERMES", IPN Orsay (France), Jan. 2006
13. C. Hadjidakis, (Seminar) "Distributions de partons generalisee et mesures de processus exclusifs a HERMES", LPSC Grenoble (France), Jan. 2006
14. D. Hasch, member of HERMES Editorial Board
15. D. Hasch, (Seminar) "How to measure transversity & friends in SIDIS", RIKEN Spin Collaboration Seminar, Brookhaven National Laboratory, Feb. 22 2006
16. D. Hasch, (Seminar) "The Spin of the Nucleon", Cagliari University, Nov. 21 2006

8 Publications of LNF Authors in Year 2006

1. A. Airapetian *et al.*, "Longitudinal Spin Transfer to the Lambda Hyperon in Semi-Inclusive Deep Inelastic Scattering", Phys. Rev. **D**74, 072004 (2006).

2. A. Airapetian *et al.*, "Double-hadron Leptoproduction in the Nuclear Medium", Phys. Rev. Lett. 96, 162301 (2006).

3. A. Airapetian *et al.*, "The Beam-Charge Azimuthal Asymmetry and Deeply Virtual Compton Scattering", Phys. Rev. **D** in print, hep-ex/0605108.

4. A. Airapetian *et al.*, "Precision Determination of the spin structure function g_1 of the proton, deuteron and neutron", Phys. Rev. **D** in print, hep-ex/0609039.

5. A. Airapetian *et al.*, "Beam-Spin Asymmetries in the Azimuthal Distribution of Pion Electroproduction", submitted to Phys. Lett. **B**, hep-ex/0612059.

6. E. Avetisyan, "Transverse spin effects in single and double hadron production at HERMES", Information Technologies and Management (Armenia), issue 3, 43 (2006).

7. E. Avetisyan, http://pos.sissa.it/archive/conferences/021/419/HEP2005_419.pdf (published in 2006), Proceeding of the International Europhysics Conference on High Energy Physics, Lisboa (Portugal), July 21-27 2005.

8. P. Di Nezza, "Spin structure of the nucleon", Nucl. Phys. **B**152, 96 (2006).

9. A. Fantoni, "The spin puzzle: recent results from the HERMES experiment", Intern. Journ. of Modern Physics **A**, in print.

10. A. Fantoni, S. Liuti and O. Rondon Editors, Proceedings of "First Workshop on Quark-Hadron Duality and the Transition to pQCD", World Scientific (2006).

11. A. Funel, "Hadron Production in Semi-inclusive Lepton DIS on Nuclei at HERMES", PhD thesis, Ferrara University, April 2006.

$\overline{\text{P}}$ANDA - $\overline{\text{p}}$ Annihilation at Darmstadt

B. Dulach, P. Gianotti (Resp. Naz.), M. Giardoni, C. Guaraldo, O.N. Hartmann (Art. 23),
M. Iliescu (Art. 23), V. Lucherini, D. Orecchini (Tecn.), E. Pace,
L. Passamonti (Tecn.), D. Sirghi (Art. 2222)

1 Introduction

$\overline{\text{P}}$ANDA is one of the biggest future experiments in nuclear and hadron physics that will be carried out at the new Facility for Antiproton and Ion Research (FAIR). It is dedicated to study annihilations of antiprotons on nucleons and nuclei up to a maximum center-of-mass energy in $\overline{\text{p}}$p of 5.5 GeV. The LNF group is involved in the design and construction of the central tracker of the $\overline{\text{P}}$ANDA detector.

2 $\overline{\text{P}}$ANDA experiment

A new facility for hadronic physics is under construction in Germany. It consists of a major upgrade of the presently running GSI accelerator complex of Darmstadt [1].

An intense, high momentum resolution antiproton beam, with momentum between 1.5 and 15 GeV/c, will be available at the High Energy Storage Ring (HESR), and the experimental activity will be carried on using a general purpose detector $\overline{\text{P}}$ANDA that will be build surrounding an internal target station installed at one of the two straight sections of the storage ring.

3 The $\overline{\text{P}}$ANDA Central Tracker

The $\overline{\text{P}}$ANDA Central Tracker has to satisfy the following requirements:

- almost full solid angle coverage;
- momentum resolution $\delta p/p \sim 1.5\%$;
- low material budget $X/X_0 \sim$ few %;
- good spatial resolution $\sigma_{r,\phi} = 150$, μm,$\sigma_z =$ few mm.

This detector will be placed around the Micro Vertex Detector (MVD) at a radial distance from the interaction point between 15 and 42 cm. Along the beam axis the allowed space is 150 cm. Presently, for this detector, two options are under discussion: a Straw Tube Tracker (STT) and a Time Projection Chamber (TPC). The LNF group is testing different straw tubes prototypes with the aim of preparing the STT final design.

3.1 Straw tube detector layout

The overall tracking volume will be divided in two half by the target pipe assembly, so that the detector will consist of two identical semi-chambers. Each one will be made of straw tubes, diameter 10 mm, length 150 cm, arranged in concentric layers. In order to avoid strong support structure, the tubes will be glued together and operated with an Ar+CO_2 gas mixture with an over-pressure of 1 bar. Some layers will be mounted with a skew angle of few degrees with respect to the beam axis to allow the reconstruction of the z coordinate.

In figure 1, the layout of one of the two semi-chamber is shown.

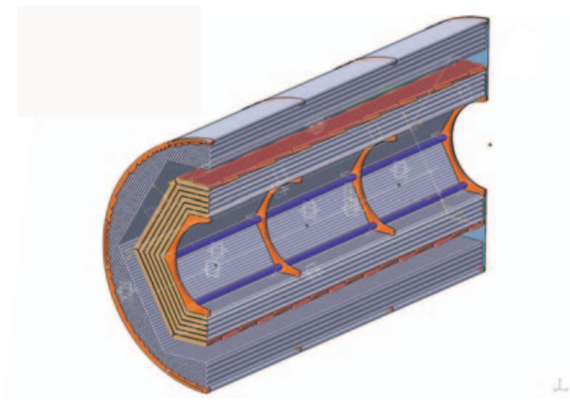

Figure 1: A possible layout for the STT. Details in the text.

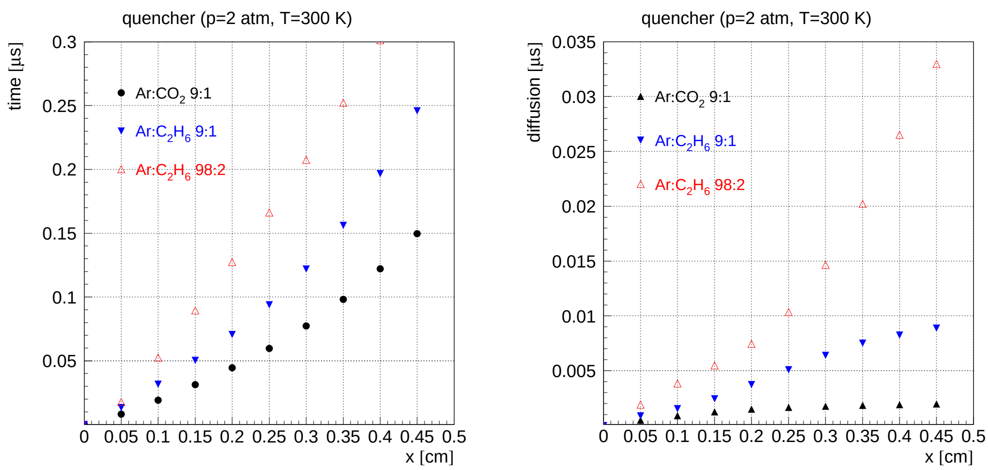

Figure 2: Behavior of different gas mixtures: (left) space time relation; (right) diffusion along the fastest drift path.

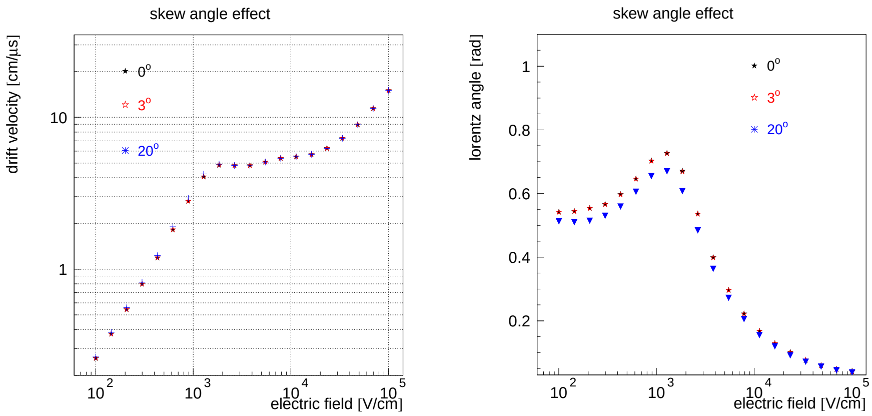

Figure 3: Effects of the shew angle on straw performance: (left) drift velocity; (right) Lorentz angle.

A small scale prototype (15 tubes) has been constructed at the LNF to allow further R&D on mechanics, electronics, gas feed, power supply, readout etc.

The behavior of the counting gas mixture for the $\overline{\text{P}}$ANDA straw tube tracker is under study using the simulation package GARFIELD and the built-in program MAGBOLTZ [4]. A single straw tube has been investigated to check the effects of different variables on its performance: magnetic field in-homogeneity, skew angle choice, gas mixture stability are the main parameter under analysis. Some results of the simulations are show in fig. 2 and 3.

4 List of publications

1. O. N. Hartmann, "Tracking in antiproton annihilation experiments", Nucl. Instr. Meth A566, 66, 2006.

5 Conference presentations

1. O. N. Hartmann, "Hadron Properties in the Nuclear Medium - the $\overline{\text{P}}$ANDA Program with $\bar{p}$-A Reactions", presented at the 9th International Workshop on Meson Production, Properties and Interaction, June 9th-13th 2006, Krakow, Poland.
2. P. Gianotti, "New Physics and Technical Challenges of $\overline{\text{P}}$ANDA", invited talk at the IVth International Conference on Quarks and Nuclear Physics, June 5th-10th 2006, Madrid, Spain.
3. O. N. Hartmann, "Charmante Hadronen in Kernmaterie", seminar at ÖAW-SMI, May 4th 2006, Vienna, Austria.
4. P. Gianotti, "Fisica con antiprotoni al GSI", invited talk at the XCII Congresso Nazionale della Societá Italiana di Fisica, Torino, 18 - 23 Settembre 2006.

References

1. http://www.gsi.de/fair/
2. http://www.gsi.de/panda/
3. PANDA Letter of Intent, 2004; PANDA Technical Progress Report, 2005.
4. http://consult.cern.ch/writeup/garfield/

SIDDHARTA

M. Bragadireanu (Bors. UE), M. Catitti (Ass. Ric.), C. Curceanu Petrascu (Co-Resp. Naz.), C. Guaraldo (Co-Resp. Naz.), M. Iliescu (Art. 2222), P. Levi Sandri, V. Lucherini, F. Lucibello (Tecn.), D. Pietreanu (Bors. PD), D. Sirghi (Art. 2222), F. Sirghi (Bors. UE), O. Vazquez Doce (Bors. UE)

1 The SIDDHARTA scientific program

The objective of the SIDDHARTA (Silicon Drift Detector for Hadronic Atom Research by Timing Application) experiment is to continue, to deepen and enlarge the successful scientific line, initiated by the DEAR experiment in performing precision measurements of X-ray transitions in exotic (kaonic) atoms at DAΦNE.

The eV precise determination of the shift and width of the $1s$ level with respect to the purely electromagnetic calculated values, in kaonic hydrogen and kaonic deuterium, generated by the presence of the strong interaction, through the measurement of the X-ray transitions to this level, will allow the first precise experimental determination of the isospin dependent antikaon-nucleon scattering lengths.

The shift ϵ and the width Γ of the $1s$ state of kaonic hydrogen are related to the real and imaginary part of the complex s-wave scattering length, a_{K^-p}, through the Deser formula (in the isospin limit):

$$\epsilon + i\Gamma/2 = 2\alpha^3\mu^2 a_{K^-p} = (412\ eV\ fm^{-1}) \cdot a_{K^-p} \tag{1}$$

where α is the fine structure constant and μ the reduced mass of the K^-p system. In the isospin limit, i.e. in the absence of the electromagnetic interaction and at $m_d = m_u$, a_{K^-p} can be expressed directly in terms of the scattering lengths for isospin I=0 and I=1:

$$a_{K^-p} = \frac{1}{2}(a_0 + a_1) \tag{2}$$

A similar relation applies to the case of kaonic deuterium and to the corresponding scattering length a_{K^-d}:

$$\epsilon + i\Gamma/2 = 2\alpha^3\mu^2 a_{K^-d} = (601\ eV\ fm^{-1}) \cdot a_{K^-d} \tag{3}$$

An accurate determination of the K^-N isospin dependent scattering lengths will place strong constraints on the low-energy K^-N dynamics, which, in turn, constraints the SU(3) description of chiral symmetry breaking in systems containing the strange quark.

The DEAR measurement on kaonic hydrogen, performed in 2002 (Phys. Rev. Lett 94 (2005), 212302), has already triggered an increased activity new of the theoretical groups working in the low-energy kaon-nucleon interaction field, as well as in more general non-perturbative QCD.

The SIDDHARTA experiment aims to improve the precision obtained by DEAR by an order of magnitude and to perform the first measurement ever of kaonic deuterium. Other measurements (kaonic helium, sigmonic atoms, precise determination of the charged kaon mass) are as well considered in the scientific program.

2 The SIDDHARTA experiment features

SIDDHARTA (Silicon Drift Detector for Hadronic Atom Research by Timing Application) represents a new phase in the study of kaonic atoms at DAΦNE. The DEAR precision was limited by a signal/background ratio of about 1/70. In order to significantly improve this ratio a breakthrough is necessary. An accurate study of the background sources present at DAΦNE was re-done. The background includes two main sources:

- synchronous background: coming together with the K^- - related to K^- interaction in the setup materials and also to the ϕ-decay process; it can be defined hadronic background;
- asynchronous background: final products of electromagnetic showers in the machine pipe and in the setup materials originated by particles lost from primary circulating beams either due to the interaction of particles in the same bunch (Touschek effect) or due to the interaction with the residual gas.

Accurate studies performed by DEAR showed that the main background source in DAΦNE is of the second type, which shows the way to reduce it. A fast trigger correlated to the negative kaon entrance in the target would cut the main part of the asynchronous background.

While DEAR used for the X rays detection the CCD (Charge Coupled Device) detectors - excellent X-ray detectors, with very good energy resolution (about 140 eV FWHM at 6 keV), but having the drawback of being non-triggerable devices (since the read-out time per device is at the level of 10 s), a recently developed device, which preserves all good features of CCDs (energy resolution, stability and linearity) but additionally is triggerable - i.e. fast (at the level of 1μs) was implemented. This new detector is represented by large area Silicon Drift Detector (SDD), specially designed for spectroscopic application. The development of the new 1 cm^2 SDD device is partially performed in the framework of an European Joint Research Activity (JRA10) within the FP6 program, the HadronPhysics I3.

Successful tests of SDD prototypes were performed in 2003, 2004 and 2005 at the Beam Test Facility of Frascati (BTF), in realistic (i.e. DEAR-like) conditions and in the laboratory. The results of this tests were very encouraging: a trigger rejection factor of $5 \cdot 10^{-5}$ was measured. Extrapolated to SIDDHARTA conditions, this number translates into a S/B ratio in the region of interest about 20/1. By triggering the SDDs, the asynchronous e.m. background (mainly due to Touschek effect) can therefore be eliminated.

3 Activities in 2006

In what follows, we present the main 2006 SIDDHARTA activities performed at LNF.

3.1 Definition of the SIDDHARTA setup

One of the main activities performed by the SIDDHARTA Collaboration in 2006 was the final definition of the setup. The structure of the target (done in kapton reinforced with fiber glass structure) was defined and the target cell built and under test; it is surrounded by SDD detectors grouped in units containing 18 SDDs 1 cm^2 each, for a total of 216 single SDDs. In Fig. 1 and 2 details on the SDD units and target cell are shown.

3.2 Laboratory tests of the 1 cm^2 SDD prototypes

The 1 cm^2 SDD chips were tested in the LNF SIDDHARTA laboratory, using a 1 mV stabilized power supply developed in the framework of SIDDHARTA, with very good results - shown in Fig. 3.

The tests are undergoing.

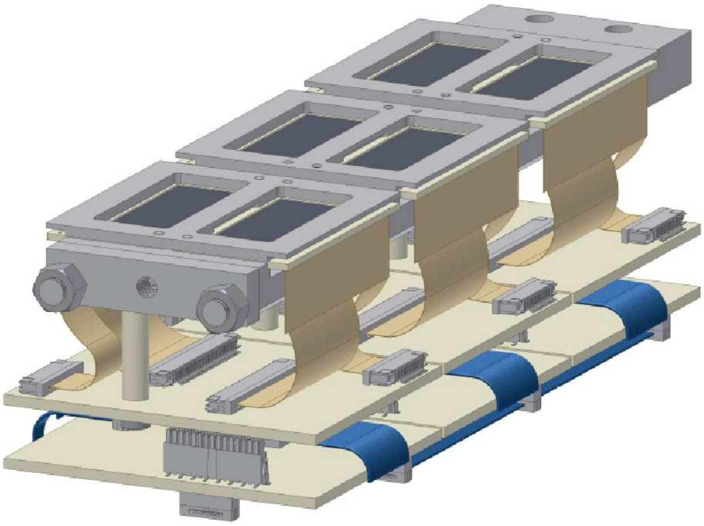

Figure 1: *An 18 cm^2 SDD unit, containing 18 SDD individual chips.*

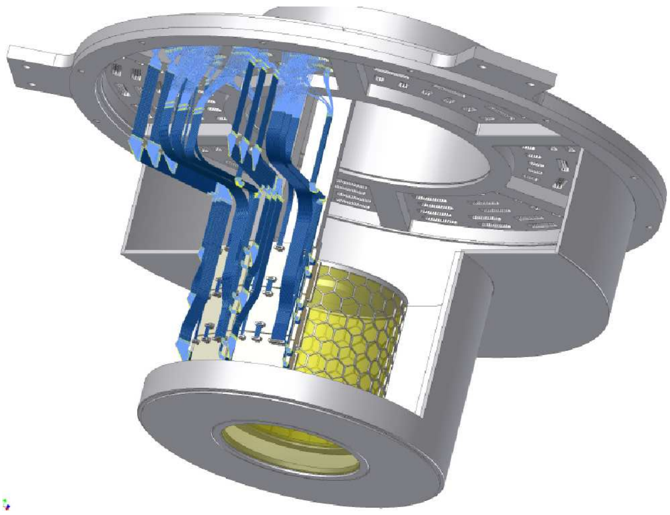

Figure 2: *The SIDDHARTA target cell surrounded by SDD units (detail).*

3.3 Design and construction of the highly stability multichannel high and low - voltages SIDDHARTA power supply

In order to be able to perform the eV precision measurements of X rays emitted in kaonic hydrogen and kaonic deuterium radiative transitions, SIDDHARTA needs a 0.1% stabilized power supply for SDDs and SDDs readout electronics. The system which realizes these tasks was developed by LNF electronic team, in collaboration with IFIN-HH Bucharest. The system, actually containing two subsystems (High Voltage Active Distributor and a Power Distributor) satisfies the following criteria: very compact and robust; well insulated; high precision on the delivered voltages; protection of the system with respect to the SDD electronics; very good thermal and groung loops control; local control, vua CAN BUS comunication in Dasy Chain configuration (so very few wires). It deliveres ± 15 V 5A; ± 20 V 2A; -340 V 120mA; -230 V 120mA. A first prototype was built and tested at LNF, with very good results. The production of all the system is undergoing.

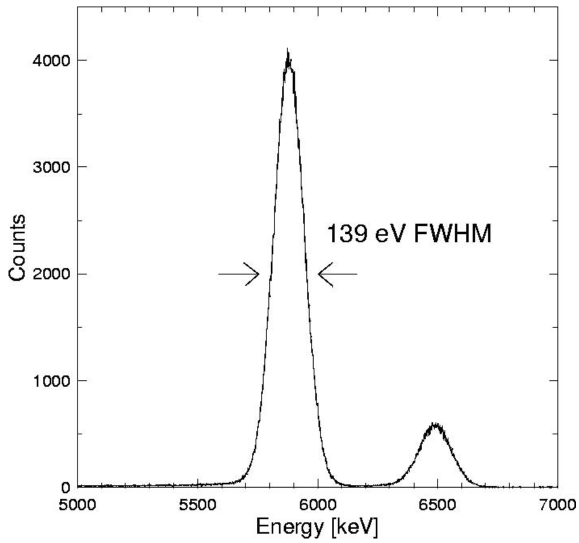

Figure 3: *The X-ray spectrum from an Iron source as measured in the laboratory with an SDD chip prototype. The experimental resolution, FWHM (Full Width Half Maximum) at 5.9 keV is 139 eV.*

3.4 The trigger system

All the PM's used in the trigger system (6 + 2 spares) were tested and characterized and their working point defined. The trigger system (a system of scintillators measuring the back-to-back delivered kaons in the ϕ-decay process) is under construction.

3.5 New general SIDDHARTA layout design

In 2006 a new scheme of the SIDDHARTA Interaction Region (IR) was put forward by the DAΦNE team. The new scheme, to be applied by the end of 2007 for the SIDDHARTA run, exploits the large crossing angle and the crabbed waist concepts and should allow to reach a luminosity of about $10^{33}\mathrm{cm}^{-2}\mathrm{s}^{-1}$. In 2006 an intense collaboration beween SIDDHARTA and DAΦNE teams, with the fundamental collaboration of the SPAS division of LNF (Bruno Dulach and Cesidio Capoccia), produced a new layout design of SIDDHARTA in the new IR, shown in Fig. 4.

4 Activities in 2007

The LNF group main activities in SIDDHARTA for 2007 are the following ones:

- end of construction and testing of the high- and low - voltages suppliers;
- end of construction and testing of the trigger system;
- end of construction and testing of the DAQ and Slow Control systems;
- continue measurements in the lab and on BTF of 1 cm^2 SDD test setup;
- finalize all the SIDDHARTA various setup components, integration and testing;
- finalize the general SIDDHARTA layout (platforms, supports) construction;
- Monte Carlo simulation of the system performance and strategy of the measurements;
- installation on DAΦNE and start data taking.

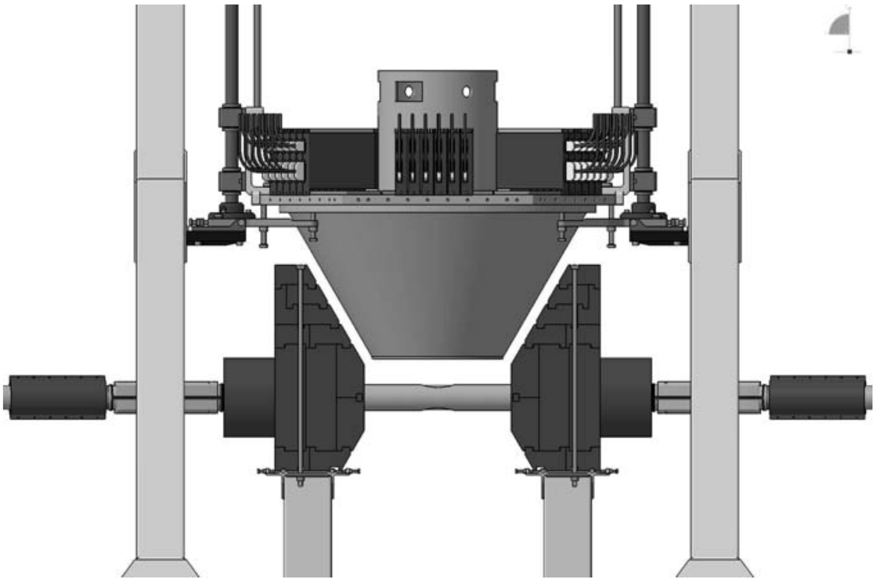

Figure 4: *The schematic drawing of the SIDDHARTA setup in the Interaction Region of DAΦNE.*

5 Publications 2006

5.1 List of Conference Talks given by LNF Authors in Year 2006

1. C. Curceanu (Petrascu), "Precision measurements of kaonic atoms at DAFNE and future perspectives", talk at the XLIV INTERNATIONAL WINTER MEETING ON NUCLEAR PHYSICS, January 29 - February 5, 2006, Bormio (Italy).

2. V. Lucherini, "Hadronic atoms physics at DAFNE", talk at the 9th International Workshop on Meson Production, Properties and Interaction KRAKW, POLAND 9 - 13 June 2006.

3. F. Sirghi, "Exotic-atom measurements at DAFNE", talk at the Frascati Spring School "Bruno Touschek" in Nuclear and Subnuclear and Astroparticle Physics, May 15th-19th, 2006.

4. C. Curceanu, "Precision measurements of kaonic atoms at DAFNE and future perspectives", talk at the QNP06, International Conference on Quarks and Nuclear Physics, Madrid, June 5th-10th 2006.

5. C. Curceanu. "The SIDDHARTA experiment at DAFNE and future perspectives", talk at the IX International Conference on Hypernuclear and Strange Particle Physics, 10-14 October 2006, Johannes Gutenberg Universitat, Mainz (Germany)

6. D. Sirghi, "Misure di Atomi Esotici: l'esperimento SIDDHARTA a DAFNE", talk at the XCII Congresso Nazionale Societa' Italiana di Fisica, Torino 18-23 Settembre 2006

5.2 Papers and Proceedings

1. T. Ishiwatari *et al.*, "New analysis method for CCD X-ray data", Nucl. Instrum. Meth.**A556** (2006), 509.

2. Catalina Curceanu, Akaki Rusetsky and Eberhard Widmann, HISKP-TH-06-28, Oct 2006. 53pp. Miniproceedings of the International Workshop on Exotic Hadronic Atoms, Deeply Bound Kaonic Nuclear States and Antihydrogen: Present Results, Future Challenges, Trento, Italy, 19-24 Jun 2006. e-Print Archive: hep-ph/0610201

3. J. Marton *et al.*, "Experimental studies on kaonic atoms at DAFNE: Recent results and perspectives", AIP Conf.Proc.842 (2006), 256.

4. J. Marton *et al.*, "Exotic Atom Research Using Large Area Silicon Drift Detectors", Proceedings of International Symposium on Detector Development for Particle, Astroparticle and Synchrotron Radiation Experiments (SNIC 2006), Menlo Park, California, 3-6 Apr 2006, pp 0196.

5. C. Curceanu, A. Rusertski and E. Widmann, " Exotic atoms cast light on fundamental questions", CERN Courier, Nr. 46 (9), (2006) 32-34.

6. M. Cargnelli *et al.*, "New Precision Studies of Strong Interaction in Exotic Atoms: Kaonic Hydrogen and Deuterium", AIP Con. Proc. 870 (2006), 475.

7. J. Marton *et al.*, "Kaonic Hydrogen Experiment", in Miniproceedings of the International Workshop on Exotic Hadronic Atoms, Deeply Bound Kaonic Nuclear States and Antihydrogen: Present Results, Future Challenges, Trento, Italy, 19-24 Jun 2006. e-Print Archive: hep-ph/0610201

8. G. Beer *et al.*, "Kaonic hydrogen X rays - experiments at DAFNE", International Workshop on Precision Physics of Simple Atomic Systems, to appear in Canadian Journal of Physics.

9. M. Cargnelli *et al.*, "Kaonic hydrogen X rays - experiments at DAFNE", to appear in Proceedings of the Workshop on Precision Physics of Simple Atomic Systems (PSAS 2006), Venice/ITALY.

10. J. Zmeskal *et al.*, "Experimental Studies on Kaonic Atoms at DAFNE", Proceedings of the 18th International IUPAP Conference on Few-Body Problems in Physics, Santos/BRAZIL.

11. C. Curceanu *et al.*, "Precision measurements of kaonic atoms at DAFNE and future perspectives", Proceedings of the XLIV INTERNATIONAL WINTER MEETING ON NUCLEAR PHYSICS, January 29 - February 5, 2006, Bormio (Italy), Universita' degli studi di Milano, Edited by I. Iori and A. Tarantola (2006) 152.

12. V. Lucherini *et al.*, "Hadronic atoms physics at DAFNE", 9th International Workshop on Meson Production, Properties and Interaction KRAKW, POLAND 9 - 13 June 2006, to appear in the International Journal of Modern Physics A.

13. C. Curceanu *et al.*, "Precision measurements of kaonic atoms at DAFNE and future perspectives", QNP06, International Conference on Quarks and Nuclear Physics, Madrid, June 5th-10the 2006, to appear in the EUROPEAN PHYSICAL JOURNAL A (EPJA)

14. C. Curceanu *et al.*, "The SIDDHARTA experiment at DAFNE and future perspectives, IX International Conferenceon Hypernuclear and Strange Particle Physics, 10-14 October 2006, Johannes Gutenberg Universitat, Mainz (Germany), to appear in the EUROPEAN PHYSICAL JOURNAL A (EPJA)

VIP

S. Bartalucci, S. Bertolucci, M. Catitti (Ass. Ric.), C. Curceanu Petrascu (Resp. Naz.),
S. Di Matteo (Art. 23), C. Guaraldo, M. Iliescu (Art. 2222), F. Lucibello (Tecn.),
D. Pietreanu (Bors. PD), D. Sirghi (Art. 2222), F. Sirghi (Bors. UE),
L. Sperandio (Dott.), O. Vazquez Doce (Bors. PD)

1 The VIP scientific case and the experimental method

The Pauli exclusion principle (PEP), which plays a fundamental role in our understanding of many physical and chemical phenomena, from the periodic table of elements, to the electric conductivity in metals, to the degeneracy pressure (which makes white dwarfs and neutron stars stable), is a consequence of the spin-statistics connection. Although the principle has been spectacularly confirmed by the number and accuracy of its predictions, its foundation lies deep in the structure of quantum field theory and has defied all attempts to produce a simple proof. Given its basic standing in quantum theory, it seems appropriate to carry out precise tests of the PEP validity and, indeed, mainly in the last 15-20 years, several experiments have been performed to search for possible small violations. The indistinguishability and the symmetrization (or antisymmetrization) of the wave-function should be then checked independently for each particle, and accurate tests were and are being done.

The VIP (VIolation of the Pauli Exclusion Principle) experiment, an international Collaboration among 6 Institutions of 4 countries, has the goal to improve the limit on the probability of the violation of the PEP for electrons, (P $< 1.7 \times 10^{-26}$ established by E. Ramberg e G. A. Snow: *Experimental limit on a small violation of the Pauli principle*, Phys. Lett. **B 238** (1990) 438) by four orders of magnitude (P $<10^{-30}$), exploring a region where new theories might allow for a possible PEP violation.

The experimental method consists in the introduction of new electrons into a copper strip, by circulating a current, and in the search for X-rays resulting from the forbidden radiative transition that occurs if one of the new electrons is captured by a copper atom and cascades down to the 1s state already filled by two electrons with opposite spins. The energy of this transition would differ from the normal K_α transition by about 300 eV (7.729 keV instead of 8.040 keV) providing an unambiguous signal of the PEP violation. The measurement alternates periods without current in the copper strip, in order to evaluate the X-ray background in conditions where no PEP violating transitions are expected to occur, with periods in which current flows in the conductor, thus providing "fresh" electrons, which might possibly violate PEP. The rather straightforward analysis consists on the evaluation of the statistical significance of the normalized subtraction of the two spectra in the region of interest.

The experiment is being performed at the LNGS underground Laboratories, where the X-ray background, generated by cosmic rays and natural radioactivity, is reduced.

2 The VIP experimental setup

The VIP setup was built in 2005, starting from the DEAR setup, reutilizing the CCD (Charge Coupled Devices) X-ray detectors, and consists of a copper cylinder, 4.5 cm in radius, 50 μm thick, 8.8 cm high, surrounded by 16 equally spaced CCDs of type 55.

The CCDs are at a distance of 2.3 cm from the copper cylinder, grouped in units of two chips vertically positioned. The setup is enclosed in a vacuum chamber, and the CCDs are cooled to

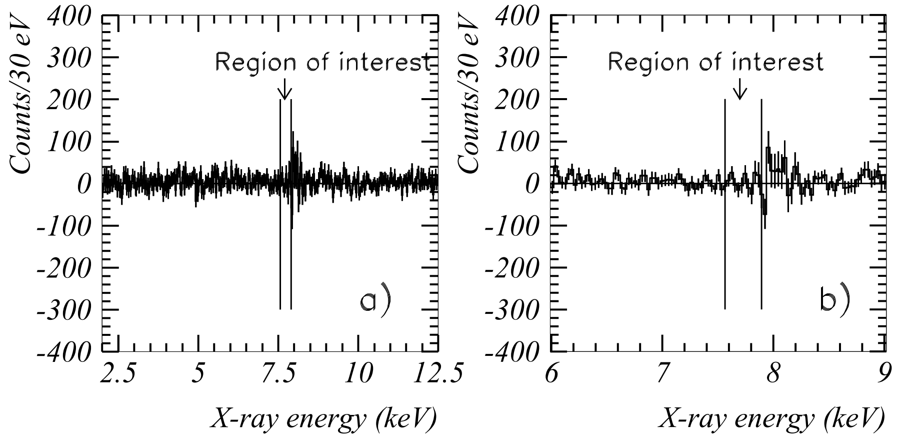

Figure 1: *Subtracted energy spectra in the Frascati measurement, current minus no-current, giving the limit on PEP violation for electrons: a) whole energy range; b) expanded view in the region of interest (7.564 - 7.894 keV). No evidence for a peak in the region of interest is found.*

about 165 K by the use of a cryogenic system.

The DAQ alternates periods in which a 40 A current is circulated inside the copper target with periods without current, referred as background.

3 Activities in 2006

3.1 First VIP results

Previous to the installation in the Gran Sasso laboratory, the VIP setup was prepared and tested in the LNF-INFN laboratory, where measurements were performed in the period 21 November - 13 December 2005. Two types of measurements were done: 14510 minutes (about 10 days) of measurements with a 40 A current circulating in the copper target and 14510 minutes of measurements without current, where CCDs were read-out every 10 minutes.

The data were analyzed in 2006. The subtracted spectrum (namely the one with current minus the one withour current) is shown in Figure 1 a) (whole energy scale) and b) (a zoom on the region of interest). Notice that the subtracted spectrum is normalized to zero within statistical error, and is structureless.

The obtained value for the probability of PEP violation is:

$$\frac{\beta^2}{2} < 4.5 \times 10^{-28} \qquad at \quad 99.7\% \quad CL. \tag{1}$$

We have thus improved the limit obtained by Ramberg and Snow by a factor about 40.

The result was published in Phys. Lett. B641 (2006) 18.

3.2 VIP at LNGS

In February 2006 the VIP setup was transferred to the LNGS underground laboratory. The setup was installed and checked and a period of DAQ without shielding followed, until April 2006, in order to check the setup behaviour in LNGS conditions previous to the compact shielding mounting. A limit on PEP violation already better than the published one was obtained (see VIP Note-IR-06, October 2006).

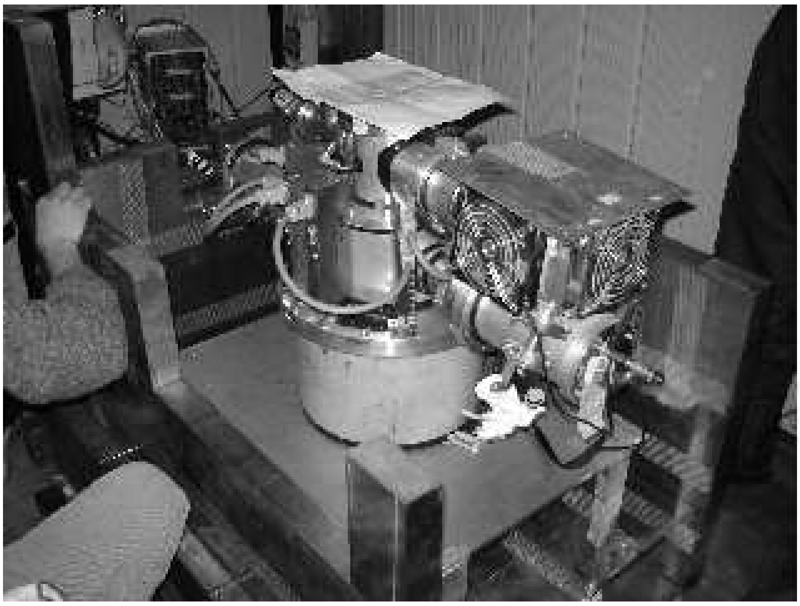

Figure 2: *Installation of the VIP setup in Gran Sasso underground laboratory.*

In April 2006 the shielding consisting in lead and copper layers completely surrounding the VIP setup was installed. In fig. 2 a picture taken during the installation phase is shown

Since April 2006 the setup is in DAQ with its final shielding configuration, alternating periods of DAQ with I=40 A current circulating in the copper target of the setup with periods of DAQ with I=0 A. Data quality check and analyses are ongoing.

4 Activities in 2007

In 2007 the VIP setup will continue the data taking at LNGS, aleternating periods of DAQ with current with periods of DAQ without current. Periodical energy calibrations, using an X-ray tube which activates foils of Ti and Zr placed inside the setup, will be performed.

The data analyses will go on in parallel with the DAQ.

The aim is to reach a limit on PEP violation by the end of 2007 in the limit of 10^{-29} - 10^{-30}.

5 Publications 2006

5.1 List of Conference Talks given by LNF Authors in Year 2006

1. L. Sperandio, "The VIP experiment", talk at "QUANTUM 2006: III WORKSHOP AD MEMORIAM OF CARLO NOVERO" Advances in Foundations of Quantun Mechanics and Quantum Information with atoms and photons, 2-5 May 2006 - Turin, Italy.
2. L. Sperandio, "Pauli Exclusion Principle: a search for possible violation", talk at the XI LNF Spring School in Nuclear, Subnuclear and Astroparticle Physics, INFN National Laboratories in Frascati, Italy, 15-19 of May, 2006.
3. D. Pietreanu, "Experimental search for a violation of the Pauli Exclusion Principle for electron: the VIP experiment", talk at The Foundations of Probability and Physics - 4, June 4 - 9, 2006, Vaxjo Univ., Sweden.

4. C. Curceanu, “New experimental limit on Pauli Exclusion Principle violation by electrons (VIP experiment at Gran Sasso)”, talk at the Third International Workshop DICE2006 , Castello di Piombino (Tuscany), September 11-15, 2006 Quantum Mechanics between Decoherence and Determinism: new aspects from particle physics to cosmology.

5. L. Sperandio, “Primi risultati dell’esperimento VIP - VIolazione del principio di Pauli per elettroni”, talk at XCII Congresso Nazionale SIF, Torino, 18-23 September 2006.

6. D. Pietreanu, “New experimental limit on the Pauli Exclusion Principle violation by electrons”, talk at the Conference Quantum Mechanics from fundamental problems to applications, Bertinoro, December 4-7 2006 (Italy).

5.2 Papers and Proceedings

1. S. Bartalucci *et al.*, “New experimental limit on the Pauli exclusion principle violation by electrons”, Phys. Lett. B641 (2006) 18-22.

2. S. Bartalucci *et al.*, “The VIP experiment”, Proceedings of ”QUANTUM 2006: III WORKSHOP AD MEMORIAM OF CARLO NOVERO” Advances in Foundations of Quantun Mechanics and Quantum Information with atoms and photons, 2-5 May 2006 - Turin, Italy, to appear in the International Journal of Quantum Information.

3. S. Bartalucci *et al.*,“VIP: an experiment to search for a violation of the Pauli Exclusion Principle”, Proceddings of the 9th International Workshop on Meson Production, Properties and Interaction KRAKW, POLAND, 9 - 13 June 2006, to appear in Int. Journ. Mod. Phys. A, and http://arxiv.org/abs/quant-ph/0608088.

4. S. Bartalucci *et al.*, “New experimental limit on Pauli Exclusion Principle violation by electrons (VIP experiment at Gran Sasso)”, Proceedings of Third International Workshop DICE2006 , Castello di Piombino (Tuscany), September 11-15, 2006 Quantum Mechanics between Decoherence and Determinism: new aspects from particle physics to cosmology, will be published by Institute of Physics (London) as a volume of Journal of Physics: Conference Series and http://arxiv.org/abs/quant-ph/0612116.

5. S. Bartalucci *et al.*, “Experimental search for a violation of the Pauli Exclusion Principle for electron: the VIP experiment”, in Proceedings of the Foundations of Probability and Physics - 4, June 4 - 9, 2006, Vaxjo Univ., Sweden.

5.3 Technical Notes

1. C. Curceanu, D. Sirghi, L. Sperandio for the VIP collaboration and A. Salvucci from Univ. Tor Vergata, VIP setup at LNGS without shielding: data analysis and results, VIP Note-IR-06, October 2006.

FA-51: FISICA ASTROPARTICELLARE

E. Nardi (Resp.)

1 Description of the 2006 activity

The main research activities of the project during the year 2006 focused on the study of the mechanism of leptogenesis as a way to generate the observed Cosmic baryon asymmetry. Two important new features have been explored, that implied relevant changes to the standard picture of leptogenesis: 1) the effects of lepton flavors, and 2) the possible effects of the two heavier seesaw Majorana neutrinos $N_{2,3}$.

Flavor effects in Leptogenesis. The effects of lepton flavors dynamics have been generally neglected in leptogenesis studies. These effects were thoroughly analyzed in ref. [1], where important quantitative and qualitative differences with respect to the case in which flavor effects are ignored were found:

i) The Cosmic baryon asymmetry can be enhanced by up to one order of magnitude;
ii) The sign of the asymmetry can be opposite to what one would predict from the sign of the total lepton asymmetry;
iii) Successful leptogenesis is possible even when the total asymmetry parameter ϵ_1 is vanishing.

From the practical point of view, the relevance of flavor effects is at least twofold:

1. The baryon asymmetry of the Universe resulting from leptogenesis can be several times larger than what would be obtained neglecting flavor effects.

2. If leptogenesis occurs in the temperature range when flavor effects are important ($T \lesssim 10^{12}\,\mathrm{GeV}$), the limit on the light neutrino masses ($m_\nu \lesssim 0.15\,\mathrm{eV}$), that was thought to be a firm prediction of successful leptogenesis, does not hold anymore.

Effects of the heavier seesaw Majorana neutrinos. In leptogenesis studies it was generally assumed that the lepton asymmetries generated in the decays of the heavier neutrinos $N_{2,3}$ are irrelevant for the computation of the final baryon asymmetry, since they would be washed out during N_1 leptogenesis by the fast N_1-related lepton number violating processes. A detailed study of the fate of a lepton asymmetry preexisting the N_1 leptogenesis era was carried out in ref. [2]. It was found that, differently from common belief, decoherence effects induced by N_1 interactions, end up projecting part of the asymmetry from $N_{2,3}$ decays onto a direction in flavor space that is protected from being washed out. Therefore, part of any preexisting asymmetry does in general survive, and must be taken into account when computing the baryon asymmetry of the Universe.

In practice, the importance of $N_{2,3}$ effects is that the standard analyses based just on considerations of N_1 related effects might incorrectly indicate that for a specific set of parameters, leptogenesis is not successful in explaining the observed baryon asymmetry. This conclusion can in fact be evaded, and after including the contribution from $N_{2,3}$ decays one might still yield the correct result.

A short review of the new results regarding flavor and $N_{2,3}$ effects in leptogenesis was recently presented in ref. [3].

References

1. Enrico Nardi, Yosef Nir, Esteban Roulet and Juan Racker,
   "The importance of flavor in leptogenesis",
   JHEP **0601**, (2006) 164; [arXiv:hep-ph/0601084].

2. G. Engelhard, Y. Grossman, E. Nardi and Y. Nir,
   "On the importance of the heavier Majorana neutrinos in leptogenesis," arXiv:hep-ph/0612187
   (Submitted to *Phys. Rev. Lett.*).

3. E. Nardi, "Topics in leptogenesis," arXiv:hep-ph/0702033.

4. Enrico Nardi, Yosef Nir, Juan Racker and Esteban Roulet,
   "On Higgs and sphaleron effects during the leptogenesis era",
   JHEP **0601**, (2006) 068; [arXiv:hep-ph/0512052].

Talks at Conferences during 2006

1. *"Flavour in Leptogenesis"*,
   Talk given at the XI Summer Institute of the Laboratori Nazionali del Gran Sasso, *"From phenomenology to Cosmology" – Sasha Dolgov Fest"*, Assergi (AQ), July 18-21, 2006.

2. *"Topics in Leptogenesis"*,
   Talk given at the *VI Simposio Latino Americano de Física de Altas Energias* (VI-Silafae), Puerto Vallarta - México October 31 - November 8, 2006.

3. *"Flavour in Leptogenesis"*,
   Talk given at the *International Workshop High Energy Physics in the LHC era*, Valparaiso – Chile, December 11 - 15, 2006.

LF-21: PHENOMENOLOGY OF ELEMENTARY PARTICLE INTERACTIONS AT COLLIDERS

G. Isidori (Resp.), G. Pancheri (Resp. Naz.),
F. Mescia (Art. 23), S. Pacetti (Ass. Ric), O. Shekhovstova (Bors. PD),
D. Temes (Ass. Ric.).

1 Summary of the project

The research topics investigated by this project can be divided into two main areas:

- Flavour physics.
- Hadronic form factors and total hadronic cross-sections.

The first area, discussed in Section 2, concerns the possibility to perform new low-energy precision tests about the mechanism of quark- and lepton-flavor mixing. The second area, discussed in Section 3, include precision studies of hadronic processes relevant to electron-positron colliders at low energy, as well as hadronic and photonic total cross-sections at high energies.

2 Flavour Physics

One of the strategies to obtain additional clues about the nature of New Physics (NP) is by means of precision tests of the Standard Model (SM) at low energies. These are particularly interesting in processes which are not mediated by tree-level SM amplitudes, such as flavour-changing neutral current (FCNC) transitions, both in the quark and in the lepton sector. Up to now there is no evidence for deviations from the SM in such rare processes, and this leads to the so-called *flavour problem*: if we insist with the theoretical prejudice that NP has to emerge in the TeV region, we have to conclude that the new theory possesses a highly non-generic flavour structure. Interestingly enough, this structure has not been clearly identified yet, mainly because the SM, *i.e.* the low-energy limit of the new theory, doesn't possess an exact flavour symmetry. The attempt to clarify this structure, both at the phenomenological level (with the help of precision data on rare decays) and at a more fundamental level (with the help of new symmetry principles), is one of the main activity of our group. [1)]

A closely related subject –which is also one of the primary research objectives of our group– is a better understanding of the SM itself, fixing his fundamental couplings (quark masses, CKM angles, non-perturbative condensates, . . .) by means of precise calculations within the framework of effective field theories and Lattice QCD.

Within this general scenario, last year we have performed a series of works on:

Grand Unification and Leptogenesis in models with MFV.

Minimal Flavor Violation (MFV) is an attractive approach to solve the flavour problem assuming that the Yukawa couplings are the only irreducible sources of flavour symmetry breaking also beyond the SM. We have shown how this hypothesis can be implemented in

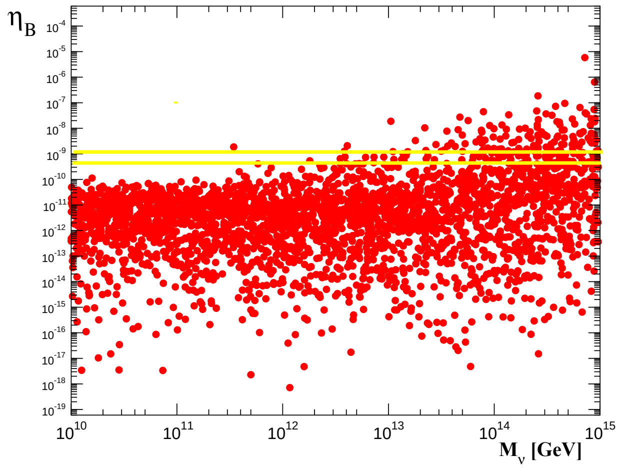

Figure 1: Baryon asymmetry (η_B) as a function of the right-handed neutrino mass scale (M_ν) in the MFV framework with right-handed neutrinos. 3) the yellow lines denote the experimental value.

Grand Unified theories. 2) We have also investigated the viability of leptogenesis in models respecting the MFV hypothesis in the lepton sector (i.e. models with three heavy right-handed neutrinos, where the charged-lepton and the neutrino Yukawa couplings are the only irreducible sources of lepton-flavour symmetry breaking). 3). We have shown that in this framework a specific type of resonant leptogenesis can generate the observed matter-antimatter asymmetry. For natural values of the free parameters, this mechanism requires a high right-handed neutrino mass scale ($M_\nu \gtrsim 10^{12}$ GeV). As a result of the high value of the scale of total lepton-number violation, in this class of models the $\mu \to e\gamma$ decay is expected to be close to the present exclusion limit.

B decays.

Motivated by the first evidence of the $B \to \tau\nu$ transition reported by Belle and by the precise ΔM_{B_s} measurement by CDF, we have analysed these and other low-energy observables in the framework of the MSSM at large $\tan\beta$. 4) We have shown that for heavy squarks and A terms ($M_{\rm squarks},\ A_U > 1$ TeV) such scenario has several interesting virtues. It naturally describes: i) a suppression of $\mathcal{B}(B \to \tau\nu)$ of $(10-40)\%$, ii) a sizable enhancement of $(g-2)_\mu$, iii) a heavy SM-like Higgs ($m_h \sim 120$ GeV), iv) small non-standard effects in ΔM_{B_s} and $\mathcal{B}(B \to X_s\gamma)$ (in agreement with present observations). The possibilities to find more convincing evidences of such scenario, with improved data on $\mathcal{B}(B \to \tau\nu)$, $\mathcal{B}(B \to \ell^+\ell^-)$, and other low-energy observables, have been analysed.

Kaon physics.

In collaboration with the KLOE experiement, we have performed improved determination of the CP and CPT violation parameters $\Re(\epsilon)$ and $\Im(\delta)$ based on the unitarity condition (Bell-Steinberger relation) and on recent results from the KLOE experiment. We find $\Re(\epsilon) = (159.6 \pm 1.3) \times 10^{-5}$ and $\Im(\delta) = (0.4 \pm 2.1) \times 10^{-5}$, consistent with no CPT violation. [5]

In view of future experiments on rare K decays, we have analysed the expecations for the two $K \to \pi\nu\bar{\nu}$ modes [6] and of the two $K_L \to \pi^0\ell^+\ell^-$ modes [7] in the MSSM and other extensions of the SM. We have shown that the information which can be extracted from precise measurements of theses rare decays turn out to be very useful in restricting the parameter space of new-physics models, even after taking into account the possible information on the new-physics mass spectrum derived from high-energy colliders, and the constraints from B-physics experiments.

Lattice QCD.

The recent B-factory activities has drawn a new deal of interest on the radiative $b \to s$ transitions. Whereas the inclusive mode $B \to X_s\gamma$ is theoretically clean but difficult to access from the experimental side, the exclusive modes are easily detectable and share the same short-distance information. On the other hand, hadronic uncertainties can dilute this type of potentiality. In the case of $B \to K * \gamma$ we have calculated the QCD relevant form factors on the lattice. [8] This allows us to extract from the corresponding branching ratios an information on the $V_{ts}^*V_{ts}$ CKM coupling.

To estimate hadronic uncertainties, lattice QCD is the only tool based on first principles. At the moment, limitations are due to the lightest quark mass that we can simulate. By using standard formulations of the lattice QCD action, we cannot simulate pions with mass below ~ 500 MeV. On the other hand, preliminary studies show that pion masses as light as 275 MeV could be accessible using the so-called twisted-fermion formulation. [9]

3 Hadronic form factors and total hadronic cross-sections

Our research interests in this area can be divided into two main categories. On the one hand, there is an intense activity to improve the theoretical predictions for low-energy processes of interest to DAΦNE, [10, 11] and to investigate its physics potential in view of possible detector/machine upgrades. [12, 13, 14] On the other hand, there is long-standing activity on the study of total pp, $p\bar{p}$ and $\gamma\gamma$ cross setions, [15, 16] which will become phenomenologically very relevant in the near future with the start of the LHC program. [17, 18]

Within this general scenario, the high-lights of the 2006 analyses can be summarised as follows:

Studies of $\sigma(e^+e^- \to \pi^+\pi^-\gamma)$ close to the Φ peak.

Effects due to non-pointlike behaviour of pions in the process $e^+e^- \to \pi^+\pi^-\gamma$ can arise for hard photons in the final state. By means of a Monte Carlo event generator, which also includes the contribution of the direct decay $\phi \to \pi^+\pi^-\gamma$, we have estimated these effects in the framework of Resonance Perturbation Theory. [10] Applying the angular cuts used in the KLOE analysis of the pion form factor at threshold, we have proposed a method to reveal the effects of non-pointlike behaviour of pions in a model-independent way.

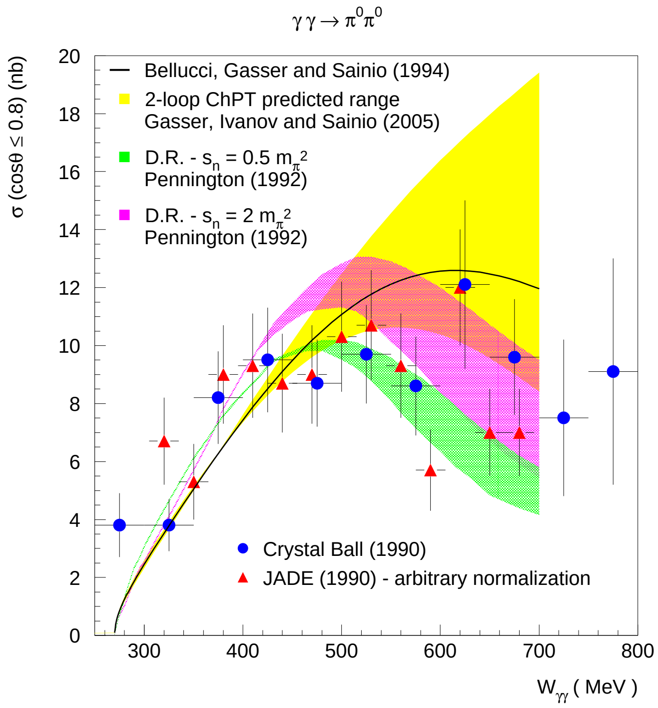

Figure 2: Present theoretical and experimental uncertainty in the $\gamma\gamma \rightarrow \pi^0\pi^0$ reaction, explored in view of proposed precision studies at DAΦNE [12] (plot made by Danilo Babusci).

A general parametrization of the $e^+e^- \rightarrow \gamma^* \rightarrow P_1P_2\gamma$ process, where the two pseudoscalar mesons are in a $J^{CP} = 0^{++}$ state, has been proposed. [11] Such a parameterization should help to shed light on the nature of light scalar mesons, indeed it allows to describe in terms of the same couplings different processes where the scalar mesons are involved.

Nucleon form factors.

Starting from the recent data on the ratio R between electric and magnetic proton form factors, collected by TJNAF and BaBar in the space- and time-like region respectively, we have defined a dispersive procedure to reconstruct the complex structure of this ratio. [14] The obtained analytic expression is in agreement with a space-like zero around $q^2 \sim -10\,GeV^2$ and it provides the asymptotic scaling $R \rightarrow \pm 1$ as $q^2 \rightarrow \pm\infty$.

Total hadronic cross-sections in QCD.

The energy behavior of total proton and photon cross-sections is the focus of this line of research and its description through QCD is the ultimate goal of this project. QCD indeed provides various mechanisms to explain the energy dependence, although quantitatively rigorous studies are yet to come. The goal would be to obtain a QCD description of the initial decrease and the final increase of total cross-sections through soft gluon summation and QCD calculable jet x-sections, also known as mini-jets in this context. The resulting physical picture includes multiple parton collisions, whose number increases with energy, and soft gluon emission dressing each collision, with a reducing effect.

In the Eikonal Minijet Model (EMM) the rise can be obtained using the QCD calculable contribution from the parton-parton cross-section, whose total yield increases with energy. For a unitary description, the jet cross-sections are embedded into the eikonal formalism, where the eikonal function contains both the energy and the impact parameter distribution in b-space. The simplest formulation, with minijets to drive the rise and hadronic form factors for the impact parameter distribution, can be applied to all the available x-sections. One finds that, with a single set of parameters, the simple eikonalized mini-jet model cannot describe both the early rise, which in proton-antiproton scattering takes place around $10 \div 50\ GeV$, and the Tevatron data.

A possible way to decrease the uncertainty in the predictions is to refine the QCD analysis, through resummation of soft gluon emission from the initial state partons, a feature absent from most simple EMM.

During a number of years, a model for the impact parameter space distribution of parton in the hadrons has been developed and applied to the proton and photon cross-sections in order to obtain a better description of total cross-section. The physical picture underlying this model is that the fast rise due to mini-jets and the increasing number of gluon-gluon collisions as the energy increases, can be reduced if one takes into account that soft gluons, emitted mostly by the initial state valence quarks, determine an acollinearity between the partons which reduces the overall parton-parton luminosity. This model, which can describe very well all available data for proton collisions, has been used to obtain a series of predictions for future high-energy colliders. [15, 16, 17, 18)]

4 Work Program for the year 2007

Most of the activity previously described will be continued into the year 2007.

References

1. G. Isidori, *Shedding light on flavour symmetries with rare decays of quarks and leptons,* in *Proceedings of the 4th Flavor Physics and CP Violation Conference (FPCP 2006)* (Vancouver, British Columbia, Canada, 9-12 Apr 2006), hep-ph/0702181.

2. B. Grinstein, V. Cirigliano, G. Isidori and M. B. Wise, *Grand unification and the principle of minimal flavor violation,* Nucl. Phys. B **763** (2007) 35 [hep-ph/0608123].

3. V. Cirigliano, G. Isidori and V. Porretti, *CP violation and leptogenesis in models with minimal lepton flavour violation,* Nucl. Phys. B **763** (2007) 228 [hep-ph/0607068].

4. G. Isidori and P. Paradisi, *Hints of large* $\tan\beta$ *in flavour physics,* Phys. Lett. B **639** (2006) 499 [hep-ph/0605012]; Nucl. Phys. Proc. Suppl. **163** (2007) 192.

5. F. Ambrosino *et al.* [KLOE Collaboration], G. D'Ambrosio and G. Isidori, *Determination of CP and CPT violation parameters in the neutral kaon system using the Bell-Steinberger relation and data from the KLOE experiment,* JHEP **0612** (2006) 011 [hep-ex/0610034].

6. G. Isidori, F. Mescia, P. Paradisi, C. Smith and S. Trine, *Exploring the flavour structure of the MSSM with rare K decays,* JHEP **0608** (2006) 064 [hep-ph/0604074].

7. F. Mescia, C. Smith and S. Trine, *$K_L \to \pi^0 e^+ e^-$ and $K_L \to \pi^0 \mu^+ \mu^-$: A binary star on the stage of flavor physics,* JHEP **0608** (2006) 088 [hep-ph/0606081].

8. D. Becirevic, V. Lubicz and F. Mescia, *An estimate of the $B \to K^* \gamma$ form factor,* hep-ph/0611295.

9. D. Becirevic, Ph. Boucaud, V. Lubicz, G. Martinelli, F. Mescia, S. Simula and C. Tarantino, *Exploring twisted mass lattice QCD with the clover term,* Phys. Rev. D **74** (2006) 034501 [hep-lat/0605006].

10. G. Pancheri, O. Shekhovtsova and G. Venanzoni, *Test of FSR in the process $e^+e^- \to \pi^+\pi^-\gamma$ at DAFNE and extraction of the pion form factor at threshold,* Phys. Lett. B **642** (2006) 342 [hep-ph/0605244].

11. G. Isidori, L. Maiani, M. Nicolaci and S. Pacetti, *The $e^+e^- \to P_1 P_2 \gamma$ processes close to the Φ peak: toward a model-independent analysis,* JHEP **0605** (2006) 049 [hep-ph/0603241]; S. Pacetti, Nucl. Phys. Proc. Suppl. **162** (2006) 172.

12. F. Ambrosino *et al.*, *Prospects for e^+e^- physics at Frascati between the Φ and the Ψ,* hep-ex/0603056.

13. P. M. Gensini, G. Pancheri, Y. N. Srivastava and G. Violini, *Low-energy kaon nucleus interactions at a Phi-factory,* presented at Meeting on e+ e- Physics Perspectives (non-K Physics), Frascati, Italy, 19-20 Jan 2006, nucl-th/0603043.

14. R. Baldini, C. Bini, P. Gauzzi, M. Mirazita, M. Negrini and S. Pacetti, *A Description Of The Ratio Between Electric And Magnetic Proton Form Factors By Using Space-Like, Time-Like Data And Dispersion Relations,* Nucl. Phys. Proc. Suppl. **162** (2006) 46.

15. R. M. Godbole, A. Grau, R. Hegde, G. Pancheri and Y. Srivastava, *Theoretical expectations for total cross-sections at the large hadron collider,* Pramana **66** (2006) 657 [hep-ph/0604214].

16. R. M. Godbole, A. Grau, G. Pancheri and Y. N. Srivastava, *Total cross sections and soft gluon resummation,* Acta Phys. Polon. B **37** (2006) 1093 [hep-ph/0604211].

17. G. Pancheri, *Photon 2005: Photons in a special year,* Acta Phys. Polon. B **37** (2006) 983.

18. C. Buttar *et al.*, *Les Houches physics at TeV colliders 2005, standard model, QCD, EW, and Higgs working group: Summary report,* hep-ph/0604120.

LF-61: SYNCHROTRON RADIATION SPECTROSCOPIES AND THE PHYSICS OF STRONGLY CORRELATED ELECTRON SYSTEMS

M. Benfatto, S. Di Matteo (Art. 23), R. Gunnella (Ass.), Y. Joly (Visit.), K. Hatada (Ass), K. Hayakawa (Ass), C.R. Natoli (Resp.), N. Perkins (Visit.), D. Sebilleau (Visit.), A. Tenore, Wu Ziyu (Visit.)

1 The Project

The aim of this project is the theoretical analysis of strongly correlated electron systems, in the light of their fundamental as well as technological interest. When appropriate, methods borrowed from field theory and statistical mechanics are used to bear on the description of the essential physics of such systems. At the same time in-depth theoretical studies of significant synchrotron radiation spectroscopies (like absorption, dichroism, elastic and inelastic resonant x-ray scattering, etc..) that can shed light on charge and magnetic correlations in such systems are carried out.

2 Physics of strongly correlated electron systems

In 2006, research in this field has developed along the following main directions:

- Analysis of synchrotron radiation (SR) experiments (resonant x-ray scattering, absorption and dichroism) in V_2O_3, $LaMnO_3$, actinides (NpO_2),$KCuF_3$, $GaFeO_3$, K_2CrO_4 and $CeFe_2$.
- Classification of the electromagnetic multipoles in matter, with an eye to chiral systems and the identification of the polar toroidal moment in magnetic systems.
- Multichannel Multiple Scattering Theory.
- Full Potential Multiple scattering Scheme.
- Fitting of XANES spectra by a full multiple scattering procedure

2.1 Analysis of synchrotron radiation (SR) experiments (resonant x-ray scattering, absorption and dichroism) in V_2O_3, $LaMnO_3$, actinides (NpO_2),$KCuF_3$, $GaFeO_3$, K_2CrO_4 and $CeFe_2$.

We have extended the tensor analysis derived for circular and linear dichroism in photoemission and photoabsorption to Bragg-forbidden reflections in anomalous diffraction. In this respect we have derived a unitary cluster approach to the calculation of several electron spectroscopies, ranging from core and valence level photoelectron diffraction and absorption to electron, Auger and anomalous diffraction. Electron energy loss and Auger-photoelectron coincidence spectroscopies could also be treated in the same frame [1]. A new European project in the framework of coordinated actions in research infrastructures, called LightNet, has been approved with the goal of interpreting and analyzing SR spectroscopies in strongly correlated systems. The extension to condensed matter of the angular correlation between Auger electron and photoelectron has been dealt with in Ref. [2], where an exact analytical expression has been derived to describe the angular distribution of the two electrons. Several studies on resonant x-ray scattering in antiferromagnetic transition-metal systems (KCuF3) and rare-earth compounds (CeFe2) have been carried out in order to measure their magnetic phase diagram. Finally, a complete polarization analysis has been made to fully describe resonant x-ray scattering experiments. We have in fact shown that incident linearly polarized x-rays can be converted into circularly polarizaed x-rays by diffraction at Cr pre K-edge in K2CrO4. The physical mechanism behind this phenomenon is a subtle interference effect between purely dipole (E1-E1) and purely quadrupole (E2-E2) transitions, leading to a phase shift between the respective scattering amplitudes [3]. We have illustrated how this effect can be exploited to disentangle two close-lying resonances that appear as a single peak in a conventional energy scan. This technique is supposed to open new potentialities for resonant x-ray diffraction as a tool to identify the different multipole order parameters involved in several exotic phase transitions.

2.2 Classification of the electromagnetic multipoles in matter, chiral systems and the identification of the polar toroidal moment in magnetic systems

This second line of research is concerned with the analysis of the polar (magnetic) and axial (non-magnetic) toroidal multipoles of a system by means of x-ray dichroism and resonant scattering. In this field a lot has been done, especially in russian literature, but there has been little investigation in connection with the detection of toroidal moments by means of x-ray resonant scattering (RXS). For this reasons, a general discussion of (magnetic and non-magnetic) toroidal multipolar expansion in condensed matter systems is needed in the community, with the aim of applying it to the theory of RXS. The idea turned out to be fruitful, and the main results of such a work regard the possibility to detect the toroidal moment and its multipoles in centrosymmetric magnetic systems by means of RXS and to separate in a similar way all the parity and time-reversal odd multipolar components. In Ref. [4] we have demonstrated that it is possible to detect the magnetic (polar) toroidal moment by means of a peculiar linear dichroism, as well as with an interference technique in resonant x-ray scattering. Based on both analitical and numerical results, we have illustrated potentialities and drawbacks of the two techniques.

2.3 Multichannel Multiple Scattering Theory

We have continued the implementation of the Multichannel multiple scattering theory into a computer code for the interpretation of various SR spectroscopies in strongly correlated systems. We have studied the problem of the branching ratio of the L_3 and L_2 edges of transition metals oxides (NiO, CuO) with an almost full 3d band. For these compounds the implementation of the Pauli principle is essential in order to obtain the correct branching ratio, which becomes again statistical for the transition metal elements at the end of the series. The study has met with success and preliminary results have been presented at the International Workshop on X-ray absorption spectroscopy and theory of XAS (February 28- March 1, 2007, Paul Scherrer Institut, Villigen, Switzerland). It is important to realize that this work represents the first successful attempt to incorporate into an independent particle description of various x-ray spectroscopies (band structure or delocalized approach) local correlation effects as given by the theory of atomic multiplets. Fig. 1 shows the calculated NiO L_3 L_2 absorption edges where the branching ratio is back to its statistical value due to the Pauli principle. The corresponding magnetic circular dichroism is also shown. The agreement with the experimental data is very good.

2.4 Full Potential Multiple Scattering Scheme

We have succeeded in developing A Full Potential Multiple Scattering (FP-MS) scheme for the interpretation of several X-ray spectroscopies that is a straightforward generalization of the more conventional Muffin-Tin (MT) version. Like this, it preserves the intuitive description of the physical process under consideration and overcomes some of the limitations of the existing FP-MS codes. The scheme hinges on a fast and efficient method for solving the single cell scattering problem that avoids the convergence drawbacks of the angular momentum expansion of the cell

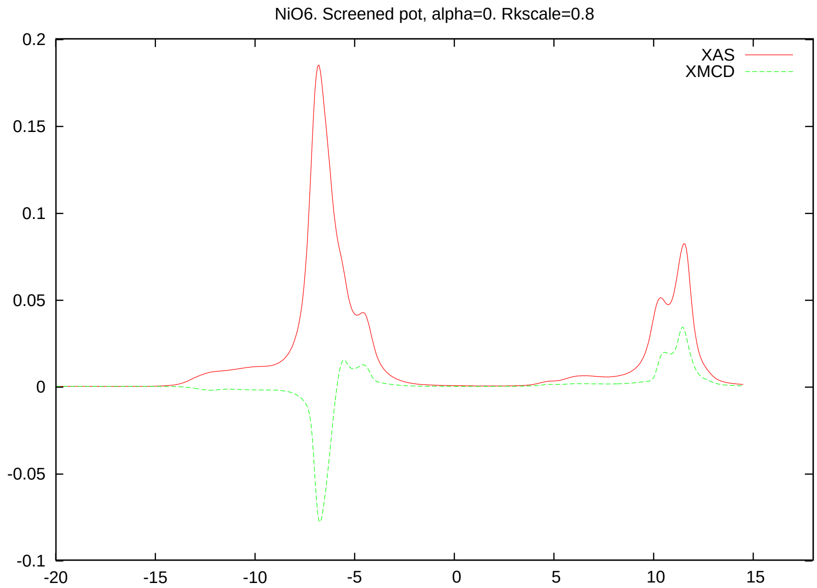

Figure 1: Calculated NiO L_3 L_2 Absorption edges. The branching ratio is back to its statistical value due to the Pauli principle. Also shown is the corresponding magnetic circular dichroism.

shape functions and relies on an alternative derivation of the multiple scattering equations (MSE) that allows us to work reliably with only one truncation parameter, i.e. the number of local basis functions in the expansion of the global scattering function, determined by the classical relation $l_{\rm max} = kR$. Tests of the method against solvable analytic models have met with remarkable success. This achievemnt eliminates the main drawback of the MT method, namely the geometrical approximation of the solid state potential, and opens the way to a better determination of the structural and electronic parameters which underly an absorption spectrum. The paper has been submitted for publication to Physical Review Letter and preliminary results have been presented at the XAS07 workshop mentioned above.

Fig. 2 shows an application of the method to the calculation of the Ge K-edge absorption spectrum of the tetrahedral molecule $GeCl_4$ [5]. The MT approximation could never reproduce the first bump after the main transition. Its appearance is due to the introduction of the anisotropy of the potential inside the atoms and the presence of four empty Voronoi cells completing the BCC unit cell. An $l_{\rm max} = 4$ was sufficient to reach convergence of the spectrum. Higher l values up to $l_{\rm max} = 8$ or the extension of the nine cell cluster with the addition of up to 34 empty cells centered at the BCC lattice sites did not substantially modify the spectrum.

2.5 Fitting of XANES spectra by a full multiple scattering procedure

The research in this field has been devoted to both the development of the MXAN code, already described in the previous reports, and its application to significant problems in collaboration with several groups. The method has been modified to analyze disordered systems and time depended XANES data. The analysis of disordered system is based on the calculation of structural averaged photo-absorption cross section. This is performed by calculating many theoretical XANES spectra from distinct molecular dynamics snapshot, each of them generating a XANES spectrum

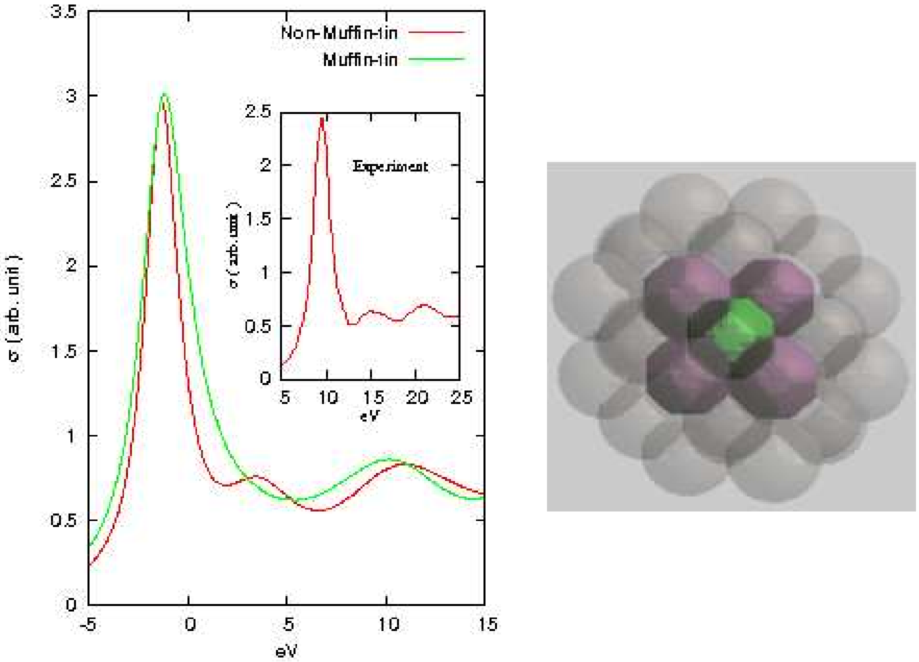

Figure 2: Cross section for $GeCl_4$ molecule with nine scattering cells located at the sites of a BCC lattice, compared with the MT result and experiment.

associated to the corresponding instantaneous geometry. The final theoretical spectrum is obtained by summing all the spectra and dividing by the total number of used molecular dynamics snapshot. The analysis of the time depended XANES data is based on the use of the difference spectrum. We have modified the MXAN code to use as the input experimental data the difference between the excited and the ground states XANES data. In other words the system under study is excited by some external probe to some new state with a defined life-time, and we analyze directly the difference between the experimental data of this state and the ones of the ground state.

3 List of Conference Talks by LNF Authors in Year 2006

1. M. Benfatto, Invited talk: Recent Theoretical Advances in the XAS Structural Analysis: Prospective for Time-Resolved Experiments at XFEL, Pump and Probe Workshop Copenhagen, January 20-21, 2006.
2. M. Benfatto, Invited talk Advances in the quantitative structural analysis of XAS data at International Conference on Porphyrins and Phthalocyanines July 2-7, 2006 Rome.
3. M. Benfatto, Invited talk Advances in the theoretical calculation of the XANES energy region: new prospective for a quantitative structural use at The 13th International Conference on X-ray Absorption Fine Structure, XAFS 13 July 9-14, 2006 Stanford (USA).
4. K. Hatada, K. Hayakawa, M. Benfatto, C.R. Natoli, Full Potential Multiple Scattering for X-ray Spectroscopies at The 13th International Conference on X-ray Absorption Fine Structure, XAFS 13 July 9-14, 2006 Stanford (USA).

References

1. D. Sebilleau, R. Gunnella, Z.-Y. Wu, S. Di Matteo, and C.R. Natoli, "Multiple Scattering approach with complex potential in the interpretation of electron and photon spectroscopies" (Topical Review), J. Phys.: Condens. Matter **18**, R175 to R230 (2006).

2. F. Da Pieve, S. Di Matteo, D. Sebilleau, R. Gunnella, G. Stefani and C.R. Natoli, "Angular correlations between photo-electron and Auger electron within scattering theory" Accepted for publication in Phys. Rev. A.

3. C. Mazzoli, S. Di Matteo, S. Wilkins, et al., accepted for publication in Phys. Rev. Lett.

4. S. Di Matteo, and Y. Joly, "Parity and time-reversal breaking effects detected by resonant x-ray scattering.", Physical Review B **74**, 014403-1/8 (2006).

5. A. Filipponi and P. D'Angelo, "Accurate determination of molecular structure by absorption spectroscopy" J. Chem. Phys., 109, 5356-5362 (1998).

6. Guo XY, Chu WS, Ma SX, *et al.* "Structural reconstruction of the catalytic center of LiPDF through multiple scattering calculation with MXAN" Radiation Physics and Chemistry **75**, 1617-1621 (2006).

7. Benfatto M, Della Longa S, Hatada K, *et al.* "A full multiple scattering model for the analysis of time-resolved X-ray difference absorption spectra" Journal of Physical Chemistry B **110**, 14035-14039 (2006).

8. Monesi C, Meneghini C, Bardelli F, *et al.* "Quantitative structural refinement of Mn K edge XANES in LaMnO3 and CaMnO3 perovskites" Nuclear Instruments & Methods **246**, 158-164 (2006).

9. D'Angelo P, Roscioni OM, Chillemi G, *et al.* "Detection of second hydration shells in ionic solutions by XANES: Computed spectra for Ni2+ in water based on molecular dynamics" Journal of the American Chemical Society **128**, 1853-1858 (2006).

10. Sarangi R, Benfatto M, Hayakawa K, *et al.* "MXAN analysis of the XANES energy region of a mononuclear copper complex: Applications to bioinorganic systems" Inorganic Chemistry **44** 9652-9659 (2006).

LF-61: LOW-DIMENSIONAL SYSTEMS AND SPIN-HALL EFFECT

S. Bellucci (Resp. Naz.), M. Cini (Ass.), F. Corrente (Dott.),
P. Onorato (Borsista PD), E. Perfetto (Borsista PD), R. Raimondi (Ass.)

1 External collaborating Institutions:

Univ. Roma La Sapienza, Univ. Roma Tor Vergata, IHEP-Protvino (Russia), Univ. Pune, India, Burnham Institute (La Jolla, CA, USA), ILL (Grenoble, France).

2 Research Activity

We investigated the ballistic electron transport in a two-dimensional quantum wire under the action of an electric field (E_y). We demonstrated how the presence of a spin-orbit coupling, due to the uniform electric confinement field gives a noncommutative effect as in the presence of a transverse magnetic field. We discussed how the noncommutation implies an edge localization of the currents depending on the electron spins also giving a semiclassical spin dependent Hall current. We also discussed how it is possible obtain a quantized Spin Hall conductance in the ballistic transport regime by developing the Landauer formalism and show the coupling between the spin magnetic momentum and the orbital one due to the presence of a circulating current.

We showed that a nanometric four-probe ballistic junction can be used to check the presence of a transverse spin Hall current in a system with a spin orbit coupling not of the Rashba type, but rather due to the in-plane electric field. Indeed, the spin Hall effect is due to the presence of an effective small transverse magnetic field corresponding to the spin orbit coupling generated by the confining potential. The strength of the field and the junction shape characterize the quenching Hall regime, usually studied by applying semiclassical approaches. We discussed how a quantum mechanical relativistic effect, such as the spin orbit one, can be observed in a low energy system and explained by using classical mechanics techniques

We developed a theoretical framework that applies to the intermediate regime between the Coulomb blockade and the Luttinger liquid behavior in multiwalled carbon nanotubes. Our main goal is to confront the experimental observations of transport properties, under conditions in which the thermal energy is comparable to the spacing between the single-particle levels. For this purpose we have devised a many-body approach to the one-dimensional electron system, incorporating the effects of a discrete spectrum. We showed that, in the crossover regime, the tunneling conductance follows a power-law behavior as a function of the temperature, with an exponent that oscillates with the gate voltage as observed in the experiments. Also in agreement with the experimental observations, a distinctive feature of our approach is the existence of an inflection point in the log-log plots of the conductance vs temperature, at gate voltages corresponding to peaks in the oscillation of the exponent. Moreover, we evaluate the effects of a transverse magnetic field on the transport properties of the multiwalled nanotubes. For fields of the order of 4 T , we find changes in the band structure that may be already significant for the outer shells, leading to an appreciable variation in the power-law behavior of the conductance. We then foresee the appearance of sizeable modulations in the exponent of the conductance for higher magnetic fields, as the different subbands are shifted towards the development of flat Landau levels.

3 List of Conference Talks by LNF Authors in Year 2006

1. S. Bellucci, Size dependent Superconductivity in Small Diameter Carbon Nanotubes, 13 Congresso Nazionale di Superconduttivita‘, Sestri Levante (Genova, Italy) 29 Marzo 2006.
2. P. Onorato, Crossover from Luttinger liquid to Coulomb Blockade regime in carbon nanotubes, 13 Congresso Nazionale di Superconduttivita‘, Sestri Levante (Genova, Italy) 29 Marzo 2006.
3. F. Corrente, Spin Hall Effect e Spin Filtering in nanogiunzioni in regime ballistico, XCII Congresso Nazionale Torino, Italy 18 - 23 Settembre 2006.
4. S. Bellucci, Electronic screening and correlated superconductivity in carbon nanotubes, STRIPES 2007 Univ. Roma La Sapienza Italy 21 December 2006.

References

1. S. Bellucci and P. Onorato PHYS. REV. B 74 (2006) 245314.
2. S. Bellucci, J. Gonza'lez, P. Onorato, and E. Perfetto PHYS. REV. B 74 (2006) 045427.
3. S. Bellucci and P. Onorato PHYS. REV. B 73 (2006) 045329.
4. S Bellucci, M Cini, P Onorato and E Perfetto J. PHYS. COND. MATT. 18 (2006) S2115.
5. Stefano Bellucci, Michele Cini, Pasquale Onorato and Enrico Perfetto J. PHYS. COND. MATT. 18 (2006) S2069.
6. S. Bellucci, P. Onorato ANN. PHYS. (N.Y.) 321 (2006) 934.
7. S. Bellucci and P. Onorato EUR. PHYS. J. B 52 (2006) 469.

MI-12: INIZIATIVA SPECIFICA

S. Bellucci (Resp.), S. Ferrara (Ass.),
E. Latini (Dott.), A. Marrani (Bors. PD), E. Orazi (Dott.)

1 Research Activity

Supersymmetric field theories, supergravity, attractor mechanism, black holes, superstrings and M-theory.

The group in Frascati focuses on supersymmetry breaking in string and M-theory compactification, relation of non-commutative supersymmetric theories with strings in different backgrounds, effective actions of bulk supergravity coupled to branes in the presence of fluxes, gauged supergravity, non-commutative superspaces and their occurrence in string theory.

We made important contributions to gauged supergravity and duality symmetry, supersymmetry algebras in diverse dimensions, super Higgs effect, supersymmetric theories in non-commutative superspaces, classification of operators in the AdS/CFT correspondence, supergravity interpretation of flux compactification, supersymmetric Born-Infeld actions.

On the side of attractors we are actively considering Charge Orbits of Symmetric Special Geometries and Attractors, as well as the Attractor Equations of N=2, d=4 supergravity in an extremal black hole background with arbitrary electric and magnetic fluxes (charges) for field-strength two-forms. We are studying the stability of non-BPS Attractor solutions corresponding to the vanishing determinant of the (fermionic) gaugino mass matrix. We are also intersted in possible consequences for the entropic functional.

The lines of future development for our group concern the following topics:

- AdS/CFT correspondence,
- Supersymmetric Yang-Mills theory and supergravity,
- Non-commutative supersymmetric field theories,
- Spontaneous supersymmetry breaking,
- Effective actions for brane dynamics,
- Attractor mechanism and black holes.

Active collaborations include: JINR-Dubna, Russia Tomsk Univ. Russia Univ. Hannover, Germany Turin Polytechnic, Italy CERN, Switzerland Annecy, LAPTH, France Valencia U., Spain

We also organized so far two Winter Schools with the participation of fair amount of collaborators, both as lecturers and as students: 1) Winter School on Supersymmetric Mechanics Frascati (Italy), 7 - 12 March 2005 2) Winter School on Attractor Mechanism Frascati (Italy), 20 - 24 March 2006

We published the Proceedings of the first School as Lecture Notes in Physics, Springer-Verlag Berlin Heidelberg 2006, two volumes, edited by S. Bellucci: Vol. 1, Lect. Notes Phys. 698, (2006) DOI 10.1007/3-540-33314-2 Vol. 2, S. Bellucci et al., Supersymmetric Mechanics Vol. 2, Lect. Notes Phys. 701 (Springer, Berlin Heidelberg 2006), DOI 10.1007/b11749356

We participate as a main node to the Project MRTN-CT-2004-005104 Constituents, Fundamental Forces and Symmetries of the Universe (Short title: ForcesUniverse), a Marie Curie Research Training Network supported by the European Community's Sixth Framework Programme. The network contract was started on 1st November 2004 with duration of 48 months.

A related noteworthy event was the RTN Winter School on Strings, Supergravity and Gauge Theories, held CERN in Geneva, January 16 - 20, 2006, with the participation of students from our group.

Another really important related event was co-organized by Frascati, i.e the RTN network conference in Naples, October 9 - 13, 2006.

2 List of Conference Talks by LNF Authors in Year 2006

1. S. Ferrara, Black hole entropy and quantum information, Winter School on Attractor Mechanism SAM 2006, 20-24 March 2006, Frascati (Roma) Italy
2. S. Ferrara, Current topics in the theory of supergravity, VII. Heineman prize session of the APS April meeting in Dallas (USA) 25 April 2006
3. A. Marrani Spin-Bits and N=4 SYM. Apr 2006. International School of Subnuclear Physics: 43rd Course: Towards New Milestones in our Quest to go Beyond the Standard Model, Erice, Sicily, Italy
4. S. Bellucci Attractor Equations of 4D, N=2 supergravity in an extremal black hole background, Convegno Informale di Fisica Teorica Cortona (Arezzo) Italy, 1 June 2006
5. S. Ferrara, Cambridge-Mitchell Conference, 21-26 August 2006, Cambridge, UK
6. S. Ferrara, Attractor Horizon Geometries of Extremal Black Holes, XVII SIGRAV Conference, 4-7 September 2006, Turin, Italy
7. A. Marrani, Extremal BH and attractors in supergravity, XCII Congresso Nazionale Torino, Italy 18 - 23 September 2006
8. S. Ferrara, Gauged Supergravities, Black-holes and Fluxes, 30 years of SUGRA, Paris, France, October 16 - 20 2006
9. S. Ferrara, Cuarta Escuela Chilena de Astrofisica, Cosmologia y Gravitacion, Valparaiso, Chile, 23-27 October 2006
10. S. Ferrara, Kaehler Geometry and Mathematical Physics, Univ. Hamburg 24-25 November 2006

References

1. S. Bellucci (Frascati) , S. Krivonos, A. Shcherbakov (Dubna, JINR) . PHYS. REV. D 74 (2006) 065016
2. S. Bellucci (Frascati) , S. Krivonos (Dubna, JINR) , A. Marrani (Enrico Fermi Ctr., Rome & Frascati) PHYS. REV. D 74 (2006) 045005
3. S. Bellucci (Frascati), S. Krivonos, A. Shcherbakov (Dubna, JINR) PHYS. LETT. B 638 (2006) 526

4. S. Bellucci (Frascati) , S. Krivonos, A. Shcherbakov (Dubna, JINR) PHYS. REV. D 73 (2006) 085014
5. S. Bellucci (Frascati) , D. O'Reilly (CUNY, Graduate School - U. Ctr.) . PHYS. REV. D 73 (2006) 065009
6. Stefano Bellucci (Frascati) , Levon Mardoyan, Armen Nersessian (Artsakh State U.) .PHYS. LETT. B 636 (2006) 137
7. Stefano Bellucci (Frascati) , Sergio Ferrara (CERN & Frascati) , Alessio Marrani (Enrico Fermi Ctr., Rome & Frascati) .PHYS. LETT. B 635 (2006) 172
8. S. Bellucci, P.-Y. Casteill (Frascati) NUCL. PHYS. B 74 (2006) 297
9. Stefano Bellucci (Frascati) , Armen Nersessian (Artsakh State U.) PHYS. REV. D 73 (2006) 107701
10. S. Bellucci (Frascati) , S. Krivonos (Dubna, JINR) , A. Marrani (Enrico Fermi Ctr., Rome & Frascati) , E. Orazi (Frascati & Rome U.,Tor Vergata) .PHYS. REV. D 73 (2006) 025011
11. S. Bellucci (Frascati) , A. Beylin, S. Krivonos, A. Shcherbakov (Dubna, JINR) PHYS. LETT. B 633 (2006) 382
12. S. Bellucci (Frascati) , S. Krivonos (Dubna, JINR) PHYS. REV. D 74 (2006) 125024
13. Stefano Bellucci (Frascati) , Sergio Ferrara (CERN & Frascati & UCLA) , Murat Gunaydin (Penn State U.) , Alessio Marrani (Enrico Fermi Ctr., Rome & Frascati) INT. J. MOD. PHYS. A 21 (2006) 5043
14. Stefano Bellucci (Frascati) , Armen Nersessian (Yerevan State U. & Artsakh State U.) , Armen Yeranyan (Yerevan State U.) PHYS. REV. D 74 (2006) 065022
15. Sergio Ferrara (CERN & Frascati & UCLA) , Eric G. Gimon (UC, Berkeley & LBL, Berkeley) , Renata Kallosh (Stanford U., Phys. Dept.) . PHYS. REV. D 74 (2006) 125018
16. Riccardo D'Auria (Turin Polytechnic & INFN, Turin) , Sergio Ferrara (CERN & Frascati & UCLA) , M. Trigiante (Turin Polytechnic INFN, Turin) . JHEP 0601 (2006) 081
17. R. D'Auria (Turin Polytechnic & INFN, Turin) , S. Ferrara (CERN & Frascati), M. Trigiante (Turin Polytechnic & INFN, Turin & UCLA) . NUCL. PHYS. B 732 (2006) 389
18. Sergio Ferrara (CERN & Frascati) , Renata Kallosh (Stanford U., Phys. Dept.) . PHYS. REV. D 73 (2006) 125005
19. Sergio Ferrara (CERN & Frascati) , Murat Gunaydin (Penn State U.) . NUCL. PHYS. B 759 (2006) 1
20. Sergio Ferrara (CERN & Frascati) , Oscar Macia (Valencia U. Valencia U., IFIC) . PHYS. LETT. B 637 (2006) 102
21. Sergio Ferrara (CERN & Frascati) , Oscar Macia (Valencia U. Valencia U., IFIC) JHEP 0605 (2006) 008

PI-11: INIZIATIVA SPECIFICA

F. Palumbo (Resp.)

Recently a new bosonization method has been used to derive, at zero fermion density, an effective action for relativistic field theories whose partition function is dominated by fermionic composites [1], chiral mesons in the case of QCD. This approach shares two important features with variational methods: the restriction to the subspace of the composites, and the determination of their structure functions by a variational calculation. But unlike standard variational methods it treats excited states at the same time and on the same footing as the ground state.

I extended [2] this method including states of nonvanishing fermion (baryon) number and derived an effective action for QCD at finite temperature and baryon density. I tested the result on a four-fermion interaction model.

References

1. Composite boson dominance in relativistic field theories, S.Caracciolo, V.Laliena and F.Palumbo, JHEP, to be published [ArXiv: hep-lat/06]
2. A semi-variational approach to QCD at finite temperature and baryon density, F.Palumbo, [ArXiv: hep-lat//0702001]

PI-31: INIZIATIVA SPECIFICA

F. Palumbo (Resp.)

We reconsidered the pairing Hamiltonian in a set of nondegenerate levels [1]. We first compared the behaviour of the ground state energy with the coupling constant in the multilevel and in the degenerate case. Next we discussed, in the multilevel case, the validity domain of a strong coupling expansion which introduces the moments of the single particle level distribution.

References

1. The Multilevel pairing Hamiltonian versus the degenerate case. M.B. Barbaro , R. Cenni , S. Chiacchiera, A. Molinari, F. Palumbo , Annals of Phys. to be published

DIAFF
Deuterium Induced Anomalous Fission Fusion

F. Celani (Resp. Naz.), A. Spallone (Ass.), E. Righi (Ass.), G. Trenta (Ass.)
A. Marcelli, V. Andreassi, A. Marmigi (Ass.), P. Quercia (Guest Res.),
G. Cappuccio (Ass.), D. Hampai (Ass.)

Collaboration with Companies/Universities:
EURESYS (Rome); Centro Sviluppo Materiali (Castel Romano, Rome);
STMicroelectronics (Cornaredo, Milan); ORIM (Macerata); CESI (Milan);
Pirelli Labs (Milan); Mitsubishi Heavy Industries (Yokohama-Japan);
Univ. Osaka (Japan);
Univ. and INFN Lecce: Vincenzo Nassisi (Resp. Loc.), Fabio Belloni, Domenico Doria;
Univ. and INFN Perugia: Giuseppe Onori (Resp. Loc.), Fabio Mazzolari, Giovanni Mazzolari

1 Foreword

The DIAFF experiment is the further development of FREETHAI experiment (see the INFN-LNF Activity Report A.R. of years 2003, 2004, 2005 for further details and deeper understanding of this report).

Starting from 2004, the experiment FREETHAI included, formally, also the activity of previous INTRABIO experiment (see the A.R. of years 2003 and 2004): biological use of Heavy Water. It was renamed DEUTER in 2004. In the last group, Researchers of Perugia Univ. and INFN Section are involved too because of a close collaboration with LNF on some scientific activity making use of the Infrared Sincrotron Light produced by DAΦNE e^+e^- collider.

First, we will report the nuclear results, key activity of DIAFF-LNF and part of Perugia Group, then and shortly, the experimental activities performed in Lecce INFN-Univ. will be related (particularly the use of a laser to stimulate the production of "new elements" in Hydrogenated or Deuteraded Palladium films).

Later one, we will report about DIAFF–Biology Group which aim is to explore the possible use of Heavy Water, heavily (17kGy) irradiated with gamma radiation (energies of 1173keV and 1332keV coming out from a high intensity ^{60}Co source "Calliope" facilities at ENEA-Casaccia), as a possible anti-cancer agent.

The common aspects of all mentioned experimental activities, both nuclear and biological, are the usage, in most of the cases, of Deuterated compounds as "active" agents and Hydrogenated as "control" ones.

2 Introduction

The experimental task of DIAFF, 1^{st} year of activity, is to develop innovative and reproducible techniques to maximize the values of Hydrogen (H) and Deuterium (D) concentrations in Palladium (Pd), i.e. the so-called overloading, (H, D/Pd$\gg$0.95) through:

a) light (H) or heavy (D) electrolytic solutions (water and/or hydro-alcoholic);

b) high pressure&high temperature D gas loading using proper nano-particles (mostly with Pd at significant concentrations).

* Our goals are the stimulation and detection of "anomalous effects" in the Metal-Deuterium system. The anomalous effects up to now detected (at the International level), in such field of Research were from nuclear (^{4}He, "transmutations", X-ray, tritium, neutrons production) and/or of thermal origin (like "excess heat" which amount can't be explained as from chemical/solid state origin).

Since beginning, the open problems of such research type were: unsatisfactory reproducibility of experiments, too small amount of effects. Anyway, in recent times, mainly thanks to experiments performed by:

a) Dr. Yasuhiro Iwamura (Mitsubishi Heavy Industries, Yokohama-Japan) on, both naturals, Strontium (to Molybdenum) and Cesium (to Praseodymium) "transmutation" (developed a sort of "Cold Fusion" multi-layered&nano-structured diode that was subjected to a flow of mild pressurized D_2, at 70 °C, for 1-2 weeks);

b) Academician Yoshiaki Arata (Osaka University-Japan), on excess heat and ^{4}He generation (used specially developed nano-Palladium embedded in a matrix of Zirconia at a pressure of 25-80 bar and temperature of 140-210 °C);

the overall situation is quite improved.

We just recall that the Strontium experiment of Iwamura was successfully reproduced by our group (at INFN-LNF), on 2002-2003, using an electrolytic environment (see A.R. of 2003) instead of gaseous one.

The Countries most involved in such type of research are: Japan, China, USA, former URSS, Italy, France, Germany, India, South-Korea, England. The number of Researchers involved is about one thousand.

Several of them are organized in the framework of the "International Society of Condensed Matter Nuclear Science" (ISCMNS), founded over 3 years ago. The President is Prof. Akito Takahashi (Univ. of Osaka-Japan). Our group collaborated with him, in several experiments, since 1992. One of us (F. Celani) was elected, for the second time, membership of the Executive Committee of that Society. The ISCMNS is a Registered Society according to the English law.

3 Experimental Activity

* In this report, we will discuss only the activity performed during year 2006.
* Four kinds of activity were carried out (a&b, c, d, e):

a) Further studies about the electrolytic loading of H and D on long (50-100cm) and thin (50μm) wires of pure Pd, according to the papers presented at ICCF12 and now published (Ref. 1, Ref. 2).

b) Refinements/improving of the phenomenon of "transmutation" of natural Strontium (Sr) to Molybdenum (Mo) and ^{133}Cesium (Cs) to ^{143}Praseodymium (Pr) that could be applied (following our International project "Scorie Zero") to their radioisotopes, i.e.:

$$^{90}\mathrm{Sr} \rightarrow {}^{98}\mathrm{Mo};\ {}^{135}\mathrm{Cs} \rightarrow {}^{143}\mathrm{Pr}(13.57\mathrm{d}) \rightarrow {}^{143}\mathrm{Nd};\ {}^{137}\mathrm{Cs} \rightarrow {}^{145}\mathrm{Pr}(5.98\mathrm{h}) \rightarrow {}^{145}\mathrm{Nd}$$

according to the paper presented at ICCF12 and now published (Ref. 3). We recall that ^{90}Sr and ^{135}Cs,^{137}Cs are the most abundant, and dangerous to any form of life, radio-isotopes produced by

fission in all the types of nuclear power plants (i.e. ^{235}U, D_2O- natural Uranium, natural Thorium, self-breeding reactors).
* A new project, to improve the reaction rate of original Iwamura experiment, is now in progress, always using natural Sr or Cs, in collaboration (since January 2006) with STMicroelectronics Researchers. It is worth to underline that the methodologies and techniques used in the microelectronics industry match very well with the requirements of the Iwamura's experiments. In order to get out the best performances from a device like that used by Iwamura, in the STMicroelectronics it has been conceived a new embodiment design. In short, a very thin Pd layer (500 nm), on a porous silicon substrate (200 μm thick), allows to obtain high flow rates using a very small amount of the precious metal (Pd), without loosing the mechanical robustness of the filter. Tests are running for the evaluation of the effective hydrogen flux increase. After that a device, with a nano-metric multilayer of Sr-Pd, Pd-CaO, Pd on porous silicon, will be manufactured and tested.

c) Replication/improvement of a crucial experiment for Cold Fusion phenomena: electrolytic compression of H (later D) inside a hollow cathode of Pd. Such kind of experiment is, de-facto, the basis for all the experimental activities on Cold Fusion by electrolysis because, just using electrolytic methods, it shows, in a very clear, elegant and unquestionable way, the possibility to compress, in an open cell, the H_2 (or D_2) at a pressure more greater than ambient one. The limiting pressure depends only on the mechanical strength of Pd, the geometry of cathode and, overall, the know-how and ability of the Researchers to generate, and keep stable, values of over-voltage (at the surface of cathode) as large as possible. The Frascati-INFN Group is well known, worldwide, for the specific know-how developed in several years of experimentations on both Pd plates and thin wires using unconventional electrolytes. Papers on this subject were presented at International (Ref. 5) and National Meeting/Congress (Ref. 4, Ref. 6). A new paper, with other recent data, is in final preparation stage to be submitted to a high impact factor journal (Ref. 7). Such kind of experiment, because of historical origin, is generally known as Arata - 1955. Our Group is proud to inform that, thanks to the before quoted high values of over-voltage, we were able to improve, by a factor as large as 5-8, the previous results of Arata about efficiency of conversion (from electrolytic current to gas stored inside the hollow cathode).

d) Cross-comparison of results obtained at LNF about large amounts of H, D absorption on thin Pd wires using nano-metric silica deposited on the surface of wire. Details of preparation are reported at A.R. 2005, pag. 183. The experiments were performed at Perugia University-INFN using a very sophisticated apparatus developed by Prof. Mazzolai. The results were in fully agreement with what was found at LNF and they were presented at annual Meeting of Italian Physical Society (Ref. 8).

e) Development of new kinds of Pd nano-particles to be employed, as "fuel", inside a high pressure and high temperature cold-fusion reactor using the recent "sauna bath approach" as developed (since July 2005) by Y. Arata. The experiment started because both our previous analysis of the reliable experiments performed at International level (see Ref. 1, and related references, for a deep understanding) and the recent (very good) results (Ref. 9, Ref. 10), before quoted, of Prof. Yoshiaki Arata. It was build, at LNF-INFN, a full stainless steel reactor able to operate between -196°C (liquid nitrogen) and 350°C temperature, and with pressure from vacuum up to 100 bar. The accuracy of pressure is 0.25% of full scale (f.s.) of electronic manometers used (typically 25 and 100 bar). The heater, thermal insulation, interface circuitry and data acquisition (LabView type) were fully developed at LNF. The system is able to measure H/Pd or D/Pd ratio with an overall accuracy of 0.02÷0.05 (the accuracy depends mainly on amount of Pd inside the chamber, increasing with larger weight of Pd) with a manometer pressure of 25 bar f.s.. Through the use of storage chamber V1 (kept at constant temperature), the reaction chamber (called V2) is able to operate both as (high resolution) testing apparatus for H/Pd, D/Pd loading measurements and as a reaction chamber (see Ref. 12). The whole system, together with some results, was recently shown both during annual Congress of Italian Physical Society (Ref. 11) and an International Workshop (Ref. 12).

4 The nano-structure approach

In the framework of Condensed Matter Nuclear Science, it has been recently shown, by Yoshiaki Arata, at Osaka University, that nano-structures of metallic Pd, stabilized in a matrix of ZrO_2, can rapidly absorb, surprisingly, extremely large amounts of H_2 or D_2, (even D/Pd as large as 3:1 at room temperature and external pressure of only 10 bar). Yoshiaki Arata and Akito Takahashi (Osaka University), independently, developed theoretic models that explain so large D/Pd ratios. In the Arata experiments, together with the abnormally high D/Pd ratios, a remarkable excess heat and production of ^{4}He were detected. On the basis of such results and of new deeper interpretation of some our previous experimental results, that (although quite interesting from the point of view of experimental effects) didn't get at that time a satisfactory explanation, we are now convinced that most of the high loading ratios (H-D/Pd) and/or anomalous effects, both thermal and nuclear (by using D), obtained (generally in a not reproducible way) by the people involved in cold fusion experiments, can be reasonably attributed to the spontaneous and uncontrolled growing-up of fractal nano-structures on the Pd surface. In our opinion, even the Sr and Cs (both natural) transmutations obtained in the experiments carried out by the Yasuhiro Iwamura team, which occur on the surface of the Pd/Pd-CaO/Pd multilayer, could be due to the formation of fractal-like structures produced during the multilayer fabrication process. In short, our experimental activity (up to June 2006) was aimed to the production of nano-structures on Pd wires both by anodic oxidation (in situ) and by air oxidation (in situ and ex situ). In situ means inside the electrolytic cell, without removing the Pd wire. In the gas experiments, the Pd wire is inside a thick SS chamber, pressurized up to 10 bar with H_2 or D_2 gas, usually at room temperature. The "good" key point of that approach is that the substrate, where the active nano-particles are located, is the Pd wire itself, not other external (and not active) materials. The drawback is that the active zone is very limited: less then 1 over 1000 of the volume of the 50μm wire's diameter. According to several previous experimental results (mainly by Arata with nano-metric Pd-black, filled inside double-structure cathode in an electrolytic environment; see, as example, the geometry of Ref. 5) in order to get stable excess heat (lasting even years) it is necessary that the amount of power density as to be not over 5-10W/g of Pd. In other words, we need several grams of nano-structured Pd, not 1/1000 (the surface) of 21mg (the weight of 1m long, 50μm diameter Pd wire). Following the excellent results of Arata (with sauna bath reactor) as before pointed out, and considering the intrinsic difficulties of the method used (melt spinning, under Argon atmosphere, from about 1200°C to -196°C in few milliseconds onto a Cu disk rotating at 20 m/s; needed of further thermal treatments and selection/purifications) we, at LNF, decided (starting from July 2006) to produce specific nano-particles using chemical approach, not a metallurgical one. The materials, fully produced at LNF, were routinely characterized by the following analysis:

a) XRPD (X Ray Powder Diffraction), c/o Dr. Giorgio Cappuccio-LNF;

b) SEM (Scanning Electron Microscope) with elemental microanalysis,
c/o CSM (Castel-Romano);

c) TGA (Thermo Gravimetric Analysis) and TDA (Thermo Differential Analysis), c/o CSM.

We experienced, up to now, the following procedures to produce materials: Pd microgranules (ultrasound treated); solutions of Pd salts with nano-metric colloidal silica; impregnation, into proper nano-porous powders, of Pd soluble salts. The work is in progress and we are planning also to develop some (metallurgical based) simplified (in respect to Arata original one) and/or hybrid procedures: the results up to now obtained, with only chemical methods, were not satisfactory about stability under thermal cycling. Results of some of the experiments performed were presented at National (Ref. 11) and International Conference (Ref. 12).

5 Activity at INFN University of Lecce

DIAFF intends to carry on and to deepen the topics started with FREETHAI experiment. It is addressed to make clear about anomalous phenomena which are ascribable to thermic and/or nuclear effects. These last occur after deuterium and hydrogen loading inside transition metals, i. e. Pd, Ti and Ni which are able to absorb huge quantity of D and H. It is well known in literature that these anomalous effects are clear only if a loading threshold is obtained equal to the atomic ratio D-metal or H-metal which has to be above to 0.85. The loading usual method of the above metals consists of electrolytical type even if the gaseous loading method has been revaluated because of the important results obtained recently in Japan from the Research Group of Iwamura at Mitsubishi Heavy Industries. The work carried out in 2006 consisted to strengthen the measurements of anomalous elements found on the Pd films of different thickness. In order to not ascribe the anomalous concentration to contaminations, it was stated to realize the film and the laser treatment keeping the sample always in vacuum, i. e. in clean condition, 10 class. For this reason a support was built to hold pure silicon substrates of 20x20 mm^2 and to put everything in the deposition system. In the figure the support grate is reported.

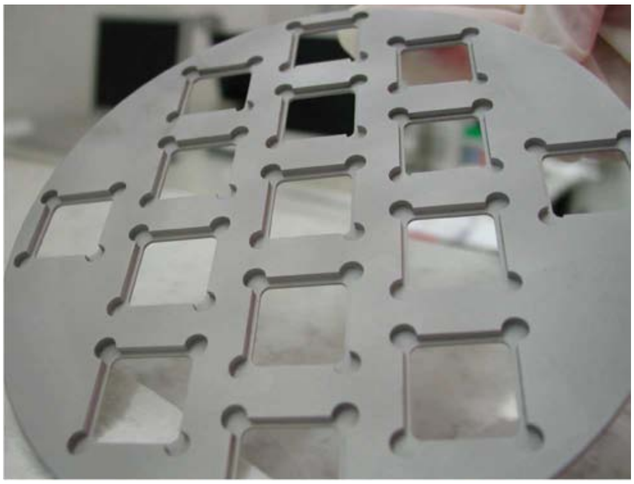

The experiment is still in progress at STMicroelectronics in Milan. At the same time a new reaction chamber was built containing porous silicon with Palladium deposition on the substrate. The project was presented during the last AISEM Conference. Finally, after the samples treatment, XRD, SEM and EDX analysis will be performed.

6 Conclusions

* The DIAFF experiment is well placed, at the International level, in the field of research of anomalies coming from the very close interaction of D with some specific metals (usually Pd).

* During 2006, by our (successful) replication (Ref. 5, Ref. 6) of the experiment of electrolytic compression, it was demonstrated, everlasting, the truthfulness, in principle, of all the Cold Fusion experiments based on electrolytic methods.
* Recently, the connection between the nano-particles and the anomalous effects in Deuterium Metal system as been elucidated in our paper presented ICCF11 (Ref. 1).
* Several experiments were independently performed (since 2000) by Prof. Yoshiaki Arata, using Pd-black (at high surface area) and, at very large efficiency, by Pd-Zirconia alloy. He was the pioneer in such field, although not enough well recognised (for several years), by other people. The his recent "sauna bath reactor" at high pressure (70-80 bar), showed very large temperature gain (of the order of 40-50 °C) at an operating temperature as large as 210 °C. The thermodynamic efficiency of "sauna bath" approach is very large if compared with the previous electrolytic methods: a very low input energy (few Watt with Pd-ZrO_2 amount of about 5g) is needed to keep the system operating over the threshold temperature value (about 140°C, Ref. 9, Ref. 10).
* Our effort is to prepare Pd nano-particles with a simpler and less costly procedure in respect to Arata one.
* A specific, continually improved apparatus, was build at LNF since July 2006 both to qualify (from the point of view of D/Pd ratio) the new materials by us produced and to study its high temperature-high pressure behaviour. The test reactor, curried out at LNF, has an accuracy and an over-all performance similar (or for some aspects better) than the Arata one.
* At moment, the fabrication of proper Pd nano-particles (to be stable over time and thermal cycling), by only chemical-physics route, looks a quite difficult task. The results, although some times interesting about temperature gain, needed further improving. Some innovative, hybrid, procedures seem necessaries: our next work will be also in such direction.

7 References

1. F. Celani *et al.*, New procedures to make active, fractal like, surfaces on thin Pd wires Condensed Matter Nuclear Science 2006, pp: 377-391. World Scientific, ISBN 981-256-901-4 Also at: http://www.lnf.infn.it/sis/preprint/pdf/LNF-06-17(P).pdf

2. A. Spallone *et al.*, Measurements of resistance temperature coefficient at H/Pd overloadings. Condensed Matter Nuclear Science 2006, pgg: 404-410. World Scientific, ISBN 981-256-901-4 Also at: http://www.lnf.infn.it/sis/preprint/pdf/LNF-06-18(P).pdf

3. Akito Takahashi *et al.*, The Italy-Japan Project: fundamental research on cold transmutation process for treatment of nuclear wastes. Condensed Matter Nuclear Science 2006, pgg: 289-292. World Scientific, ISBN 981-256-901-4
Also at: http://www.lnf.infn.it/sis/preprint/pdf/LNF-06-19(P).pdf

4. F. Celani *et al.* (DIAFF Collaboration), Replica, con grossi miglioramenti, ai LNF-INFN, dell'esperimento di Yoshiaki Arata-1955: conseguenze per la Fusione Fredda ed implicazioni sperimentali nell'immediato futuro. Invited Paper at Coherence 2006, Borghetto di Roma, April 21-23, 2006.

5. F. Celani *et al.* (DIAFF Collaboration), Electrochemical compression of Hydrogen inside a Pd-Ag thin wall tube, by alcohol-water electrolyte. Invited Paper at: The 7^{th} Meeting of Japan CF Research Society, April 27-28, 2006. Kagoshima University, Japan. Ed. by Hiroshi Yamada, (with Referee), Vol. 7, pgg. 38-46 (2006). http:// wwwcf.elc.iwate-u.ac.jp/jcf/
Also at: http://www.lnf.infn.it/sis/preprint/pdf/LNF-06-20(P).pdf

6. F.Celani *et al.* (DIAFF Collaboration), Macroscopica compressione elettrochimica dell'Idrogeno, dentro un catodo cavo di Pd-Ag, tramite elettrolita idroalcoolico e sali di Th-Sr-Hg (concentrazione micromolare). Contributed Paper at: XCII Congresso Nazionale Societá Italiana di Fisica. Torino, 18-23 Settembre 2006, Italy. http://www.sif.it

7. F. Celani, *et al.* (DIAFF Collaboration), Electrochemical compression of Hydrogen, inside Pd hollow cathode, at high Faradaic efficiency Submitting to: International Journal of

8. F. Celani, *et al.* (DIAFF Collaboration), Misura del rapporto H/Pd in fili di Pd, PdO, Pd-SiOx tramite tecniche di tipo Sieverts e confronto con il metodo dellla resistivitá, Contributed Paper at: XCII Congresso Nazionale Societá Italiana di Fisica. Torino, 18-23 Settembre 2006, Italy. http://www.sif.it

9. F. Celani, Latest results on Arata's D_2 reactor, 7^{th} International Workshop on Anomalies in Hydrogen/Deuterium Loaded Metals. Asti (Italy), September 23-25, 2006 http://www.iscmns.org/asti06/program.htm

10. F. Celani, *et al.* (DIAFF Collaboration: INFN, Euresys, STM, ORIM, CSM, CESI, Pirelli Labs.), Ulteriori sviluppi degli esperimenti di Yoshiaki Arata: macroscopici eccessi termici (40°C) ad alta temperatura (210°C) utilizzando opportune nano-particelle di Palladio con Deuterio pressurizzato, Convegno Nazionale CSB, Chemical Dep., Univ. La Sapienza, Rome, Dec. 14, 2006.

11. F. Celani, *et al.* (DIAFF Collaboration), Studio dell'assorbimento di Idrogeno in microgranuli di Pd, PdO, Pd-SiOx, Contributed Paper at: XCII Congresso Nazionale Societá Italiana di Fisica. Torino, 18-23 Settembre 2006, Italy. http://www.sif.it

12. F. Celani, *et al.* (DIAFF Collaboration), Toward the use of nanoparticles for stable excess heat in Pd-D system: progress report at INFN-LNF, 77^{th} International Workshop on Anomalies in Hydrogen/Deuterium Loaded Metals. Asti (Italy), September 23-25, 2006. http://www.iscmns.org/asti06/Celani.pdf

13. E. Chiadroni, "Porous Silicon Based High Flow Rate Hydrogen Filter", Proceedings XII Conferenza Nazionale AISEM, Napoli 12-14 Febbraio 2007. p.40-41.

14. A.A. 2005-2006 "UV laser cleaning e analisi EDXRF", L.S. Leo, Rel. G. Buccolieri e V. Nassisi, Tesi di Laurea in Fisica, Università di Lecce.

DIAFF Biology

F. Celani, G. A. Marcelli, G. Onori (Ass.), E. Righi (Resp. Naz..), G. Trenta (Ass.)

As a consequence of a serious lack of biological laboratory personnel, the DEUTER research Group during the 2006 year was looking for a reconstruction of the competence trough the activation of a collaboration with the “Laboratorio Eccellenza Cancerogenesi Ambientale” of Emilia-Romagna Region Environmental Protection Agency (ARPA) and with the “Carcerogenesi Ambientale” Unit of the “Istituto Nazionale per la Ricerca sul Cancro” in Genoa. As a matter of fact both institutions gave expression of their interest to collaborate with our Group for a research on the heavy irradiated water effects at genomic and citogenetic level.

A similar relationship was brought in action with the “Cattedra di Immunologia Clinica e Allergologia” at the 2^{nd} Medical and Surgery Faculty of the La Sapienza University (Rome) to study the qualitative and quantitative immune answer to the ROS produced in the heavy water (D_2O) by a high radiation dose. The activities on this subject are already started and the preliminary experimental results are available. The research activity to study the processes through witch the immune system responds to a low dose stimulation is now outstanding. On this last subject about the effects of the low radiation doses to the immune cells, which we are carrying out with the “Cattedra di Immunologia Clinica e Allergologia” at the 2^{nd} Medical and Surgery Faculty of the La Sapienza University, the full professor R. DAmelio asked the Direzione del Corpo Nazionale dei Vigili del Fuoco for trying benefits, in conventional regime, from the irradiator in use at Capannelle Center in Rome. We hope to actuate the irradiation of cellular culture at defined doses during the 2007 year to point out the answer (particularly as far as the lymphokine production) of the irradiated lymphocytes.

With regard to the irradiation of the heavy water at high doses, we set going the first feasibility evaluation with the responsible of the Linac Laboratory of ENEA Frascati, to execute the necessary irradiations at high doses of D_2O to use it in the foregoing pointed out experience. At this purpose, it was designed and fulfilled a suitable glass container to optimize the dose and its distribution with reference to the electron beam and electron $\rightarrow$ gamma conversion target characteristics.

The interest of the “Laboratorio Eccellenza Cancerogenesi Ambientale” of Emilia-Romagna Region, Environmental Protection Agency (ARPA), in the heavy water researches and in the effects of low radiation doses brought forth a first meeting in a congress where the people participation and the concern of the public operators was very successful.

On the base of the specific and consolidated competence our research Group ripened in biodosimetric matter and with regard to a real radiation protection need at the national level, a relevant enterprise is now in progress to realize an operative national Centre for Citogenetic Dosimetry with adhesion of experts belonging to University, Institutions and to some other scientific Institutions.

Promoting Committee: DIAFF-Biology research Group of LNF; General Direction of Istituto Nazionale per la Ricerca sul Cancro; Chair of Immunologia Clinica e Allergologia at the 2^{nd} Medical and Surgery Faculty La Sapienza Rome; Chairs of Medicina del Lavoro of the University of Bologna, Padova e Pisa; Direzione Centrale di Sanità del Dipartimento della Pubblica Sicurezza Ministero dell'Interno.

This enterprise was promoted as a result of some meetings devoted to biodosimetric themes during 2006 year. The final result was the indication that the best seat for the National Centre, because of its competence and availability, was that of the "Carcerogenesi Ambientale" Unit of the Istituto Nazionale per la Ricerca sul Cancro in Genoa. At the same time, for the biodosimetric purposes, at the national level was foreseen a settlement of a task-group of qualified slide lecturers associated to the Genoa seat, and a validated instrument for an automatic computerized scanning of the radio induced chromosomal aberrations.

The biological DIAFF Group carried on an intense didactic and formative activity on the risk due to the ionizing radiation exposure trough the direct organization or trough the participation at courses, congress, seminars sponsored by INFN or by other scientific public institutions. Biological, environmental and health aspects were analyzed in lessons or reports with reference to normal, incidental or intentional exposure events. As regards this aspect we can point out, the Advanced Course in Medical Radiation Protection (September 2006) celebrative of 20^{th} year always supported and financed by INFN, Course that in this occasion experienced the official participation of the towns and autonomous districts Authorities.

1 Publications and Conferences

1. E. Righi, "Stima degli effetti tardivi a seguito di eventi accidentali", Corso di Formazione e Perfezionamento in Radioprotezione; Università degli Studi di Napoli "Federico II"; Napoli, 6 Aprile, 2006.

2. E. Righi, "Radiopatologia Deterministica e Radioprotezione. Danni stocastici e basse dosi: problema centrale della Radioprotezione", Corso Squadre Speciali Nucleari-Radiologiche Vigili del Fuoco. Roma: 10 Maggio, 15 Giugno, 21 Settembre, 26 Ottobre 2006.

3. E. Righi, "Stima degli effetti radioindotti tardivi a seguito di eventi accidentali ed ostili", 1^a Conferenza sulla Difesa NBC e la Tutela dellAmbiente. Centro Sperimentale Volo; Pratica di Mare-Roma, 16-18 Maggio 2006.

4. E. Righi, "La costruzione radioprotezionistica tra teoria e realtá", Convegno Nazionale: La Radioprotezione Nell'era Delle Basse Dosi, Bologna, 19 Maggio 2006.

5. E. Righi, "Stima degli effetti tardivi a seguito di eventi accidentali", Corso di Formazione in RADIOPROTEZIONE. Anno Accademico 2005/6, Napoli, Università Federico II, 3 Aprile 2006

6. E. Righi, "Gli effetti sanitari immediati - Chernobyl ventanni dopo", Giornata di Studio 3 Luglio 2006, CNR-Roma.

7. E. Righi, "Disastro di Chernobyl: danni immediati ed effetti tardivi", CABLIT Conferenza "Disastro di Chernobyl: 20 anni dopo", Centro Addestramento Sanitario Professionale Aeronautica Militare. Roma, 20 Dicembre 2006.

8. E. Righi, "Radioepidemiologia: percezioni di un medico autorizzato", 20° Corso Avanzato di Radioprotezione Medica, Bressanone, 4-8 Settembre 2006.
9. E. Righi, "Chernobyl: gli effetti immediati", 20° Corso Avanzato di Radioprotezione Medica, Bressanone, 4-8 Settembre 2006.
10. E. Righi, "Lezioni di radiopatologia e biodosimetria" , Master di II livello in Difesa dalle Armi NRBC, II Facoltà di Medicina e Chirurgia Università La Sapienza Roma, Anno Accademico 2006.
11. G. Trenta, Serie di lezioni su: "Contaminazione ambientale", "Le armi atomiche", "Scenari incidentali", "Contaminazione umana", "Fisiopatologia dell'irradiato", "Scenari nucleari", "L'incidente di Chernobyl", Master di 2° livello in "Difesa da Armi Nucleari, Radiologiche, Chimiche e Biologiche", II Facoltà di Medicina e Chirurgia, Università degli Studi di Roma "La Sapienza", Osp. S. Andrea, Febbraio e Luglio 2006.
12. G. Trenta, Serie di lezioni su: "Principi generali di Radioprotezione", "Valutazione della Probabilità causale", "Incidenti nucleari ed altre emergenze", "Gestione degli interventi sanitari in caso di evenienze accidentali", "Diagnosi e denuncia di malattie professionali", "Sorveglianza medica: il polmone", 1° Corso di formazione e aggiornamento in Radioprotezione medica, AIRM, Roma, Febbraio 2006.
13. G. Trenta, "L'epidemiologia: strumenti interpretativi", 20° Corso Avanzato di Radioprotezione Medica, Bressanone, 4-8 Settembre 2006.
14. G. Trenta, "PC: rassegna casistica", 20° Corso Avanzato di Radioprotezione Medica, Bressanone 4-8 Settembre 2006.
15. G. Trenta, "La Radioprotezione oggi: innovazione e conservazione", 20° Corso Avanzato di Radioprotezione Medica, Bressanone, 4-8 Settembre 2006.
16. G. Trenta, "L'evoluzione della prevenzione nell'impiego delle radiazioni", Convegno: L'uso pacifico dell'energia nucleare da Ginevra 1955 ad oggi: il caso italiano. Roma, 8-9 Marzo 2006.
17. G. Trenta, "Effetti delle radiazioni ionizzanti: loro estensione ed interpretazione alle basse dosi", Corso di formazione in tecnologie nucleari. ENEL, Roma, 20-31 Marzo 2006.
18. G. Trenta, "Fisica e metrologia delle radiazioni", Corso di Formazione in Radioprotezione, Anno Accademico 2005/6, Napoli, Università Federico II, 3 Aprile 2006
19. G. Trenta, "Rifiuti radioattivi e Radioprotezione", Seminario a: Scuola di specializzazione in Sicurezza e Protezione. Palazzo Baleani, Roma, 26 Aprile 2006.
20. G. Trenta, "Nesso di causalità nella Radiopatologia stocastica", Convegno su: La Radioprotezione nell'era delle basse dosi; Bologna, 19 Maggio 2006.

21. G. Trenta, ICRP Pubblicazione n. 96 NCRP Report n. 138: Dirty bombs, Radiological Dispersion Device, Improvised Nuclear Device. Corso: Le emergenze radiologiche e nucleari; Taormina, 25-27 Maggio 2006.

22. R. Moccaldi, G. Trenta “Application of probability of causation in professional exposure to radiation”, 28^{th} International Congress on Occupational Health: Renewing a century of commitment to a healthy, safe and productive life; Milano, 11-16 Giugno 2006.

23. G. Trenta, “L’evoluzione del concetto di protezione del paziente”, 42° Congresso Nazionale della Società Italiana di Radiologia Medica; Milano, 23-27 Giugno 2006.

24. G. Trenta, “Medical surveillance”, Scuola Europea di Studi Avanzati in “Tecnologie nucleari e delle radiazioni ionizzanti” Anno accademico 2005-2006, Istituto Universitario di Studi Superiori, Pavia, 12 Luglio 2006.

25. G. Trenta, “Radioprotezione medica. Convegno su: Attualità di Radioprotezione in campo sanitario”, Università “La Sapienza” Scuola di specializzazione in Sicurezza e Protezione. Palazzo Baleani, Roma, 15 Settembre 2006.

26. G. Trenta, “Basse dosi di radiazioni ionizzanti: la dottrina e la pratica di protezione”, dBA 2006, 4 Convention nazionale dei responsabili dell’igiene e sicurezza in ambiente di lavoro. Modena, 12-13 Ottobre 2006.

27. G. Trenta, “La sorveglianza sanitaria: il ruolo del medico competente nella protezione dai campi elettromagnetici. La figura dell’esperto nella sorveglianza fisica dei campi elettromagnetici nei luoghi di lavoro”, Frascati, 14 Novembre 2006.

28. G. Trenta, “Giustificazione e ottimizzazione negli impieghi medici delle radiazioni ionizzanti”, Convegno INPRAT su: “La relazione rischi benefici: impiego delle tecnologie ed ottimizzazione”, Roma, 24 Novembre 2006.

29. G. Trenta, “L’incidente e le conseguenze ambientali“, CABLIT Conferenza “Disastro di Chernobyl: 20 anni dopo“, Centro Addestramento Sanitario Professionale Aeronautica Militare; Roma 20 Dicembre 2006.

ETRUSCO

G. Bellettini, (Ass.), A. Boni (Bors.), C. Cantone (Bors.), S. Dell'Agnello (Resp.),
G. O. Delle Monache, M. Garattini (Bors.), N. Intaglietta (Tecn.), M. Martini (Bors.),
R. Tauraso (Ass.), R. Vittori (Ass.)

1 Introduction

A Space Climatic Facility (SCF) has been built at INFN-LNF (Frascati, Italy) in 2006. The SCF is described in detail in ref. 1) and 2). The initial purpose of the SCF was to study the non-gravitational perturbations on the LAGEOS and LARES satellites, used for precision Space Geodesy measurements and tests of General Relativity.

The modular and evolutionary design of the SCF turned out to be well suited to characterize the thermal and laser-ranging performance of cube-corner retro-reflector (CCR) arrays deployed on GNSS[1] constellations, like the existing US GPS-2, the imminent European GALILEO and the future GPS-3. The integration of satellite laser ranging (SLR) with the standard microwave ranging (MWR) to improve the satellite navigation capabilites has become another SCF goal.

With minor upgrades, the SCF can also test the laser-ranging performance of spherical test masses in the outer Solar System for DSGP (Deep Space Gravity Probe), which is a satellite formation of an active spacecraft and a few masses laser-tracked by the active spacecraft. DSGP is being conceived to accurately study the Pioneer effect (ie, deviations from the $1/r^2$ gravity force law) and to perform important (inter)planetary science investigations. For this purpose, the groups of INFN-LNF, Rome-Tor Vergata, plus R. Vittori[2] in 2006 proposed to INFN a new experiment, ETRUSCO (Extra Terrestrial Ranging to Unified Satellite COnstellations). ETRUSCO was approved by INFN in October 2006, with the recommentation to focus the activity on GNSS applications. The R&D for DSGP will be reconsidered at a later stage. We describe the first preliminary thermal measurements on a *flight* model of CCR array to be deployed soon on the GPS-2 constellation and the upgrade of the SCF to perform simultaneous thermal and laser-ranging tests.

2 Extra Terrestrial Ranging to Unified Satellite COnstellations

A space-climatic characterization of the detailed thermal properties and of the laser ranging response of the GALILEO CCR arrays will strongly enhance the integration ("unification") of SLR with MWR. For each CCR fo the array, the characterization will include the measurement of the thermo-optical parameters (emissivity and reflectivity), the thermal relaxation time and the variation of the laser far field diffraction pattern in a realistic space environment. This will be done with the arrays inside the SCF, exposed to simulators of the Sun and Earth illuminations. Since SLR gives a fundamental contribution to the definition of the Earth center of mass and of the absolute scale of length, this test program will improve the accuracy and long-term stability of the determination of the GALIELO orbits. The ultimate satellite positioning accuracy that can be reached is less than 1 cm. This in turn will propagate to the final end used on the Earth and all civil and commercial services provided by GALILEO will benefit from it. Since the large-scale deployment of SLR on GALILEO will be a world-first in GNSS, it is of the utmost importance that a full-fledged space-climatic characterization is performed. The experience of SLR with GPS-2 (two

[1] Global Navigation Satellite System.
[2] Italian Air Force and European Astronaut Corps.

satellites) and GLONASS was a test more than a mission critical deployment. Over several years, these few satellites have indicated how crucial the proposed characterization is and how difficult it is to model climatic effects without experimental measurements. A third CCR array exists, which will be deployed soon on a satellite of current GPS-2 constellation. This array is property of the University of Maryland (UMD, College Park, MD, USA) and is now at INFN-LNF for space climatic tests, following a special agreement with NASA-GSFC, IRLS[3] and UMD (C. O. Alley, D. G. Currie). Testing this third array is very important because the previous identical versions of the arrays when tracked with lasers show significant periods of low light returns. Climatic tests and simulations are important to assure that no failures occur in GALILEO, in the long term and with a large multiplicity of satellites. The Frascati SCF offers the unique possibility to understand in detail the effects of the severe space environment on the many years of expected lifetime of the CCR arrays of GALILEO. In addition, the proposed test program can help keep GALILEO competitive with the next generation of GPS-3 (about 2011-2012), which might take advantage of proposed innovative retro-reflectors, like the hollow type, as opposed to the traditional solid, fused-silica reflectors used by GLONASS, GPS-2 and GALILEO.

3 The "GPS3" Array

This so-called GPS3 array is identical to the ones installed on the GPS-35 and GPS-36 satellites in orbit. The three arrays have been manufactured in Russia. Mechanical drawings for its correct modelling have been provided courtesy of V. P. Vasiliev of the Russian IPIE (Institute for Precision Instrument Engineering of the Federal Space Agency of Russia, Moscow). Since this is a *flight* model, in 2006 it was decided not to start with a full test in the harsh SCF environment. Figure 1 shows a photo of the GPS3 and the warm-up and cool-down curve of a central retro-reflector, measured with a digital infrared camera. This preliminary test was conducted with the Solar simulator as the main thermal load, at 75% of its nominal intensity. A space-climatic test in the SCF will follow in 2007, under the supervision of D. G. Currie of UMD.

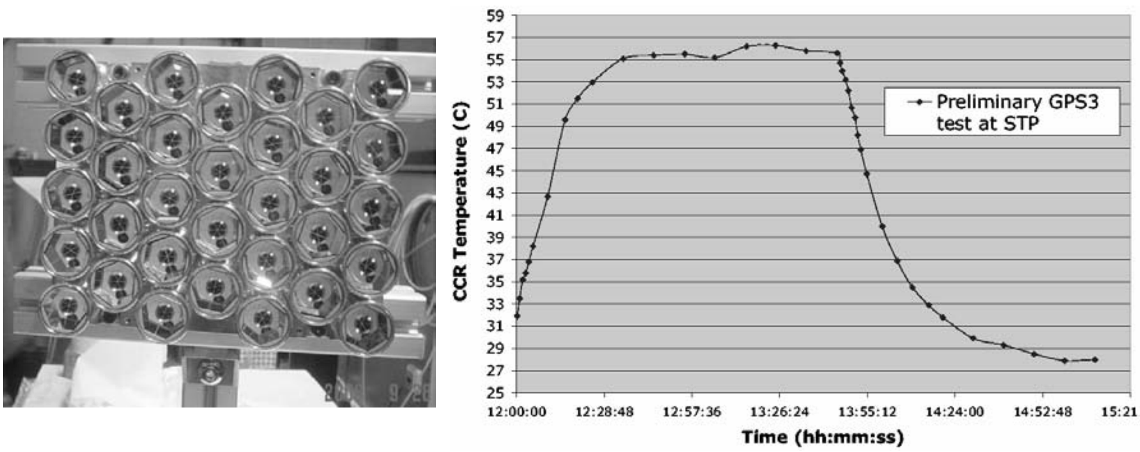

Figure 1: Left: the GPS3. Right: warm-up and cooldown curve of the GPS3 at STP.

[3] International Laser Ranging Service

4 Far Field Diffraction Pattern (FFDP) Measurement

The most basic test of the SLR performance, is the measurement of FFDPs. The optical circuit for FFDP measurements with CCRs is shown in fig. 2. The laser beam profiler (by Spiricon) uses a PtGrey CCD 2 MPix camera, readout via Firewire by a PC. These tests are currently done in STP conditions to check the optical instrumentation, but final tests will be performed with the CCR array in the SCF. Figure 3 shows a preliminary measurement of an FFDP of a flat mirror, in place of the CCR. Optical flats like this with known reflectivity will be used as a normalization to determine the absolute intensity of the SLR return to Earth from the CCR under test.

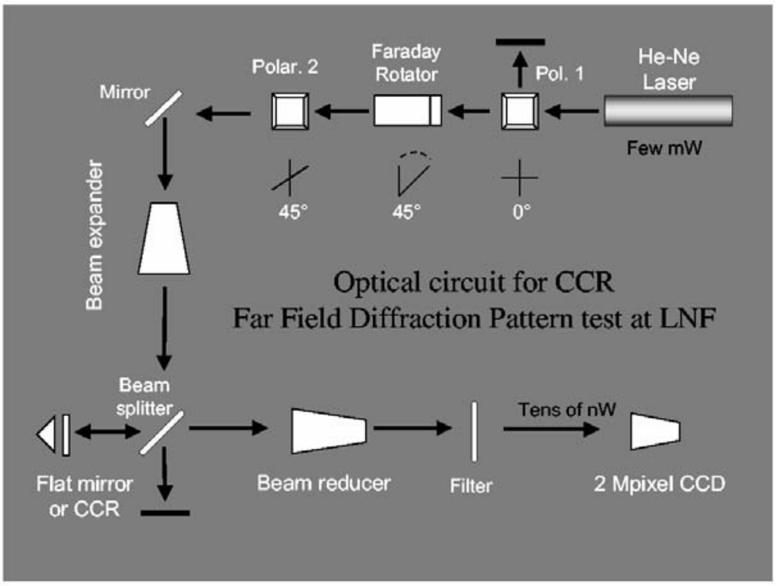

Figure 2: Scheme of the optical circuit for the FFDP measurement at LNF.

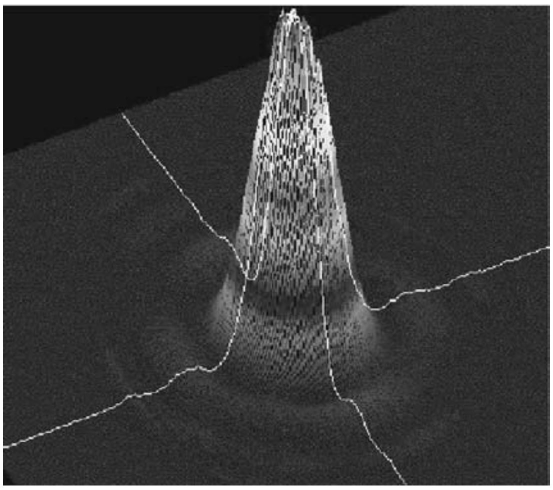

Figure 3: Preliminary FFPD measured for a flat optical mirror.

5 SCF Upgrade

The upgraded SCF is shown in the top view of fig. 4: the existing left window for the IR camera, the new central window for FFDPs and the new right spare window. The side view of fig. 4 shows the sketch of the LARES satellite ($\phi = 32$ cm) and of a GALILEO CCR array (~ 53 cm $\times$ 43 cm). Each CCR will be first exposed to the Sun and the Earth simulators and its thermogram taken. Then, the CCR will be moved in front of the *central* window to take its FFPD.

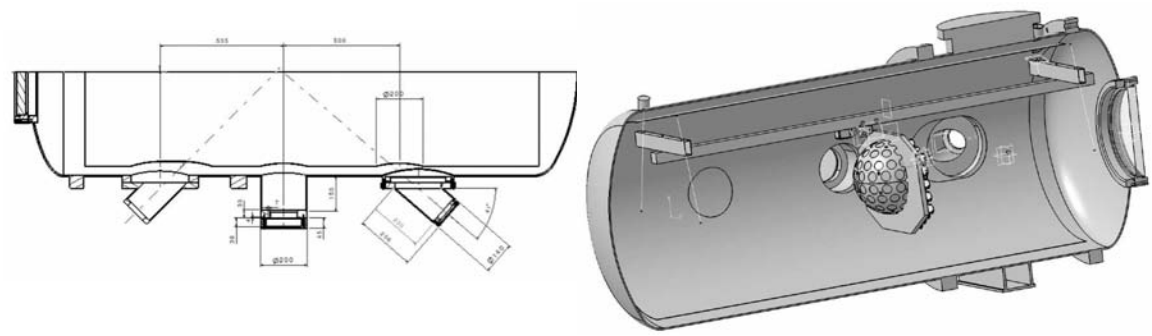

Figure 4: Upgraded SCF. Left: top view (Sun enters left). Right: side view (Sun enters right).

SCF measurements are complemented by simulations done with commercial software [3) 1)].
1) Autocad INVENTOR for mechanical drawings and ANSYS for Finite Element. Meshing is done with great detail and in a complete *parametric* way for model portability, modularity and debugging.
2) Space-climatic simulations are handled by THERMAL DESKTOP (geometric thermal modeler) + RADCAD (radiation analysis) + SINDA-Fluint (solver) + orbital simulator, by $C\&R - Tech$ (`www.crtech.com`). This consists of thermal modelization coupled to satellite attitude and orbital motion in the whole Solar System. Models are tuned to the SCF data.
3) CODEV, by Optical Research Associates (`www.opticalres.com`) to analyze the FFDPs.

Talks in 2006 by ETRUSCO Collaborators

C. Cantone, Experimental Gravity in Space GGI Workshop, Florence, Italy, Sep. 2006.
G. O. Delle Monache, Int. Laser Ranging Service Conference, Canberra, Australia, Oct. 2006.

6 Conclusions

In September 2006 the SCF has become a permanent, small-size, experimental apparatus of INFN-LNF. During the last two years the collaboration of LNF with ILRS has been very fruitful. The current upgrade of the SCF, consisting of the integration of the thermal and the laser-ranging tests has been funded by INFN, and by LNF, explicitly for GNSS studies. An additional, dedicated optical table can thus be operated next to the SCF, when alternating among exposure to the heat simulators, IR thermography and laser ranging. At the end of 2006, LNF has become member of the "Signal Processing" Working Group of the IRLS.

References

1. LNF Report LNF-06-24(P); to be published on Int. Jour. Mod. Phys. D.
2. G. Bellettini et al, LNF Report LNF-06-26(IR).
3. A. Bosco, Thesis, Univ. of Rome Tor Vergata, 2006, LNF Report LNF-06/32(T).

FLUKA2

M. Carboni, M. Pelliccioni (Resp.), S. Villari (Ass.)

1 Report year 2006

The development of FLUKA code applications as part of the FLUKA collaboration is the main purpose of this experiment.

In order to validate FLUKA predictions on the neutral pion production by the GCR in atmosphere, the high-energy component of the calculated vertical photon fluence has been compared with the experimental data. An excellent agreement has been found with BETS (Balloon-born Electron Telescope with Scintillation fibers detector) observations between 15000 m and 25000 m. The calculated results are slightly underestimating the experimental data out for this altitude range.

The study on the angular dependence of the neutron fluence on altitude, latitude and solar activity at low-medium altitudes (less than 20000 m) is in progress.

The calculation of the new conversion coefficients fluence-to-effective dose for neutrons using voxel phantoms has been launched in collaboration with the ICRP.

The FLUKA code has been widely engaged to study the radiation problems of the CNAO (i.e. dump activation, skyshine, etc.).

2 Conference Talks in 2004

1. M. Pelliccioni, Simulazioni in radioprotezione. Convegno: Il metodo Monte Carlo nella Fisica Medica: codici di calcolo e loro applicazioni. A.O. San Camillo Forlanini, 28-29 novembre, 2006.

3 List of Publications 2006

1. F. Ballarini et al., GCR and SPE organ doses in deep space with different shielding: Monte Carlo simulations based on the FLUKA code coupled to anthropomorphic phantoms, Advances in Space Research, Volume 37, Issue 9, p. 1791-1797, 2006.

2. F. Ballarini et al., The FLUKA code: an overview, J. Phys., Conf. Ser., 41 151-160, 2006.

3. F. Ballarini et al., Modelling human exposure to space radiation with different shielding: the FLUKA code coupled with anthropomorphic phantoms, J. Phys., Conf. Ser., 41 135-142, 2006.

4. G. Battistoni et al., The hadronic models for cosmic ray physics; the FLUKA code solutions, SLAC-PUB-12333, Dec. 2006.

5. S. Trovati et al., Human exposure to space radiation: role of primary and secondary particles. Radiation Protection Dosimetry, 2006 (in press).

KLONE

S. Bertolucci, A. Ferrari, S. Florin Catalin, M. Iliescu,
M. Martini(Dott.), S. Miscetti(Resp.Naz.), B. Sciascia

1 Measurement of detection efficiency to low energy neutrons

Detection of neutrons with energies from a few to hundreds MeV is usually performed with organic scintillators. The high concentration of hydrogen atoms provides a proton target and the elastic scattering of neutrons produces recoil protons which originate a visible response. Typical efficiency is of the order of 1 %/cm of scintillator thickness. On the other hand, when inserting one layer of a medium high Z material in the organic scintillator there is an enhancement of the neutron response through inelastic processes. The KLOE calorimeter [1] was primarily designed to detect photons with very high efficiency. However, during a KLOE study of kaon interactions in the apparatus walls, hints of a high efficiency for low energy neutrons (< 20 MeV) were observed. We therefore planned to make a systematic study of the calorimeter response to neutrons, both exposing it to a dedicated neutron beam and by performing a complete simulation of the detector geometry and response. An high detection efficiency to neutrons could open the road to inexpensive and compact neutron counters and have an impact for the future experimentation at DAΦNE.

The used prototype is composed of ~ 200 layers of 1 mm diameter blue scintillating fibers glued inside grooved lead layers of 0.5 mm thickness with total external dimensions of $13 \times 24 \times 65$ cm^3. The readout is organized in four planes along the calorimeter depth for the first 16.8 cm. Each plane is then subdivided in 3 columns along the horizontal coordinate originating cells of 4.2×4.2 cm^2. When running with neutron beam, the calorimeter was positioned with fibers running vertically, the lower (upper) end is called side A (B). Each PM signal has been split in three replicas to allow measurements of charge and time and to create two analog signals for the trigger. With their discriminated signals, SA and SB, a coincidence, $SA \cdot SB$, was formed to trigger on the calorimeter. A reference counter for efficiency was built with a 5 cm thick bulk of NE110 organic scintillator, of transversal dimensions 10×20 cm^2. When running with the beam, the scintillator was positioned with its longest dimension along the horizontal coordinate. To trigger on the scintillator, the PM signals, $S1$ and $S2$, were discriminated and a coincidence, $S1 \cdot S2$, formed.

We ran our experiment at TSL high-energy neutron facility [2] for two weeks in October 2006. In our setting, 178.7 MeV protons were directed on a ^{7}Li target generating a neutron beam geometrically shaped by an iron collimator block with a 2 cm diameter cylindrical hole. The neutron energy spectrum is dominated by a peak at a few MeV below the primary proton energy, and a long tail down to thermal neutrons. The neutron beam time structure was in phase with the cyclotron RF which had a period, T_{RF}, of ~ 45 ns. The beam was emerging from the collimator at 3 m distance from the target. In order to ensure full beam acceptance we have run at a distance of 5.1 m from the target and centered the beam in the middle of our detectors. Very low intensity neutron beams, from 1.5 kHz/cm^2 to 6 kHz/cm^2, have been required in order to minimize the probability of counting more than a neutron per event. The neutron rate has been measured by an ionization-chamber monitor (ICM), with an absolute accuracy estimated at the level of 10 %.

All discrimination and trigger signals were formed with NIM logic while the DAQ was based on VME standard. The trigger signal was either $SA \cdot SB$ or $S1 \cdot S2$ after phase locking with the cyclotron RF replica. We acquire data at a rate of 1.7 kHz. Typical runs consist of $\sim 0.5 - 1.5 \times 10^6$ events.

The detector efficiency to the overall neutron spectrum has been determined by making the

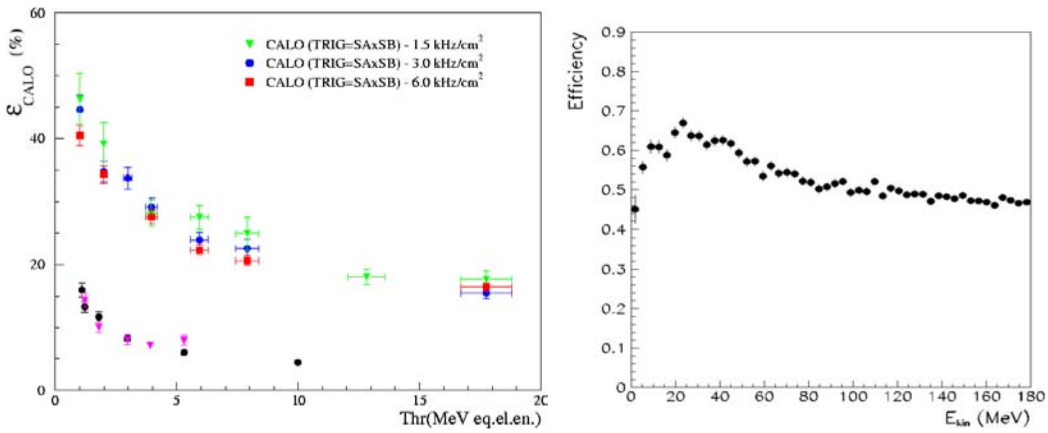

Figure 1: *(Left-plot) Calorimeter detection efficiency (upper points) and expected efficiency for an equivalent thickness of NE-110 (lower points) to neutrons of 5-175 MeV as a function of the threshold. (Right plot) Detection efficiency as a function of neutron energy as estimated by FLUKA.*

ratio of the counted detector rate with the neutron beam rate estimated by the ICM. The measured efficiency for the calorimeter is shown in Fig. 1.left as a function of the trigger threshold in MeV. These preliminary results show that at the lowest trigger threshold the neutron detection efficiency of the calorimeter ranges from 40 % to 50 %, depending on the beam intensity. It corresponds to a sizeable enhancement with respect to the expected 8−16 % based on the amount of scintillator only. For comparison, the efficiency of the 5 cm thick NE110 scintillator ranges from 4 % to 10 %, for values of the trigger threshold below 5 MeV of electron equivalent energy, in good agreement with the available measurements in literature.

The Monte Carlo code FLUKA [3, 4] has been used for a detailed simulation of the calorimeter structure and of the TSL experimental beam-line. The primary reason for the observed efficiency enhancement appears to be the huge inelastic production of neutrons on the lead planes. For neutrons in the high energy peak (175 MeV), the probability to have an inelastic interaction is 31.4 % on the lead, compared to 7.0 % on the fiber and 2.2 % on the glue. The secondary particles generated in such inelastic interactions are on average 5.4 per event, counting only the secondary neutrons above 19.6 MeV. Among the produced secondaries, 62 % are neutrons, 27 % photons, 7 % protons while the remaining 4 % are nuclear fragments. The high sampling frequency of the calorimeter appears also to be a crucial point in the efficiency enhancement. In Fig. 1.right the detection efficiency estimated by FLUKA is shown as a function of the kinetic energy of the neutron impinging on the calorimeter. By weighting the efficiency curve with the neutron spectrum, the overall efficiency turns out to be 50 %, in agreement with the measured integrated value.

References

1. The KLOE collaboration, NIM **A 482** (2002) 364-386.
2. A.V. Prokofiev et al., PoS (FNDA2006) 016 (2006).
3. A. Fassò et al., CERN 2005-10 (2005), INFN/TC_05/11, SLAC-R-773.
4. A.Fassò et al., eConf C0303241 (2003), arXiv:hep-ph/0306267.

MARIMBO

G. Celentano (Ass.), A. Della Corte (Ass.), U. Gambardella (Resp.)

1 Purposes of the project

The *MARIMBO* experiment was devoted to study the applications of superconducting wires and tapes made of magnesium diboride MgB_2. As MgB_2 becomes superconducting at temperatures below 39 K and being a low cost material, it looks potentially attractive especially in a cryogen free, low field, magnet applications. As the tape technology has been developed relatively fast, making available 1600 m long pieces of MgB_2 tapes with good transport properties, we proposed to build a demostrating application of MgB_2 tapes: the fabrication of a small racetrack coil designed and tested by INFN and realized by Ansaldo Superconduttori SpA. Three INFN sections are involved: Genova (group leader), Milano, and LNF, in collaboration with Ansaldo Superconduttori SpA, Genova.

2 The Frascati group activity

The Frascati group, made of LNF and ENEA Frascati researchers, have studied in more details some MgB_2 features,and have analyzed the stability properties of the Columbus tape under the transport current as a function of the temperature and the applied magnetic field.

2.1 Material features

Two kind of studies have been carried out: one concerning the the influence of the disorder introduced by neutron irradiation on polycrystalline MgB_2 material, and another concerning the MgB_2 phase nucleation by means of MgB_2/Mg multilayers. In the first study [1] we analyzed the magnetic properties of polycristalline MgB_2 which were exposed to different neutron fluences in order to make in-depth analysis of the critical field and current density behaviour and to identify what scattering and pinning mechanisms come into play.

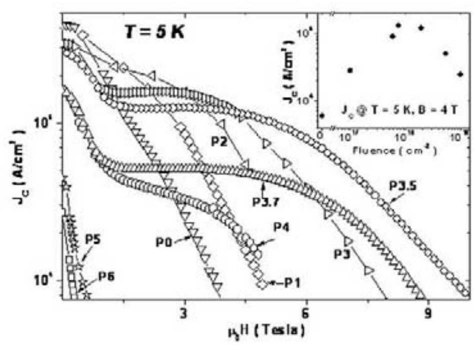

Figure 1: *Critical currents measured in samples which had different neutron doses*

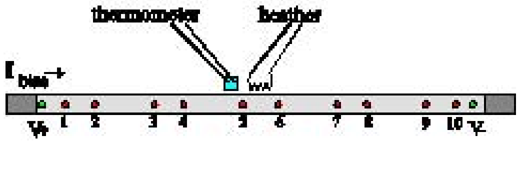

Figure 2: *Connection layout along the MgB_2 tape (not to scale). Darker edges represent the 3 cm long welded area also acting as heat sink.*

In the second study 2) we analyzed the chemical composition and electronic structure of the multi layer films and compared these results to the corresponding MgB_2 bulk case to investigate the causes for the low transition temperature in our *in-situ* low-temperature processed MgB_2 films.

2.2 Stability and quench propagation against thermal disturbances

In this work 3) we analyzed short straight samples of the Cu-stabilized, 14 filaments, MgB_2 tape manufactured by Columbus Superconductors, Genova, taken from a 1.6 *km* length production, being used to realize a cryogen free, double pancake style, magnet. The shape of the conductor is a tape, 3.6 mm wide and 0.65 *mm* thick, manufactured with the PIT (Powder In Tube) method. There is copper inside, included in an iron barrier, and finally the MgB_2 filaments are compressed in a Ni matrix. The superconducting fraction is less than 10% of the whole section. In fig.2 it is shown the experimental setup to analyze the normal zone propagation along the tape. Tape edges were welded over 3 *cm* on the bulk copper sample holder used for the tests, performed in a He gas flow cryostat. Two brass counter flow cooled current leads, designed for 200 A, are used to bias the tape. The wire is shielded from the direct exposure of the cold gas by means of thick polystyrene. A 3 *mm* wide heater, made of NiCr wire, is wound and glued in the middle of the tape. Voltage contacts, at known positions are used to determine the presence of dissipative regimes. A calibrated cernox thermometer is located on the tape, few *mm* far from the heater side.

In Fig. 3 (left) the propagation velocity v_p as a function of the delivered energy $\mathbf{E}$ is reported at two temperatures and bias currents while in Fig. 3 (right) the v_p is reported as a function of the temperature at two values of bias current, each one triggered by a constant energy pulse.

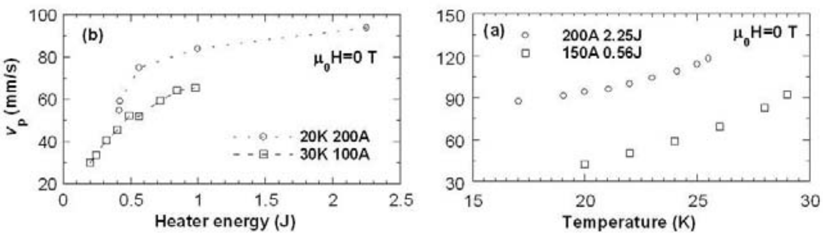

Figure 3: *Normal zone propagation velocity as a function of both the heater energy (left) and the temperature (right)*

The v_p-vs.-energy curve indicates a fast increase of v_p at low heater energy followed by a weak dependence for higher energy values. This $v_p(\mathbf{E})$ behavior at low **E** values may be ascribed to the short distance between voltage taps and heater, where the equilibrium balance between the heat loss by conduction and the generated heat is not yet achieved. The v_p increases with the temperature because dissipation grows up narrowing the temperature margin T_g-T_0, where T_0 and T_g are the operating temperature and the generation temperature, respectively.

References

1. C. Tarantini, H. U. Aebersold, V. Braccini, G. Celentano, C. Ferdeghini, V. Ferrando, U. Gambardella, F. Gatti, E. Lehmann, P. Manfrinetti, D. Marre', A. Palenzona, I. Pallecchi, I. Sheikin, A. S. Siri and M. Putti, "Effects of neutron irradiation on polycrystalline $Mg^{11}B_2$", Physical Review **B73**, 134518 (2006)

2. A. Santoni, U. Besi Vetrella, G. Celentano, U. Gambardella, A. Mancini, *X-ray photoemission study of MgB_2 films synthesized from in-situ annealed MgB_2/Mg multilayers* , Applied Physics **A** (2007), to be published

3. U. Gambardella, A. Saggese, P. Sessa, A. Guarino, S. Pace, G. Masullo, A. Matrone, E. Petrillo, R. Quarantiello, *Stability Measurements in Multi-Filamentary MgB_2 Tapes*, IEEE Applied Superconductivity (2007), to be published

NEXT

S. Bellucci (Resp. Naz.), C. Balasubramanian (bors. PD),
M. Bottini (Ass.), F. Corrente (Dott.), D. De Bellis (Laur.), G. Giannini (bors. PD),
A. Grilli (Tecn.), A. Marcelli, F. Micciulla (Laur.), R. Pastore (bors., specializ.),
A. Raco (Tecn.), M. Regi (Ass.), A. Tiberia (bors., specializ.)

1 External collaborating Institutions:

Univ. Roma La Sapienza, Univ. Roma Tor Vergata, IHEP-Protvino (Russia), Univ. Pune, India, Burnham Institute (La Jolla, CA, USA), ILL (Grenoble, France).

2 Relevant results achieved:

We continued the study of the stability of the emitted current from field emission of carbon nanotubes, which is a very important constraint for the proposed applications, such as vacuum sensors, electron guns and high-brilliance X-ray sources, based on point-like emitters. We also repeated the measurements of the emitted current for samples obtained using different synthesis methods and conditions. We started sample purification procedures using nitric acid, thermal oxidation, as well as sonication. Fourier Transform Infra Red (FTIR) characterization of the nano-AlN samples produced in collaboration with the Univ. of Pune were performed for both mid-IR (600 - 4000 cm-1) as well as far-IR (200 - 600 cm-1), in collaboration with the LNF Dafne Luce laboratory. In collaboration with the Aerospace Engineering School at the Univ. Rome La Sapienza, we carried out electrical (and started structural and thermal) characterizations of composite materials based on polymeric matrix, with physical performances enhanced by the added filler containing carbon nanotubes, for aerospace applications. In collaboration with the Univ. of Roma Tor Vergata and the Burnham Institute, we characterized carbon nanotube-silica nanobead composite structures for biomedical applications. A PRIN 2006 (Medical Sciences, coordinated by E. Bergamaschi) was recently approved by the MIUR for our collaboration. We also studied the toxicity of nanotubes, in collaboration with the INFN Servizio Medicina del Lavoro and SELEX SI. A project on NMP materials regarding our collaboration with the Finmeccanica nanotechnology group coordinated by C. Falessi, was recently approved by the MoD (Segredifesa). We continued our study of channeling of particle beams in carbon nanotubes.

3 List of Conference Talks by LNF Authors in Year 2006

1. S. Bellucci, "Nanotechnology for Bio-medical and other Applications", International Symposium on Nano-Bio Interface 2006, Calcutta(India), 1-3 March 2006.

2. C. Balasubramanian, "Study of field emission of multiwalled C nanotubes from arc discharge", Boston(USA), 7 May 2006.

3. S. Bellucci, "Nanostructures for Biomedical Applications", Scuola Scienza delle Formulazioni Farmaceutiche, Pula (Italy) 23 May 2006.

4. S. Bellucci, "Carbon Nanotubes: Bio-medical Applications and Cytotoxicity", 28th International Congress on Occupational Health, Milano(Italy) 11-16 June 2006.

5. S. Bellucci, "Nanotechnology Applications in Biology and Medicine", Corso di Formazione su enzimi da ipertermofili e nanotecnologie: aspetti applicativi, IBP-CNR Napoli (Italy) 26-27 June 2006.

6. S. Bellucci, "Carbon Nanotubes: Biomedical Applications and Cellular Toxicity", NanoSEA 2006, Aix-en-Provence(France), 6 July 2006.

7. S. Bellucci, "Applications of Carbon Nanotubes-Silica Nanoparticles Composites to Biology and Medicine", NIS Centro G. Scansetti Torino (Italy), September 19th, 2006

8. S. Bellucci, Electrical properties of CNT based composites for aerospace applications, CANEUS 2006 Conference on Micro-Nano Technologies for Aerospace Applications From Concepts to Systems Toulouse, France Aug. 27 - Sep. 1, 2006.

9. S. Bellucci, Propriet elettriche di nanocompositi per applicazioni aerospaziali", WORKSHOP NANOTECNOLOGIE Dalla diffusione scientifica allevoluzione industriale nei trasporti Sala Auditorium CEA, Orbassano (Torino, Italy)- 10 novembre 2006.

References

1. Bottini M., Bruckner S., Nika K., Bottini N., Bellucci S., Magrini A., Bergamaschi A., Mustelin T., Toxicology Letters, 160, 121 (2006).

2. M. Bottini, C. Balasubramanian, M. I. Dawson, A. Bergamaschi, S. Bellucci, T. Mustelin, J. Phys. Chem. B, 110, 831 (2006).

3. M. Bottini, A. Magrini, A. Di Venere, S. Bellucci, M. I. Dawson, N. Rosato, A. Bergamaschi, T. Mustelin, Journal of Nanoscience and Nanotechnology, 6, 1381 (2006).

4. S. BELLUCCI, C. BALASUBRAMANIAN, A. IVANOV, A. POPOV and H. SCHOBER, Journal of Neutron Research, Vol. 14, No. 4, December 2006, 287291.

5. L Galfetti, L T De Luca, F Severini, L Meda, G Marra, M Marchetti, M Regi and S Bellucci, J. Phys.: Condens. Matter 18 (2006) S1991S2005

6. H.H. Andersen (Bohr Inst.) , S. Bellucci (Frascati) , V.M. Biryukov (Serpukhov, IHEP) . NUCL. INSTRUM. METH. B252 (2006) 1

7. C Balasubramanian, S Bellucci, G Cinque, A Marcelli, M Cestelli Guidi, M Piccinini, A Popov, A Soldatov and P Onorato J. PHYS. COND. MATT 18 (2006) S2095

8. V.T. Baranov, V.M. Biryukov, G.I. Britvich, V.N. Chepegin, Y.A. Chesnokov, V.I. Kotov, A.E. Kushnirenko, V.A. Maisheev, V.A. Pikalov, V.I. Terekhov, V.N. Zapolsky Serpukhov, IHEP S. Bellucci, C. Balasubramanian, G. Giannini Frascati V. Guidi, G. Martinelli, E. Milan Ferrara U. U.I. Uggerhoj Aarhus U. NUCL. INSTRUM. METH. B252 (2006) 32

9. S. Bellucci, S. Balasubramanian, A. Grilli, F. Micciulla, A. Raco (Frascati) , A. Popov (Latvia U., ISSP) , V. Baranov, V. Biryukov, Y. Chesnokov, V. Maisheev (Serpukhov, IHEP) JETP LETT. 83 (2006) 95

10. S. Bellucci J. PHYS. COND. MATT. 18 (2006) S1967

11. S Bellucci and V A Maisheev J. PHYS. COND. MATT. 18 (2006) S2083

12. S. Bellucci, C. Balasubramanian, A. Grilli, F. Micciulla, A. Raco (Frascati) , A. Popov (Riga, Inst. Phys.) , V. Baranov, V. Biryukov, Yu. Chesnokov, V. Maisheev (Serpukhov, IHEP) NUCL. INSTRUM. METH. B252:(2006) 3

13. S. Bellucci NUCL. PHYS. B (Proceedings Supplements) 150 (2006) 339

14. S. Bellucci (Frascati) , V.A. Maisheev (Serpukhov, IHEP) NUCL. INSTRUM. METH. B252 (2006) 339

15. V.M. Biryukov (Serpukhov, IHEP) , S. Bellucci (Frascati) NUCL. INSTRUM. METH. B252 (2006) 7

16. Yu F Zhukovskii, A I Popov, C Balasubramanian and S Bellucci J. PHYS. COND. MATT. 18 (2006) S2045

17. Bellucci S, Balasubramanian C, Micciulla F, Rinaldi G, 2006 Nanotech 2006 Vol. 1, p. 129-133, ISBN 0-9767985-6-5

18. Bellucci S, Balasubramanian C, Giannini G, Marchetti M, Micciulla F, Regi M, 2006 Nanotech 2006 Vol. 3, p. 129-132, ISBN 0-9767985-8-1

PRESS-MAG-O

M. Cestelli Guidi, G. Della Ventura, D. Di Castro, D. Di Gioacchino (Resp.),
A. Marcelli, A. Mottana, M. Piccinini, P. Postorino, P. Tripodi

1 Purposes and *PRESS-MAG-O* Activity

PRESS-MAG-O experiment, one of the 2005 highlights of the INFN Vth Committee, is devoted to the investigation of new materials and new phenomena in condensed matter under extreme conditions. The proposal is based on the R&D of an apparatus that will allow performing ac magnetic measurements and magneto-optic experiments on samples under high pressure and high DC magnetic field in a wide temperature range. The device has been designed to perform experiments using SINBAD, the brilliant IR synchrotron radiation beam line operational at Frascati. A large collaboration is involved in this proposal joining the 'LNF-INFN magneto-dynamic' group, the SINBAD team, the 'High-pressure Raman Spectroscopy group' of the Department of Physics of "La Sapienza" University and the Department of Geological Science of the Roma Tre University. In the second year of the project the main activities of the PRESS-MAG-O collaboration can be summarized as: **a)** the acquisition of the 8 Tesla 'AMI' superconducting magnet device; **b)** the construction of a cryostat for the superconducting magnet with four access ports; **c)** the design of the magnetometer insert for the diamagnetic Diamond Anvil Cell (DAC) based on the SQUID technology. This insert will allow performing both IR experiments and ac susceptibility measurements.

2 Cryostat and superconducting magnet

The 8 tesla split magnet built by AMI Inc. is shown in figure 1 after delivery. The cryostat is characterized by four ports, two of which will be dedicated to infrared optical windows, and allows the insertion from the top of an insert containing a DAC cell equipped with the magnetometer.

Figure 1: *Photograph of the 8 Tesla superconducting split magnet.*

Figure 2: *Two views of the cryostat device.*

The system has been realized in cooperation with the DG-Tecnology Service and is actually under test. Two views of the cryostat are showed in figure 2.

3 PRESS-MAG-O insert

In the last months of 2006 we completed the design of the 'PRESS-MAG-O' insert. A scheme of the system that had to host the DAC cell is showed together with the vertical section of the cryostat in the figures 3A,B. To finalize the design, during the second year we take care of the following aspects: ***I*)** thermal analysis of the contact of the bottom insert with the cryostat cold finger. The contact will be realized by Cu-Be springs on the 'SQUID magnetic screen cylinder' located at the bottom end of the insert. This part will fit in the hole of the cold finger cryostat as illustrated in figures 4A and 4B; ***II*)** magnetic tests of the Nb_3Sn around the SQUID system to screen the stray maximum field of 0.9Tesla at 100 Gauss; ***III*)** design and construction of the pickup coils gradiometer and the related holder for the DAC cell (see figure 5A). The holder will be actually made by a Si chip $0.4 - 0.5$mm tick glued to a Cu or a CuBe block. The chip will be in a thermal contact with the holder of the DAC cell; ***IV*)** design study of the coil geometry and of the field spatial distribution with a field of 10 gauss to evaluate the magnetic response of a sample inside the DAC cell. Simulations have been performed with the OPERA 3D SW package(figure 6) considering that in the middle of the 'PRESS-MAG-O insert' an ac exiting split coil around the DAC cell will be installed (figure 5B). Finally we started the study of the x-y-z micrometric insert positioning system to make possible the alignment within a few microns of the DAC cell to the IR beam of the SINBAD synchrotron radiation beamline.

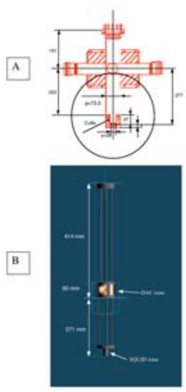

Figure 3: *A vertical section of the cryostat with the insert zone (panel A) and the layout of the 'PRESS-MAG-O INSERT' (panel B).*

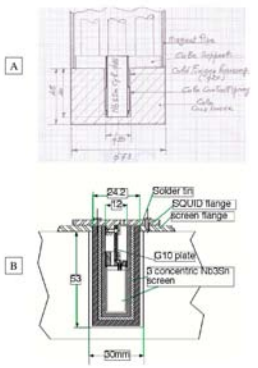

Figure 4: *Layout of the CuBe spring contact between the SQUID and the cryostat cold finger (A panel); The SQUID system flange and the magnetic Nb_3Sn screen (panel B).*

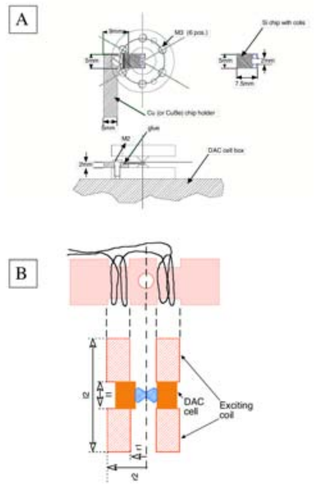

Figure 5: *The gradiometer pick-up coils holder inside the DAC cell (panel A) and the a.c. exciting split coil around the DAC cell (panel B).*

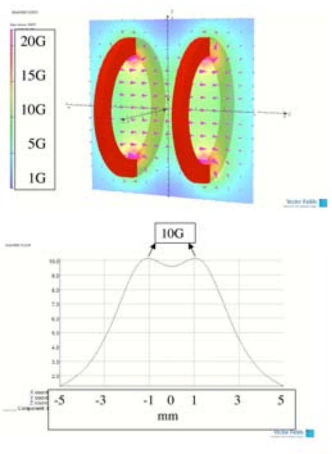

Figure 6: *The spatial distribution of the magnetic field of the split exciting coil.*

References

1. D. Di Gioacchino, P. Tripodi, A. Marcelli, M. Cestelli Guidi, M. Piccinini, P. Postorino, D. Di Castro, "PRESS-MAG-O: a new facility to probe superconducting phenomena under extreme conditions", contribution presented at the Appl. Superconductivity Conference (Seattle, 2006).

R2PC: A PROGRAM TO DEVELOP FREON-LESS PARALLEL PLATE DETECTORS

A. Calcaterra, L. Daniello (Tecn.), R. de Sangro, G. Mannocchi (Ass.)
P. Patteri, M.Piccolo(Resp.), L. Satta (Ass.)

Collaboration with:
INFN Milano and INFN Torino

1 Abstract

Following the work carried out with "CAPIRE" a program to develop large area float-glass parallel plate detectors, that showed vulnerability of glass material to gas mixture containing a sizeable ($\approx$ 50%) quantity R134A, the same collaboration tried during 2006 to develop a parallel plate detector operating with a freon-less gas mixture. The quenching of the streamers was obtained mechanically using an hexcell structure inserted in the gas volume. Results obtained at the BTF are reported,

2 Results

Few chambers have been built using the technique mentioned in the abstract. Fig. 1 shows the building details of this detector.

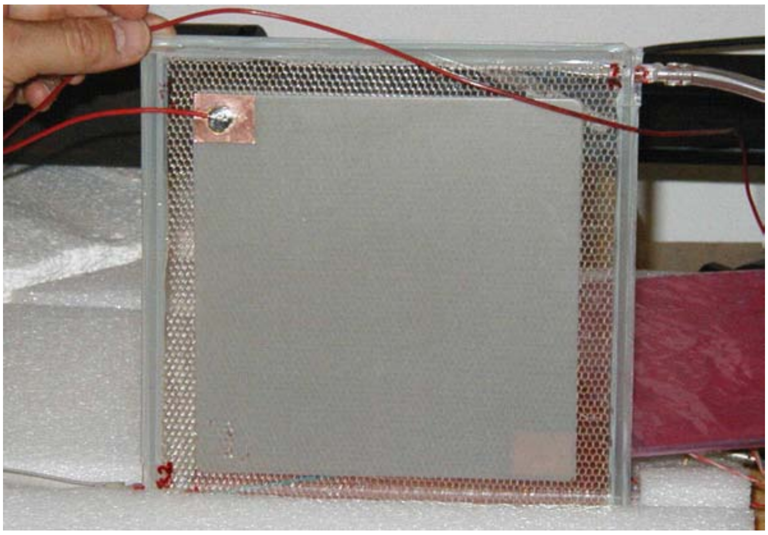

Figure 1: *One of the mechanically quenched parallel plates detectors.*

The Hexcell is a commercially available epoxy impregnated cardboard mainly used as a plane wings filler.

A small telescope of six of these detectors was exposed to the BTF beam to evaluate performances. As a reference a traditional (no Hexcell) chamber was added to the telescope in order to have a direct comparison.

Typical results obtained with single particles hitting the detectors are shown in fig 2 where the response of the different detectors can be seen with a gas mixture containing 92% Ar. 7.5% Isobutane and 0.5% SF_6.

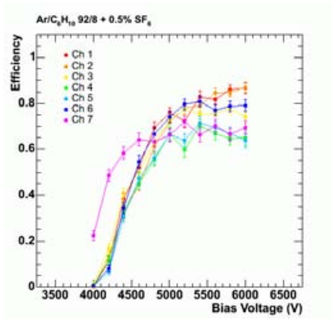

Figure 2: *Plateaux curves for the six detectors built with Hexcell structure in the gas volumes. The curve number 7 refers to a "traditional" RPC.*

The efficiency to detect minimum ionizing particles marginally improves , increasing the amount of isobutane in the mix: fig 3 shows the detectors behavior with a 80% Ar. 19.75% Isobutane and 0.25% SF_6. Unfortunately the detectors we built and operated do not reach 100%

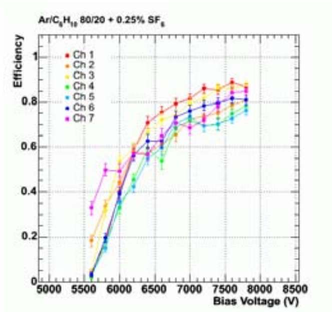

Figure 3: *Plateaux curves for the six detectors built with Hexcell structure in the gas volumes. The curve number 7 refers to a "traditional" RPC.*

efficiency in detecting minimum ionizing particles; an alternative design with only one high resistivity (glass) electrode will be tested shortly to check whether improved performances could be obtained.

SAFTA2

D. Alesini (Art. 23), V. Fusco (Ass.), M. Migliorati (RU),
L. Palumbo (PO), B. Spataro (PR) (Resp.), M. Zobov (PT)

1 Aim of the experiment

The activity of SAFTA2 group is mainly related to the study of the electromagnetic interaction between a particle beam and the accelerator pipe wall of the LHC and SPS machines of the CERN. In both cases the analysis of the results has suggested an optimization of the design in order to obtain acceptable values of the coupling impedance and energy loss.

The activity, done in collaboration with AB/ABP group at CERN, consists in the estimation of the longitudinal and transverse impedance budget, the generation of the parasitic fields, the evaluation of the energy loss and the instability effects. Results obtained with simulations have been compared with analytical estimations and whenever possible with experimental results.

2 Main results of 2006

The energy losses, the parasitic resonances and the longitudinal and transverse impedances of several beam pipe components have been studied with the MAFIA3D, HFSS, ABCI, OSCAR2D and SUPERFISH codes. In particular we have analyzed the modified recombination chambers (Y-chambers) of the LHC, the cold to warm transitions with different geometries for the SPS machine, and the vertical and horizontal beam position monitors for SPS.

The recombination chamber is a piece of equipment which allows the separated beams to merge into a common vacuum chamber surrounding the interaction points. Such a chamber is therefore located in the experimental areas. The chamber is composed of a common cylinder of diameter 180 mm which splits into two smaller cylinders of 54 mm diameter each. Given this particular shape, it is often referred to as the Y-chamber. We already carried out in detail the study of the Y-chamber some years ago [1, 2, 3, 4]. Recently, for beam dynamics reasons it has been decided to modify slightly the smaller vacuum chamber. Therefore, it has been necessary to evaluate again the behaviour of the modified Y-chamber in order to obtain acceptable values of the coupling impedances and energy loss.

In order to reduce strongly the heating of the cold section, the change of the shape and sizes of the previous installed vacuum chamber inside the SPS machine has been required [5]. As a final design study result, the new and innovative cold transition proposed is in OFHC Cu with inner diameter 67 mm and 2232 long. The slots are 2 mm wide, 9.5 mm long with a 1 mm radius at the extremity. The longitudinal distance between the slots axes is 16.3 mm. There are two rows of 132 slots each. In a cross-sectional view the slots are located at 42 and +42 degrees. The numerical calculations have been carried out by using the MAFIA3D code in time domain and by carrying out the Fourier transform of the wake potential for the impedances estimations. Measurements have shown a good agreement with the simulation results [6]. As an interesting result, we strongly reduced the energy losses due to the coupling impedance and we showed that they are mainly caused by the electron cloud effects.

The shape of the warm transition is similar to the previous one, and from the study results no specific problem was determined. In this case the results obtained from simulations with ABCI have been cross-checked with analytical estimations.

Machine studies performed at the CERN SPS in 2003 and 2004 have shown that single-bunch proton beams with low longitudinal emittance are affected by heavy energy losses after less than one synchrotron period as a result of a fast vertical instability. The observed instability indicates that this could be a Beam Break-Up or Transverse Mode Coupling Instability (TMCI) [7, 8].

These observations have triggered a detailed study of the impedance of the main elements of the SPS machine in order to complete the work already started in the longitudinal plane at the end of the nineties to create a data-base of the longitudinal and transverse impedances of the elements of the SPS machine. It has been therefore completed the study of the beam position monitors, installed in some dedicated positions of the SPS machine. Concerning the 108 horizontal and 108 vertical beam position monitors (Fig. 1), simulations with MAFIA3D in time and frequency domain have been performed, revealing the presence of four potentially dangerous transverse trapped modes (two horizontal and two vertical). As a conclusion, the basic parameters of these modes revealed that the TMCI threshold is one order of magnitude higher that the observed one and that the beam position monitors alone cannot explain the observed fast instability.

Figure 1: *SPS beam position monitor slant-cut diagonally.*

3 2007 Activity

It is foreseen the continuation of the activity with the AB/ABP of CERN in order to study additional components to be installed in the SPS machine. In particular it will be investigated the pumping port cavities and other type of beam position monitors.

References

1. B. Spataro et al., "Impedance of the LHC recombination chambers", LHC Project Note 254 (2001).

2. B. Spataro et al., "On trapped modes in the LHC recombination chambers: experimental results", LHC Project Note 266 (2001).

3. B. Spataro et al., "Coupling impedance of LHCb recombination chamber (IR8)", LHC Project Note 348 (2004).

4. B. Spataro et al., "On trapped modes in the LHC recombination chambers: numerical and experimental results", NIM A **517**, 9 (2004).

5. B. Spataro et al., "Impedances of the cold bore experiment, COLDEX, installed in the SPS machine", NIM A **564**, 38 (2006).

6. To be published.

7. E. Métral et al., “Transverse mode coupling instability in the Cern Super Proton synchrotron”, Proc. of EPAC04, Lucerne, Switzerland, 1843 (2004).

8. E. Métral, B. Spataro et al., “The fast vertical single-bunch instability after injection into the Cern Super Proton synchrotron”, Proc. of EPAC 06, Edinburgh, UK, 2913 (2004).

SALAF

D. Alesini (Art. 2222), R. Boni (D.T.), A. Gallo (P.T.), F. Marcellini (T.), M. Migliorati (R.U.)
A. Mostacci (Ass.), B. Spataro (D.T.), L. Ficcadenti (Ass.)

1 Aim of the experiment

The aim of SALAF group is related to the design, realization and measurements of a compact standing wave accelerating structure operating at 11 GHz to be used for linearizing the longitudinal space phase in the Frascati coherent light source (SPARC). Two different structures have been analyzed, the first one is a 9-cell cavity operating on a standing wave mode, and the second one is bi-periodic accelerating section operating on the $\pi/2$ standing wave mode. The standing wave sections have been designed with the HFSS, ABCI, OSCAR2D, SUPERFISH and ANSYS codes. Prototype for both the structures have been built and have been successfully characterized.

2 Periodic π-mode cavity

The 9 cells X-band cavity designed to operate on the π-mode at 11.424 Ghz and to obtain 42 MV/m accelerating gradient with 3 MW of peak input power is fed by a central coupler. The design of the structure, the cavity dimensions and parameters is reported on [1], [2] and [3]. The picture of the brazed periodic cavity [4] is reported in Fig. 1.

Figure 1: *Brazed periodic cavity prototype.*

The transmission coefficient between the small antenna, fixed on the lateral cell, and the central coupler compared with the one of the non brazed prototype is reported in Fig.2, as it is possible to see the brazing procedure has reduced the visibility of the unwanted modes having a zero field in the central cell. The measured dispersion curve before and after brazing, is compared with the one from HFSS simulation in Fig.2. The quality factor of the operating π-mode has been measured on the brazed structure and compared with both the one measured on the non brazed cavity and the one calculated by HFSS and SUPERFISH codes as we can see in Tab.1.

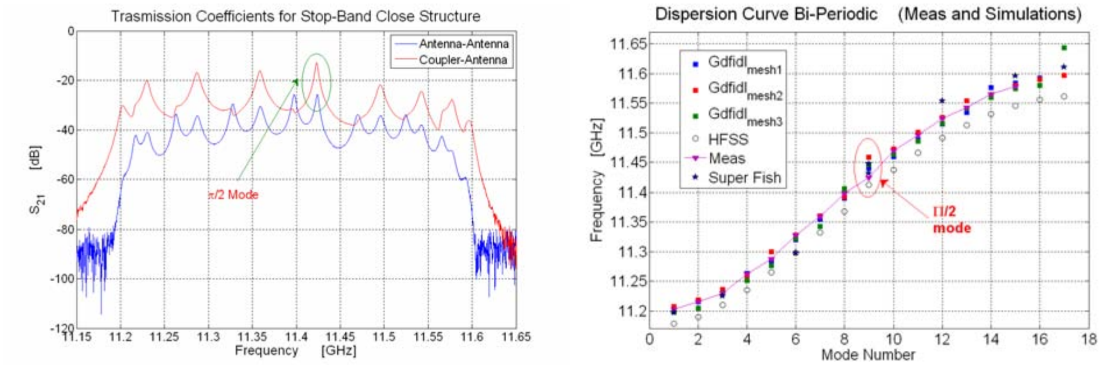

a) *b)*

Figure 2: *a)Transmission coefficient between the lateral antenna and the central coupler, b) Dispersion curve before and after brazing.*

Table 1: *Quality and form factors measured before (I) and after (II) brazing on the prototype compared with the numerical results.*

	HFSS	Superfish	Meas I	Meas II
$f_0(Ghz)$	11.4244	11.4240	11.4239	11.4244
Q_0	8500	8070	7900	8066
$R/Q(\Omega/m)$	9138	9232	9440(90)	9070(20)

With the bead pull technique we measured the electric field on axis. To calculate R/Q we have calibrate the bead form-factor in simple pillbox cavity. The measured longitudinal electric field on axis, for the brazed prototype, compared with the one of the non brazed cavity, is plotted in Fig.3. The field flatness is of the order of 4% at the measured frequency of 11.4244 Ghz. The measured R/Q per unit length is reported in Tab.1.

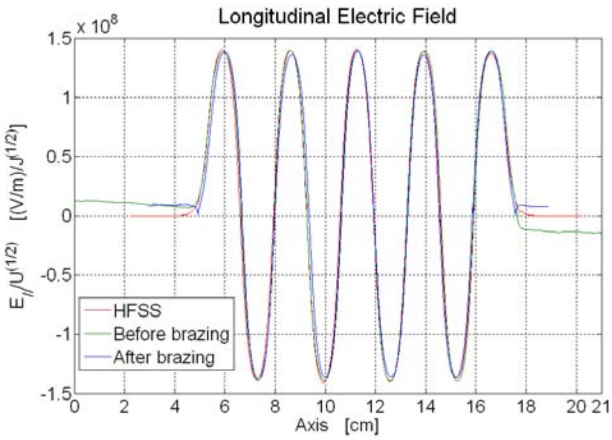

Figure 3: *Measured longitudinal electric field on axis.*

3 Bi-Periodic $\pi/2$-mode cavity

The proposed 17 cells $\pi/2$-mode accelerating section represents an alternative design to the standard π-mode cavity, as the lower sensitivity (of the cavity field distribution and resonant frequency) to the machining errors, cell-to-cell temperature variations and assembly errors. The price to be paid is a lower shunt impedance per unit length and major fabricating costs because of the presence of the coupling cells, with respect to the π-mode structure. As the periodic structure this cavity is design to obtain 5 MV accelerating voltage with an input power of 3 MW and is fed by a central coupler. The design of the structure, the cavity dimensions and parameters is reported on [5] and [6]. The 2D design have been performed using SUPERFISH code and 3D simulation code (HFSS and GDFIDL) have been used to design a proper feeding system for the cavity in the central cell. The full scale copper prototype has been constructed and it is shown in Fig.4. To feed the structure two lateral small antennas are also inserted (position 1,2 of Fig.5)

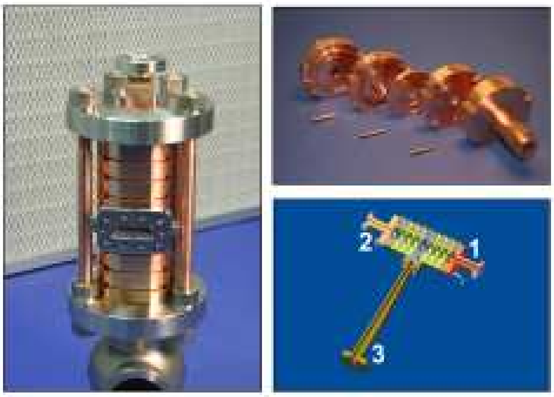

Figure 4: *Copper prototype of the structure.*

The transmission coefficient between the two small lateral antennas and between the antennas and the central coupler (position 3 of Fig.4) have been measured both in the stop-band open and stop-band close structures. We can excite only nine over seventeen possible modes by central coupler because we impose a non-zero field in the central cell. On the contrary with the two antennas we can excite all the possible modes as reported in Fig.5 in stop-band close case.

The quality factor of the resonance has been measured and compared with the numerical ones. The Q factor of the $\pi/2$ mode in the case of stop-band close is reported in Tab.2; the measured Q is lower than the calculated ones since the cavity are not brazed yet. The measured dispersion curve, compared with the one obtained from HFSS, GDFIDL and SUPERFISH, is reported in Fig.6.

With the bead pull technique we measured the electric field on axis. To calculate R/Q we have calibrated the bead form-factor in a pillbox cavity working at 1.91 GHz on the TM010 mode. Using different resonant modes of the pillbox cavity we also checked that the form factor does not depend on the frequency, within our measure uncertainty. The measured longitudinal electric field on axis, for the stop-band close structure, is plotted in Fig.7. The tuning procedure allow a field-flatness of the order of 3% at the nominal resonant frequency of 11.424 Ghz. The measured R/Q per unit length is reported in Tab.2 and it is in very good agreement with the simulation results.

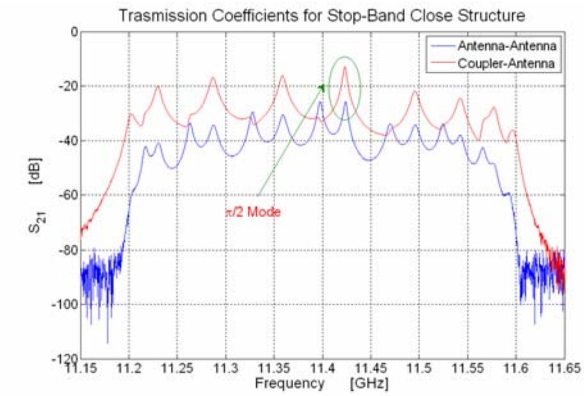

Figure 5: *Transmission coefficient between the two lateral antenna in stop-band close case.*

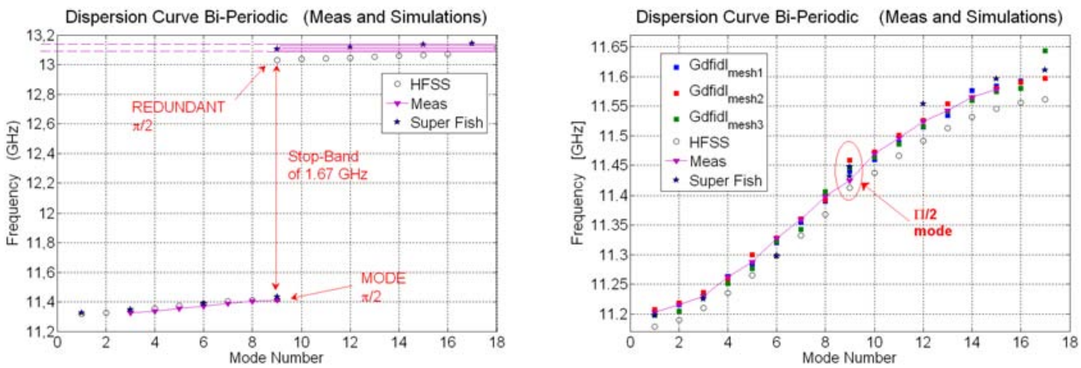

Figure 6: *Measured dispersion curve in the case of: a) stop-band open and b) stop-band close, compared to simulation results.*

Table 2: *Quality and form factors measured on the stop-band close prototype compared with the numerical results.*

	HFSS	Superfish	Meas
Q_0	7412	7101	5815
$R/Q(\Omega/m)$	9452	9639	9150200

4 Activity 2007

The continuation on the design and realization of the linear accelerating structures is foreseen in order to determine the final choice of the section to be installed on the SPARC LINAC. In particular the behaviour of the thermal stress will be investigated in detail with simulations and by comparing the results with dedicated measurements. In order to get a satisfactory know-how on the design and realization of the linac sections at high frequency, more investigations will be made on the brazing and electroforming procedures.

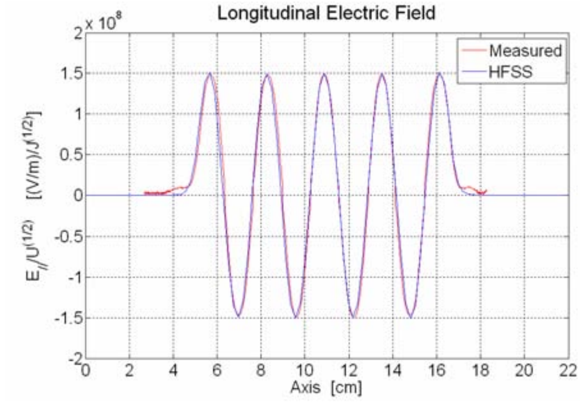

Figure 7: *Measured longitudinal electric field on axis.*

References

1. D. Alesini *et al.*, "Design and RF measurement of an X-band accelerating structures for linearizing the longitudinal emittance at SPARC", Nucl. Inst. And Meth. A 554 (2005) 1-12.

2. A. Bacci *et al.*, "An X-Band structure for longitudinal emittance correction at SPARC", LNF-03/008 (R), LNF-INFN, 6 May 2003.

3. D. Alesini *et al.*, "Design and RF measurement of an X-band accelerating structures for linearizing the longitudinal emittance at SPARC", LNF-05/07 (P), LNF-INFN, 19 May 2005.

4. P. Chimenti *et al.*, "First results on vacuum brazing of RF, 11Ghz, linear accelerating structures at Frascati laboratory",LNF-05/22 (IR), LNF-INFN, 14 November 2005.

5. B. Spataro *et al.*, "Studies on a Bi-Periodic X-band structure for SPARC", LNF-03/013 (R), LNF-INFN, 25 August 2003.

6. D. Alesini *et al.*, "R&D on X-band accelerating structures at the INFN-LNF", SPARC-RF-06/002, LNF-INFN, 27 February 2006.

SI-RAD

L.Bongiorno (Bors.), M.A.Franceschi, G.Mazzenga (Tecn.), M.Ricci (Resp.), B.Spataro

Participant Institutions:

ITALY: INFN LNF, Firenze, Roma Tor Vergata, Trieste; University of Genova
GERMANY: SIS (Darmstadt)
RUSSIA: MePhi, IBMP, RKK "Energia" (Moscow)
SWEDEN: KTH (Stockholm)
ESA European Astronaut Center

1 Introduction

The SI-RAD experiment is a continuation of the activities carried out for the experiments SIEYE1 and SIEYE2 on board the Russian Space Station MIR and for the experiments SIEYE3/ALTEINO on board the International Space Station (ISS) in the years 1995-2002 [1) 2) 3) 4) 5)].

The experimental task of the SI-RAD experiment is to develop a detector to be placed on the external part of the ISS. The detector will be used to monitor cosmic rays and radiation environment in Low Earth Orbit. Long (Solar modulation) and short (coronal mass ejections, orbit dependence) of the particle flux and the dose absorbed by the astronauts will be monitored. In addition, data will be compared with measurements taken inside the ISS with ALTEA (see below) and ALTEINO detectors to validate radiation transport and dose estimation codes. At the same time, the investigation, with a more sophisticated instrument, of the "Light Flashes" phenomenon [6)], will be conducted to improve and refine the results obtained with the previous SIEYE experiments.

To meet these goals, a precursor mission in space with a high performance cosmic ray detector, LAZIO/SIRAD [7)], has been accomplished to measure and identify all particles traversing the detector separating nuclei from electrons/positrons, in the energy range ~ 10 to $\sim 100 MeV$. LAZIO/SIRAD has been launched in April 2005 on a Soyuz rocket and placed aboard the ISS by the italian astronaut Roberto Vittori. We refer to the previous Annual Report LNF 2005 for details on this mission [8)].

Moreover, in July 2006, the ALTEA experiment [9)], launched with the Space Shuttle Discovery, has been placed on board the ISS by the Swedish astronaut Christoph Fuglesang and has started taking data one month later.

The preparation of the next SI-RAD extended mission is advancing towards the completion of the full flight instrument consisting of a 16-plane tower of double-sided silicon detectors (8x8 cm^2 area) equipped with trigger and anticoincidence counters. The total weight is about 15 kg and the total power consumption should not exceed 30 W. The hardware set-up is accomplished through three steps by the construction of a laboratory prototype model, an engineering model and the final flight, space qualified model. The activity in 2006 has been focused on the development of the following systems of the engineering model:

- Trigger system.
- Development of Silicon Photomultiplier (SI-PM) technology for space applications and test of different SI-PM configurations at the LNF-BTF beam.

- Completion of a highly integrated silicon board (16 cm x 16 cm).
- Production and test of a low-power, low-mass Digital Processing Unit (DPU).

Starting from 2007, the SI-RAD acronym will be replaced by a new one, ALTCRISS (Alteino Long Term monitoring of Cosmic Rays on the International Space Station), meaning that all the described activities on board the International Space Station will be coordinated as branches of one same scientific and technological program. In 2007, the planned activity includes the completion of the engineering SI-RAD unit and the set-up of the flight configuration equipped with autotrigger capabilities for heavy nuclei and a trigger for crossing protons and nuclei. The interface with the ISS Space Station will be realized with an intermediate CPU to manage the telecommands from ground and the download of the data. Beam tests at the LNF-BTF, GSI/Darmstadt and other facilities are also planned together with the continuation of the R&D on the SI-PM technology.

2 Activity of the LNF group

The LNF group has taken the responsibility of the design, construction and test of the mechanical structures and interfaces of the three models of the detector also contributing to the integration of the mechanical support for the DAQ. This activity is carried out with the support and the participation of the LNF Service of Development and Costruction of Detectors (SSCR). The activity in 2006 has been mainly devoted to the completion of the mechanical support of the engineering model and to the interfaces of the front-end and DAQ with the detector. These systems will be developed for the final space-qualified flight configuration in the year 2007. The LNF group participates as well in the beam test activities at the above mentioned facilities having the responsibility of the beam trigger counters.

3 Selection of publications in 2006

1. M. Casolino *et al.*,“Relative nuclear abundances inside ISS with Sileye-3/Alteino experiment”, Adv. Space Res. **37**, 1685 (2006).
2. M. Casolino *et al.*,“Detector response and calibration of the cosmic-ray detector of the Sileye-3/Alteino experiment”, Adv. Space Res. **37**, 1691 (2006).

References

1. V.Bidoli *et al.*,“In-flight performances of SilEye-2 Experiment and cosmic ray abundances inside space station MIR”; Journal of Physics G: Nuclear and Particle Physics **27**, 2051(2001).
2. S.Avdeev *et al.*,“Eye light flashes on the Mir Space Station”; Acta Astronautica, **50**, 511 (2002).
3. M.Casolino *et al.*,“The Sileye/3-Alteino experiment on board the International Space Station”; Nucl.Phys. **113B**, 88 (2002).
4. V.Bidoli *et al.*, “Dual origin of light flashes in space”, Nature **422**, 680 (2003).
5. P.Maponi *et al.*,“A syncitium model for the interpretation of the phenomenon of anomalous light flashes occurring in the human eye during space missions”, Nuovo Cim., **116B**, 1173 (2001).

6. G. Horneck, "Radiobiological experiments in space: a review", Nucl. Tracks Radiat. Meas., **20**, 185 (1992).

7. F.Altamura *et al.*,"Preliminary results from the LAZIO-Sirad experiment on board the International Space Station", Proc. XXIX ICRC, Pune (2005), SH35 p.101.

8. "LNF 2005 Annual Report", LNF-06/10 (IR), March 2006.

9. L.Narici *et al.*,"ALTEA: Anomalous long term effects in astronauts. A probe on the influence of cosmic radiation and microgravity on the central nervous system during long flights", Adv. Space Res. **31**, 141 (2003).

DAΦNE

The DAΦNE Team: D. Alesini, M.E. Biagini, C. Biscari, R. Boni, M. Boscolo, B. Buonomo, A. Clozza, G. Delle Monache, E. Di Pasquale, G. Di Pirro, A. Drago, L. Falbo, A. Gallo, A Ghigo, S. Guiducci, M. Incurvati, P. Iorio, C. Ligi, F. Marcellini, C. Marchetti, G. Mazzitelli, C. Milardi, L Pellegrino, M. Preger, L. Quintieri, P. Raimondi, R. Ricci, U. Rotundo, C. Sanelli, M. Serio, F. Sgamma, B. Spataro, A. Stecchi, A. Stella, S. Tommasini, C. Vaccarezza, M. Vescovi, M. Zobov

The DAΦNE Technical Staff: G. Baldini, P. Baldini, A. Battisti, A. Beatrici, M. Belli, B. Bolli, A. Camiletti, G. Ceccarelli, R. Ceccarelli, A. Cecchinelli, S. Ceravolo, R. Clementi, O. Coiro, S. De Biase, M. De Giorgi, N. De Sanctis, R. Di Raddo, M. Di Virgilio, G. Ermini, G. Fontana, U. Frasacco, C. Fusco, F. Galletti, M. Giabbai, O. Giacinti, E. Grossi, F. Iungo, R. Lanzi, V. Lollo, V. Luppino, M. Marchetti, C. Marini, M. Martinelli, A. Mazzenga, C. Mencarelli, M. Monteduro, A. Palleschi, M. Paris, E. Passarelli, V. Pavan, S. Pella, D. Pellegrini, R. Pieri, G. Piermarini, G. Possanza, S. Quaglia, F. Ronci, M. Rondinelli, F. Rubeo, M. Sardone, M. Scampati, G. Sensolini, R. Sorchetti, A. Sorgi, M. Sperati, A. Sprecacenere, P. Tiseo, R. Tonus, T. Tranquilli, M. Troiani, V. Valtriani, R. Zarlenga, A. Zolla

1 Introduction

DAΦNE is an "electron-positron factory" operating at Frascati since 1997. Factories are storage rings for electrons and positrons delivering a high rate of mesons to high resolution experiments which require an extremely large number of events. To reach such high rates, the factories are designed to work at the energies of the meson resonances, where the production cross section peaks. To obtain the required production rate it is also necessary that the collider luminosity (the number of events per unit time of the reaction under investigation divided by its cross section weighted by the acceptance of the detector) is very high, between one and two orders of magnitude larger than that obtained in the conventional colliders with a single ring, where electrons and positrons run on the same orbit in opposite directions. When sharing the same ring the two N-bunch trains cross in 2N points and the maximum obtained luminosity is limited by the electromagnetic beam-beam interaction. The unwanted effects of this interaction can be reduced with a very strong focussing (called "low-β") at each of the crossing points, obtained by means of quadrupole doublets or triplets. At the same time these magnetic structures take up much room and excite chromatic aberrations which must be corrected elsewhere in the ring. A large number of bunches can be stored only with twice the number of low-β points and due to the compactness of the DAΦNE machine only two of these regions can be realized, and therefore only a single electron bunch and a single positron one could be stored in a single ring.

This limitation does not hold for the double ring option, consisting in two separate rings crossing at two low-β points. The number of bunches that can be stored in such a collider is limited only by the geometry of the IR's.

DAΦNE is a system consisting of a double-ring collider, a linear accelerator (LINAC) an intermediate damping ring to make injection easier and faster and 180 m of transfer lines connecting these machines. The beam accelerated by the Linac can also be switched into a laboratory called "BEAM Test Facility BTF)", for dedicated experiments and calibration of detectors. The accelerator complex has been designed to fit into the existing ADONE buildings (ADONE was the 3 GeV center of mass electron-positron collider in operation at LNF from 1969 to 1993); the complex is shown schematically in Fig. 1.

In the DAΦNE collider the two beam trajectories cross at the interaction point (IP) at an angle of ≈1.5 degrees in the horizontal plane. A positron bunch leaving the IP after crossing an electron one will reach the following electron bunch at a distance of half the longitudinal separation between bunches from the IP. Due to the horizontal angle between the trajectories of the two beams, the distance in the horizontal direction between the two bunches is equal to the horizontal angle times half the longitudinal distance between the bunches in the beam. The beam-beam interaction can be harmful to the beam stability even if the distance in the horizontal direction between bunches of opposite charge is of the order of few bunch widths at points where the β function is high and this sets a lower limit on the bunch longitudinal separation and therefore on the number of bunches which can be stored in the collider. For DAΦNE the minimum separation is 80 cm, and the maximum number of bunches to be stored in each ring is 120. This number determines the frequency of the radiofrequency cavity which replaces at each turn the energy lost in synchrotron radiation, which must be 120 times the revolution frequency. The luminosity of the collider can therefore be up to 120 times larger than that obtainable in a single ring with the same size and optical functions.

Crossing at an angle could in principle be a limitation to the maximum single bunch luminosity. In order to make the beam-beam interaction less sensitive to this parameter and similar to the case of single ring colliders where the bunches cross head-on, the shape of the bunches at the IP is made very flat (typical r.m.s. sizes are 30 mm in the longitudinal direction, 2 mm in the horizontal and 0.01 mm in the vertical one).

The double ring scheme with many bunches has also some relevant drawbacks: the total current in the ring reaches extremely high values (5 A in the DAΦNE design) and the high power emitted as synchrotron radiation (≈50 KW) needs to be absorbed by a complicated structure of vacuum chambers and pumping systems in order to reach the very low residual gas pressure levels necessary to avoid beam loss. In addition, the number of possible oscillation modes of the beam increases with the number of bunches, calling for sophisticated bunch-to-bunch feedback systems.

The double annular structure of the DAΦNE collider is shown schematically in Fig. 2.

Both rings lay in the same horizontal plane and each one consists of a long external arc and a short internal one. Starting from the IP the two beams travel together inside a common vacuum chamber and their distance increases until it becomes ≈12 cm at the level of the magnetic separators called "splitters" (SPL). These are special magnets with two regions of opposite field which deflect the two beams in opposite directions, allowing them to reach the separate vacuum chambers of the long and short arcs. Each arc consists of two "almost achromatic" bends (deflecting the beam by 81 degrees in the short arc and 99 degrees in the long one) similar to those frequently used in synchrotron radiation sources, with a long straight section in between. Each bend consists of two dipoles, three quadrupoles, two sextupoles and a wiggler. This structure is used for the first time in an electron-positron collider and it has been designed for the particular requirements of DAΦNE: the amount of synchrotron radiation power emitted in the wigglers is the same as in the bending magnets and the wigglers can be used to change the transverse size of the beams. The increase of emitted power doubles the damping rates for betatron and synchrotron oscillations, thus making the beam dynamics more stable, while the possibility of changing the beam sizes

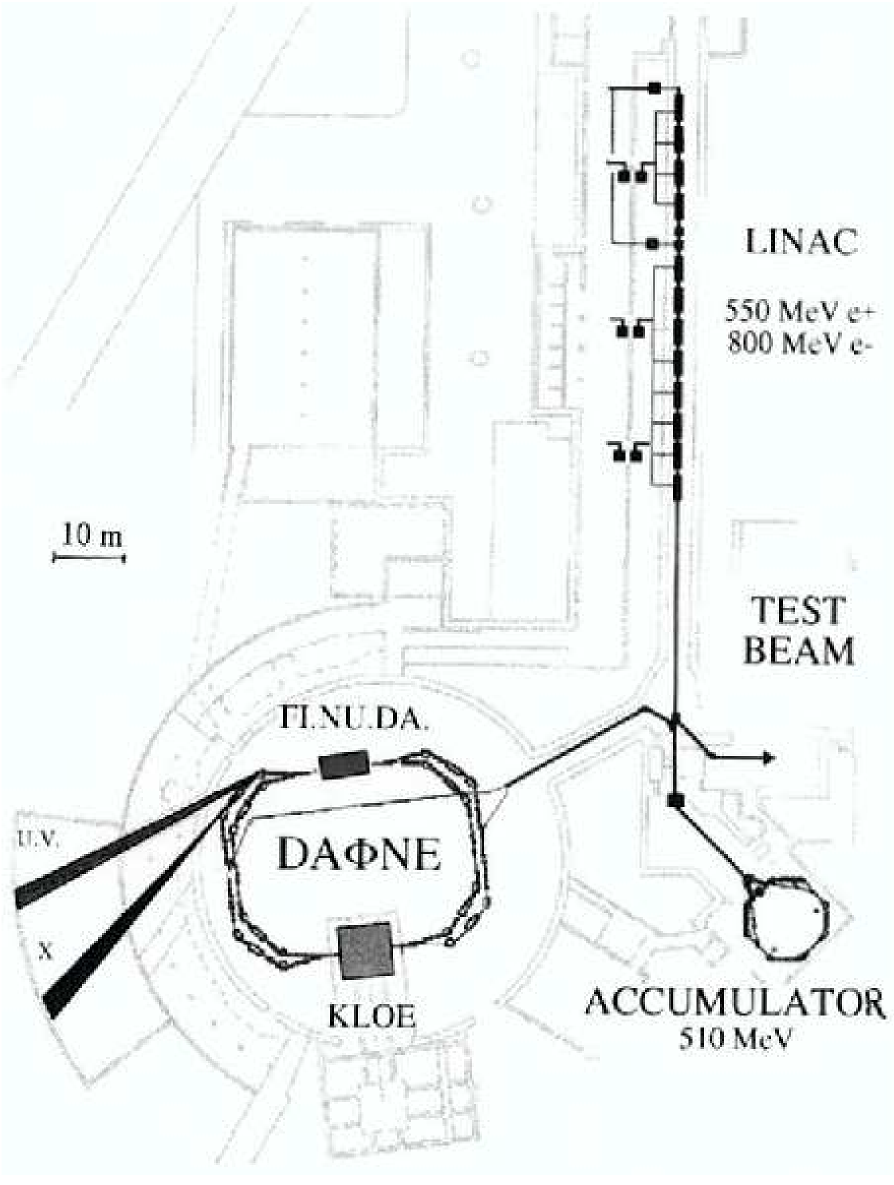

Figure 1: *The layout of the DAΦNE accelerator complex inside its buildings.*

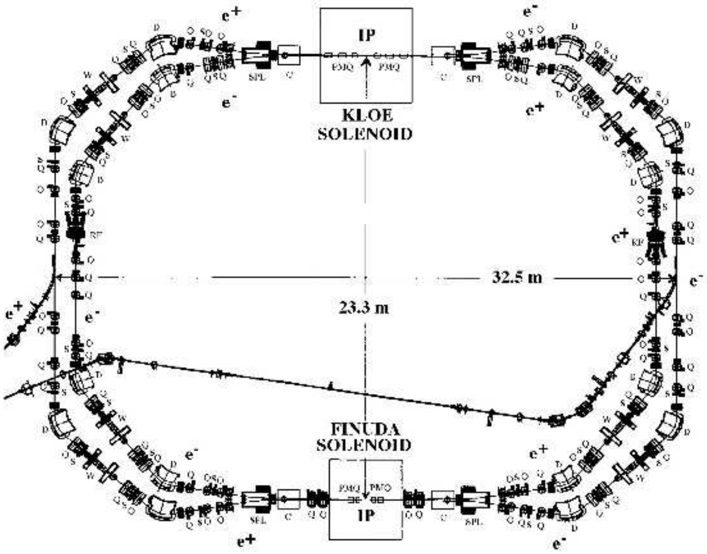

Figure 2: *The DAΦNE Main Rings.*

makes the beam-beam interaction parameters more flexible.

The straight section in the long arc houses the pulsed magnets used to store into the rings the bunches coming from the injection system, while in the short straight arc there are the radiofrequency cavity and the equipment for the feedback systems which are used to damp longitudinal and transverse instabilities.

The most delicate part of the whole structure are the IR's. The collider can host two experiments, even if up to now only one at a time can get useful luminosity. Three detectors have been realized, KLOE, DEAR and FINUDA. KLOE is permanently installed in the first IP, while DEAR and FINUDA are alternatively running on the second one. The detectors of KLOE and FINUDA are surrounded by large superconducting solenoid magnets for the momentum analysis of the decay particles and their magnetic fields represent a strong perturbation on the beam dynamics. This perturbation tends to induce an effect called "beam coupling", consisting in the transfer of the betatron oscillations from the horizontal plane to the vertical one. If the coupling is not properly corrected, it would give a significant increase of the vertical beam size and a corresponding reduction of luminosity. For this reason a superconducting solenoid magnet with half the field integral of the detector one and of opposite direction is placed near each splitter in such a way that the overall field integral in the IR's vanishes. However, this is not sufficient to obtain full compensation of the beam coupling induced by the main solenoids. In the case of KLOE the low-β at the IP was originally designed with two quadrupole triplets. Due to the flat shape of the beam at the IP, the low-β is realized only in the vertical plane. The quadrupole cannot be of the conventional electromagnetic type for two reasons: the first is that the iron of the joke would degrade the flatness of the magnetic field in the detector and the second is that the overall transverse size of a conventional quadrupole is at least twice its useful aperture. Therefore quadrupoles realized with permanent magnets have been built, which exhibit an excellent field quality, very small transverse size and are fully transparent to external fields. The region of space around the IP occupied by machine elements, which is unavailable for the detection of decay particles by the experiment consists in two cones with the vertex at the IP and a half aperture of only 9 degrees. In order to obtain a good compensation of the above mentioned coupling effects induced by the solenoids, these quadrupoles are rotated around their longitudinal axis by angles between 10 and 20 degrees and are provided with actuators to finely adjust their position and rotation.

The structure of the FINUDA IR is quite similar. Since its superconducting solenoid magnet has half the length (but twice the field) of the KLOE one, the low-β focusing at the IP is obtained by means of two permanent magnet quadrupole doublets inside the detector and completed with two other conventional doublets outside. Both IR's have been further modified during the 2003 shutdown.

The DEAR experiment, which was installed on the IR opposite to KLOE, took data during the years 2002-2003. It does not need magnetic field and therefore only conventional quadrupoles were used for the low-β. FINUDA rolled-in at DEAR's place in the second half of 2003 and took data until spring 2004. It was then removed from IP2 in order to run the KLOE experiment with only one low-β section at IP1.

Two synchrotron radiation lines, one from a bending dipole and the other from the wiggler are routinely operated by the DAΦNE-LIGHT group in a parasitic mode, providing to users radiation from the infrared to soft x-rays.

The vacuum chambers of the arcs have been designed to stand the high level of radiation power emitted by the beams (up to 50 KW per ring): they consist of 10 m long aluminum structures built in a single piece: its cross section exhibits a central region around the beam and two external ones, called the antechambers, connected to the central one by means of a narrow slot. In this way the synchrotron radiation hits the vacuum chamber walls far from the beam and the desorbed gas particles can be easily pumped away. The chambers contain water cooled copper absorbers placed where the radiation flux is maximum: each absorber has a sputter ion pump below and a titanium sublimation pump above.

The single cell copper radiofrequency cavities, one in each ring, are capable of running at 368 MHz and 250 KV and are designed with particular care to avoid high order modes which could induce longitudinal instabilities in the particular multibunch structure of the beams. This is obtained by means of external waveguides terminated on 50Ω loads. A sophisticated longitudinal feedback has, however, been built to maintain a reasonable safety margin on the threshold of multibunch instabilities. The system is based on the digital signal processing technique and acts on each single bunch individually. Additional feedback systems on the betatron motion have been also realized following the observation of coherent instabilities during collider operation.

The correct superposition of the beams at the IP is of course critical for the luminosity of the ring. For this reason, 46 beam position monitors are available in each ring and 31 small dipoles can be used to steer the beam and correct orbit distortions caused by alignment errors or wrong currents in the magnetic elements by means of sophisticated software procedures implemented in the Control System of the collider. Additional beam diagnostics are two synchrotron radiation outputs, from which the transverse and longitudinal size of the beam can be measured, total beam current monitors and strip-line pickups delivering the charge of each bunch.

In a low energy electron-positron collider, such as DAΦNE, the lifetime of the stored current is mainly limited by the Touschek effect, namely the particle loss due to the scattering of the particles inside the bunches. In the present operating conditions it is of the order of half an hour. It is therefore necessary to have a powerful injection system, capable of refilling the beam without dumping the already stored one. In addition, flexibility of operation requires that any bunch pattern can be stored among the 120 available buckets. The injection system of DAΦNE is therefore designed to deliver a large rate of particles in a single bunch at the working energy of the collider.

It consists of a linear accelerator (LINAC, see Fig. 1) with a total accelerating voltage of 800 MV. In the first section electrons are accelerated to $\approx$250 MeV before hitting a tungsten target (called positron converter) where positrons are generated by bremsstrahlung and pair production with an efficiency of ≈1%. The positrons exit from the target with an energy of few MeV and are then accelerated by the second section of the LINAC to their final energy of ≈0.51 GeV. The positrons are then driven along a transfer line and injected into a small storage ring, called Accumulator, at a frequency of 25 Hz. Up to 19 positron pulses are stacked into a single bucket of the Accumulator, then injection stops and the bunch damps down to its equilibrium beam size and energy spread, which are much smaller than the LINAC ones. Damping takes ≈0.1 seconds and then the beam is extracted from the Accumulator and injected into the positron main ring at an overall repetition rate of 2 Hz. A powerful and flexible timing system allows the storage of any desired bunch pattern in the collider. In the electron mode, the converter is extracted from the LINAC and electrons are directly accelerated to 0.51 GeV and injected into the Accumulator in the opposite direction with respect to positron operation. They are then extracted like in the positron case and injected into the electron main ring through the second transfer line.

The Accumulator has been introduced for the following reasons. The first is that the LINAC can deliver 10 ns pulses with a charge of ≈1 nC. Since the design charge of the main ring at the maximum luminosity is 1.5 μC and the longitudinal acceptance of the main rings is only 2 ns, the number of pulses necessary to fill the ring is of the order of 10^4. In order to avoid saturation it is therefore necessary that at each injection pulse a fraction smaller than 10^{-4} of the already stored beam is lost, and this is not easy to achieve. The Accumulator instead can work with a lower frequency RF cavity and therefore with a larger longitudinal acceptance. In this way the full charge coming from the LINAC can be stored. The number of pulses into the Accumulator is only 19, and after damping the whole charge stacked into an Accumulator bunch can be stored into the main ring. In this way a single main ring bucket can be filled with only one pulse from the Accumulator, reducing to 120 the number of injection pulses into each main ring. As an additional benefit, the transverse beam size and energy spread of the beam coming from the Accumulator are at least one order of magnitude smaller than those of the LINAC beam, and this strongly reduces the aperture requirements of the main ring and, as a consequence, the overall cost of the collider.

2 DAΦNE main changes during 2003

During the six months shutdown occurred in 2003 the main machine modifications can be summarized as follows:

- KLOE IR extraction and reassembling according to a modified optics design and vacuum chamber upgrade: the IR lattice was changed from a a triplet to a doublet structure in order to have the same low-β^* characteristics while lowering the chromaticity with an overall improvement of the beam lifetime and beam-beam performance. At the same time the increased tunability of the low-β^* lattice allows to double the number of colliding bunches (from 50 t0 100) avoiding the parasitic crossings drawback on the luminosity.

- FINUDA detector installation, together with the insertion of a new Be vacuum chamber and four Permanent Magnet (PM) quadrupoles; as for the KLOE IR, the mechanics has been modified in order to allow for full rotation of the PM quadrupoles.

- wiggler magnets modification to increase the width of the good quality field region and get rid of the high order terms of the magnetic field. Yhe main effect on the beam dynamics is a strong octupole term contribution affecting the dynamic aperture of the ring. A reduction of the octupole term by a factor ≈2.5 turned out from the measurements.

Further details of the overall machine modifications performed in 2003 can be found in the previous LNF Activity Report. In the following section the activities carried on during the year 2004 are described in detail.

3 Year 2006 activity

In March 2006 the KLOE experiment completed its data taking. The total integrated luminosity between May 2004 and November 2005 at the Φ resonance energy of 1020 MeV was $2fb^{-1}$ with a maximum peak luminosity of $1.53 * 10^{32} cm^{-2} s^{-1}$ and a maximum integrated luminosity per day of $\approx 10pb^{-1}$. Between November 2005 and March 2006, according to the KLOE experiment requirements, the accelerator has been set up for runs at different energies (between 1000 and 1030 MeV). The total integrated luminosity at these different energies has been $\approx 300pb^{-1}$. The evolution of the DAΦNE peak and daily integrated luminosity since April 2004 is reported in Fig. 3 and Fig. 4. The last bins with lower integrated luminosity correspond to the off-energy operations.

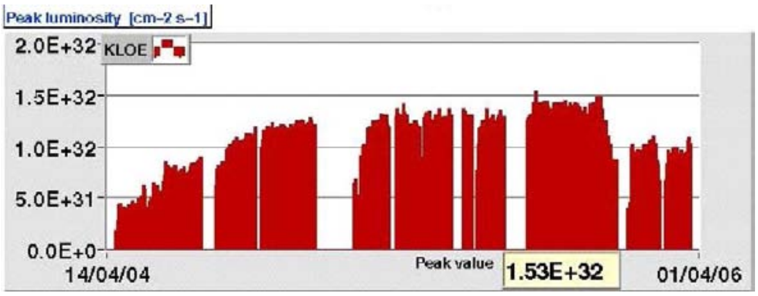

Figure 3: *Evolution of the DAFNE peak luminosity since April 2004 (KLOE run).*

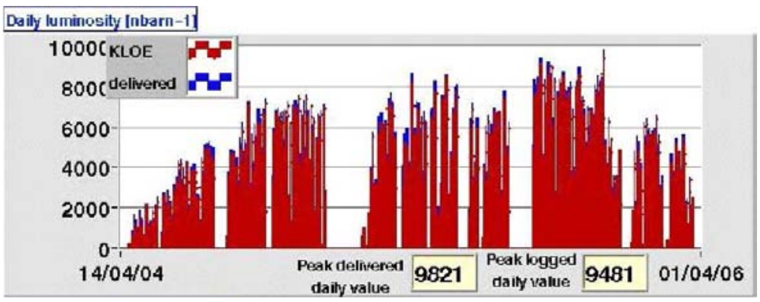

Figure 4: *Daily integrated luminosity during the KLOE run. It exhibits a steady improvement and its maximum value of 10 pb-1 per day has been obtained in November 2005. The last bins with lower integrated luminosity correspond to the off energy operations.*

In the last two weeks of March 2006 dedicated runs for machine studies have been done. All machine studies were aimed at improving DAΦNE performance for the next FINUDA run and at defining design criteria for an upgraded machine. In particular the following measurements have been done:

- detailed study of background to KLOE during injection;

- test on the wires for Beam Beam Long Range interaction compensation;
- analysis of the KLOE background as a function of the scrapers position;
- test of the new transverse feedback in the e+ vertical plane;
- injection from the Linac without the chicane downstream the e+ converter;
- test on the new acquisition system for the single turn orbit measurements;
- test on the timing system to control the new power supply of the BTF pulsed magnet;
- bunch length measurements with a large negative momentum compaction (≈ -0.036) optics;
- optics measurements on the Transfer Lines.

Figure 5: *Wiggler cooling system upgrade.*

In the following shutdown, started on April 2006 and finished on September 2006 the following operations have been done:

- the KLOE detector has been removed from the collider and parked in the KLOE hall. At the same time its interaction region (IR) has been replaced with a straight section equipped with electromagnetic quadrupoles. With this new section the collider has only one low beta point at the FINUDA IR with smooth optical functions in the other one, allowing for a more efficient separation of the two beams;
- maintenance of the LINAC, cooling, vacuum, RF and control systems, magnet power supplies, cryogenic and electric plants. In particular all the spigots (input of water cooling to the coils, ≈ 150 in each wiggler), which were the main source of downtime due to magnet faults, have been replaced with new ones of improved design (Fig. 5).

Figure 6: *ICE removed from e- wigglers.*

- removal of the ion clearing electrodes (ICE) in the e- ring wigglers with a dedicated positioning and cutting system (Fig. 6). This operation has been done in order to reduce the e- ring beam coupling impedance, thus increasing the current threshold of vertical beam blow up due to microwave instability and the current threshold of the quadrupole instability that limited the longitudinal feedback performances;
- upgrade of the feedback system with the implementation of a third generation digital system. The new device is extremely compact, it has gain and phase digital and remote control, allows to manage any betatron or synchrotron tunes monitoring real time parameter and it is less sensitive to large oscillations at injection;
- upgrade of the control system with new CS servers, implementation of new front-end processors (Pentium/Linux), extension of the CS Ethernet network in the LINAC area, BTF experimental hall, Damping Ring area, DAΦNE hall;
- roll-in of the FINUDA Experiment.

DAΦNE operation for FINUDA restarted in October 2006 with the goal of delivering $1fb^{-1}$ integrated luminosity within May 2007. Commissioning started with the compensation of the betatron coupling by rotating the permanent quadrupoles inside the FINUDA solenoid, reaching an optimal value of $\approx 0.3\%$. To reduce the total wall-plug power of the machine the wiggler current has been reduced by $\approx 25\%$. This gives $\approx 5\%$ field reduction and allows to save $\approx 50\%$ ($\approx 1MW$) of total wall-plug power with respect to the last KLOE run corresponding to $\approx 100keuro/month$.

First collisions started on November 2006; then, with a continuous optimization involving mainly the main ring optics and the feedback systems, the peak luminosity has been increased up to $\approx 1.0 * 10^{32} cm^{-2} s^{-1}$ with a maximum daily integrated luminosity of $\approx 5 pb^{-1}$. Also the background level has been progressively reduced and, in December 2006, the rates were better if compared with those obtained during the last FINUDA run ($L_{peak} \approx 0.6{*}10^{32}$ and $\int_{day} L \approx 4pb^{-1}$). The daily and total integrated luminosities since October 2006 are reported in Fig. 7. The 2006 best performances have been reached with 96+96 colliding bunches with 1.5 A stored in the e- ring and .85 A stored in the e+ ring.

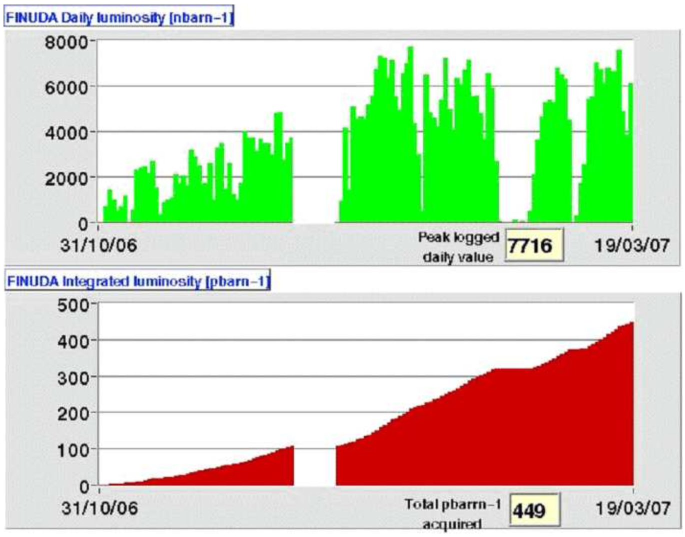

Figure 7: *Daily and total integrated luminosity during the 2006 FINUDA run.*

It is important to remark that, after the new startup with the FINUDA experiment:

- vacuum recovered in few weeks;
- all the upgrades done are in operation and have shown to be effective in optimizing machine operation and uptime as well as in providing new efficient diagnostic tools;
- ICE removal in the e- ring gave the expected results in term of bunch shortening, no quadrupole instability for the e- beam and no blow-up of the vertical beam size. The bunch length measurements before (KLOE run) and after (FINUDA run) the ICE removal are reported in Fig. 8.

4 Future Plans

FINUDA should complete its data collection by the end of May 2007 and the whole detector will be removed from the collider. In the next five months the SIDDHARTA experiment will be installed in IP1 with a new Interaction Region designed to exploit the large crossing angle and crabbed waist concepts. This new scheme for luminosity increase in e+e- colliders has been extensively studied both analytically and with numerical simulations. A combination of large crossing angle, together with very small transverse beam sizes at the IP, and the crabbed vertical waist, should in principle give us the possibility of reaching a maximum luminosity $L_{max} > 5 * 10^{32} cm^{-2} s^{-1}$, with few modifications of the machine and beam currents similar to those stored during the last KLOE run.

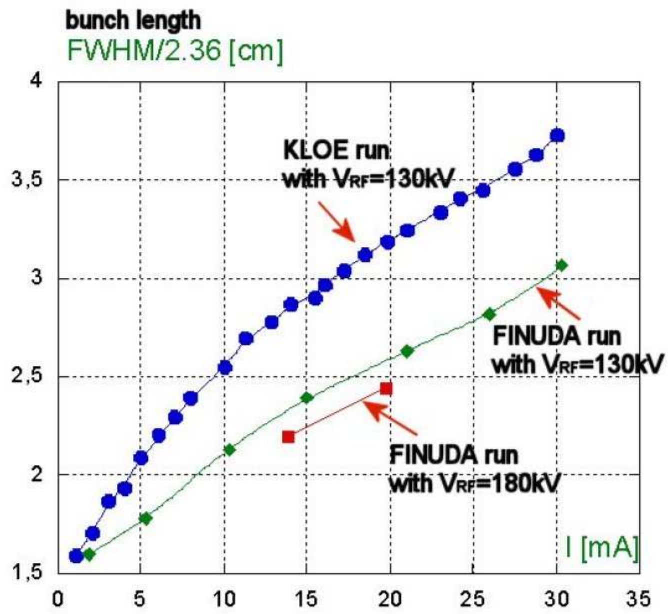

Figure 8: *Bunch length measurement before and after the ICE removal.*

Other improvements to DAΦNE will be the installation of fast stripline kickers, as those foreseen for the ILC damping rings. The new kickers have been designed to improve the injection efficiency of DAΦNE, and, compared to the present ones, exhibits much shorter pulse ($\approx 5ns$ instead of $\approx 150ns$), better transverse uniformity of the deflecting field, reduced broadband impedance and possibility of 50 Hz rep rate. Wiggler poles will also be modified in order to improve the dynamic aperture, with benefits in beam lifetimes and background. TiN coating deposition in the positron wiggler vacuum chambers is under study in order to cope with the e-cloud instability which is presently limiting the machine performances.

5 Publications

1. M.Zobov, D. Alesini, M.E. Biagini, A. Drago, A. Gallo, C. Milardi, P. Raimondi, B. Spataro, A. Stella: "DAFNE Experience with Negative Momentum Compaction", Presented at the 10th Particle Accelerator Conference (EPAC2006), 26-30 June, 2006 - Edinburgh, UK; LNF-06-23(P), 07/09/06.

2. L. Falbo, D. Alesini, M. Migliorati: "Beam Dynamics Simulation in e- Rings in SRFF Regim", Presented at the 10th Particle Accelerator Conference (EPAC2006), 26-30 June, 2006 - Edinburgh, UK; LNF-06-23(P), 07/09/06.

3. A. Gallo, D. Alesini, M.E. Biagini, C. Biscari, R. Boni, M. Boscolo, B. Buonomo, A. Clozza, G. Delle Monache, E. Di Pasquale, G. Di Pirro, A. Drago, A. Ghigo, S. Guiducci, M. Incurvati, P. Iorio, C. Ligi, F. Marcellini, C. Marchetti, G. Mazzitelli, C. Milardi, L. Pellegrino, M.A. Preger, L. Quintieri, R. Ricci, U. Rotundo, C. Sanelli, M. Serio, F. Sgamma, B. Spataro, A. Stecchi, A. Stella, S. Tomassini, C. Vaccarezza, M. Vescovi, M. Zobov (INFN/LNF, Frascati), E. Levichev, S. Nikitin, P. Piminov, D. Shatilov (BINP SB RAS, Novosibirsk), G.

Benedetti (CELLS, Bellaterra), L. Falbo (INFN-Pisa), J. Fox, P. Raimondi, D. Teytelman (SLAC, Menlo Park): "DAFNE Status Report", Presented at the 10th Particle Accelerator Conference (EPAC2006), 26-30 June, 2006 - Edinburgh, UK; LNF-06-23(P), 07/09/06.

4. A. Gallo, D. Alesini, F. Marcellini, P. Raimondi, M. Zobov (INFN/LNF, Frascati): "Preliminary Study of a Crab Crossing System for DAFNE", Presented at the 10th Particle Accelerator Conference (EPAC2006), 26-30 June, 2006 - Edinburgh, UK; LNF-06-23(P), 07/09/06.

5. A. Stella, M. Serio: "Turn by Turn Measurements at DAFNE Based on the Libera Beam Position Processor", Presented at the 10th Particle Accelerator Conference (EPAC2006), 26-30 June, 2006 - Edinburgh, UK; LNF-06-23(P), 07/09/06.

6. D. Alesini, S. Guiducci, F. Marcellini, P. Raimondi: "Design and Tests of New Fast Kickers for the DAFNE Collider and the ILC Damping Rings", Presented at the 10th Particle Accelerator Conference (EPAC2006), 26-30 June, 2006 - Edinburgh, UK; LNF-06-23(P), 07/09/06.

7. M. Zobov, D. Alesini, C. Milardi, M.A. Preger, P. Raimondi (INFN/LNF, Frascati), D. Shatilov (BINP SB RAS, Novosibirsk): "Wire Compensation of Parasitic Crossings in DAFNE", Presented at the 10th Particle Accelerator Conference (EPAC2006), 26-30 June, 2006 - Edinburgh, UK; LNF-06-23(P), 07/09/06; LNF-06-23(P), 07/09/06.

8. D. Teytelman, R. Akre, J. Fox, A.K. Krasnykh, C.H. Rivetta, D. Van Winkle (SLAC, Menlo Park), A. Drago (INFN/LNF, Frascati), J.W. Flanagan, T. Naito, M. Tobiyama (KEK, Ibaraki): "Design and Test ing of Gproto Bunch-by-bunch Signal Processor", Presented at the 10th Particle Accelerator Conference (EPAC2006), 26-30 June, 2006 - Edinburgh, UK; LNF-06-23(P), 07/09/06.

9. D. Alesini, D. Babusci, M.E. Biagini, R. Boni, M. Boscolo, F. Bossi, B. Buonomo, A. Clozza, G. Delle Monache, G. Di Pirro, A. Drago, A. Gallo, S. Guiducci, M. Incurvati, C. Ligi, F. Marcellini, G. Mazzitelli, C. Milardi, L. Pellegrino, M. Preger, L. Quintieri, P. Raimondi, R. Ricci, U. Rotundo, C. Sanelli, M. Serio, F. Sgamma, B. Spataro, A. Stecchi, A. Stella, S. Tomassini, C. Vaccarezza, M. Zobov, LNF-INFN; A. D'Angelo, R. Messi, D. Moricciani, Rome II University Tor Vergata; S. Bettoni, CERN; I. Koop, E. Levichev, P. Piminov, D. Shatilov, V. Smaluk, BINP: "DAFNE Upgrade for Siddharta Run", LNF-06-33(IR), 13/12/2006.

The DAΦNE Beam Test Facitily (BTF)

The BTF Staff: B. Buonomo (Art.22), G. Mazzitelli (Resp.), L. Quintieri (Art.23) P. Valente

The DAΦNE Operation Staff: G. Baldini, P. Baldini, A. Beatrici, M. Belli, B. Bolli, G. Ceccarelli, R. Ceccarelli, A. Cecchinelli, S. Ceravolo, R. Clementi, O. Coiro, S. De Biase, M. De Giorgi, N. De Sanctis, M. Di Virgilio, G. Ermini, C. Fusco, O. Giacinti, E. Grossi, F. Iungo, C. Marini, M. Martinelli, M. Masciarelli, E. Passarelli, V. Pavan, D. Pellegrini, R. Pieri, G. Piermarini, S. Quaglia, M. Sardone, M. Scampati, G. Sensolini, A. Sorgi, M. Sperati, A. Sprecacenere, R. Tonus, T. Tranquilli, M. Troiani, R. Zarlenga

The DAΦNE Technical Staff: R. Di Raddo, U. Frasacco, F. Galletti, V. Lollo, A. Mazzenga, C. Mencarelli

1 Description of the DAΦNE BTF 2006 Activities

The DAΦNE Beam Test Facility had a very intense activities during 2006, providing electron or positron and now also photons in various range of energy (25-750 MeV) and intensity, from single particle up to 10^{10} particle per spill. The facility hosted tens of high energy physics experiments coming from all over Europe, operating in very different conditions of multiplicity and energy.

The schedule has been divided in four periods:

- **Parasitic runs (KLOE)**: From January to 4^{th} March the BTF delivered beam in parasitic mode during the data taking of the KLOE experiment, i.e. beam was delivered to the BTF transfer line when not injecting into the main rings. The duty cycle was then limited to about 40% (see figure 1) due to the continuous topping-up during the operation of DAΦNE during the KLOE running.

- **DAΦNE shutdown**: From 4^{th} March to 19^{th} June the DAΦNE LINAC underwent several maintenance works. In particular, a pulsed power supply for the first BTF transport dipole placed at end of the LINAC has been put in operation in order to allow almost continuous delivering of beam in the BTF experimental area. The power supply has been realized in collaboration of CERN [1]. In the same period an upgrade of the tagged photons source has been performed: the design of vacuum system of the transfer line inside the BTF experimental hall has been optimised and the arrangement of the silicon micro-strip tagging detectors has been modified, in order to increase the efficiency of the photon tagging system.

- **Dedicated runs**: From 19^{th} June to 25^{th} September a major shutdown of the DAΦNE complex was performed: during this period the roll-out of the KLOE and the roll-in of FINUDA experiments have been completed, so that DAΦNE LINAC and BTF only could be operated. Besides, the operation mode with the new pulsed dipole magnet was defined and tested in this period.

- **Parasitic runs (FINUDA)** : From 25^{th} September to the end of the year, during the data taking of FINUDA. Thanks to new operation mode of the facility, a duty cycle of 90% (see figure 2) has been reached in the new operation mode: the fast pulsed magnet successfully delivered the LINAC beam to the damping ring transfer line and in the test beam area alternatively, allowing a DAΦNE BTF simultaneous operation mode.

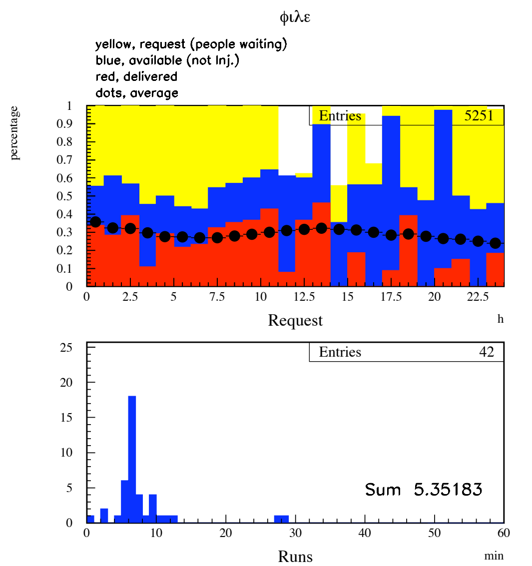

Figure 1: BTF duty cicle during KLOE run

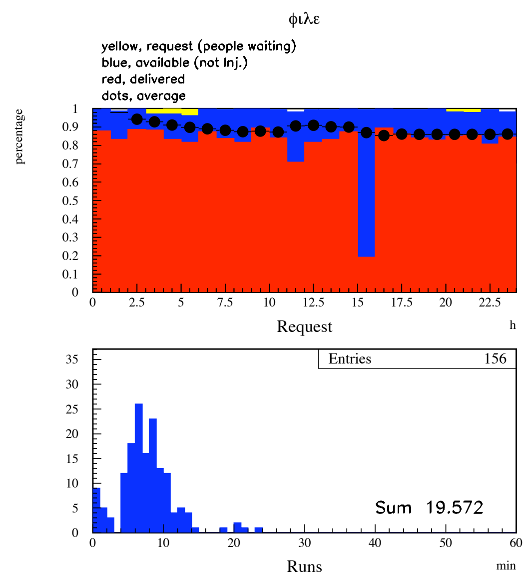

Figure 2: BTF duty cicle during FINUDA run

2 2005 User Experiences

During the 2006 many different test-beam and experiments have used the DAFNE-BTF, operating in very different conditions:

P326: The P326 experiment is aimed to measure the very rare decay $K^+ \rightarrow \pi + \nu\nu$, immersed in an overwhelming background of $K^+ \rightarrow \mu + \nu$ and $K^+ \rightarrow \pi + \pi^0$, so that it is very important to veto events with a single pion track plus photons in the decay volume. The experiment will re-use part of the NA48 experiment at the CERN SPS, while a new set of photon veto detectors should be designed, optimized and built, with the requirement of reaching a $1-10^{-4}$efficiency below 1 GeV. Several experimental solutions are being investigated in order to reach this kind of performance, and different calorimeter prototypes have been tested both with electron and photon beams, not only in terms of efficiency, but also energy resolution, timing performance, uniformity, etc.

OPERA: The aim of the OPERA experiment is to observe tau flavour from a pure muonic neutrino beam in order to confirm the theory of the neutrino oscillations. It exploits the nuclear emulsions technique: films with dimensions 12.5x10cm^2 and 45 micron of thickness are constituted of gel with interspersed AgBr crystals to reach a precision of 16 grains per layer. The BTF has allowed to study the sensibility of such emulsions exposing them with beam of electrons with fixed energy (usually 100 MeV) varying the electron number and the position (from the center to the edges of the films) with the incidence angle that was chosen longitudinal or orthogonal.

MEG: The experiment is devoted to the search for the decay (flavour violating)$\mu \rightarrow e + \gamma$ with a sensitivity of 10^{-13}. The test performed at the BTF measured the time resolution of two scintillator samples, studying the response as a function of the positrons impact position and angle.

PASSRA: Study of the particle channeling effect via a bent crystal. Positrons were sent to a crystal sample optimally aligned (with as setup similar to the one of the NANO experiment). The profile of channeled positrons was monitored 5 meters far from the sample, by means of the BTF scintillating fiber hodoscope.

LHCb-RICH: The experiments aim was to test the Pixel Hybrid Photo-Detectors (PHPD) of the Ring Imaging Cherenkov counters for the LHCb experiments. The photon detection and the data collection efficiency of the LHCb-RICH read-out system have been measured.

LHCb-LNF Test of efficiency for the MWPC and GEM detectors that will be installed in Large Hadron Collider beauty experiment. A multiplicity of a few electrons has been delivered at the maximum repetition rate of 49 Hz.

MICE: Test combined system of particle detectors constituted by scintillation counters and electromagnetic calorimeter "type KLOE" realized with some constructive variations. The results of the test have been positive and they are:

- the temporal intrinsic resolutions of various types of plastic (UPS95F, BC420 and BC404) scintillators, destined to the construction of the calorimeter of the experiment has been of 50-60 ps;
- the energetic and time resolutions of calorimeter, to the recognition of the electrons present inside the beam of muon, has been esteemed in $7\%/\sqrt{E[GeV]}$ and $70\mathrm{ps}/\sqrt{E[GeV]}$ respectively.

LAZIO: Test of silicon and scintillators detectors. The experiments requires 1-10 electrons/s and 1-10 ns variable pulse length and an energy around 500 MeV.

MIMOSA: The experiment goal is the study of the monolithic active pixels for particle physics application like the ILC (International Linear Collider).The sensor main properties are spatial resolution at micrometer level, small material budget and easy realization due to the use of standard ASIC technology. During the year 2006 we started at the BTF facility the characterization of a microstrips reference telescope built by us to measure the spatial resolution and detection efficiency of the pixel sensors.

R2PC: Test consisted in mapping the efficiency of large glass RPC chamber as a function of the beam impinging position, gas mixture and repetition rate.

3 Upgrade of Tagged photon source

During the 2006 DAΦNE shutdown, an upgrade of the hardware and software of the tagged photon source has been realized [2], [3]. The photons are produced by Bremsstrahlung of electrons with a maximum momentum of 750 MeV/c on a pair of x-y silicon micro-strip chambers, placed before the last bending magnet of the BTF transfer line. For this reason the transfer line has been interrupted for a length of about 10 cm hosting the micro-strip chambers. The divergence of the beam arriving from the LINAC, is minimized by using thin (0.5 mm) beryllium windows located just in front of the chambers. On the other side, the out-coming photons and electrons enter in the bending area where a vacuum has been ensured by three 40 microns mailer windows. No electron/positron beam degradation has been seen during standard BTF operation. The micro-strip chamber has been assembled together with its electronic in a new box (see figure 3) and has been mounted on a system of rails by means of which it can be easily inserted to the centre of the beam path when photons are requested (see figure 4). The photons are tagged in energy using the same bending

Figure 3: The new box of silicon microstrip chamber

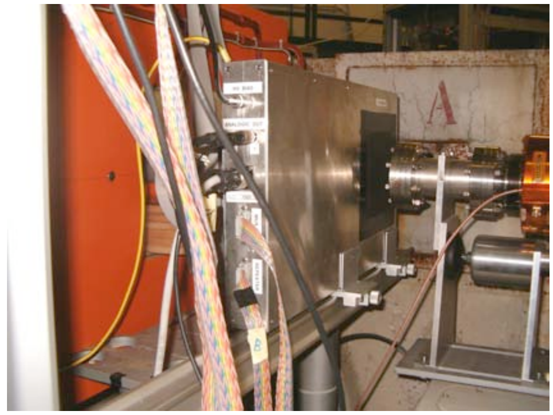

Figure 4: The silicon microstrip chamber before the the dipole

dipole, whose internal walls have been covered by 10 modules of silicon micro-strip detectors. Depending on the energy loss in the photon production, the electrons impinge on different strips once the dipole current has been set to the nominal value. The correlation between the directions on the electron measured by silicon chambers and the impinging position on the tagging module inside the magnet, allows the tagging of the photon momentum. To increase the resolution of the system, we have design and installed a new vacuum chamber inside the downstream dipole in the BTF transfer line. The new vacuum chamber is made in aluminum has with a total thickness of 1mm (only in the inner wall) with respect to the old chamber, made of 3mm steel. This gives a strong reduction of the multiple scattering of the particles impinging the inner face of the curved beam-pipe inside the dipole magnet. Moreover, three thin windows made of Mylar ($40\mu m$) close the chamber, inside which a vacuum at the level of 1 mbar or less is kept by a turbo-pump. A new mechanical support for the tagging modules inside the bending magnet has been design and constructed (see figure 5). By means of this new support the 10 modules are now mounted along the internal magnet curvature (see figure 6), increasing the spatial resolution on the determination of impact point of the emitting electrons. The tagging detectors are divided in 10 modules of 2.6 cm active height and 384 strips each, with a readout pitch of 300 m (actually 394, 10 strips at the very edges are not readout). Adding the four chamber planes, a total of 5376 micro-strip signals are read by TAA1 ASICs (IDEAS, Norway, 128 channels/chip), the analog signals are then multiplexed with a 5 MHz clock and acquired by sampling ADCs and C-RAMs (CAEN V550). All the electronic read-out of the Photon Tagging Source has been fully integrated in the BTF data acquisition system in order to record on disk the reconstructed photon energy together with the electron beam parameters.

4 The new pulsed dipole magnet

As already described, during the last DAΦNE shutdown in 2006, a pulsed dipole magnet has been inserted at the end of the LINAC to increase the duty cycle of the facility. Even when beams are injected into the DAΦNE main rings, the BTF beam can still be delivered, with a lower repetition rate, since not all the LINAC bunches are needed for the filling the accumulator ring. One pulse is in any case sent to hodoscope system for energy measurement and injection tune up. Obviously, in this operation scheme the pulse duration and the primary beam energy must be the same of

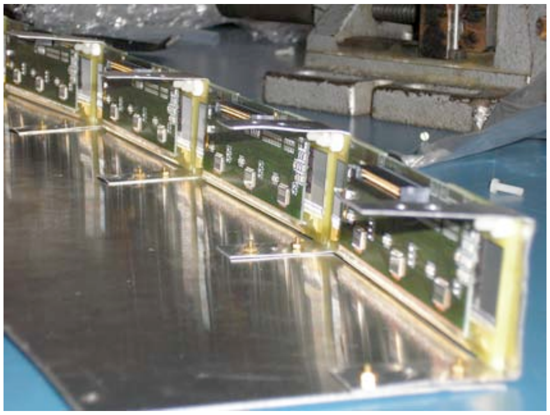

Figure 5: The tagging modules mounted on the new supporting structure

Figure 6: Insertion of the new set-up inside the bending dipole

DAΦNE . This is not a strong limitation, since the facility is mainly operated in single particle mode (electrons/positrons), which is the ideal configuration for detectors calibration and testing.

5 Conclusion

The DAΦNE Beam Test Facility is continuing showing very good performance, both from the point of view of operation reliability and the flexibility needed in order to cope with very different experimental needs. Diagnostics, data acquisition system, and tools available for experiments are continuously improving.

References

1. R. Maccaferri, F. Chiusano, "*The BTF (Beam Transfer Facility) DC/Pulsed 50 kW Power Supply for DAΦNE injector*", (MCS)CERN/AT 2006-14

2. A. Mozzanica, F. Risigo, A. Bulgheroni, M. Caccia,C. Cappellini, M.Prest, L. Foggetta, B.Buonomo, G. Mazzitelli, P. Valente, E. Vallazza, "*High Granularity Silicon Beam Monitorsfor Wide Range Multiplicity Beams*" LNF-05/25 (IR), 25 November 2005

3. S. Hasan, M. Prest, L. Foggetta, C. Pontoni, A. Mozzanica, G. Barbiellini, M. Basset, F. Liello, F. Longo, E. Vallazza, B. Buonomo, G. Mazzitelli, L. Quintieri, P. Valente, F. Boffelli, P. Cattaneo, F. Mauri, "*A Photon Tag Calibration Beam for the AGILE Satellite*", LNF-05/24(IR) 25 November 2005

DAΦNE-Light Laboratory and Activity

A. Balerna (Resp.), A. Bocci (Dott.), P. Calvani (Ass.), G. Cibin (Dott.), R. Cimino (Resp.), M. Cestelli Guidi (Art. 23), A. Frani (Tecn.), A. Grilli (Tecn.),A. Nucara (Ass.), E. Pace (Ass.), M. Piccinini (Ass. Ric.), M. Pietropaoli (Art. 15), A. Raco (Tecn.), V. Sciarra (Tecn.), F. Tombolini (Ass. Ric), V. Tullio (Tecn.), G. Viviani (Art. 15).

1 Summary

In 2006 a new organization was given to the scientific and technical activities of the DAΦNE-Light laboratory. Italian research groups interested in using synchrotron radiation must now submit their experimental proposals to a Scientific Committee that includes internal (LNF) and external members and whose President for the first three years is M. Benfatto. This Committee is planned to meet 2-3 times a year to scientifically judge and give priorities to the present and future activities of the entire DAΦNE-Light activities. In addition to the Scientific Committee a Technical Committee, having A. Balerna has chairperson for the first three years, has been created and is formed by all the responsibles of the different synchrotron beamlines and the responsible of the technical staff. This Committee meets on a regular basis 1-2 times a month in order to follow and distribute resources in agreement with the scientific priorities given by the Scientific Committee, to organize all the experimental activities and evaluate the technical feasibility of the incoming experimental proposals.

In 2006 the DAΦNE-L laboratory has lost the collaboration of two scientists: in April, G. Cinque, who was working on the soft X-ray beamline, achieved a permament position at DIAMOND (UK), while in June 2006, C. Marcelli, responsible of the infrared (IR) SINBAD beamline and of the UV branch line, resigned from the position.

During 2006 the main experimental activities were related to the organization and improvement of the existing soft X-ray, IR and UV beamlines but also to the realization of a complementary new beamline that will cover the energy range going from 60 eV to 1000 eV. On the IR and soft X-ray beamlines, new experiments were performed by Italian and European users in parasitic mode, during KLOE runs, but also using dedicated days for some specific experiments from January 2006 up to the end of March 2006 when the DAΦNE shutdown started. In particular, several EU teams got access to the syncrotron facilities within the Integrated Infrastructure Initiative for Transnational Access to Research Infrastructure (TARI).

The synchrotron infrared beamline (SINBAD) was equipped in 2006 with two end stations, as shown in Fig. 1 with one hosting the IR microscope Hyperion 3000, working both in transmission and reflection mode and operating in the near- mid- and far-IR range down to about 200 cm^{-1},whose commissioning and complete characterization with synchrotron radiation will be concluded at the beginning of 2007. Among the many initiatives of 2006 at SINBAD, great mention should also be given to the organization in May and October of the first and second *FTIR Microspectroscopy School*. Both schools have been organized by the SINBAD team with the support of Bruker Optics, and were attended by about 50 people. The schools were mainly oriented to introductory lectures and student training, including experimental sessions using the SINBAD instrumentation.

On the soft X-ray beamline many improvements have been performed concerning the x-ray beam definition and the sample movement. New apparata were designed and are now being realized in order to improve as much as possible the opportunities for the soft x-ray users. The use of the UV beamline, after the conclusion of the SUE experiment funded by the INFN Vth

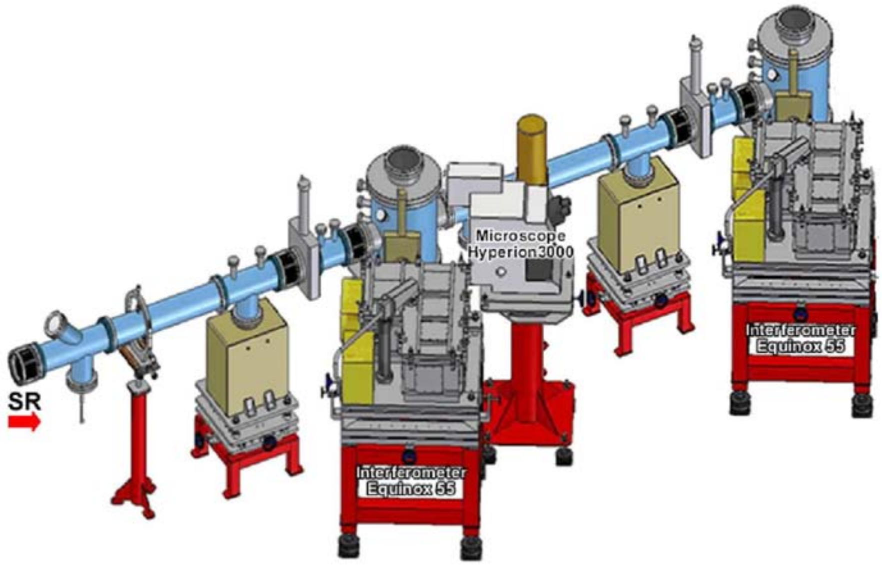

Figure 1: Layout of the two end stations installed on the SINBAD IR beamline.

Committee, was required by a new Vth Committee experiment named SOURCE or Synchrotron Optical Ultraviolet Radiation for Calibration Experiments which includes in its main goals also the test of large mirrors for space applications. Concerning the new X-UV beamline, an existing laboratory has been equipped with all the necessary items to be ready to host it together with its related experimental end-stations. The beamline construction started with the realization of the first optical UHV chamber.

2 Activity

2.1 SINBAD

The SINBAD infrared beamline is composed by three sections: the front-end, the section that transfers radiation from the bending magnet to a first focus - where the image of the source is demagnified by an ellipsoidal mirror - and, finally, a third section that transmits the radiation as a parallel wave to the wedged diamond window located at the entrance slit of the interferometer.

The beamline in 2006 was equipped with two end stations: the first one is the new Equinox 55 interferometer hosting on one of its exit ports the microscope Hyperion 3000 that can be also remotely controlled via internet, to allow interaction among scientist working on the same experiment from different laboratories. The second end station is another Equinox 55 interferometer, owned by the University of Rome *La Sapienza*, and is actually working with conventional sources. The vacuum chamber for the mirror that focus the synchrotron radiation in this second interferometer has been realized and tested, and its installation on the beamline is planned in the next months, when the focusing mirror will be available. At that point both interferometers will be able to use, alternatively, synchrotron radiation as a source for IR experiments.

The commissioning of the experimental station is going on and it will be concluded in the first part of 2007, including the complete characterization of the Hyperion 3000 microscope with synchrotron radiation. The beamline has been equipped with a Helium-cooled cryostat, which was adapted to the existing instrumentation and tested. Among the planned upgrades of the IR beamline a new Focal Plane Array detector for the IR microscope was bought in 2006 and will be probably installed by the end of 2007.

The scientific activity at SINBAD was associated to experiments performed with Italian teams that submitted scientific proposals approved by the LNF synchrotron radiation Scientific Committee and by European scientists that achieved the access within the EU framework of the TARI I3 program. In 2006 more than 30 experimental teams were hosted at the IR beamline. The EU funded experimental runs related to about 15 experimental proposals, accounted for a total of about 30 users and 230 experimental days. Several Italian scientists, including graduates and PhD had access to the IR beamline performing experiments in cooperation with the SINBAD staff. Almost all of these teams re-applied to continue their researches or submit their new applications. Some of the 2006 scientific highlights achieved by the performed experimental activities are here summarized:

1. *High-pressure study of the competition between insulating and metallic ferromagnetism in the low doped* $La_{1-x}Sr_xMnO_3$.

   Polycrystallines of the stoichiometric compounds $La_{1-x}Sr_xMnO_3$ with x=0.12, 0.14 and 0.16 and $Pr_{0.8}Ca_{0.2}MnO_3$ have been synthesized. The former are prototype materials giving rise to a competition between FM (ferromagnetic metal) and FI(ferromagnetic insulator) states at high temperature, while in the latter the FI state is very stable. Transmission spectra have been measured over the energy range 500 cm^{-1} to 6000 cm^{-1} at room temperature as a function of the pressure up to 20 Gpa (Fig. 2). Such mid-infrared spectra have been taken in

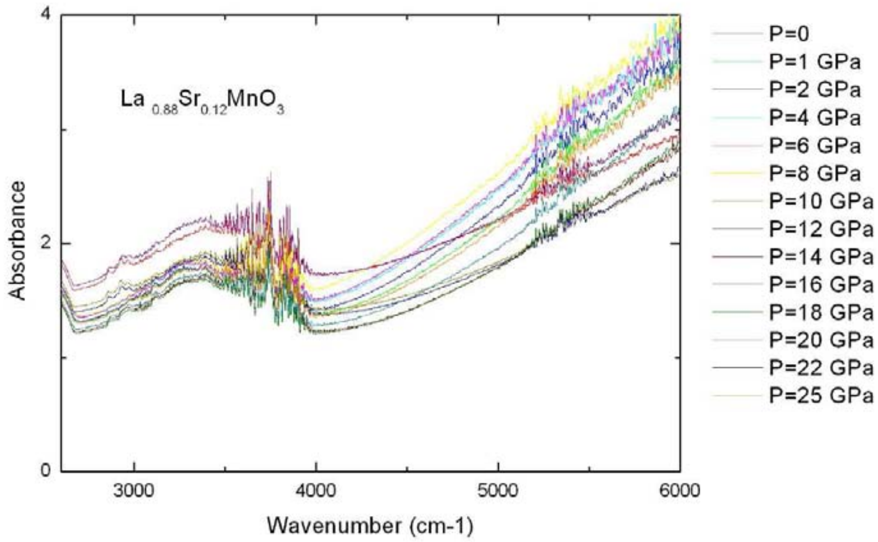

Figure 2: Absorbance of the $La_{0.88}Sr_{0.12}MnO_3$ sample.

   a diamond anvil cell and required the use of synchrotron radiation. These measurements show the role of Jahn-Teller interactions in the FI state. The main finding published on Physical Review Letters (see Ref. 1 in this report) is an increase in the low-energy spectral weight as the pressure is raised (Fig. 3). This continuous trend towards increasing metallicity suggests an increase in the bandwidth due to the reduction of Jahn-Teller distortions. However, in such scenario, the spectral weight should reach a constant value above a certain threshold pressure. In fact, the variation in the spectral weight with pressure shows a plateau following by an other increase. This unexpected observation suggests that other interactions play an essential role in the competition between FM and FI states.

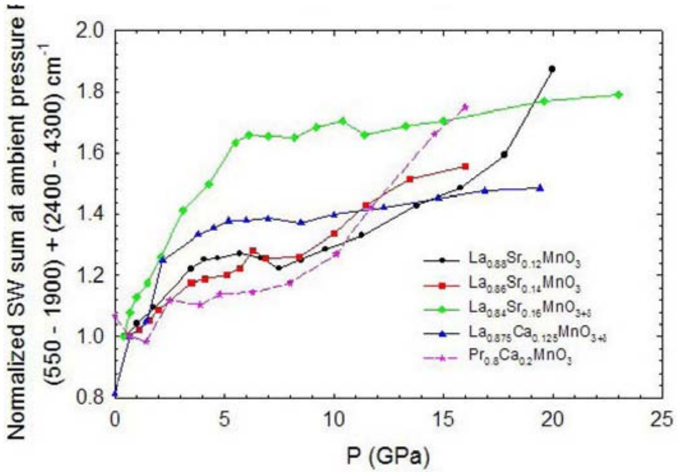

Figure 3: Sum of the low and high frequency spectral weight.

2. *Pituitary Gland in the infrared light.* In pituitary gland studies with infrared light different pathological tissues were obtained from patients undergoing surgery of removal. The fresh tissues were immediately frozen in liquid nitrogen and cut using a microtome in 15 μm slices. The slices of tissues were carefully placed on thin (0.9 μm) Mylar foils. In order to obtain reliable information about different patterns of pituitary samples two dimensional scans on chosen areas using microscopic FT-IR spectrometer (BRUKER Hyperion 3000 IR-Microscope) were performed. For each spectra 1000 scans were collected. During the experiments (two experimental days in 2006 were allocated for this project) only the internal Globar source was used. This is the first work that shows a difference in secondary conformational structure of different human pituitary diseases. FTIR microspectroscopy is a unique analytical method and can be used to classif y the human pituitary abnormalities more easily than the complicated immunochemical analysis. But more investigation of FTIR microspectroscopy must be undertaken to give a high level of confidence of obtained results. Measuring the changes in the pituitary gland may well lead to not only a better understanding of the disease progression but also an ability to prediction outcome.

2.2 Soft X-ray Beamline

The DAΦNE soft X-ray beamline, DXR-1, is mainly dedicated to photo-absorption spectroscopy. The X-ray source of the soft X-ray beamline is one of the 6-poles equivalent planar wiggler devices installed on the DAΦNE electron ring (0.51 GeV) for the vertical beam compaction. The wiggler forces the accelerated electrons to emit a wide, intense and polarized fan of electromagnetic radiation. Due to the wiggler higher magnetic field, with respect to the bending magnet one, the critical energy of the emitted synchrotron radiation spectrum moves from 219 eV to about 296 eV with the wiggler at its maximum field of 1.8 Tesla. The 6 wiggler poles and the high storage ring current (higher then 1 A) give a useful X-ray flux for measurements well beyond ten times the critical energy. The useful soft X-ray energy range in 2006 was 1200 eV - 3200eV. During this year the main improvements performed on the beamline concern the design and realization of many different but fundamental elements like:

1. a double wire beam monitor to control the X-ray beam dimension and position
2. remotely controlled output slits
3. new motorized support for the experimental chamber
4. He cryostat for sample cooling.

Clearly all these elements will be tested and installed in 2007. Another important improvement will be given by the acquisition of a SDD detector that will be used to perform X-ray absorption measurements in fluorescence mode. The scientific activity at the soft X-ray beamline included experiments performed by Italian teams and by European scientists that achieved the access within TARI program. In the first three months of 2006 about 6 experimental groups were hosted at the soft X-ray beamline. The EU funded experimental runs related to the feasibility of an experimental proposal, accounted for a total of 2 experimental weeks with 1 dedicated beamtime day.

Several Italian scientists coming from different Italian Universities or related to INFN Vth Committee experiments used the beamline with dedicated and parasitic beamtime for about 7 weeks (6 dedicated days). In parasitic mode X-ray imaging measurements have been performed on leaves accumulating toxic metals as effective agents for the so-called phytoremediation of polluted environment. Images were taken above and below the lead M_V absorption edge (A. Reale MIDIX INFN - Vth Committee) and above and below the S K-edge. For the same experiment also the XANES spectra at the K edge of Mg were measured in treated and untreated leaves (1 week with 1 day dedicated). Beamtime was given to complete (2 weeks with 2 dedicated days) the ARCHIMEDE (ARCHItects of Mirrorsfor Euv DEvices) experiment of the INFN - Vth Committee for a final set of measurements on new multilayer devices in the soft X-ray energy domain (V. Rigato of LNL and G. Cinque of LNF) and to measure (1 week parasitic beamtime) the performances as x-ray detectors of diamond based detectors (proposal by E. Pace and A. Desio from University of Firenze). Beamtime was also given to complete some studies on natural mica crystals in transmission mode measuring the XANES spectra at the potassium K-edge, and at the Al and Mg K edges (2 weeks and 2 dedicated days)(proposal by A. Mottana and G. Cibin, Roma III University).

The LNF staff performed also some tests at the Si and S K edges measuring extended X-ray absorption fine structure spectra (1 week and 1 dedicated day). Some of the 2006 scientific highlights achieved by the performed experimental activities are here summarized:

1. *Preliminary study on the chemical speciation of sulfur in cancerous tissues.* Sulfur is vital for almost all living organisms by participating in a wide variety of metabolic processes. Nevertheless its biochemistry is only partially understood, due to it a few tools such as X-ray absorption near edge structure may be used to determine its chemical speciation in biological system. This study was mainly based on the analysis of the composition and elemental distribution in tissue structures of biological samples like cancerous and non-cancerous prostate tissues. X-ray absorption near edge structure spectra have shown two main types of sulphur that are represented by X-ray peaks at 2476 eV and 2484 eV in the XANES spectra.

2. *Al K-edge XANES Measurements in $NaAlH_4$ Doped with $TiCl_3$ by Ball Milling.* Al K-edge X-ray absorption spectroscopy has been applied to investigate pure sodium alanate and doped sodium alanate with Ti on the basis of $TiCl_3$ by ball milling. First experimental data indicate that the chemical state of Al in $NaAlH_4$ does not change upon cycling and confirm also that the valence state of Al is an oxidation state higher than that of metallic Al in NaAlH4. Moreover, a change in the orbital occupancy of Al atoms and/or increasing structural disorder in the local Al surroundings is occurring most probably after doping sodium alanate and subsequent cycling under hydrogen. Indeed, an evolution of the XANES features was observed with increasing number of cycles under hydrogen compared to the pure alanate sample. After several cycles, a new phase containing metallic Al was formed, which corresponds to the mixture of Al and the formation of small Ti-Al clusters already observed in Ti K-edge measurements. The preliminary results suggest the presence of molecular-scale inhomogeneities within the average structure of sodium alanate.

2.3 UV branch Line

In 2005 the experimental proposal submitted by E. Pace of the University of Florence named SOURCE (Synchrotron Optical Ultraviolet Radiation for Calibration Experiments) devoted to test of VUV optics for space applications and novel optical devices based on multilayer technology, was been approved by the INFN Vth Committee. According to the schedule of the project, in 2006 an upgrade of the UV branch line was planned with a new UV monochromator and the set up of a larger experimental area. The project of the new set-up of the experimental area was done and will be realized in 2007.

2.4 New X-UV beamline

The characteristics of the DAΦNE accelerator as a synchrotron radiation (SR) source are very interesting, mainly due to its very high flux in the vacuum ultraviolet and soft x-ray region (5-1000 eV). The flux per mRad of the bending magnets at DAΦNE is even higher than the one from a third generation machine like ELETTRA up to 500 eV. For this reason a great number of specific spectroscopy experiments, which require high flux but not a very high energy resolution and brilliance can be, therefore, optimally performed like e.g. angle resolved photoemission, surface XAFS from shallow core levels and so on. In the recent past, the construction of two bending magnet beamlines covering the range from 5 eV to 1000 eV has been proposed and studied in detail. The optical project has been done for two beamlines , an high Energy Beamline (HEB from 60 eV -1000 eV) and a Low Energy Beamline (LEB from 5 eV - to 150 eV- see Ref. 16 in this report).

The SR Scientific Committee of LNF has decided to give priority in the construction of the High energy beamline (whose energy range covers the one expected from the SPARX project, in construction in the Tor Vergata Campus) keeping the option of inserting the second beamline in the future. With this in mind, in 2006, the UHV chamber hosting the first optical elements, which will collimate the emitted radiation into a parallel beam entering the existing laboratory n 13, has been designed and ordered. This is shown in figure 4, where the constructive details of the Front end and the optical system have been adapted to the existing bending magnet output and to the geometrical constraints. The design is as compact as possible in order to collect as many horizontal milliradiants a possible, keeping the mirrors as close as possible to the source. The installation of the described optical system is foreseen during the machine shut-down in the summer 2007, and we plan to have a parallel beam in the laboratory within 2007. The coupling of such pre-optics with an existing monochromator is under study as well as the possibility of maintaining the original optical design if fundings will become available.

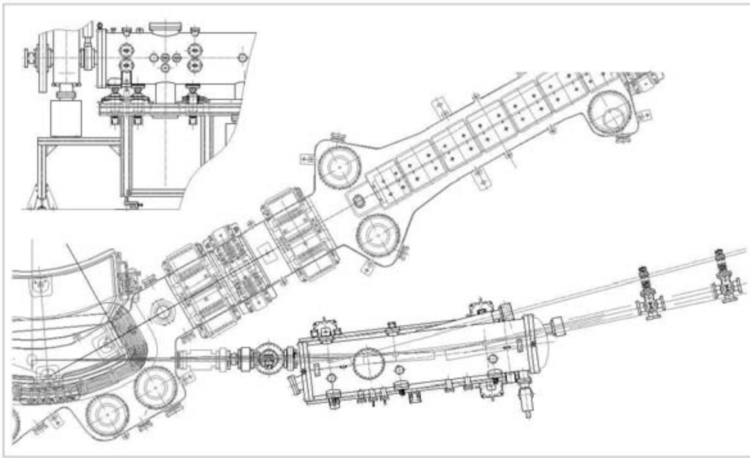

Figure 4: Constructive drawing of the optical UHV chamber and of the front end to be installed in the summer 2007 (courtesy of RMP).

References

1. A. Sacchetti, M. Cestelli Guidi, E. Arcangeletti, A. Nucara, P. Calvani, M. Piccinini, A. Marcelli, P. Postorino, Far-infrared absorption of $La_{1-x}Ca_xMnO_{3-y}$ at high pressure, Physical Review Letters **96**, 035503 (2006)

2. B.V. Robouch, A. Kisiel, A. Marcelli, M. Cestelli Guidi, M. Piccinini, E. Burattini, A. Mycielski, Statistical model of sphalerite structured quaternary $A_{1-x}B_xY_yZ_{1-y}$ systems, Journal of Alloys and Compounds **426**, 31 (2006)

3. P. Zajdel, A. Kisiel, J. Polit, B.V. Robouch, E.M. Sheregii, J. Warczewski, J. Cebulski, E. Burattini, A. Marcelli, M. Cestelli Guidi, M. Piccinini, A. Mycielski, Model considerations on hydrogen distribution in hydrogenated CdTe, Journal of Alloys and Compounds **426**, 12 (2006)

4. P.Innocenzi, T. Kidchob, J. Mio Bertolo, M. Piccinini, M. Cestelli Guidi, A. Marcelli, Time-resolved infrared spectroscopy as an in situ tool to study the kinetics during self-assembly of mesostructured films, Journal of Physical Chemistry B **110**, 10837 (2006)

5. M. Piccinini, G. Cibin, A. Marcelli, G. Della Ventura, F. Bellatreccia, A. Mottana, Synchrotron radiation FT-IR micro-spectroscopy of fluorophlogopite in the O-H stretching region, Vibrational Spectroscopy **42**, 59 (2006)

6. M. Piccinini, G. Cibin, A. Marcelli, A. Mottana, G. Della Ventura, F. Bellatreccia, Synchrotron radiation FTIR micro-spectroscopy of natural layer-silicates in the O-H stretching region, Infrared Physics and Technology **49**, 64 (2006)

7. A. Sacchetti, M. Cestelli Guidi, E. Arcangeletti, P. Postorino, A. Nucara, M. Piccinini, P. Calvani, A. Marcelli, High pressure far-infrared absorption measurements on $La_{1-x}Ca_xMnO_{3-y}$ by means of synchrotron radiation, Infrared Physics and Technology **49**, 92 (2006)

8. J. Polit, E.M. Sheregii, J. Cebulski, A. Kisiel, M. Piccinini, A. Marcelli, B.V. Robouch, M. Cestelli Guidi, A. Nucara, A. Mycielski, High resolution spectra of defects in CdTe obtained in far-infrared region using synchrotron radiation, Infrared Physics and Technology **49**, 23 (2006)

9. E.M. Sheregii, J. Polit, J. Cebulski, P. Sliz, A. Kisiel, M. Piccinini, A. Marcelli, B.V. Robouch, M. Cestelli Guidi, P. Calvani, V.I. Ivanov-Omskii, First interpretation of phonon spectra of quaternary solid solutions using fine structure far-IR reflectivity by synchrotron radiation, Infrared Physics and Technology **49**, 13 (2006)

10. J. Cebulski, E.M. Sheregii, J. Polit, B.V. Robouch, A. Marcelli, M. Cestelli Guidi, M. Piccinini, A. Kisiel, A. Mycielski, Anisotropy of oriented mono-crystalline ZnCdTe phonon spectra obtained by synchrotron radiation, Infrared Physics and Technology **49**, 19 (2006)

11. C. Balasubramanian, S. Bellucci, G. Cinque, A. Marcelli, M. Cestelli Guidi, M. Piccinini, A. Popov, A. Soldatov, P. Onorato, Characterization of aluminium nitride nanostructures by XANES and FTIR spectroscopies with synchrotron radiation, Journal of Physics: Condensed Matter **18**, S2095 (2006)

12. J. Polit, E.M. Sheregii, B.V. Robouch, A. Marcelli, J. Cebulski, M. Cestelli Guidi, M. Piccinini, A. Kisiel, P. Zajdel, E. Burattini, A. Mycielski, Phonon and Vibrational spectra of hydrogenated CdTe, Journal of Applied Physics **100**, 013521 (2006)

13. G. Cinque, G. Bellisola, M. Colombatti and E. Burattini, X-ray absorption near edge spectroscopy of sulfur in biomolecules: Two examples from glutathione and insulin, Acta Phys. Pol. A **109**, 335 (2006)

14. A. Marcelli, G. Cibin, G. Cinque, A. Mottana and MF. Brigatti, Polarized XANES spectroscopy: The K edge of layered K-rich silicates, Radiat. Phys. Chem. **75**, 1596 (2006)

15. W.M. Kwiatek, A. Banas. K. Banas, A. Kisiel, G. Cinque and G. Falkenberg, Preliminary study on chemical speciation of sulphur in cancerous tissues, Acta Phys. Pol. A **109**, 383 (2006)

16. G. Naletto, G. Tondello, R. Cimino, Design of a high-flux low-energy synchrotron radiation monochromator, Nulclear Intrum. Methods A **556**, 371 (2006)

GILDA - GENERAL PURPOSE ITALIAN BEAMLINE FOR DIFFRACTION AND ABSORPTION - AT ESRF.

A. Balerna, A. Grilli (Tecn.), S. Mobilio (Resp.), A. Raco (Tecn.),
V. Sciarra (Tecn.), V. Tullio (Tecn.)

1 Introduction

GILDA (General Purpose Italian BeamLine for Diffraction and Absorption), is the Italian CRG beamline, built to provide the Italian scientific community with an easy access to the European Synchrotron Radiation Facility to perform experiments with a high energy and brilliance X-ray photon beam. GILDA is today funded by the Italian public research Institutes: Consiglio Nazionale delle Ricerche (CNR) and Istituto Nazionale di Fisica Nucleare (INFN). Experimental stations for X-ray Absorption Spectroscopy, Anomalous X-ray Scattering and X-ray Diffraction (XRD) are present at the GILDA beamline.

2 Activity on the GILDA beamline during 2006

In 2006 many activities were performed:1) a new He cryostat was installed in the absorption hutch of the beamline; a valuable increase of the thermal stability and a decrease of the dead-time associated with cooling and heating of the samples during measurements was achieved. 2) The migration of the operating system of the beamline control system from Microware OS9 to LINUX was completed in the optical hutch. 3) Sample environment systems were implemented in the diffraction hutch to perform (high-resolution) experiments in controlled atmosphere, to perform grazing incidence experiments and to control the overall humidity of the sample. 4) The support of the new second mirror, installed during 2005, was modified to recover the possibility to expose both the mirror coatings to the X-ray beam: in such a way the beam-line now can work in the overall energy range of the low energy configuration. 5) An oscillating total yield detector working at liquid He temperature was installed and commissioned in the absorption hutch; this detector allows measuring thin films grown on crystalline substrate eliminating diffraction Bragg peaks from the substrate. 6)First tests and depositions using the magneto-sputtering cluster sources were planned.

3 Beamtime use during 2006 and scientific outcomes

During 2006 ESRF delivered beam for about 5300 hours; 4000 hours were used for user's experiments,the remaining for in-house research, beamline improvements, maintenance and alignment. Totally 49 experiments were performed, 36 of Italian users and 13 of European users. Two experiments were published in the ESRF Highlights 2006. Studies and results to be mentioned are the following:

1. *Iron oxidation, interfacial expansion and buckling at the Fe/NiO(001) interface.* In order to provide a structural basis for a physical understanding of exchange bias in metal-magnetic-oxide interfaces, the structure of the Fe/NiO(001) interface was determined by means of XAFS spectroscopy and ab initio density functional theory calculations. A Fe-Ni alloyed phase on top of an interfacial FeO planar layer is formed. The FeO layer exhibits a 7% expanded interlayer distance and a 0.3 buckling; its presence is predicted to increase the spin magnetic moment of the interface Fe atoms by 0.6 mB, compared to the ideally abrupt interface.

2. *Er site in Er-implanted Si nanoclusters embedded in SiO_2.* The local order around Er atoms introduced by ion implantation in substoichiometric silica films was investigated by EXAFS. The results show that Er atoms are surrounded by a first shell of O atoms and no Er-Si direct correlations are observed; moreover, while the variation of the preimplantation annealing temperature has no effect on the Er site, it is observed that the increase of the Er concentration determines an increase of both the Er first shell coordination number and the Er-O interatomic distance, becoming more similar to those of Er_2O_3. In the presence of an extensive phase separation between Si and SiO_2 the local environment around Er plays a crucial role on the efficiency of the photoluminescence emission at 1.54 μm, which is significantly increased when the first shell of atoms around Er is closer to that of Er_2O_3.

3. *Sub-nanometric metallic Au clusters as Er^{3+} efficient sensitizers in silica.* This study is related to the enhancement of the Er photoluminescence in Er-doped silica films that contain either metallic aggregates or metallic ions. The open question is that it is not clear to what extent this enhancement is triggered by the surface plasmon resonance of the metal nanoclusters (that occurs for cluster size of more than about 1nm). For this reason the structure and the optical response of Au+Er-doped silica, choosing the Au concentration to obtain subnanometer size Au clusters has been investigated. The EXAFS analysis, performed at Au and Er L_3-edges, supports the hypothesis of an energy transfer process mediated by sub-nanometric Au aggregates and that the Au clusters size is less than 1 nm.

4. *Negative Thermal Expansion.* Some materials present a negative thermal expansion effect (NTE), i.e. their lattice parameter shortens as temperature increases, originating an effect which deserves attention both from a fundamental and a technological point of view. NTE was investigated in $CuScO_2$ and in $CuLaO_2$ where it is originated by lattice interactions and in Au cluster where it is originated by the finite size of the metal particles. In this case the presence of NTE was confirmed by EXAFS measurements performed on the GILDA beamline and its origin was explained as due to the presence of discrete electron energy level in the conduction band due to the finite cluster size.

4 2007 - GILDA Forseen Activity

During the 2007, the activity foresees: 1) completion of the migration of the operating system of the beamline from Microware OS 9 to LINUX; 2)the installation of a new and more flexible and fast imaging plate detector in the diffraction hutch; 3)the conceptual study and preliminary design of the beamline implementation needed for the foreseen updates of the ESRF storage ring; 4)the end of the commissioning and the beginning of the operating phase of the magneto-sputtering cluster source.

References

1. C. Monesi, C. Meneghini, F. Bardelli, M. Benfatto, S. Mobilio, U. Manju, D. D. Sarma, Quantitative structural refinement of Mn K edgeXANES in $LaMnO_3$ and $CaMnO_3$ perovskites, Nucl. Inst. and Met. B **246**, 158-164 (2006).

2. F. Liscio, F. Bardelli, C. Meneghini, S. Mobilio, Sugata Ray, D. D. Sarma, Local structure and magneto-transport in Sr_2FeMoO_6 oxides, Nucl. Inst. and Met. B **246**, 189-193 (2006)

3. G. Deganello, F. Giannici, A. Martorana, G. Pantaleo, A. Prestianni,A. Balerna, LF. Liotta, A. Longo, Metal-support interaction and redox behaviour of Pt 1% in $Ce_0.6Zr_0.4O_2$, J. of Chem. Phys. B **110**, 8731-8739 (2006)

NTA-DISCORAP

G. Celentano (Ass.), A. Della Corte (Ass.), U. Gambardella (Resp.)

1 Purposes of the project

The *DISCORAP* (DIpoli Super COnduttori RApidamente Pulsati) program comes out from the new requirement of developing fast ramped superconducting dipoles for the FAIR accelerators at GSI, Darmstadt, Germany. It is a four year program to develop a fully working bent dipole long 3.8 m in its horizontal cryostat. The dipole has to generate a field of 4.5 tesla with ramping rate of 1 tesla/sec [1]. Among other requirements it has to keep dissipation at reasonable levels as well as to generate low harmonic contents. To achieve these targets a suitable wire must be developed. DISCORAP also encloses the ending activities on the Nb_3Sn wire realized in the framework of the previous NTA-CANDIA program (see the 2005 Activity report). Three INFN sections are involved: Genova (group leader), Milano, and LNF, in collaboration with LUVATA (former Outukumpu Copper Superconductors) Italy, Fornaci di Barga (LU), and Ansaldo Superconduttori Genova, Italy.

2 The Frascati group activity

The Frascati group, made of *LNF* and *ENEA* Frascati researchers, in 2006 took care of wire characterizations, analyzing the newly developed low losses NbTi superconducting wires and the the Nb_3Sn wires in the framework of the NED activity. We have performed magnetic measurements in high magnetic field, from which information about the intrinsic magnetization losses, the critical current, and the filament size can be extracted. Due to the high transport current density of the NbTi and Nb_3Sn it became advisable deriving transport and losses properties from magnetization measurements before setting up a long length production. In addition as the low losses NbTi requires extremely narrowed filaments, in the range 2-4 μ, we also provided morphological SEM as well as compositional analysis on the first wire prototypes. In Figure 1 it is shown a SEM picture for sample 87696 (left side), a NbTi wire with a 2 μm filament size. On the right it is shown the element composition as detected from a linear scan among filaments. The filament deformation seems acceptable.

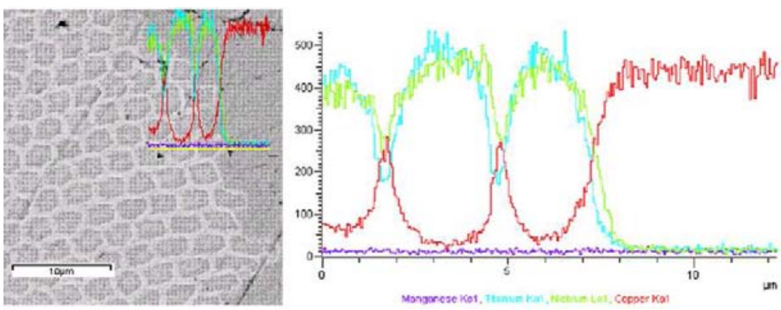

Figure 1: *SEM picture and analysis of 2μm filament prototype NbTi wire*

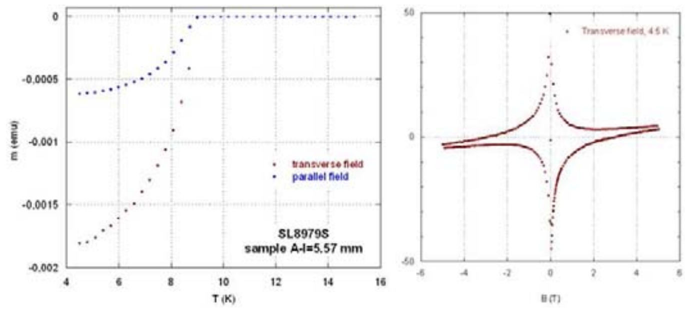

Figure 2: *Magnetic moment for low filament size NbTi wire*

The one cycle hysteretic losses Q in a superconducting wire may be computed from the wire radius a and the critical current density J_c with eq.1 (in J/m^3) :

$$Q = \frac{8}{3\pi} J_c a B_m \tag{1}$$

where B_m is the maximum value of the ramping magnetic field. This simple consideration makes advisable to develop low filament size wires, in order to save cryogenic costs for fast ramped dipoles. Though the NbTi alloy is well known, the production of μ-size filaments is not yet well developed and may suffer of many problems: filament sausaging and/or breaks, weak superconductor creation at the Nb-matrix interface (proximity effect), etc.. Further dissipation, when the magnetic field is rapidly changing, comes from the filament couplings, which are connected through the metallic matrix. To minimize this additional loss source, beside to the usual filament twisting, a resistive barrier, such as $CuMn_{0.5wt}$ alloy, around filaments can be used. These considerations, and additional problems when realizing the 36 strand Rutherford cable, require a dedicated analysis just for the wire to be used in the fast ramped dipole.

To analyse the magnetization M of NbTi and Nb_3Sn wires we used VSM (Vibrating Sample Magnetometer) operating in the range [300 $\div$ 4] K under a maximum field up to 16 Tesla. All the tests were carried out in the ZFC (Zero Field Cooling) situation, to have the opportunity of recording the purely diamagnetic response at low magnetic field, useful for studying the shielding regimes. In Fig. 2 there are shown magnetic measurements for a 2μm filament prototype NbTi wire. A total of 13 measurement runs were carried out on both NbTi and Nb_3Sn wires providing a fast and reliable feedback on their superconducting properties.

References

1. P. Fabbricatore, S. Farinon, U. Gambardella, M. Greco, G. Volpini, "Rapid cycling superconducting magnets", Nucl. Phys. (Proc. Suppl.) **154**, 157 (2006)

2. Michela Greco, Pasquale Fabbricatore, Carlo Ferdeghini, Umberto Gambardella, "Magnetization Measurements of Nb_3Sn Wires for the Next European Dipole (NED)", IEEE Transaction on Magnetics, **16**, 1164 (2006)

NTA TTF

L. Cacciotti (Tecn), M. Castellano (Resp), E. Chiadroni, A. Clozza, G. Di Pirro,
O. Giacinti (Tecn), R. Sorchetti (Tecn)

1 Introduction

The TESLA Test Facility (TTF) is an international effort, based at Desy (Hamburg), aiming at the development of the technologies required for a Superconducting e^+e^- Linear Collider. High gradient superconducting RF cavities, with their high power coupling and tuning device, and low cost cryostats were the main goal of the project, but also the production of a high power, long pulse electron beam from a RF gun was required. This involved the development of new photocathode, an adequate laser source and new beam diagnostics. In addition to prove the possibility of producing and accelerating the kind of beam required for the future superconducting Lineal Collider, TTF has also demonstrated that this beam was of enough good quality to be successfully used for the production of UV coherent radiation with the Self Amplified Spontaneous Emission (SASE) Free Electron Laser process. TTF is now trasformed in FLASH (Free-electron LASer in Hamburg), becoming a test bench not only for the Linear Collider, but also for the European X-ray FEL Facility. INFN contribution comes from LNF, LNL, Sezione di Milano and Sezione di Roma2.

2 Activities in the year 2006

The maintenance activity in 2006 mainly consisted in the replacement of a camera, damaged by the radiation, and in the better alignment of a couple of optical systems. The whole OTR diagnostics worked very well for the long user delivery time. The scientific activity was concentrated in the installation and preliminary data taking of the experiment on the Optical Diffraction Radiation for non-intercepting beam size measurement. In March 2006, during the period of machine development, we used two set of shifts, 5 shifts each, for the commissioning of the experiment, the understanding of the strong background problem and a first preliminary data taking at a rather low energy. The results have been really satisfactory and were presented at the 6^{th} Channeling Conference. As a result of these test, in October, during a machine shutdown, we changed the optics alignment procedure, using an intense light source injected far upstream in the vacuum pipe and obtaining a much better alignment. We also inserted a screen with a hole as a tentative of reducing the synchrotron radiation background. What was clear from these test was the need for a higher energy and a smaller beam size, that were scheduled for 2007.

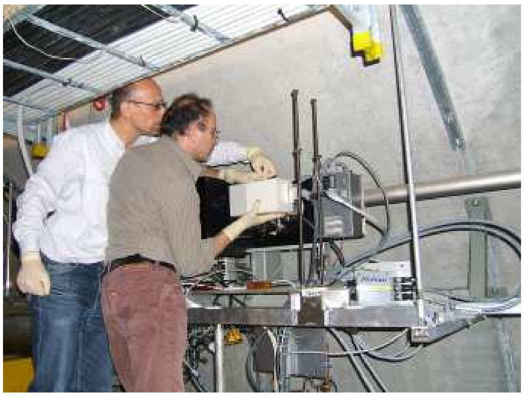

Figure 1: *Installation of the high sensitivity Camera.*

Figure 2: *Bringing the beam on the screen..*

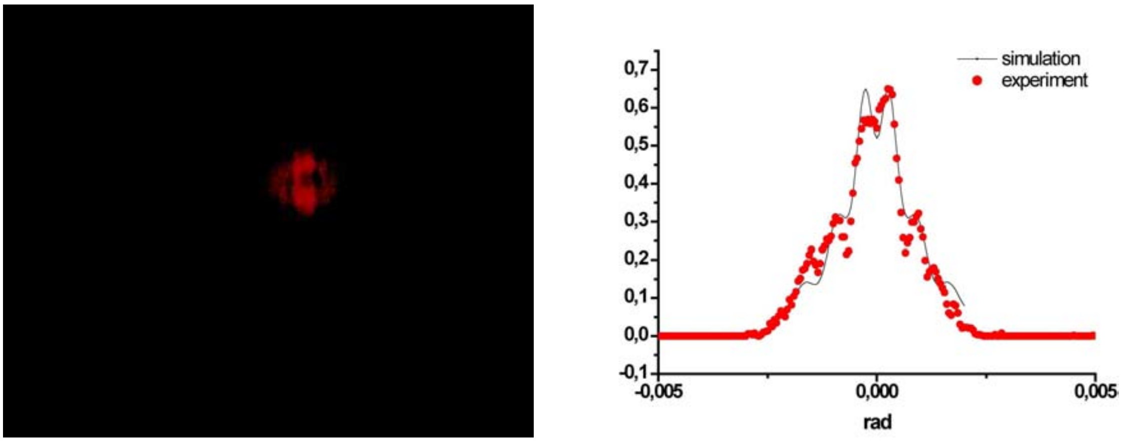

Figure 3: Image of ODR angular distribution (left) and its projection on the orizontal axis compared with the theoretical distribution from a beam with the measured parameters (right).

3 Publications

1. F. Löhl, S. Schreiber, M. Castellano, G. Di Pirro, L. Catani, A. Cianchi, and K. Honkavaara, "Measurements of the transverse emittance at the FLASH injector at DESY", Phys. Rev. ST Accel. Beams 092802 (2006).

2. E. Chiadroni, "Bunch length characterization downstream from the TTF VUV-FEL", Proc. of the EPAC Conference 2006, Edinburgh.

3. E. Chiadroni, M. Castellano, A. Cianchi, K. Honkavaara, G. Kube, "Status of the Electron Beam Transverse Diagnostics with Optical Diffraction Radiation at the DESY FLASH Facility", International Conference on Charged and Neutral Particles Channeling Phenomena, S. Dabagov Ed., to be published in Proc. SPIE 2007.

RADIATION SAFETY

A. Esposito (Resp.), R. Bedogni (Art. 23), M. Chiti (Tecn.),
A. Gentile (Tecn.), L. Fioretti (Tecn.), G. Carinci(Tecn.)

1 Institutional duties

The LNF Radiation Protection Group is in charge of the radiation safety and the radiation protection surveillance at the LNF. Environmental and individual radiation monitoring are routinely performed by means of active and passive dosemeters. The environmental dosimetry is based on a lattice of about 100 measurement points distributed over four "rings" around the DAΦNE accelerator complex, up to the boundary of the center. Each point is monitored by means of two dosemeters, provided and processed by the U.F. Fisica Sanitaria itself and the ENEA dosimetry Service, respectively. The same double dosemeter system is used for the individual monitoring of the "Category B" workers. A lattice of active monitoring units, each formed by a rem-counter and an ion chamber, are located around the DAΦNE accelerator complex, and operate as complementary ambient dosimetry system. In case the instantaneous ambient dose rate exceeds a given threshold level, the units provide an "alarm signal" which immediately shuts down the accelerator. Moreover, a confirmation monitoring with active neutron and gamma portable instruments is periodically performed over the center. The radiation induced activity in the components and the instruments inside the accelerator buildings is also periodically assessed. A series of low background Germanium detectors are used to check the potentially activated component and instruments before clearance or manipulation. The Groups is holding a series of Standards for the calibration of the instruments used for the radiation protection surveillance. Whilst radioactivity measuring devices are calibrated with portable alfa, beta and gamma sources, the active and passive dosemeters are calibrated with reference photon and neutron fields.

The Radiation Protection Group is also in charge of the workers classification, the radiation protection and safety training, the dose recording and all licensing and communication activities required by the Italian Radiation Protection Law, D.Lgs. 230/95.

The introduction, detention and use of radioactive sources or X-rays apparatus at the LNF is regulated and controlled by the Group.

The Group is involved in the radiation protection and safety aspects for the commissioning of the following projects: DAΦNE Upgrading, SPARC, DANAE, and SPAR-X.

2 Research and Development activities during 2006

The LNF Radiation Protection Group is involved in the study and the improvement of modern dosimetric and spectrometric techniques for the ambient and individual radiation monitoring, with special attention to the mixed neutron/photon fields characterizing the areas around high energy particle accelerators. Participation to collaborations, International Working Groups and inter-comparison activities in the mixed-field dosimetry field have been set up at national and international level.

2.1 Neutron spectrometry

In the field of the computational techniques applied to the neutron dosimetry, the LNF group developed the FRUIT code (Frascati Unfolding InTeractive Tool) for the determination of the energy distribution of the neutron fields with the Bonner Sphere Technique. The whole spectrometry system (Bonner Spheres + unfolding code) operates in the energy range from thermal to hundreds MeV neutrons, allowing an accurate characterization of the neutron fields around high energy accelerator based facilities. The LNF Bonner Sphere spectrometer and the code have been validated in different radiation environments [1], [2], such as the reference neutron fields of the ENEA-Bologna Institute for Radiation Protection and the ENEA-Frascati Fast Neutron Generator. This technique has been extended to different radiation environments by using integrating passive detectors, such as TLDs (thermoluminescence detectors) [3], [4] , [5], or gold foils.

The LNF Radiation Protection Group is contributing to the European Networks EURADOS (European Radiation Dosimetry Group) / CONRAD (Coordinated Network for Radiation Dosimetry), with direct participation to the following working packages: - WP4 computational dosimetry. This group organized and distributed worldwide the computational exercise Uncertainty assessment in computational dosimetry, based on data taken with the Frascati Bonner Sphere Spectrometer. - WP6 Complex mixed radiation fields at workplaces. This group organized an international neutron spectrometry and dosimetry experimental intercomparison, held in the GSI Darmstadt (17-23 July 2006).

In the framework of the EURATOM program Transnational Access to Large Infrastructures, the LNF Rad. Prot. Group carried out the experiment *Experimental validation of a multisphere spectrometric system used for radiation protection applications around high energy electron accelerators and medical LINACs* . The experiment was performed at the Van de Graaff accelerator of the Institute for Reference Materials and Measurements (IRMM), EC JRC Geel, Belgium (23-27 Jan. 2006).

In the framework of the bilateral INFN/MEC agreement, the LNF Rad. Prot. Group is continuing the Collaboration *Development and validation of experimental and computational techniques for neutron spectrometry in radiation protection* with the Radiation Physic Group of the Universidad Autonoma de Barcelona (UAB).

During 2006 a collaboration with the Hospital S. Camillo Forlanini (Rome) has been established with the aim to measure the neutron fields generated by a 18 MV radiotherapy electron LINAC. An external student of the Health Physics post graduate school (La Sapienza University, Rome) is involved. The measurements are going to be performed with the LNF Bonner Sphere set equipped with gold activation foils. The experimental technique and the computational method to derive the neutron spectra have been developed and tested [6] at the LNF Rad. Prot. Group.

2.2 Ambient neutron monitoring

In order to improve the accuracy of the neutron ambient dosimetry at the LNF, a new CR-39 based fast neutron dosimetry service has been established by the Rad. Prot, Group [7] [8], providing ambient dosemeters suitable for the monitoring of high energy accelerator based fields. Adequate chemical procedures and an automated image analyzer [9] have been developed for processing and reading the dosemeters. The LNF neutron dosemeter shows adequate sensitivity in the energy interval 0.1 - 20 MeV and a very low Minimum Detectable Dose Equivalent, 0.05 mSv per monitoring period. This kind of dosemeter provides a valuable contribution to the routine physical survelliance since its response is not influenced by photon radiation. An external researcher from the FAI program (M.J. Garca from the Universidad Autonoma de Barcelona) has been involved in the establishment of quality assurance procedures for the dosimetric service. The definitive implementation of the CR-39 for the ambient surveillance of the LNF is planned for half 2007.

2.3 Radiometric characterization of activated waste

The decommissioning of ADONE, in 1993, produced a considerable amount of potentially activated metallic scraps and slightly activated tritiated water. An experimental study for the characterization of the waste and the study of the clearance/storage options is in progress [10]. An external researcher in the framework of the FAI program (J. C. Mora) contributed to this work during 2006.

2.4 Secondary Standard calibration Laboratory

The Rad. Prot. Group holds a multi-source irradiation unit for the production of reference photon fields for the routine calibration of dosemeters and survey-meters. The reference fields of ^{241}Am, ^{137}Cs and ^{60}Co are available with a kerma rate interval from 0.0005 to 2 mGy.h^{-1}. A preparation work is in progress for the accreditation of the facility according to the SIT (Servizio di Taratura in Italia) network.

2.5 Standardization

Since 2006, A. Esposito and R. Bedogni are members of the UNI (Ente Nazionale Italiano di Unificazione) / Commissione Tecnica 85 Energia Nucleare / SC2 (Protezione dalle Radiazioni) and project leaders for the revision of the standards UNI 8144 *Radioprotezione per apparecchiature per analisi di diffratotometria e fluorescenza a raggi X* (A. Esposito); UNI 9880 *Strumentazione per dosimetria neutronica ambientale* (R. Bedogni). As Italian delegates at the ISO, they are participating to the International Standardization Organization ISO / TC85 (Nuclear Energy) / SC2 (Radiation Protection) for the production of the standards in the fields of: *Dosimetry for exposures to cosmic radiation in civilian aircraft* (Working Group 21) A. Esposito, *Reference Radiation fields* (Working Group 2), R. Bedogni.

2.6 Archaeometry

The Group supervised an Under graduated student in Roman Archaeology (F. Gonnella) which discussed her thesis during 2006. The work consisted in the characterization of roman finds by means of the X-rays fluorescence technique [11] [12]. An external associated scientist (A. Gorghinian) contributed to this activity.

3 Educational activities

The following experimental activities were performed with high school students during 2006: *Gamma Spectrometry with NaI(Tl)* (Stages invernale) *Measurements of environmental radioactivity with a Geiger Muller counter* (Stages estivi).

References

1. R. Bedogni.*Neutron spectrometry and dosimetry for radiation protection around a high energy electron/positron collider.* Ph. D. Thesis. Universidad Autonoma de Barcelona, Barcelona, Spain (2006). .

2. R. Bedogni, A. Esposito, C. Domingo, F. Fernandez, M. J. Garca, M. Angelone. *Performance of the UAB and the INFN-LNF Bonner sphere spectrometers in quasi mono-energetic neutron fields. Radiat. Prot. Dosim.,* accepted for publication.

3. R. Bedogni, A. Esposito, M. Chiti, M. Angelone. *Neutron spectrometry around a high energy electron-positron collider using a multi-sphere system with passive detectors. Radiat. Prot. Dosim.,* accepted for publication.

4. R. Bedogni, A. Esposito, M. Angelone and M. Chiti. .*Determination of the Response to Photons and Thermal Neutrons of New LiF Based TL Materials for Radiation Protection Purposes.* IEEE Trans. Nucl. Sci. 53(3), 1367-1370 (2006). ISSN 0018-9499.

5. R. Bedogni, M. Angelone, A. Esposito and M. Chiti. *Inter-comparison among different TLD-based techniques in a standard multisphere assembly for the characterization of neutron fields.* Radiat. Prot. Dosim. 120(1-4) part 2, 369-372 (2006). ISSN 0144-8420.

6. A. Esposito, R. Bedogni, L. Lembo, M. Morelli. *Tecniche per la spettrometria neutronica attorno ad acceleratori di particelle: acceleratori medical.* Proceed. Convegno Nazionale di Radioprotezione - La radioprotezione nella ricerca. La ricerca in radioprotezione, Catania, 15-17 Settembre 2005. ISBN 88-88648-03-8.

7. R. Bedogni, A. Esposito, G. Lovestam, M. J. Garca, M. Virgolici. *The new CR-39 based fast neutron dosimetry system of the INFN-LNF.* Submitted to Radiat. Meas.

8. A. Esposito, R. Bedogni, A. Gentile. *Monitoring the ambient neutron radiation around a high energy electron/positron collider using CR-39 dosemeters.* Submitted to Radiat. Meas.

9. R. Bedogni *Development of a reader for the routine analysis of CR-39 fast neutron dosemeters: improvement of the dosimetric performance using automatic vision and motion tool.* Radiat. Meas. 36(1-6), 239-243 (2003).

10. J. C. Mora, R. Bedogni, A. Esposito and D. Cancio. *Investigation of induced radioactivity in the LINAC-ADONE accelerator complex for the management of the decommissioned material.* Health Phys., accepted for publication.

11. A. Esposito, G. Cappuccio, F. Gonnella, A. Gorghinian, A. Jaia. *XRF Applied to Archaelogical Samples.* EXRS 2006 European Conference on X-Ray Spectrometry Paris, France June 19-23 2006

12. A. Esposito, G. Cappuccio, F. Gonnella, A. Gorghinian, A. Jaia. *Studio di reperti ceramici repubblicani (IV-I sec a.c.) a vernice nera.* Congresso Societ italiana di Fisica - Torino 18-22 settembre 2006

SPARC

D. Alesini, M. Bellaveglia, S. Bertolucci, R. Boni, M. Boscolo, M. Castellano, A. Clozza, L. Cultrera, G. Di Pirro, A. Drago, A. Esposito, M. Ferrario, L. Ficcadenti, D. Filippetto, V. Fusco, G. Gatti, A. Gallo, A. Ghigo, M. Incurvati, C. Ligi, F. Marcellini, M. Migliorati, A. Mostacci, L. Palumbo, L. Pellegrino, M. Preger, R. Ricci, C. Sanelli, M. Serio, F. Sgamma, B. Spataro, A. Stecchi, A. Stella, F. Tazzioli, S. Tomassini, C. Vaccarezza, M. Vescovi, C. Vicario **(INFN/LNF)**

F. Alessandria, A. Bacci, I. Boscolo, F. Broggi, S.Cialdi, C. De Martinis, D. Giove, C. Maroli, M. Mauri, V. Petrillo, M. Romè, A. R. Rossi, L. Serafini **(INFN/Milano)**

D. Levi, M. Mattioli, P. Musumeci, G. Medici, D. Pelliccia, M. Petrarca **(INFN/Roma1)**

L. Catani, E. Chiadroni, A. Cianchi, E. Gabrielli, S. Tazzari **(INFN/Roma2)**

A. Perrone **(INFN/Lecce)**

F. Ciocci, G. Dattoli, A. Dipace, A. Doria, G.P. Gallerano, L. Giannessi, E. Giovenale, G. Messina, P.L. Ottaviani, S. Pagnutti, L. Picardi, M. Quattromini, A. Renieri, G. Ronci, C. Ronsivalle, M. Rosetti, E. Sabia, M. Sassi, A. Torre, A. Zucchini **(ENEA/FIS)**

J. Rosenzweig, G. Travish, S. Reiche **(UCLA)**

1 Aim of the experiment

The aim of the SPARC project is to promote an R&D activity oriented to the development of a high brightness photoinjector to drive SASE-FEL experiments. It has been proposed by a collaboration among ENEA-INFN-CNR-Universita‘ di Roma Tor Vergata-INFM-ST and funded by the Italian Government and INFN.

The main goals of the SPARC project are:

1. the generation of a high brightness electron beam able to drive a Self Amplified Spontaneous Emission Free Electron Laser (SASE FEL) experiment in the green visible light, Seeding and Higher Harmonics Generation,

2. the development of an ultra-brilliant beam photo-injector needed for the future SASE FEL-based X-ray sources, as for the recently funded 1 GeV 10 nm FEL project SPARX whose SPARC is become its test facility.

The SPARC injector will allow also investigations into the physics of ultra-short beams, plasma wave-based acceleration, and production of X-ray Compton back-scattering as reported in the PLASMON activity section.

The first phase of the SPARC project consists in characterizing the electron beam out of the photoinjector at low energy (5 MeV) before the installation of the three accelerating sections. The design goal in terms of peak current (100 A) and emittance (2 mmmrad) has been successfully achieved during the year 2006 by the team shown in Fig. 1. The experimental layout for this phase of the project is shown in Fig. 2.

Figure 1: *Picture of SPARC team, taken at the end of phase I run.*

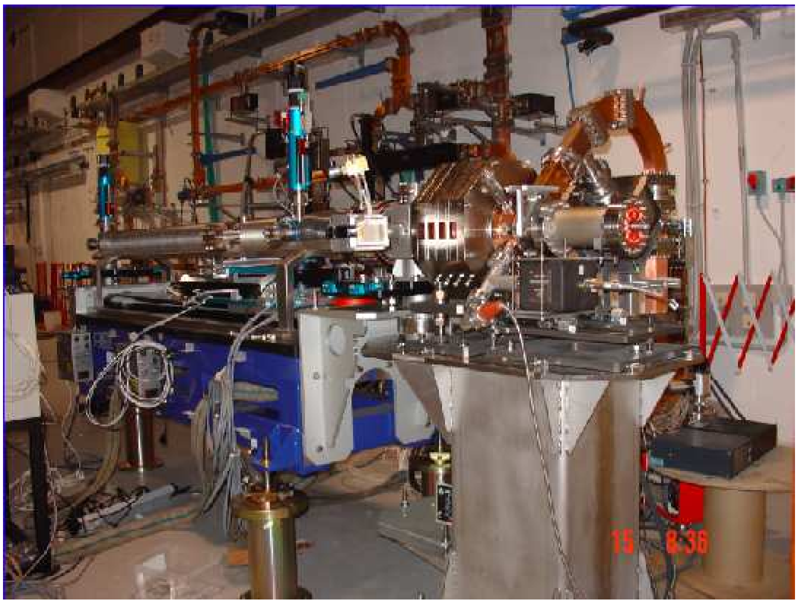

Figure 2: *Picture of the SPARC photoinjector showing the RF gun with solenoid and emittance meter installed.*

To reach this results a lot of efforts has been done to make all the SPARC components work properly, as will be discussed in this report.

The SLAC/BNL/UCLA 1.6 cell S-band RF gun was conditioned up to 10 MW, corresponding to a field of 120 MV/m at the beginning of 2006.

The photocathode drive laser has been characterized in terms of pulse shape and quality and the first generation of an UV flat top laser pulse has been achieved. In combination with a quite high Quantum Efficiency (QE) up to 10^{-4} of the copper photocathode, obtained after a dedicated laser cleaning, the nominal beam electron beam parameters have been obtained (1 nC , 10 ps long).

In order to study the first few meters of beam propagation where space charge effects and plasma oscillations dominate the electron dynamics, a new sophisticate diagnostic tool has been installed and commissioned: the movable emittance-meter.

Emittance oscillations driven by space charge in the drift downstream ther RF gun have been observed, in agreement to what expected from our theoretical model and numerical simulations, and the first experimental observation of the double emittance minima effect, on which is based the optimized matching with the SPARC linac, has been achieved.

In addition the particular design of the emittance-compensating solenoid with 4 different coils inside the magnetic yoke allowed a study of how different magnetic field configurations affect the electron beam dynamics in particular varying (in sign and absolute values) independently the current setting for each coil power supply.

Additional parallel activities in the framework of future higher energy FEL experiments (SPARX) have been brought ahead and the recent results from R&D on new photocathode materials, X-band RF structures and advanced diagnostic will be also reported.

2 Group activity in 2006

2.1 Cathode and Laser system

Challenging requests are made on laser temporal pulse profile (flat top pulse with ∼1 ps rise time and ripples limited to 30%) to minimize the e-beam emittance, consequently the main activity of the laser group has been devoted to optimize pulse shaping techniques. The Laser system layout is shown in Fig. 3.

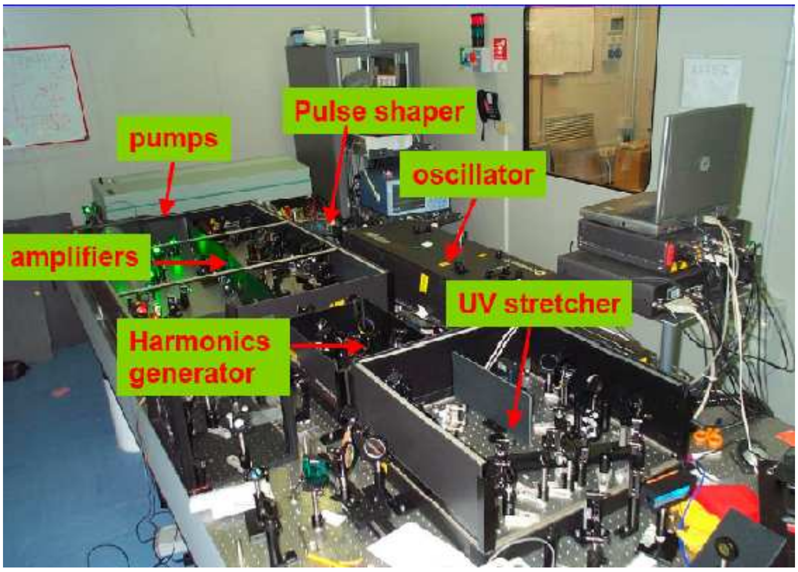

Figure 3: *Laser system layout.*

We currently use a mono-cristalline Cu cathode with a quantum efficiency (QE) of 10^{-4} at 120 MV/m, achieved after a successful in situ laser cleaning treatment, therefore it is required about 50 μJ to extract 1 nC at the operating phase. The SPARC laser is a 10 Hz TW system produced by Coherent. The laser system is composed by a Ti:Sa oscillator that generates 100 fs pulses with a repetition rate of 79:3 MHz and an energy of 10 nJ. An acousto-optic programmable dispersive filter called "DAZZLER", used to modify the spectral amplitude and phase is placed between the oscillator and the amplifier to obtain the target temporal profile in the UV. The regenerative and two multi-pass amplifiers delivers pulses with bandwidth of at 10 nm FWHM $\lambda = 800$ nm with energy of $\sim$50 mJ and divergence less than 1 mrad. The amplified pulses go to the third harmonic generator (THG) where UV pulses with an energy up to $\sim$ 4 mJ are produced. The THG is characterized by two type-I BBO (Beta Barium Borate) crystals of 0:5 mm and 0:3 mm thickness used to produce respectively the second and third harmonics. The crystal lengths have been chosen to allocate enough bandwidth to preserve the pulse shape and, at the same time, to guarantee good efficiency. The efficiency of the first conversion is about 50% and the overall conversion efficiency is more than 10%. After the THG the pulse is sent to a pair of 4300 g/mm UV parallel gratings, that forms a negative group velocity dispersion two passes stretcher. Varying the distance L between the gratings it is possible to obtain the output pulse length . The energy efficiency of the UV stretcher is about 30% producing a energy up to 1.5 mJ with an amplitude jitter of 5%RMS. To characterize the pulse time profile a multishot crosscorrelator with 200 fs resolution was built. The diagnostics uses part of the sub-ps IR pulse to cross-correlate the UV pulse and generating the frequency difference at 400 nm. According with the theory and experimental measurements, when a large chirp is imposed, such as for our the UV stretcher, the pulse spectrum allows the direct reconstruction of the time intensity distribution. For the spectral measurements in the UV it has been designed a spectrometer using a UV grating with 4350 g/mm and a converging lens to focus the different wavelength on a ccd camera. This diagnostic proved a the resolution of 0.02 nm. The optical transfer line to the cathode has been designed to increase the pointing stability, to easily change the spot dimension and to provide a normal incidence on the cathode surface.

In Fig. 4 the mesured flat top laser pulse is reported, showing a 10 ps (FWHM) longitudinal profile with rise and fall time less that 2 ps. Additional work is under way to make this results more stable and improve also the uniformity of transverse distribution.

2.2 RF system and synchronization

The SPARC RF system is mainly constituted by two RF chains. The power sources, are the 45 MW peak, 2856 MHz klystrons TH2128C. The klystron n.1 presently feeds only the RF gun with 3 sec long pulses and it is designed to feed also one accelerating section via a 3dB waveguide coupler and an RF deflecting cavity for beam diagnostic purposes.

The RF gun, has been successfully conditioned without relevant problems and we fed into it more than 10 MW of RF power that corresponds to an accelerating field of about 120 MV/m. Klystron n. 2 and its waveguide distribution lines are now under test and they will feed two high gradient accelerating sections through an energy compressor that allows to obtain a 60 MW - 0.8 μsec RF pulse.

The timing distribution system is installed and it provides the 79.33 MHz reference to lock the laser system to the RF oscillator using a home-designed frequency divider board. It also furnishes the 10 Hz repetition rate signal to the machine, synchronous with the external line and to the 2856 MHz internal distribution.

The synchronization diagnostic is working with good and stable performances and the time jitter from each location of the machine (relative to the main oscillator) is displayed in the control room monitors. Also an RF phase feedback system was implemented to correct slow drifts due to

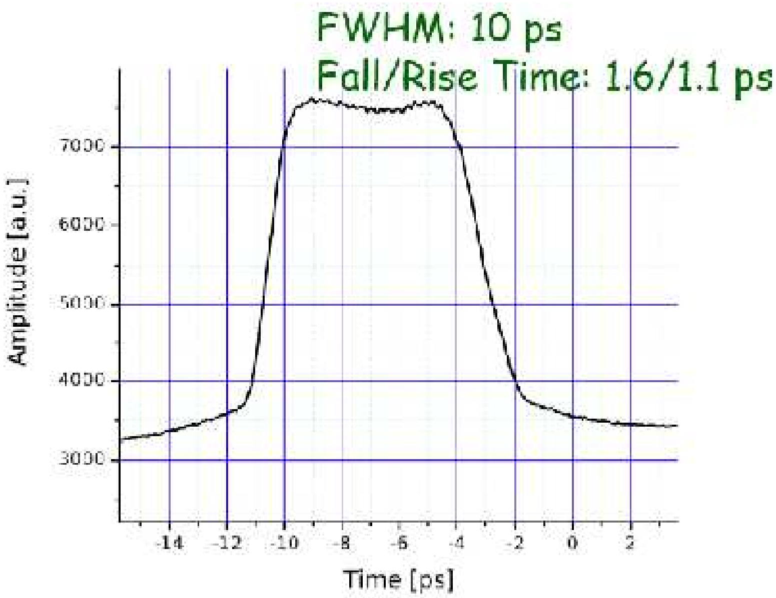

Figure 4: *Measured flat top laser pulse, showing a 10 ps (FWHM) longitudinal profile with rise and fall time less than 2 ps.*

temperature. The observed rms time jitter of the accelerating field inside the gun is 250 fs and the laser oscillator rms time jitter is 350 fs.

2.3 The control system

The control system is working and it is ready to be extended to the SPARC full configuration. The SPARC main server with a RHEL3 operating system, is in a LTSP configuration so that the consoles are identical diskless workstations. The photo-injector device drivers are installed in industrial PCs placed in the bunker.

Two machines form a connecting bridge from the front-end industrial PCs to the control room consoles. The data server: it accepts a request of information from the consoles and send them the data read from the proper industrial PC. The data can be software variables (that identify the controlled devices), sampled signals, images or information about the status of the computer itself. And the command server: it elaborates the queue coming from the consoles and, once identified legal commands, it delivers them to the front-end PCs to control the photo-injector devices.

2.4 Advanced Diagnostic devices: the emittance meter and the RF deflector

The complete characterization of the beam parameters at different distances from the cathode is important to find the injector settings optimizing emittance compensation and for code validation. For this purpose, a dedicated moveable emittance measurements device (emittance-meter) is used allowing to measure the RMS emittance downstream the gun in the range from about z=86 cm to z=210 cm. More than a simple improvement over conventional, though non-trivial, beam diagnostic tools this device defines a new strategy for the characterization of novel high performance photo-injectors, providing a tool for detailed analysis of the beam dynamics and the phase space.

The technique to measure the beam emittance and the phase space, in both the horizontal and vertical planes, makes use of a double system of horizontal and vertical slit masks. Each mask consists of a slit array (7 slits, 50 μm width spaced of 500 μm, 2 mm thick) and two single slits, 50 and 100 μm width. The slits are realized by photo-chemical etching providing, compared to mechanical machining, higher precision and improved smoothness of slits edges. The multislits are used for single shot measurements, provided the beam size is large enough for an adequate beam sampling by the slit array. Alternatively, a single slit can be moved across the beam spot. In this case the accuracy of transverse sampling can be freely chosen adjusting the step between the different positions of the slit. This measurement is an integration over many pulses. Linear actuators with stepper motors are used to control the insertion of the slits masks into the beamline. A differential encoder and a reference end switch guarantee reproducibility and accuracy of the movement to better than 2 μm, required for single-slit multi-shots measurements.

The projected cross-section of beamlets emerging from the slit-mask are measured by means of a downstream Ce:YAG radiator. Because beam size and divergence depend on the device longitudinal position, the slit to screen distance must be properly adjusted in order to optimize the accuracy of the beamlet profiles measurement. A bellow is therefore interposed between the slit mask and the screen, allowing their relative distance to be changed from 22 to 42 cm, to optimize the drift in order to fit several scenarios (converging beam, diverging beam, single or multi-slits).

Radiation emitted in the forward direction from the Ce:YAG crystal is collected by a 45 degrees mirror downstream from the radiator. The back face of the transparent crystal radiator is observed, thus minimizing degradation of the spatial resolution due to the depth of field of the optics.

Images are acquired using digital CCD cameras (Basler 311f) equipped with simple 105 mm "macro" type objective from SIGMA. The magnification of 0.66 gives a calibration of 15.4 μm per pixel. Such cameras offer the advantage that the signal is digitalized directly by on-board electronic so that there is no need for a frame grabber and the output signal, being digital, is less sensitive to environmental noise. Furthermore, the IEEE1394 (firewire) link allows simpler cabling topology because it carries both pixels readout and commands to the camera. Charge is measured by means of a Faraday cup, placed in a cross together with a cromox screen to image the beam at 60 cm from the cathode. This screen is also used to monitor the position of the laser spot on the cathode. The emittance-meter is followed by a magnetic spectrometer measuring the beam energy and energy spread.

The six-dimensional beam phase space characterization at the exit of a photoinjector is another important measurement we have foreseen to conduct in the second phase of the SPARC commissioning. This measurement is based on the use of an RF deflector that allows measuring the temporal profiles of the beam, as well as the complete longitudinal phase space by adding a dispersive system. Using the quadrupole scan technique the horizontal beam slice emittances as a function of longitudinal position in the beam can also be measured. Simulations made by the ELEGANT code have shown the feasibility of this diagnostic system.

The RF deflector design has been made by the use of the e.m. codes MAFIA and HFSS. The RF deflector proposed is a 5-cell SW structure working on the π mode at 2.856 GHz and fed by a central coupler with β=1 . Since the transverse shunt impedance is 2.5MΩ and the maximum input power is 2MW, it is possible to obtain a resolution length of the order of 12 mm. Two small longitudinal rods have been inserted to shift the resonant frequency of the 90 deg rotated polarity modes with respect to the working mode. By the bead-pull technique we have measured the deflecting field on axis. A tuning procedure has been implemented in order to reach a field flatness of the order of a few percents. External quality factor measurements have also been done, showing good agreement with expectations.

2.5 Experimental results with the beam

We performed a detailed characterization of the photoinjector, studying the beam dynamics as function of relevant parameters such as the solenoid field, the beam charge and size, the laser pulse length and its shape. First of all we made charge versus gun RF phase measurement (phase scan) that allow us to choose day by day the optimal phase for the electron extraction and to collect information about the accelerating gradient and cathode quantum efficiency. Moreover this kind of measurement allows to obtain a rough estimation of the beam duration. Fig. 5 shows some phase scans performed in different photo-injector working points.

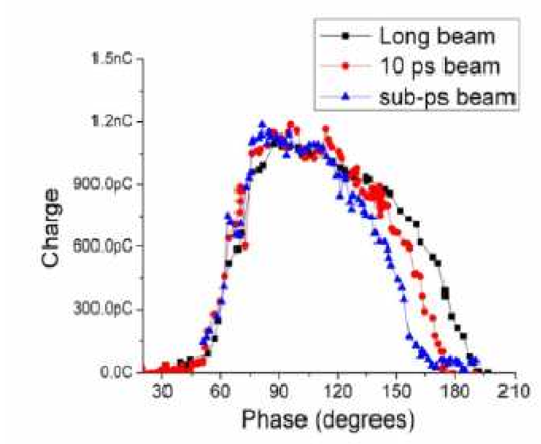

Figure 5: *Charge vs phase in three different beam configurations.*

The spectrometer and its transport line (constituted by a FODO cell) are placed at the end of the diagnostics chain to measure energy and energy spread. We performed these measurements in low and high charge configurations versus the launching phase as shown in Fig. 6. The difference both in maximum energy and energy spread between the low and high charge case are due to longitudinal space charge effects (including the image charge at the cathode).

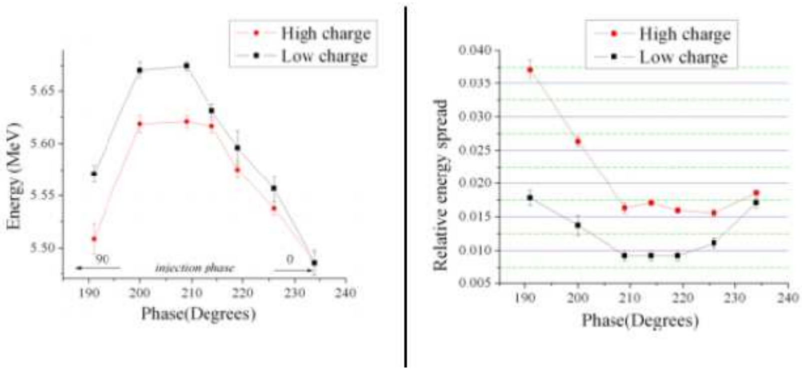

Figure 6: *Energy (a) and energy spread (b) for low and high bunch charge.*

The e-meter gives also the possibility to investigate the longitudinal dynamics by inserting a slit and selecting a low charge beam slice at different longitudinal locations.

By doing so, as shown in Fig. 7, we can 'froze' the space charge contributions to energy

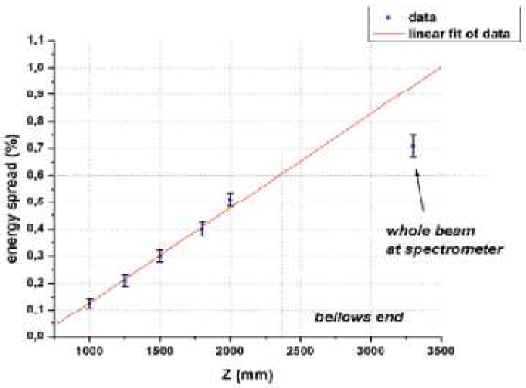

Figure 7: *Energy spread versus z.*

spread growth and measure its evolution at different locations along the beamline. Moving the slit over the beam and measuring the energy and the energy spread in the spectrometer gives information of possible correlation between position and energy. Also centering the slit on the beam and moving along the emittance meter allows the measure of the energy spread in different longitudinal positions.

A longitudinal diagnostic, based on Cherenkov radiation produced by the beam passing through a 5 mm thick aerogel slab with index of refraction n = 1.017, was installed with the main purpose of studying the photoinjector response to different laser pulses length. A field-lens narrow band filtering optical system delivers the Cherenkov light to the entrance slit of a 2ps resolution Hamamatsu streak camera enabling direct pulse length measurements see Fig. 8.

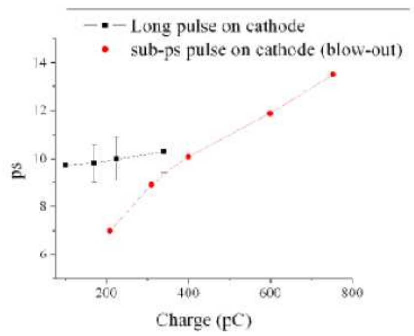

Figure 8: *Bunch length measurements with streak camera.*

With the emittance meter is possible to follow the emittance evolution, and tuning the machine parameters. A typical emittance measurement with the single-slit mask consists of collecting

15 beam images for each slit position. The center of mass and RMS size of beamlets are then calculated for each image and averaged. From the beamlets images we calculate the projection on the axis, subtract the baseline, try a gaussian fit to find the best position for the distribution center, reduce the number of the relevant points skipping these that are outside the 3 standard deviation from the centre and only on the remaining points we calculate the RMS parameters.

The use of big magnification, an high efficiency YAG and a CCD with a gain remotely controlled give a good signal to noise ratio and large number of sampling point for every beamlet in all the conditions.

The 1-D pepper pot technique allows not only to measure the beam and the Twiss parameters, but also to reconstruct the phase space. In Fig. 9 the phase space reconstruction in different

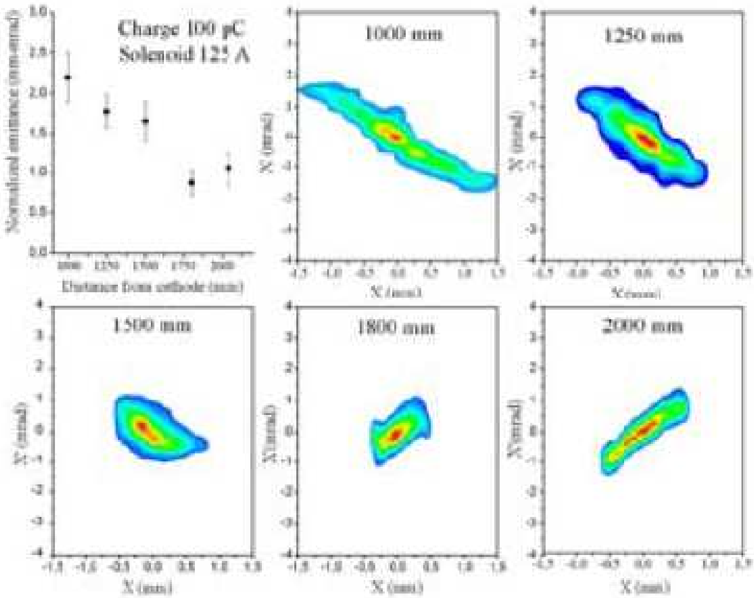

Figure 9: *Phase space reconstruction.*

positions, measured at low charge, 100 pC is shown.

A careful data analysis is still under way and final results will be published at the beginning of 2007. We report hereafter for example two results that are consistent with PARMELA simulations performed taking in to account the real machine parameters. The first one (Fig. 10) shows the envelope and the emittance behaviour downstream the gun exit obtained with 1 nC Gaussian longitudinal charge distribution in 12 ps FWHM long pulse, corresponding to 83 A peak current. The achieved emittance minimum, 2 mm-mrad, is very close to the simulation result and to the theoretical best performances obtainable with this bunch parameters.

The second case (Fig. 11) is 1 nC Flat Top longitudinal charge distribution in 10 ps FWHM long pulse, corresponding to a higher peak current: 100 A. Better results are expected with a Flat Top distribution when an improved transverse uniformity distribution will bw achieved, a subject of investigation in the next SPARC run.

In the following plot, Fig. 12, is reported the emittance measured at a fixed position (z=1.5 m) as a function of the solenoid current, the so called B-scan. The interpretation of this results is

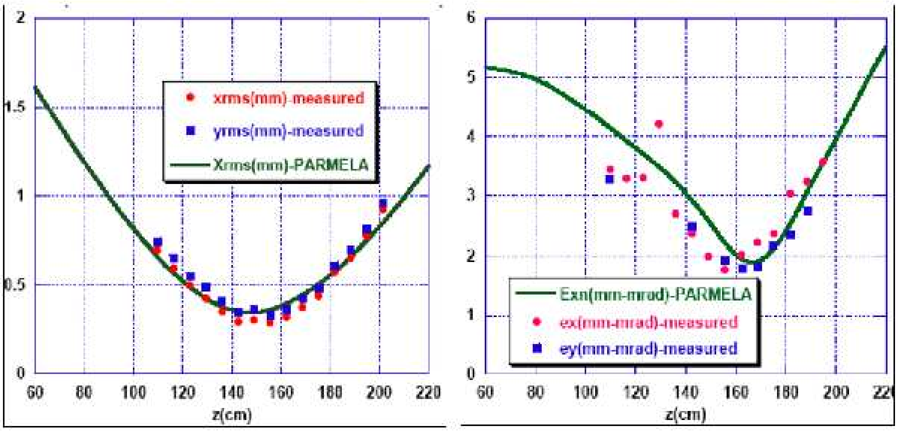

Figure 10: *Envelope and emittance versus z for a Gaussian pulse.*

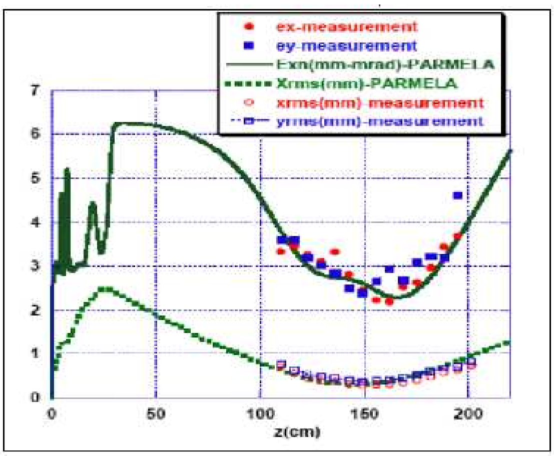

Figure 11: *Envelope and emittance versus z for a Flat Top pulse.*

still subject of investigation. Nevertheless it seems quite evident the double emittance minimum behavior on which is based the optimized matching with the SPARC linac.

2.6 New Cathode developments

Among the parallel activities of the SPARC project new cathode developments gave very interesting result during the year 2006. We investigated the deposition of high quality metal films directly on the RF gun cavity end plate, to be used as photocathodes. Main aim of this study is to circumvent problems of RF breakdown shown at the metal junction by Mg disks inserted by press fitting in the end Cu plate of the gun. A key parameter determining the adherence of a deposited film is the kinetic energy of the particles impinging on the substrate. Therefore it is worthwhile to study alternative deposition processes with inherent higher particle energies, as pulsed laser deposition (PLD) and vacuum arc discharge.

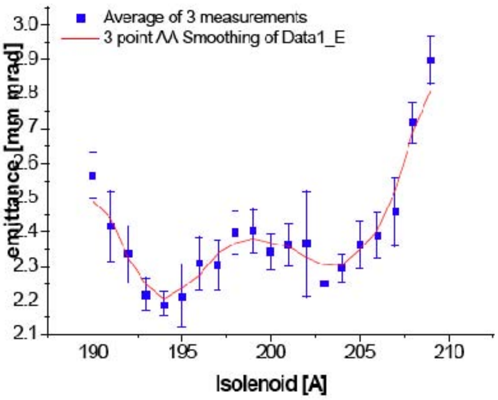

Figure 12: *Emittance versus solenoid current at a fixed position , z=1.5 m.*

The PLD deposition apparatus used in this study is made up of an UHV chamber containing the Mg target to be ablated and the substrate to be coated. A powerful laser beam from a XeCl excimer laser (pulse duration 30 ns), impinges on the target and forms a plume of Mg vapor. The substrate is placed in the plume cone at a suitable distance from the target.

Films with thickness from 0.2 to 2.5 μm, covered or not with thin protective layer either of graphite, palladium or silicon have been synthesized. A computer controlled laser cleaning procedure has been implemented in order to clean the surface gradually and uniformly, thus allowing a controlled removal of the contaminated surface layers and avoiding pure film deterioration. Mg films grown by PLD either with or without protective layers gave remarkable results in terms of QE, ranging from 1.4x10^{-4} up to 7.9x10^{-4} at low dc electric field (1 MV/m), see Fig. 13.

2.7 X-band structure

An 11 GHz π-mode cavity for linearizing the longitudinal phase space in SPARC has been realised and brazed. Experimental tests have given satisfying results. The electromagnetic behaviour, in terms of E field on axis, Q factor and R/Q form factor does not show substantial variations. The brazing procedure has been successfully studied and carried out. A cooling system has been designed and calculated and simulations prove that it works correctly. Alternative solutions to reduce the peak surface field and thus to allow higher accelerating gradients have been considered and analyzed.

A Bi-Periodic X-Band accelerating section has been also proposed and the copper prototype, shown in Fig. 14, has been realized. Resonant frequency, quality factors and electric field have been measured on the copper prototype in the open and close stop-band cases. Even if the prototype is not brazed the measurement results are very close to the expectation. Thermal analysis has been carried out using ANSYS code. Brazing tests are now in progress in the LNF for the construction of the final device.

References

1. S. Cialdi, M. Petrarca, C. Vicario, "High-power third-harmonic flat pulse laser generation", Opt. Lett. Vol 31, (2006), 2885, and Virtual Journal of Ultrafast Science Oct. 2006.

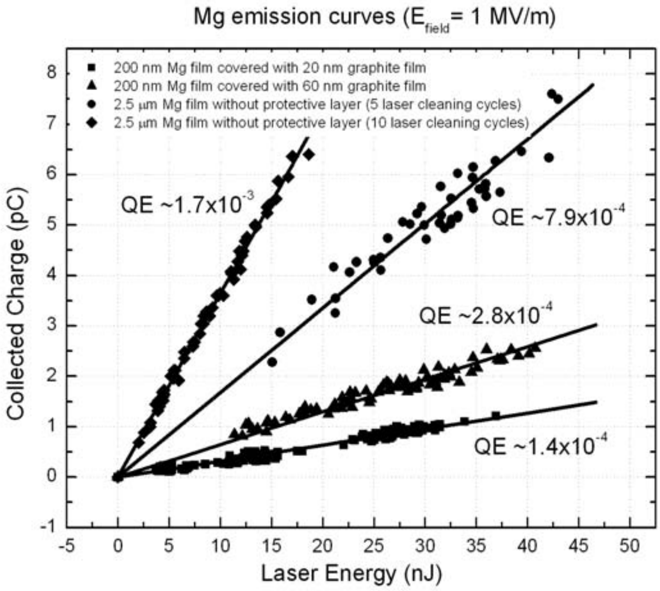

Figure 13: *Emission curves of different Mg samples deposited by PLD on Cu substrates, after the laser cleaning of the protective or contaminated layers.*

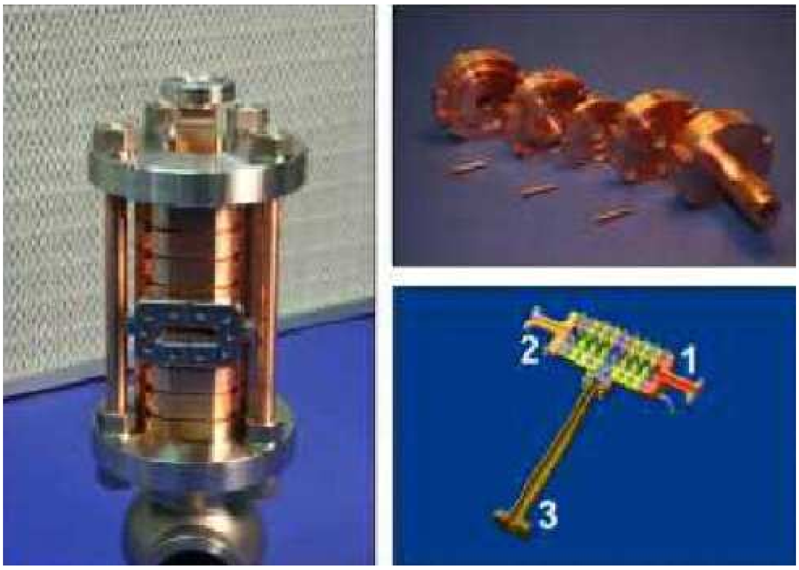

Figure 14: *Copper prototype of the structure.*

2. D. Alesini, G. Di Pirro, L. Ficcadenti, A. Mostacci, L. Palumbo, J. Rosenzweig, c. Vaccarezza, "RF deflector design and measurements for the longitudinal and transverse phase space characterization at SPARC", NIM A, Vol: 568 Issue: 2 (2006).

3. M. Ferrario, V. Fusco, C. Ronsivalle, L.Serafini, C. Vaccarezza, "Beam dynamics in a high brightness linac for short wavelength SASE-FEL experiments", New Journal of Physics 8 (2006) 295.

4. M. Ferrario, "Overview of FEL Injectors", Invited talk, EPAC 06 , Edinburgh.

5. P. Musumeci, "Inverse Free Electron Lasers for Advanced Light Sources", Invited talk, FEL 06, Berlin.

6. E. Chiadroni, "Recent Results with the SPARC Emittance Meter", Invited talk, EUROFEL Workshop, Daresbury.

7. M. Bellaveglia, G. Di Pirro, A. Gallo, "A new radiofrequency data acquisition system in the SPARC project at LNF" presented at "Forum Tecnologico sulla strumentazione Virtuale - NIDays".

8. D. Filippetto, "Commissioning of the Sparc Photo-Injector", FLS Workshop, Hamburg.

9. M. Boscolo et al., "Laser Comb: Simulations of Pre-modulated E- Beams at the Photocathode of a High Brightness RF Photoinjector", EPAC 06, Edinburgh.

10. P. Musumeci et al., "Status of the SPARC Project", EPAC 06, Edinburgh.

11. C. Ronsivalle et al., "Study of the Effect of Multipolar Components in the SPARC Emittance Compensation Gun Solenoid", EPAC 06, Edinburgh.

12. V. Petrillo et al., "Analysis of Radiative Effects in the Electron Emission from the Photocathode and in the Acceleration inside the RF Cavity of a Photoinjector using the 3D Numerical Code RETAR", EPAC 06, Edinburgh.

13. M. Ferrario et al., "Electron Beam-laser Interaction near the Cathode in a High Brightness Photoinjector", EPAC 06, Edinburgh.

14. J.B. Rosenzweig et al., "Optimum Beam Creation in Photoinjectors Using Space-charge Expansion", EPAC 06, Edinburgh.

15. A. Cianchi et al., "Characterization of the SPARC Photo-injector with the Movable Emittance Meter", EPAC 06, Edinburgh.

16. B. Spataro et al., "A Biperiodic X-band RF Cavity for SPARC", EPAC 06, Edinburgh.

17. B. Spataro et al., "Progress on the Pi-mode X-band RF Cavity for SPARC", EPAC 06, Edinburgh.

18. M. Bellaveglia et al., "Commissioning of the SPARC Photo-Injector", FEL 06, Berlin.

19. J.B. Rosenzweig et al., "Optimum Beam Creation In Photoinjectors Using Space-Charge Expansion", FEL 06, Berlin.

20. L. Catani et al., "Operational Experience with the Emittance-Meter at SPARC", FEL 06, Berlin.

21. L. Giannessi et al., "Future Seeding Experiments at SPARC", FEL 06, Berlin.

22. R. Boni et al., "Status of the Sparc Photoinjector", LINAC 06, Knoxville.

23. M. Bellaveglia et al., "The RF System of the Sparc Photo-Injector LNF", LINAC 06, Knoxville.

YEAR 2006 FRASCATI PUBLICATIONS

Available at www.lnf.infn.it

1 – Frascati Physics Series

Volume XL
Frontier Science 2005 – New Frontiers in Subnuclear Physics
Eds.: A. Pullia, M. Paganoni
Milano, September 12 - 17, 2005
ISBN—88–86409–46–X

Volume XLI
Discoveries in Flavour Physics at e^+e^- *Colliders*
Eds.: L. Benussi, S. Bianco, C. Bloise, R. de Sangro, C. Gatti, G. Isidori, M. Martini, F. Mescia, S. Miscetti
Frascati, February 28th - March 3rd, 2006
ISBN—88–86409–51–6

Volume XLII – Special Issue
Les Rencontres de Physique de la Vallée d'Aoste –
Results and Perspectives in Particle Physics
Ed.: M. Greco
La Thuile, Aosta Valley, March 5 – March 11, 2006
ISBN—88–86409–47–8

2 – LNF–Frascati Reports

LNF - 06 / 1(P)
F. Terranova, S.V. Bulanov, J.L. Collier, H. Kiriyama, F. Pegoraro
Enabling Pulse Compression and Proton Acceleration in a Modular ICF Driver for Nuclear and Particle Physics Applications
Accettato su Nucl. Instrum. Meth. A

LNF - 06 / 2(NT)
Angelo Veloce
VPN at LNF - User Guide

LNF - 06 / 3(P)
Olaf N. Hartmann
Tracking in Antiproton Annihilation Experiments
Published on Nuclear Instr. and Meth. Presented at the Workshop on Tracking In High Multiplicity Environments (TIME05) October 2005, Zurich, Switzerland

LNF - 06 / 4(P)
B.V. Robouch, A. Kisiel, A. Marcelli, M. Cestelli Guidi, M. Piccinini, E. Burattini, A. Mycielski
Statistical Model of Sphalerite Structured Quaternary A1–xBxYyZ1-y Systems
Journal of Alloys and Compounds (article accepted)

LNF - 06 / 5(NT)
Claudio Bisegni
Software per il Monitoring dei Parametri Oracle

LNF - 06 / 6(IR)
G. Bellettini, A. Bosco, C. Cantone, I. Ciufolini, D. Currie, S. DellAgnello, G. Delle Monache, M. A. Franceschi, M. Garattini, T. Napolitano, A. Paolozzi, E. C. Pavlis, D. P. Rubincam, V. J. Slabinski, R. Tauraso
Applicazioni Tecnologiche della Camera Spaziale Climatica dei Laboratori Nazionali di Frascati

LNF - 06 / 7(P)
Alessio Bocci, Massimo Piccinini, Alessandro Drag, Mariangela Cestelli, Diego Sali, Pierangelo Morini, Emanuele Pace, Jozef Piotrowski, Augusto Marcelli
Detection of Pulsed Synchrotron Radiation Emission with Uncooled Infrared Detectors
Review of Scientific Instruments

LNF - 06 / 8(IR)
INFN - (Frascati, Genova, L'Aquila, Roma, Roma2), University of Genova, University of Lieden
SFERA - Proposal for a Sperical Gravitational Wave Detector

LNF - 06 / 9(P)
N. Nasonov, V.A. Likhaekev, S.B. Dabagov
Modification of Radiation by Relativistic Particles in Thin Target Due to Transition Radiation
Proc. of SPIE Vol 5974 Presented at International Workshop on Charged and Neutral Particles Channeling Phenomena - 'Channeling 2004', 2-6 November 2004, Frascati (Rome), Italy

LNF - 06 / 10(IR)
AA VV
2005 Annual Report

LNF - 06 / 11(IR)
F. Ambrosino, F. Anulli, D. Babusci, S. Bianco, C.Bini, N.Brambilla, R.De Sangro, P.Gauzzi, P.M. Gensini, S. Giovannella, V. Muccifora, M. Negrini, F. Nguyen, S. Pacetti, G.Pancheri, M. Passera, A. Passeri, A.D.Polosa, M.Radici, Y.N. Srivastava, A.Vairo, G.Venanzoni, G.Violini
Prospects for e^+e^- physics at Frascati between the ϕ and the ψ 03-04-2006

LNF - 06 / 12(IR)
S. Bellucci, S. Ferrara
Lessons in SuperGravity
(In press)

LNF - 06 / 13(NT)
S. Bianco, M.A.Caponero, F.L. Fabbri, A.Paolozzi
Omega-Like Fiber Bragg Grating Sensors as Position Monitoring Device: A Possible Pixel Position Detector in CMS?

LNF - 06 / 14(IR)
L. Benussi, M. Bertani, S. Bianco, M.A. Caponero, D. Colonna, F.L. Fabbri, F. Felli, M. Giardoni, A. La Monaca, F. Massa, B. Ortenzi, M. Pallotta, A. Paolozzi, L. Passamonti, B. Ponzio, D. Pierluigi, C. Pucci, A. Russo
Primi Risultati DI Fluidodinamica (CFD) Gassosa in Rivelatori RPC dell'Esperimento CMS e Studio Sem-Eds dei Materiali in Presenza di Acido Fluoridrico
(In press)

LNF - 06 / 15(P)
S. Bellucci, S. Krivonos, A. Shcherbakov
N=4, d=3 Nonlinear Electrodynamics
(In press)

LNF - 06 / 16(P)
Stefano Bellucci, Sergio Ferrara, Murat Gùnaydin and Alessio Marrani
Charge Orbits of Symmetric Special Geometries and Attractors
(In press)

LNF - 06 / 17(P)
Francesco Celani, A. Spallone, E. Righi, G. Trenta, G. DAgostaro, P. Quercia, V. Andreassi, O. Giacinti, P. Marini, V. DI Stefano, M. Nakamura, F. Todarello, E. Purchi, A. Mancini, P. G. Sona, F. Fontana, L. Gamberale, D. Garbelli, E. Celia, F. Falcioni, M. Marchesini, E. Novaro, U. Mastromatteo
New Procedures to Make Active, Fractal Like, Surfaces on Thin PD Wires
Invited paper at the International Conference on Cold Fusion, ICCF12, Yokohama (Giappone), 28 Novembre al 5 Dicembre 2005

LNF - 06 / 18(P)
Antonio Spallone, Francesco Celani, Paolo Marini, Vittorio di Stefano
Measurements of the Temperature Coefficient of electric Resistivity of hydrogen Overloaded Pd
Contributed paper on International Conference on Cold Fusion, ICCF12, Yokohama (Giappone), 28 Novembre al 5 Dicembre 2005

LNF - 06 / 19(P)
Akito Takahashi, Francesco Celani, Yasuhiro Iwamura
The Italy-Japan Project-Fundamental Research on Cold Transmutation Process for Treatment of Nuclear Wastes
Invited Talk to Conference on Cold Fusion, ICCF12, Yokohama (Giappone), 28 Novembre al 5 Dicembre 2005

LNF - 06 / 20(P)
Francesco Celani, A. Spallone, P. Marini, V. Di Stefano, M. Nakamura, V. Andreassi, A. Mancini, E. Righi, G. Trenta, E. Purchi, U. Mastromatteo, E. Celia, F. Falcioni, M. Marchesini, E. Novaro, F. Fontana, L. Gamberale, D. Garbelli, P.G. Sona, F. Todarello, G. Dagostaro, P. Quercia
Electrochemical Compression of Hydrogen inside a PD-AG Thin Wall Tube, by Alcohol-Water Electrolyte
Invited Paper at JCF7 Kagoshima University-Japan, April 26-28 2006

LNF - 06 / 21(IR)
G. Modestino, G.Pizzella and F.Ronga, for the ROG Collaboration
Optimal Strategy for the Search of Coincident Events Between EXPLORER and NAUTILUS

LNF - 06 / 22(P)
Olaf N. Hartmann
Hadron Properties in the Nuclear Medium – the PANDA Program with $\overline{p}A$ Reactions
Published on Talk given at the Ninth International Workshop on Meson Production, Properties and Interaction (MESON2006), 9-13 June 2006, Cracow, Poland

LNF - 06 / 23(P)
Accelerator Division
Papers presented at EPAC 2006

LNF - 06 / 24(P)
A. Bosco, C. Cantone, S. Dellagnello, G. O. Delle Monache, M. A. Franceschi, M. Garattini, T. Napolitano, I. Ciufolini, S. Negri, A. Agneni, F. Graziani, P. Ialongo, A. Lucantoni, A. Paolozzi, I. Peroni, G. Sindoni, G. Bellettini, R. Tauraso, E. C. Pavlis, D. G. Currie , D. P. Rubincam, D. A. Arnold, R. Matzner, V. J. Slabinski
Probing Gravity in Neo with High-Accuracy Laser-Ranged Test Masses
Presented by S. DellAgnello at the Quantum to Cosmos NASA International Workshop, Warrenton, VA (USA), May 2006 – To be published in a Special Issue of International Journal of Modern Physics D (IJMPD)

LNF - 06 / 25(P)
M. Agnello, L. Benussi, M. Bertani, H.C. Bhang, S. Bianco, G. Bonomi, E. Botta, M. Bregant, T. Bressani, L. Busso, D. Calvo, P. Camerini, P. Cerello, B. Dalena, F. De Mori, G. D'Erasmo, D. Di Santo, D. Elia, F. L. Fabbri, D. Faso, A. Feliciello, A. Filippi, V. Filippini, R. Fini, M. E. Fiore, H. Fujioka, P. Gianotti, N. Grion, B. Kang, A. Krasnoperov, V. Lucherini, V. Lenti, V. Manzari, S. Marcello, T. Maruta, N. Mirfakhrai, O. Morra, T. Nagae, H. Outa, E. Pace, M. Pallotta, M. Palomba, A. Pantaleo, A. Panzarasa, V. Paticchio, S. Piano, F. Pompili , R. Rui, G. Simonetti , H. So, V. Tereschenko, S. Tomassini, R. Wheadon, A. Zenoni
DAΦNE Monitored by FINUDA
Submitted to Nucl. Inst. Meth. A

LNF - 06 / 26(IR)
G. Bellettini, A. Bosco, C. Cantone, I. Ciufolini, D. Currie, S. DellAgnello, G. Delle Monache, M. A. Franceschi, M. Garattini, T. Napolitano, A. Paolozzi, E. C. Pavlis, D. P. Rubincam, V. J. Slabinski, R. Tauraso
Applicazioni Tecnologiche della Camera Spaziale Climatica dei Laboratori Nazionali di Frascati
Contributo alla Fiera InnovAction (Udine, Feb/2006, www.innovactionfair.com), sul trasferimento tecnologico dalla scienza fondamentale del CERN e dellINFN allindustria. Presentato da M. Garattini

LNF - 06 / 27(IR)
M. Abbrescia, A. Colaleo, R. Guida, G. Iaselli, R. Liuzzi, F. Loddo, M. Maggi, B. Marangelli, S. Natali, S. Nuzzo, G. Pugliese, A. Ranieri, F. Romano, R. Trentadue, L. Benussi, M. Bertani, S. Bianco, M.A. Caponero, D. Colonna, D. Donisi, F.L. Fabbri, F. Felli, M. Giardoni, B. Ortenzi, M. Pallotta, A. Paolozzi, L. Passamonti, B. Ponzio, C. Pucci, G. Saviano, G. Polese, I. Segoni, N. Cavallo, F. Fabozzi, P. Paolucci, D. Piccolo, C. Sciacca, G. Belli, A. Grelli, M. Necchi, S.P. Ratti, C. Riccardi, P. Torre, P. Vitulo
Proposal for a Systematic Study OF THE CERN Closed Loop Gas System Used by the RPC Muon Detectors in CMS

LNF - 06 / 28(IR)
G. Bellettini, C. Cantone, S. DellAgnello, G. O. Delle Monache, M. Garattini, N. Intaglietta
MoonLIGHT-M: Moon Laser Instrumentation for General Relativity High-Accuracy Tests

LNF - 06 / 29(IR)
Andrea La Monaca, Giorgio Cappuccio, Roberto De Masi, Andrea Maria Di Lellis, Paolo Di Muro, Roberto Favilla, Fabrizio Fiori, Pasqualino Gaudio, Michele Maffia, Paolo Mariani, Alberto Mazzini, Ivan Micetich, Domenico Nanni, Maria Richetta, Franco Rustichelli, Benedetto Salvato, Francesco Spinozzi
Fluorescence Analysis by Spectroscopy Transmission and Electron Streak Camera (FASTEST-CAM. A proposal for detecting time-synchronized ultra-fast light phenomena

LNF - 06 / 30(P)
A. Donini, E. Fernandez-Martinez, P. Migliozzi, S. Rigolin, L. Scotto Lavina, T. Tabarelli de Fatis, F. Terranova
A Beta Beam Complex Based on the Machine Upgrades for the LHC
Submitted to Eur. Phys. J. C

LNF - 06 / 31(Thesis)
Cristiano Pucci
Tesi di Laurea
in press

LNF - 06 / 32(Thesis)
Student: Arianna Bosco;
Thesis Advisor: Prof. G. Bellettini;
Co-Thesis Advisor: Ing. G. O. Delle Monache
Simulation of the Thermo-Optical Properties of the Lares and Lageos Satellites for a Precise Measurement of the Lense-Thirring Effect in General Relativity

LNF - 06 / 33(IR)
D. Alesini, D. Babusci, M.E. Biagini, R. Boni, M. Boscolo, F. Bossi, B. Buonomo, A. Clozza, G. Delle Monache, G. Di Pirro, A. Drago, A. Gallo, S. Guiducci, M. Incurvati, C. Ligi, F. Marcellini, G. Mazzitelli, C. Milardi, L. Pellegrino, M. Preger, L. Quintieri, P. Raimondi, R. Ricci, U. Rotundo, C. Sanelli, M. Serio, F. Sgamma, B. Spataro, A. Stecchi, A. Stella, S. Tomassini, C. Vaccarezza, M. Zobov, A. D'Angelo, R. Messi, D. Moricciani, S. Bettoni, I. Koop, E. Levichev, P. Piminov, D. Shatilov, V. Smaluk
DAΦNE Upgrade for Siddharta Run

3 – INFN Reports

INFN / AE–06 / 1
Nicoleta Dinu, Emanuele Fiandrini, Livio Fanò
Overview of the Electrical Characterization of the AMS/CMS Silicon Microstrip Detectors

INFN / AE–06 / 2
Elvio Di Salvo
Q^2 *Dependence of Azimuthal Asymmetries in Semi-Inclusive Deep Inelastic Scattering*

INFN / TC–06 / 1
Alessandra d'Alessandro, Franco Marenco, Federico Mazzei, Silvia Nava, Paolo Prati, Roberta Vecchi
Particolato Atmosferico A Modena Nellestate 2004 Risultati dellAnalisi Elementale e Statistica

INFN / TC–06 / 2
Lucio Rossi, Massimo Sorbi
MATPRO: a Computer Library of Material Property at Cryogenic Temperature

INFN / TC–06 / 3
D. Mascali, G. Ciavola, S. Gammino, L. Celona, F. Consoli, S. Passarello, S. Barbarino, F. Maimone
Measurement of the Trips Source Plasma Parameters by Means of a Langmuir Probe

INFN / TC–06 / 4
A.Badalà, F. Blanco, F.Fichera, P. La Rocca, E.Leonora, F.Librizzi, G.S.Pappalardo, O.Parasole, A.Pulvirenti and F. Riggi
Tests with GPS Camac Units for Educational Experiments on Cosmic Ray Physics

INFN / TC–06 / 5
Antonio Codino, Franois Plouin
Galactic Basins of Helium and Iron around the Knee Energy

INFN / TC–06 / 6
Andrea Domenici, Flavia Donno, Gianni Pucciani, Heinz Stockinger
CONStanza: Data Replication with Relaxed Consistency

INFN / TC–06 / 7
F. Maimone, D. Mascali, F. Consoli, S. Barbarino, L. Celona, G. Ciavola, S. Gammino
Simulations and Measurements about the Electromagnetic Properties for the Cylyndrical Cavity of the Serse Ion Source

INFN / TC–06 / 8
Riccardo de Asmundis
Analisi Gas-Cromatografiche Effettuate Presso la Sezione di Napoli, sulla Miscela Impiegata negli RPC di ATLAS

INFN / TC–06 / 9
A.Badalà, F. Blanco, F.Fichera, P. La Rocca, E.Leonora, F.Librizzi, G.S.Pappalardo, O.Parasole, A.Pulvirenti and F. Riggi
A Case Study FOR Educational Collaborations between High Schools in Cosmic Ray Physic

INFN / TC–06 / 10
A. Anastasio
Il Sistema di Controllo di un Bruciatore per Lanalisi ed il Monitoraggio del Rischio Ambientale

INFN / TC–06 / 11
Michelle Stancari
Starting Generators for ABS Intensity Calculations and Magnet System Design

INFN / TC–06 / 12
P. Parascandolo, V. Sipala.
Un Operazionale Full Custom in Tecnologia 0.35 Micron

INFN / TC–06 / 13
Francesca Del Corso
Strategie per lUpdate Management Process

INFN / TC–06 / 14
M. Anghinolfi, A. Calvi, A. Cotrufo, M. Ivaldi, O. Yershova, F. Parodi, D. Piombo, A. Plotnikov and L. Repetto
A Fiber Optic Air Backed Mandrel Hydrophone to Detect High Energy Hadronic

INFN / TC–06 / 15
Agnese Cartocci, Mariaelena Fedi, Marco Manetti, Francesco Taccetti
AMS 14C Measurements At Labec on Viri (Fifth International Radiocarbon Inter-Comparison) Samples

INFN / TC–06 / 16
S. Energico
Disegno e Layout di un OP-AMP Full Custom in Tecnologia da 0.35 μ

INFN / TC–06 / 17
M. Anghinolfi, A. Calvi, A. Cotrufo, M. Ivaldi, O. Yershova, F. Parodi, D. Piombo, A. Plotnikov and L. Repetto
The Realization of an Optic Fiber Air Backed Mandrel Hydrophone for Frequencies up to 20 KHz

INFN / TC–06 / 18
S. Cerchi, S. Cuneo, S. Minutoli, P. Musico, E. Robutti, D. Torazza
Qualification of a Thermal GAP Filler to be Used as Electronics to Structure Interface

Glossary

These are the acronyms used in each status report to describe personnel qualifications other than Staff Physicist:

Art 15	Term Contract (Technician)
Art. 23	Term Contract (Scientist)
Ass.	Associated Scientist
Ass. Ric.	Research Associate
Bors.	Fellowship holder
Bors. PD	PostDoc Fellow
Bors. UE	European Community Fellow
Dott.	Graduate Student
Laur.	Undergraduate Student
Loc. Coor.	Local Coordinator
Osp.	Guest Scientist
Perfez.	PostLaurea Student
Resp.	Local Spokesperson
Resp. Naz.	National Spokesperson
Specializ.	PostLaurea Student
Tecn.	Technician